Measuring and Modeling the Concentrations of Individual Organic Compounds in the Urban Atmosphere

Thesis by

Matthew Paul Fraser

In Partial Fulfillment of the Requirements

for the Degree of

Doctor of Philosophy

California Institute of Technology

Pasadena, California

1998

(Submitted January 7, 1998)

As Their Land Is

After all anybody is as their land and air is.
Anybody is as the sky is low or high,
the air heavy or clear
and anybody is as there is wind or no wind there.
Is that which makes them and the arts they make
and the work they do and the way they eat
and the way they drink
and the way they learn and everything.

–Gertrude Stein

Acknowledgements

There are many people who I would like to acknowledge for their assistance and friendship during my time here at Caltech. First and foremost, my advisor Glen Cass has provided a constant stream of ideas, encouragement and support during my graduate student career. His commitment to perfection and insight into the field of air pollution has greatly improved the quality of my research and presentation of this work.

I am deeply grateful for the assistance of many people who have helped me in my work. While there are too many to list, I would especially like to thank Mike for helping me with the modeling, Jamie for all his help with organizing the lab and mixing standards, Lynn for helping set up samplers and running the analytical equipment. My work has been aided by numerous reseachers at other locations too. I am grateful for the opportunity to have worked with Bernie Simoniet of Oregon State University, Eric and Daniel Grosjean of DGA, Inc., and Rei Rasmussen of the Oregon Graduate Institute. Ed Ruth of UCLA was a big help with the GC/MS analysis and a great excuse to get off campus for a day.

My path in the Environmental Engineering Science Department here at Caltech has crossed with numerous individuals who have aided and inspired me. I thank Rayma Harrison, our librarian, who is always ready for our requests, and Professor Norman Brooks, whose love of teaching is inspirational. I am indebted to those graduate students before me who showed me the ropes. Annmarie's view of life helped me keep things in perspective

whenever things got hectic, and Rob's Mapomatica is just about the coolest thing ever.

My field sampling program pulled together the talent of many graduate students and staff of the EES Department. They had to cross picket lines of burley IBEW workers, run from exploding electrical transformers, and, worst of all, put up with me running around dazed and confused. I am very appreciative for the help of Aaron, Annmarie, Chris, Christos, Darrell, Denis, Jim, Linda, Lynn, Nicole, Pat, and Selena. Two people that my words cannot thank and praise highly enough are Clo and Mike. You are the only reason I made it through 1993, and I thank you two for your help and friendship.

Finally, I have to thank my friends and family. I am truly blessed to have such wonderful people around me, and it goes without saying that I wouldn't have made it without them. There are many memories of good times with my friends. I will never forget the camping trips to J-Tree; hanging at the Red Door with Neil and Anders; the roadtrips to Colorado and skiing trips to Mammoth; golfing with The Linda Weavers Fan Club; missing the last plane off San Nicolas Island with Mike and getting stuck out there; Y-hiking with Clo; catching waves before dawn with Mark and marveling at the color of the sky; Lisa's incredible Sunday night feasts; Hali-daze in Yosemite; and the night that saw me diving the depths with Dave and then climbing the heights of Keck with Mike, Don and Pat. I'm expecting y'all to come to Houston and visit. And to my family, your love and support is a bright light on the hill for me.

Abstract

Field experiments and atmospheric models are used to explore the relationships between source emissions and ambient air quality for individual organic compounds.

Measurements are made at a 5-station air monitoring network in the Los Angeles area during a severe photochemical smog episode. Air samples taken in stainless steel canisters are analyzed for 141 volatile organic compounds by GC/FID, GC/ECD and GC/MS; PAN and PPN are measured by GC/ECD; 82 vapor-phase semi-volatile organics are analyzed by GC/MS after collection on polyurethane foam, and 103 particulate organic compounds are determined by GC/MS. Twenty-three carbonyls are quantified. It is discovered that the high molecular weight carbonyls collectively are as important to atmospheric reactivity as formaldehyde or acetaldehyde individually. Organic compounds concentrations reflect recent changes in gasoline composition, show the decline in alkenes and aromatics concentrations due to atmospheric reactivity while oxy-PAH and nitroaromatics concentrations increase due to formation by atmospheric reactions over downwind transport across southern California. Low molecular weight aliphatic dicarboxylic acids in the air at San Nicolas Island upwind of Los Angeles are found at 44%-76% of urban concentrations, indicating that these compounds are contributed in part by long distance transport, by marine sources, or by oxidation of background biogenic hydrocarbons.

The emissions rates of 221 vapor-phase, semi-volatile and particulate or-

ganic compounds from motor vehicle traffic are measured in a Los Angeles roadway tunnel. Carbon monoxide and organic vapor emissions are found to be much higher than current governmental estimates. Petroleum biomarkers (e.g. hopanes and steranes) emissions rates are measured and used to trace motor vehicle exhaust particles in the urban atmosphere. Elevated ammonia emissions apparantly from three-way catalyst-equipped vehicles were discovered during the highway tunnel experiment. These previously undocumented NH_3 emissions have the potential to increase atmospheric NH_4NO_3 aerosol concentrations.

An Eularian photochemical airshed model is adapted to simultaneously predict the concentrations of nearly 100 individual gas phase, semi-volatile and particle phase organic compounds directly from data on source emisssions. Most organic compounds concentrations are predicted within the correct order of magnitude over 6 orders of magnitude difference in concentrations between the species studied.

Contents

List of Tables

List of Figures

1 Introduction

1.1 Motivation

Many of the air quality problems facing the country today are all closely interlinked. Emissions of gas-phase hydrocarbons and oxides of nitrogen lead to ozone as well as fine particulate formation [1, 2]. Urban haze can be transported hundreds of kilometers and lead to visibility degradation in National Parks and other scenic locations [3]. The emission of sulfur dioxide from the power plants in the midwest leads to sulfate aerosol haze over the East Coast, acidification of streams and lakes in Canada and the United States [4], and has been linked to changes in global radiative forcing [5].

One such linking of air quality concerns revolves around atmospheric organic compounds, which constitute a complicated mixture of vapors and particle-bound species. Direct emissions to the atmosphere of organic gases and particles from anthropogenic and natural sources undergo chemical reaction and gas-to-particle conversion leading to a complicated suite of ambient organic compounds. These atmospheric chemical reactions lead to ozone formation and secondary organic compounds which include toxic air contaminants and non-volatile species which partition into the particle phase contributing to secondary organic aerosol mass. This linking of atmospheric photochemistry leading to ozone and secondary particulate matter formation at least partly motivated the U.S. Environmental Protection Agency's decision in 1997 to simultaneously change the National Ambient Air Quality Standard for ozone and to adopt a new standard for fine particulate matter

($d_p \leq 2.5\ \mu m$). In order to understand the complex mixture of organic compounds that arise from primary emissions sources and secondary atmospheric chemical reactions, one cannot simply look at the bulk organic material in the atmosphere, or separately investigate either the organic vapors or the particulate organic compounds. Rather a comprehensive view of the individual organic compounds present in both the gas and particle phases is required in order to address all of the interactions that occur.

Hundreds of different compounds present in the atmosphere each contribute to the overall atmospheric organic compound burden. However, individual volatile organic compounds (VOCs) can have dramatically different reactivity [6], potential for ozone production [7], secondary organic aerosol formation potential [8], or toxicity. Carbonaceous material constitutes about 30% of the atmospheric fine particle mass concentration, and is composed of hundreds of individual organic compounds, many present at only trace levels [9]. These trace contaminants include highly mutagenic compounds as well as tracer compounds which can be used to track portions of the ambient particulate matter back to the specific primary sources from which they were originally emitted [10, 11]. To obtain an accurate assessment of the role of atmospheric organic compounds in urban air pollution, the chemical complexity of the ambient suite of organic compounds should be fully described.

The air pollution problem of Southern California has been studied extensively in the past, and a complete review of the previous studies of atmospheric organic compounds in the South Coast Air Basin (SoCAB) that surrounds Los Angeles is presented later this work. Previous field studies have focused attention on determining either bulk measures of organic matter (e.g., total organic carbon concentrations), or concentrated on speciating

either the vapor-phase organics or the particle-phase organics [12, 13]. No previous investigation has undertaken a coordinated effort to examine the individual organic compound concentrations in both the vapor-phase and the particle-phase simultaneously.

In past research, when gas-phase organic compounds were characterized, measurements generally were made only of the most abundant species that are present in the molecules with 10 to 12 or fewer carbon atoms. When particle phase species were measured, the simultaneous existence of some of these higher molecular weight species in the gas phase usually was ignored as well. As a result, there exists a broad category of high molecular weight semi-volatile gas-phase species whose composition and concentration generally have not been determined. Recent work has shown that these semi-volatile organic compounds (those compounds which partition between the vapor-phase and particle-phase) are important in accurately describing the ambient concentrations of carbonaceous particles [14] and the formation of secondary organic aerosol [8]. When added to the accounts of atmospheric compounds, these semi-volatile organic compounds lead to the view that organics in the atmosphere exist as a continuum from the lightest VOC to the heaviest particle-bound organic compounds, with a region of overlap in the middle in which many compounds exist simultaneously in both the gas and particle phases. This understanding leads to questions about the wisdom of arbitrarily measuring only compounds lower than a certain volatility for assessing the role of VOCs in ozone formation, or ignoring the vapor-phase concentrations of compounds which partition into the particle-phase.

1.2 Research Objectives

The principal objective of this research effort is to advance a computer-based air quality model which simultaneously accounts for the vapor-phase, semi-volatile, and particle-phase organic compounds present in the urban atmosphere.

A grid-based mathematical model is sought that describes the following atmospheric processes: emissions of gases and particles, atmospheric advection and dispersion, photochemistry, and deposition of both gas-phase and particle-phase species. Mathematical air quality models which can accurately predict the effect of emissions reductions can be used as an efficient means of predicting the outcomes of proposed air quality improvement strategies. The ambient organic pollutants that are tracked within this model are described at the level of individual organic structures. This provides a valuable tool in studying urban air pollution because it allows the chemical fingerprints of different emissions source categories to be carried through the model in a way that helps to assess the relative contribution of different emissions sources to ambient pollutant concentrations. Maintenance of a detailed account of the individual organic compounds also helps to evaluate the accuracy of source emissions inventories.

In order to test the performance of this air quality model, extensive new data are needed on both source emissions and the ambient concentrations of individual organic compounds. A further objective of this research thus is to acquire that data base and use it to evaluate the performance of the air quality model.

In pursuit of this research objective, the ambient concentrations of individual vapor-phase, semi-volatile and particle-phase organic compounds are

measured during a severe photochemical smog episode in Southern California. The ambient concentrations of these individual organic compounds first are displayed and described in order to provide insight into the relationship between vapor and particle phase organic compounds, to attempt to identify those compounds whose ambient concentrations are dominated by atmospheric formation, to track the emissions from different sources which have different organic molecular compositions, and to assess the importance of semi-volatile organic compounds, which are often not considered in emissions estimates or ambient field studies, to atmospheric photochemistry and fine particle concentrations. To evaluate the importance of vehicular exhaust on urban air quality, sampling also is conducted in a local roadway tunnel. By sampling in a roadway tunnel, the emissions of many thousands of vehicles are quantified as they drive under actual operating conditions. Through chemical analysis of the vapor-phase, semi-volatile and particle-phase organic compounds, motor vehicle emissions can be described at the level of detail needed to adequately evaluate the effect of vehicle exhaust on ambient air quality.

1.3 Approach

This section provides an overview of the research presented later in this work. Chapters 2 through 6 detail the data collected during the ambient field sampling program. In Chapter 2, the bulk chemical composition of the atmospheric gases and particles collected during the field project and the gas/particle distribution factors calculated from the data are presented. A review of previous studies of carbonaceous air pollutants in the Southern California atmosphere is provided along with a general overview of the summer 1993 atmospheric sampling program conducted as part of the present

research. Overall mass balances on the totality of the carbonaceous air pollutants and the nitrogen-containing air pollutants in the southern California atmosphere are constructed and used to show the relative contribution of the major vapor-phase and particle-phase air pollutants. The extent of transformation of vapor-phase species into condensed particle-phase products of atmospheric chemical reactions is tracked by displaying the fraction of carbon and nitrogen in the particle-phase compared to total measures of ambient carbonaceous and nitrogenous air pollutants.

In Chapter 3, the ambient levels of carbonyls and peroxyacetyl nitrates are discussed. Included in the data presented in Chapter 3 are the ambient concentrations of 23 carbonyl compounds and two peroxyacyl nitrates. The data are analyzed to reveal that the higher molecular weight aliphatic aldehydes ($\geq C_3$) that are seldom, if ever, measured in source emissions or in the atmosphere are important contributors to atmospheric photochemistry. Calculations are presented which show that the amount of peroxyacetyl nitrate (PAN) that undergoes thermal decomposition at about the time of the daily ozone peak is comparable to the remaining ambient PAN concentration, implying that thermal decomposition of PAN provides a very important reservoir from which release of nitrogen dioxide and radical species can raise the daily ozone peak.

Chapter 4 reports the atmospheric concentrations of non-aromatic hydrocarbons. The data include the ambient concentrations of normal alkanes homologs from ethane (C_2) to hexacontane (C_{36}) which are analyzed to illustrate the transition from vapor-phase compounds to semi-volatile compounds that partition between the gas-phase and particle-phase, to compounds that are found entirely in the particle-phase. Data from San Nicolas Island are used to describe the background atmosphere upwind of the Los Angeles ur-

ban area, and long-term trends in hydrocarbon concentrations are discussed.

Chapter 5 details the ambient levels of aromatic compounds in the urban atmosphere. The data on aromatic hydrocarbons are analyzed to infer relative chemical reaction rates based on depletion during downwind transport, and the spatial and diurnal variations in ambient concentrations are used to identify those compounds whose ambient concentrations in this study are dominated by atmospheric chemical reactions.

In Chapter 6, the ambient concentrations of organic acids are presented. Included in these data are ambient levels of alkanoic acids, benzoic acids, benzene polycarboxylic acids and alkanoic diacids. Relatively low molecular weight aliphatic dicarboxylic acids (e.g., butanedioic acid, hexanedioic acid and propanedioic acid) are found at San Nicolas Island at surprizingly high concentrations (44% to 76% of the concentrations in the urban area), indicating that these compounds, which are generally thought to be formed by atmospheric chemical reactions, or their precursors may have an important component that is derived from long distance transport or natural background sources.

Chapters 7 and 8 describe the results from the characterization of motor vehicle emissions as measured within the Van Nuys tunnel, where Sherman Way crosses under the runway of Van Nuys Airport in the San Fernando Valley area of Los Angeles. The tunnel study is a means of determining emissions from the in-use vehicle fleet under actual operating conditions. Chapter 7 discusses the emissions of organic compounds, including particle-phase, vapor-phase and semi-volatile compounds. The detailed analysis allows comparison of these emissions to the composition of unburned gasoline. That comparison illustrates the relative contribution of combustion products versus unburned fuel components to the composition of vehicle exhaust. Chemical analysis

of particulate matter emitted in the tunnel allows the determination of the contribution of road-dust and tire wear particles to the overall emissions of particle-phase carbon from vehicle traffic within the tunnel.

Chapter 8 describes the emission of ammonia from in-use vehicles in the Van Nuys tunnel. The results show a considerable excess of ammonia emissions from in-use vehicles above and beyond the emissions estimates contained in previous emissions inventories. This finding has important implications for the control of atmospheric fine particle ammonium nitrate concentrations in Los Angeles.

Chapter 9 relates the emissions of petroleum biomarkers from motor vehicle traffic within the Van Nuys tunnel to the ambient concentrations of these same compounds determined during the summer 1993 field experiments. From these data, calculations are made that estimate the contribution of primary emissions of carbonaceous particles from motor vehicles to the ambient atmosphere.

Chapter 10 describes an Eularian photochemical model designed to track the emissions of vapor-phase, semi-volatile and particle-phase organic compounds through the atmospheric chemistry, transport and deposition processes which govern the ambient concentrations of these organic compounds.

Finally, in Chapter 11 the major results of this research are summarized. Important accomplishments are highlighted, and areas for future research are identified.

Bibliography

[1] National Research Council. *Rethinking the ozone problem in urban and regional air pollution.* National Academy Press, Washington, D.C., 1991.

[2] Z. Meng, D. Dabdub, and J. H. Seinfeld. Chemical coupling between atmospheric ozone and particulate matter. *Science*, 277:116–119, 1997.

[3] National Research Council. *Protecting visibility in National Parks and Wilderness areas.* National Academy Press, Washington, D.C., 1993.

[4] R. J. Charlson and H. Rodhe. Factors controlling the acidity of natural rainwater. *Nature*, 295:683–685, 1982.

[5] R. J. Charlson, S. E. Schwartz, J. M. Hales, R. D. Cess, J. A. Coakley, and J. E. Hansen. Climate forcing by anthropogenic aerosols. *Science*, 255:423–430, 1992.

[6] R. Atkinson. Gas-phase tropospheric chemistry of organic compounds: a review. *Atmos. Environ.*, 24A:1–41, 1990.

[7] W. P. L. Carter. Development of ozone reactivity scales for volatile organic compounds. *J. Air Waste Manage. Assoc.*, 44:881–899, 1994.

[8] J. R. Odum, T. P. Jungkamp, R. J. Griffin, H. J. L. Forstner, R. C. Flagan, and J. H. Seinfeld. Aromatics, reformulated gasoline and atmospheric organic aerosol formation. *Environ. Sci. Technol.*, 31:1890–1897, 1997.

[9] B. R. T. Simoneit. Characterization of organic-constitutents in aerosols in relation to their origin and transport- a review. *Intern. J. Environ. Anal. Chem.*, 23:207–237, 1986.

[10] M. P. Hannigan, G. R. Cass, B. W. Penman, C. L. Crespi, A. L. Lafleur, W. F. Busby, and W. G. Thilly. Human cell mutagens in Los Angeles air. *Environ. Sci. Technol.*, 31:438–447, 1997.

[11] J. J. Schauer, W. F. Rogge, L. M. Hildemann, M. A. Mazurek, G. R. Cass, and B. R. T. Simoneit. Source apportionment of airborne particulate matter using organic compounds as tracers. *Atmos. Environ.*, 30:3837–3855, 1996.

[12] R. A. Harley and G. R. Cass. Modeling the atmospheric concentrations of individual volatile organic compounds. *Atmos. Environ.*, 29:905–922, 1995.

[13] W. F. Rogge, L. M. Hildemann, M. A. Mazurek, G. R. Cass, and B. R. T. Simoneit. Mathematical modeling of atmospheric fine particle-associated primary organic compound concentrations. *J. Geophys. Res.*, 101:19373–19394, 1996.

[14] B. J. Turpin, J. J. Huntzicker, and S. V. Hering. Investigation of organic aerosol sampling artifacts in the Los Angeles basin. *Atmos. Environ.*, 28:3061–3071, 1994.

2 Bulk Chemical Composition and Gas/Particle Distribution Factors

2.1 Introduction

The hundreds of organic compounds contained in urban atmospheres are important contributors to the problems caused by air pollution. Volatile organic compounds (VOCs) have long been known to promote ozone formation when combined with oxides of nitrogen [1,2]. Higher molecular weight and less volatile organic compounds are a sizable fraction of the mass of aerosol particles with aerodynamic diameters less than 2 μm [3,4]. These fine particles are mainly responsible for the visibility degradation in the Los Angeles area [5], and are easily respirable and have been linked to a number of human health problems [6].

Mathematical models can be developed that simulate the atmospheric transport and chemical reactions which relate source emissions to ambient pollutant concentrations. These models can then be used to evaluate the effect of alternative emission control programs so that the most effective control program can be identified and implemented. Atmospheric models have been

Reference: Fraser, M. P.; Grosjean, D.; Grosjean, E.; Rasmussen, R. A.; Cass, G. R. Air Quality Model Evaluation Data for Organics. 1. Bulk Chemical Composition and Gas/Particle Distribution Factors. *Environ. Sci. Technol.*, **30**, 1996: 1731-1743.

developed that track inorganic pollutants, such as the oxides of nitrogen and sulfur, from their emission as gases, atmospheric conversion to form low vapor pressure products, condensation onto particles, accompanied by atmospheric transport to downwind smog receptor sites [7-10]. While atmospheric pollutants include both inorganic and organic compounds, the atmospheric fate of single inorganic compounds has been more extensively studied than the fate of single organic compounds. This is because the number of inorganic pollutants is small compared to the number of organic compounds in the atmosphere, and also because inorganic pollutants are more easily measured than organic pollutants.

Air quality modeling of organic compounds has progressed primarily along two fronts: (1) aerosol processes modeling of particulate organics [9, 11-13], and (2) separate photochemical modeling of vapor phase organics with respect to ozone formation and air toxics [14-19]. Research in aerosol modeling of atmospheric organics has led to an understanding of source/receptor relationships for primary particulate organic compounds (those compounds that are emitted directly from sources; [13]). Air quality modeling of VOCs has led to the capability to predict the atmospheric concentrations of more than 50 individual VOCs [19]. However, there has been little attempt to unify the treatment of the gas and particle phases in modeling individual organic compounds and to investigate interactions between the two phases.

The long-term objective of the research begun here is to enable the creation and testing of a photochemical airshed model that predicts the concentrations of individual airborne organic compounds within a combined framework that encompasses both VOC and organic aerosol modeling, and that includes within the model a new ability to account for the concentrations of semi-volatile organics (those compounds that are present simultaneously in

both the gas phase and the particle phase). By tracking vapor-phase and particle-phase organics simultaneously, it should be possible to account more accurately for the formation of secondary organic compounds (those formed by atmospheric chemical reactions). A major barrier to the development and testing of such a comprehensive model for atmospheric organic air pollutants is the absence of an equally comprehensive experimental data base against which such a model can be tested.

The purpose of this article is to describe the design and execution of an experiment to collect the data base needed for performance evaluation of a comprehensive regional airshed model for atmospheric organic compounds. To this end, a field study was conducted in Southern California during 1993. The atmospheric concentrations of individual organic compounds were measured in the gas and particle phases simultaneously at a network of air monitoring sites over consecutive short averaging times in a format that can be used for subsequent evaluation of a comprehensive model of atmospheric organics. The resulting data provide observations for hundreds of organic compounds in the particle and gas phases simultaneously at five sites during a two-day photochemical smog episode. In the present paper, the severity of the photochemical smog event and concentrations of bulk chemical species in both the particle and gas phases will be discussed. The partitioning of carbon, nitrogen and chlorine between the gas and particle phases will be tracked as the smog episode evolves over time. Subsequent papers will describe the measurement and atmospheric behavior of the individual organic compounds present within major classes of organic compounds: hydrocarbons, aldehydes and other carbonyl compounds, peroxyacyl nitrates, and organic acids.

2.1.1 An Overview of Previous Studies in Southern California

The South Coast Air Basin (SoCAB), which surrounds Los Angeles, has the nation's most extensively studied air pollution problem. The research spurred by Los Angeles's well-known smog formed much of the foundation for the current understanding of urban photochemical air pollution and has led to significant improvements in air quality in recent decades.

Experiments to characterize the volatile organic compounds in the Los Angeles atmosphere date back at least to the early 1960s when VOCs were examined as an important component of photochemical smog. Ambient air samples speciated for volatile organic compounds were collected in Central Los Angeles during the morning rush hour [20,21] and at Riverside, California [22]. Comparisons between speciated hydrocarbons in the Los Angeles and the New York-New Jersey metropolitan areas were presented by Lonneman et al. [23]. Lagrangian air monitoring of speciated hydrocarbons was preformed during the Los Angeles Reactive Pollutant Program (LARPP) from early September to mid-November, 1973 [24,25]. Additional sampling campaigns investigated spatial variations in VOCs in the SoCAB by sampling at two sites, Downtown Los Angeles and Azusa, [26]; spatial variations in speciated hydrocarbons were measured during three daily sampling periods between June and September 1974 at six sites in the basin [27, 28]. Simultaneous measurements of more than 50 vapor-phase compounds, including hydrocarbons and carbonyl compounds at Downtown Los Angeles during 1981 were collected in an attempt to measure those compounds important to simultaneously modeling both ozone formation and organic aerosol formation [29]. These studies of ambient volatile organic compounds have underscored the importance of measurements of individual hydrocarbons rather than bulk concentration measurements, and have led to the development of reactivity

scales that account for the relative importance of single organic species to ozone production and secondary organic aerosol formation [30-32].

In a separate series of investigations, the composition, concentration, spatial and temporal distributions of particulate matter in the SoCAB has been studied through a number of field experiments and associated modeling efforts. Beginning with a chemical element balance based on aerosol samples collected in Pasadena [33], experiments have continued to correlate source contributions to ambient particulate matter concentrations. The California Aerosol Characterization Experiment (ACHEX) produced intensive field observations in the Los Angeles area between September 1972 and October 1973 [34], providing data on particle size distributions and chemical composition for a number of sites in the SoCAB. The ACHEX experiment demonstrated the variability of aerosol composition, and suggested the need to study changes in aerosol behavior over short time periods. The ACHEX chemical characterization included analysis of elemental composition by X-ray fluorescence [35], sulfate and nitrate concentrations [36], and individual organic compounds and organic compound classes in the particle phase [37-40]. Other studies of organic particulate matter in the air basin focused on analyzing certain individual organic compounds within specific compound classes including polycyclic aromatic hydrocarbons (PAHs; [41,42]); aliphatic dicarboxylic acids [43], as well as aggregate quantities of organic aerosol components contained within lumped compound classes [44, 45].

During the 1980s, a number of long-term studies of aerosol concentrations provided information on the chemical composition of particulate matter in Southern California over long enough periods of time that a stable statistical measure of the time series of ambient concentrations could be obtained in detail sufficient to support emission control program development. Gray et al.

[3] describe an experiment to investigate particulate organic and elemental carbon concentrations, as well as ionic species and trace metals levels at 10 sites in the SoCAB and at one offshore island by taking samples of 24 h duration every sixth day during 1982. A subsection of the samples collected in this experiment were analyzed by high-resolution gas chromatography/mass spectrometry to identify and quantify the single organic compounds present [4]. Ambient aerosol carbon samples from this study also were analyzed to determine their isotopic composition (^{12}C / ^{14}C ratios; [46]) and their bacterial mutagenicity [47]. A program of source testing accompanied by determination of the elemental composition [48], emission rates of specific organic compounds [49-55], carbon isotopes [46], and bacterial mutagens [47] in the effluent from Southern California aerosol sources was coordinated with the 1982 ambient fine particle characterization experiments. Air quality models that track source contributions to fine particle organic carbon, elemental carbon, individual particulate organic compounds, carbon isotopes and bacterial mutagens have been developed and tested against the 1982 Southern California fine aerosol field experimental data base [13,46,47,56,57]. A related study conducted during 1986 to determine the characteristics of PM_{10} in Southern California provided chemical speciation of particulate matter based on 24-h average samples taken every sixth day at nine sites throughout the basin [58] that has subsequently been used as the basis for the current PM_{10} control plan for the SoCAB.

While the chemical properties of Southern California fine particles over averaging times of 24-h to one year are known in detail from the 1982 and 1986 annual studies just described, much more detailed information on the size distribution of the aerosol and concentration changes from hour-to-hour are needed in order to test the predictions of the next generation of photo-

chemical airshed/aerosol air quality models. A comprehensive set of data on bulk aerosol chemical composition and concentration changes over consecutive short-term (e.g., four-hour) sampling periods was collected during the Southern California Air Quality Study (SCAQS; for an overview of SCAQS, see [59]). A detailed description of the spatial and temporal variations in the size distribution and chemical composition of particulate matter was obtained [60-66]. The SCAQS experiment provides data [67,68] on the detailed speciation of the volatile organic compounds that are precursors to secondary organic aerosol production [11,12].

The SCAQS data base comprises the most complete set of short-term average particulate and gas phase air quality, visibility, and meterological observations assembled in Southern California. Speciated vapor-phase hydrocarbon measurements taken at 9 sites throughout the basin during SCAQS were the basis for chemical mass balance receptor models that seek to trace non-methane hydrocarbons in the atmosphere back to their original sources, including motor vehicle exhaust, unburned whole gasoline, gasoline headspace vapors, natural gas leaks, architectural and industrial coatings and biogenic emissions [69,70]. Source contributions to ambient particulate matter concentrations also were quantified using the SCAQS data set based largely on elemental analysis of aerosol samples; source contributions to atmospheric particle concentrations were identified for sources including primary geological material, primary motor vehicle exhaust, primary marine aerosol, primary lime/gypsum, secondary sulfates and nitrates [71]. Measurements of elemental concentrations alone, however, were unable to resolve source contributions from primary meat cooking operations; use of elemental data alone did not permit quantification of the contribution of secondary organics to ambient aerosol loadings, and could not distinguish the differ-

ence between diesel-powered and gasoline-powered vehicle primary particulate emissions [71]. Secondary organic aerosol levels during SCAQS were estimated by examination of particulate organic and elemental carbon concentration ratios determined from an in-situ carbon analyzer [72], and by mathematical modeling of the formation, transport and deposition of secondary organic aerosol [11,12]. In spite of the abundance of detail available in the SCAQS data base, certain important features are missing. In particular, semi-volatile organics and the specific organic compounds present in the aerosol and the semi-volatile organics were not measured. For that reason, interactions between gas-phase and particle-phase organics cannot be examined simultaneously and in detail through use of the SCAQS data. Indeed, in spite of the tremendous body of literature on atmospheric organics just reviewed, there are no field experimental studies that simultaneously account for gas-phase and particle-phase organics at the single compound level.

2.1.2 Comprehensive Determination of Atmospheric Organics

During the summer of 1993, a field experiment was undertaken whose major objective was to measure the concentrations of as many individual organic compounds as possible in both the particle and gas phases simultaneously. The observational experiment was conducted at five sites in Southern California. Samples of 4-h duration were taken every six hours to obtain time series data on the short-term concentrations of individual organic compounds in a format suitable for evaluation of photochemical airshed model performance for single organic compounds.

Four urban sites (Long Beach, Central Los Angeles, Azusa and Claremont) were selected to represent the different air pollution characteristics within the greater Los Angeles area, and one offshore site (San Nicolas Is-

land) was selected to represent air quality upwind of the city. These five sites are among the air monitoring site locations that are shown in Figure 2.1, along with topographic contours that outline the location of local mountain ranges. The air pollution in Long Beach reflects primary emissions from industrial sources, including local oil refineries, power plants and activities in the harbor. Central Los Angeles, at the center of Southern California's highway system, has air quality characterized by high concentrations of primary organics from motor vehicle exhaust as well as some secondary photochemical reaction products. Air quality in Azusa and Claremont, photochemical smog receptor sites that are downwind of the primary emission sources located in the western portion of the air basin, is characterized by high levels of ozone and secondary air pollutants. The offshore background site (San Nicolas Island) is characterized by cleaner marine air from the near-coastal Pacific Ocean. Because of the low pollutant levels at this site and restricted access to the site, four air sampling periods of longer duration than at the urban sites were defined at San Nicolas Island during the experiment reported here. Little variation in the chemical composition was seen between the four samples taken at San Nicolas Island. For this reason, all San Nicolas Island data will be lumped to form a single background concentration measurement.

Five separate ambient samplers were deployed to measure the organic compounds in the atmosphere at each air monitoring site. High volume dichotomous samplers followed by polyurethane foam (PUF) cartridges were used to characterize the particulate organic air pollutants by filtration and semi-volatile organics by collection on the PUF cartridges. Low volume filter-based samplers were used to measure aerosol mass concentrations and aerosol elemental composition as well as the concentrations of several gas-phase inorganic species using denuder difference and tandem filter pack techniques. A

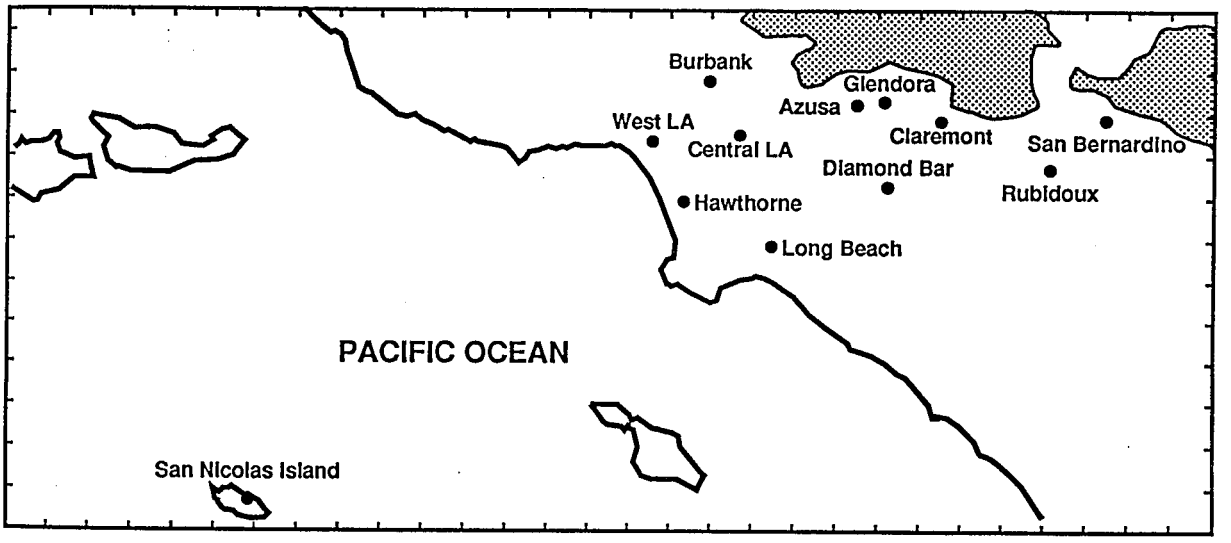

Figure 2.1:
Map of southern California, showing the air monitoring sites mentioned in the text. Local mountain ranges extending above 1200 meters elevation are shown within the shaded contours.

volatile organics sampler employing internally electropolished stainless steel canisters was used to capture gas-phase organics. Electron capture gas chromatographs were used to measure peroxyacyl nitrates. Collection on cartridges impregnated with dinitrophenylhydrazine (DNPH) was used to measure carbonyl compounds. Each of these samplers will be described briefly.

A low volume sampler, shown schematically in Figure 2.2, was used to collect ambient samples of the fine (diameter, $d_p \leq 1.6$ μm) and total airborne particulate matter, and certain inorganic gases at the four urban sites over 4-hr sampling periods centered within sequential 6 hour intervals. Longer sampling periods were used at San Nicolas Island. The fine particle stream was first passed through a Teflon-coated AIHL cyclone separator to remove the coarse particles with $d_p \leq 1.6$ μm [73]. The air flow was then divided between five parallel sampling assemblies. For total particle samples, a separate manifold was used, pulling air through three sampling assemblies. Each sampling assembly contained filter substrates which were chosen to be compatible with particular chemical analyses. Organic and elemental carbon samples were collected on quartz fiber filters (Tissuquartz 2500 QAO, Pallflex, Putnum, CT) which were heat treated at 550 degrees C for at least 6 hours to lower their carbon blank values. Organic and elemental carbon concentrations were determined from the quartz fiber filters by the method described by Huntzicker et al. [74] and Cary [75]. Fine particle and total particle mass concentrations were determined gravimetrically by repeated weighing of the Teflon filters at 50% RH using a Mettler Model M-55-A mechanical microbalance. Ion chromatography and atomic absorption spectrophotometry were used to measure the particulate inorganic species NO_3^-, Cl^-, SO_4^{2-}, Na^+, Mg^{2+} collected on the Teflon filters. The denuder difference method employing nylon filters (Nylasorb, Gelman, Ann Arbor, MI) was used to mea-

sure gas phase nitric and hydrochloric acids as well as fine particle nitrate and chloride [76-82]. Before use, the nylon filters were washed with dilute sodium bicarbonate to ensure a low chloride blank value. An indophenol colorimetric procedure [83] was used to determine particle-phase ammonium ion from analysis of collections on Teflon pre-filters and gas-phase ammonia from oxalic acid impregnated glass fiber backup filters (Gelman AE) located downstream of Teflon prefilters. Samples were collected on KOH impregnated glass fiber filters located downstream of Teflon prefilters for later analysis of gas-phase organic acids. After collection all samples were sealed in petri dishes with Teflon tape, and chilled while being transported back to the laboratory, where they were frozen at -21 degrees C prior to analysis.

High volume dichotomous virtual impactors [84] were used to collect the relatively large amounts of size-separated organic material over the short 4-hr sampling periods needed to identify individual compounds in the particle phase by GC/MS techniques [4,85]. Following the fine particle filter of the high volume dichotomous sampler, polyurethane foam plugs were used to collect the semi-volatile organic compounds [86,87].

Electropolished stainless steel canister samplers were used to capture volatile organic compounds. The 6 liter canisters were shipped and deployed into the field under high vacuum, used to collect 4 hour integrated samples through PFA Teflon sample lines purged with ambient air, sealed and returned to the lab for analysis. Total non-methane organic compounds in the gas phase were measured by cryogenic preconcentration and direct flame ionization detection according to EPA Method TO12 [88]. Individual organic compounds from the stainless steel canister samples were analyzed by gas chromatography/electron capture detection, gas chromatography/flame ionization detection, and gas chromatography/mass spectroscopy. The bulk con-

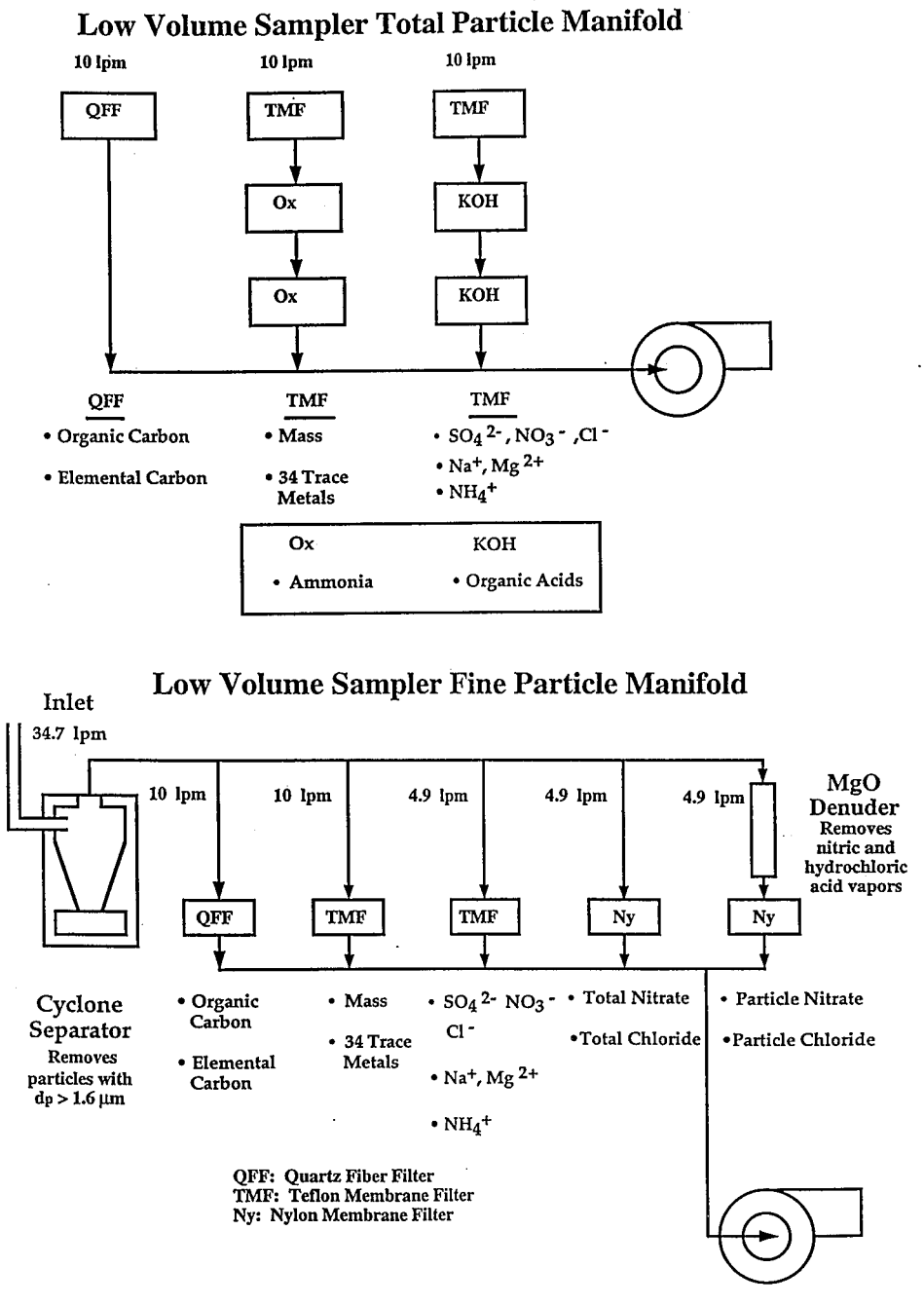

Figure 2.2:
Schematic drawing of the low-volume particulate matter sampler.

centrations of major organic compound classes (chlorinated organics, alkanes, alkenes and aromatic hydrocarbons) will be presented here.

Twenty-three aldehydes and other carbonyl compounds were measured by collection on DNPH impregnated C_{18} cartridges [89]. Air was drawn through these cartridges at a flow rate of circa 1 lpm for 4-hr, and the carbonyl compounds trapped were analyzed by liquid chromatography.

The peroxyacyl nitrates peroxyacetyl nitrate (PAN) and peroxypropionyl nitrate (PPN) were measured by on-site electron capture gas chromatography [90]. Data were collected every half hour at the four onshore sampling sites.

Levels of other gas-phase pollutant levels, including NO, NO_2, O_3, CO and SO_2 were measured hourly by the South Coast Air Quality Management District (SCAQMD) at their 31 continuous air monitoring stations within the SoCAB. Our sampling sites at Long Beach, Central Los Angeles, and Azusa were co-located with SCAQMD air monitoring stations. Ozone concentrations were measured at Claremont as part of our measurement program using a Dasibi Model 1003-PC nondispersive ultraviolet absorption photometer. Meteorological data collected for this experiment included temperature, relative humidity, wind speed and wind direction measurements made at 70 existing governmental monitoring stations. The SCAQMD also provided information that describes inversion base height and winds aloft from upper air soundings taken at 0600 hours PDT in West Los Angeles. Measurements of solar and ultraviolet radiation were also taken by the SCAQMD at Central Los Angeles. A NOAA upper air profiler was operated at the Claremont site as part of a separate study by the California Air Resources Board (CARB) [91] that provided high resolution data on inversion base height and winds aloft. Meterological observations also include a large number of temperature, relative humidity, cloud cover, visual range, wind speed and direction

observations from airports throughout the region.

2.2 Results

The two photochemical smog episodes examined occured on 2-3 Sept. and 8-9 Sept. 1993, with efforts concentrated on analyzing samples from the latter episode. The photochemical smog episode of Sept. 8-9 included the highest one-hour average ozone concentration observed in the SoCAB during 1993. A high pressure system developed over the air basin during the episode; the extent of vertical mixing was decreased due to a strong temperature inversion aloft while atmospheric photochemical reactions were induced by sunny hot weather. Peak temperatures in the eastern portion of the air basin reached greater than 40 degrees C on the second day of the episode. Onshore winds developed in the afternoon transporting pollutants inland and bringing marine moisture and fog to the coastal region of the basin during the early morning hours of both days. The onshore air flow in the summer transports air parcels from over the Pacific Ocean which next pass over the heavily urbanized western section of the basin, accumulating primary emissions of both gas-phase and particle-phase pollutants. These air parcels become aged as they are advected inland, with the result that the eastern half of the air basin experiences the highest levels of the secondary air pollutants that are formed due to atmospheric chemical reactions. Ozone data for the second day of the episode studied here show that peak ozone levels occur progressively later in the day with increasing distance inland from the coast, which is consistent with the passage over the air basin of masses of heavily polluted air originally generated over the western portion of the air basin. Figure 2.3 shows the diurnal variations in ozone and nitrogen dioxide concentrations at two of the sampling sites. At the western edge of the air basin, 1-hr average

ozone concentrations peaked on September 9 at 50 ppb at 1300 hours PDT in Hawthorne and West Los Angeles, and at 90 ppb in Long Beach. Further inland hourly average ozone concentrations peaked at 110 ppb in Central Los Angeles, at 230 ppb in Azusa, and at 280 ppb in Glendora at 1400 hours PDT in the afternoon. The highest ozone levels were measured at our Claremont sampling site, reaching 290 ppb 1-hr average at 1500 hours PDT on September 9 with excursions above 300 ppb over shorter averaging times. At sites further inland from Claremont, the peak ozone levels begin to decline. The eastern end of the basin experienced peak 1-hr average ozone concentrations of 240 ppb in Upland, 260 ppb in Rubidoux/Riverside, and 190 ppb in San Bernardino, all at 1500 hours PDT.

Unusually high levels of nitrogen dioxide were also observed during this experiment. The highest NO_2 concentrations were observed in the mid-morning, following the atmospheric oxidation of NO, which peaks during the morning rush hour. Hourly average NO_2 concentrations peak on the first day of the episode (Sept. 8) at Central Los Angeles at 200 ppb at 1100 hours PDT, and at Diamond Bar at 210 ppb at 1000 hours PDT on the second day (Sept. 9). Peak hourly average NO_2 concentrations on the second day of the episode, moving from the western edge of the air basin inland, are: 110 ppb at Long Beach at 1100 hours; 160 ppb at Central Los Angeles at 1000 hours, and 160 ppb at Burbank at 0900 hours; 150 ppb at Azusa at 0900 and at 1000 hours, and 210 ppb at Diamond Bar at 1000 hours PDT. Such high NO_2 levels, nearing the 250 ppb State of California 1-hr average air quality standard for NO_2, are unusual for an extreme ozone concentration event in the Los Angeles area; the highest NO_2 concentrations typically occur in the colder months which have lower early morning mixing depths. The mean of the daily NO_2 maxima at Central Los Angeles for the summer

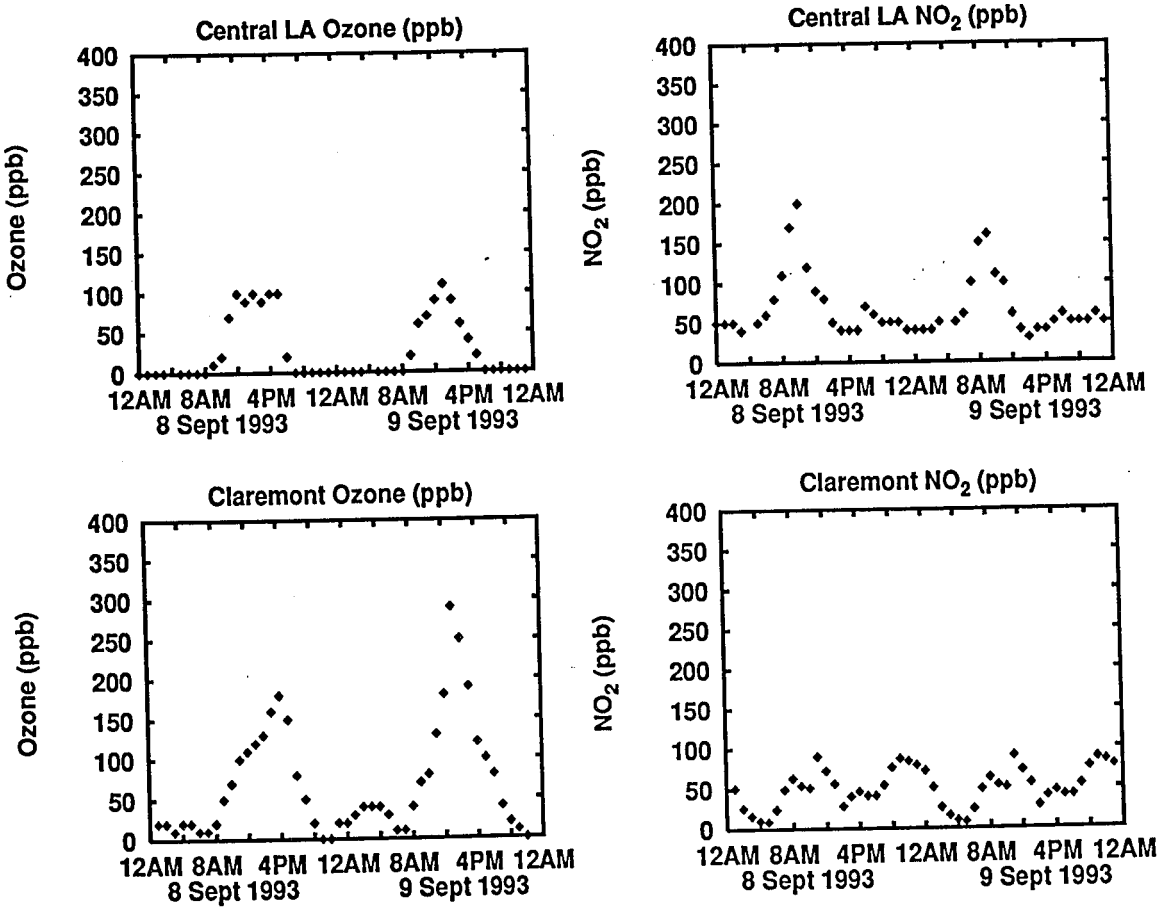

Figure 2.3:
Diurnal variation of ozone and nitrogen dioxide at Central Los Angeles and Claremont during the period studied.

(June-Sept) of 1993 is only 64 ppb. NO_2 concentrations during the Sept. 8-9, 1993, episode are much higher than those that accompanied the highest ozone events observed during the Southern California Air Quality Study (SCAQS) (see model evaluation data presented by reference [17]).

2.2.1 Carbonaceous Air Pollutants

A material balance on the composition of the entire assemblage of the organic air pollutants measured during the September 8-9, 1993, episode was constructed as shown in Figure 2.4 to investigate the spatial and temporal variations in these organic air pollutants. From data collected by the ambient samplers, all pollutant concentrations were converted to an equivalent basis (μg C m^{-3}).

Total carbon is calculated as the sum of the total organic carbon in the vapor phase as measured by cryogenic preconcentration followed by direct flame ionization detection (according to EPA Method TO12) plus total particulate carbon measured as the sum of elemental carbon and organic carbon in the particle phase. Thus methane, CO, and CO_2 are excluded from the carbon balance while all more complex species are included. Total carbon is highest at the Central Los Angeles and Azusa air monitoring sites during the morning rush hours. A sharp decrease in the organic carbon levels occurs between the morning sampling period, which includes the morning traffic rush hours, and the early afternoon sampling period. This reflects the increasing mixing depth due to solar heating and the decreased emission levels from vehicular sources once the morning commute to work is completed. Total carbon concentrations at Claremont are lower than those at Central Los Angeles, and do not show strong diurnal variations. During the morning hours, Claremont is affected by direct emissions from local motor vehicle traffic, but

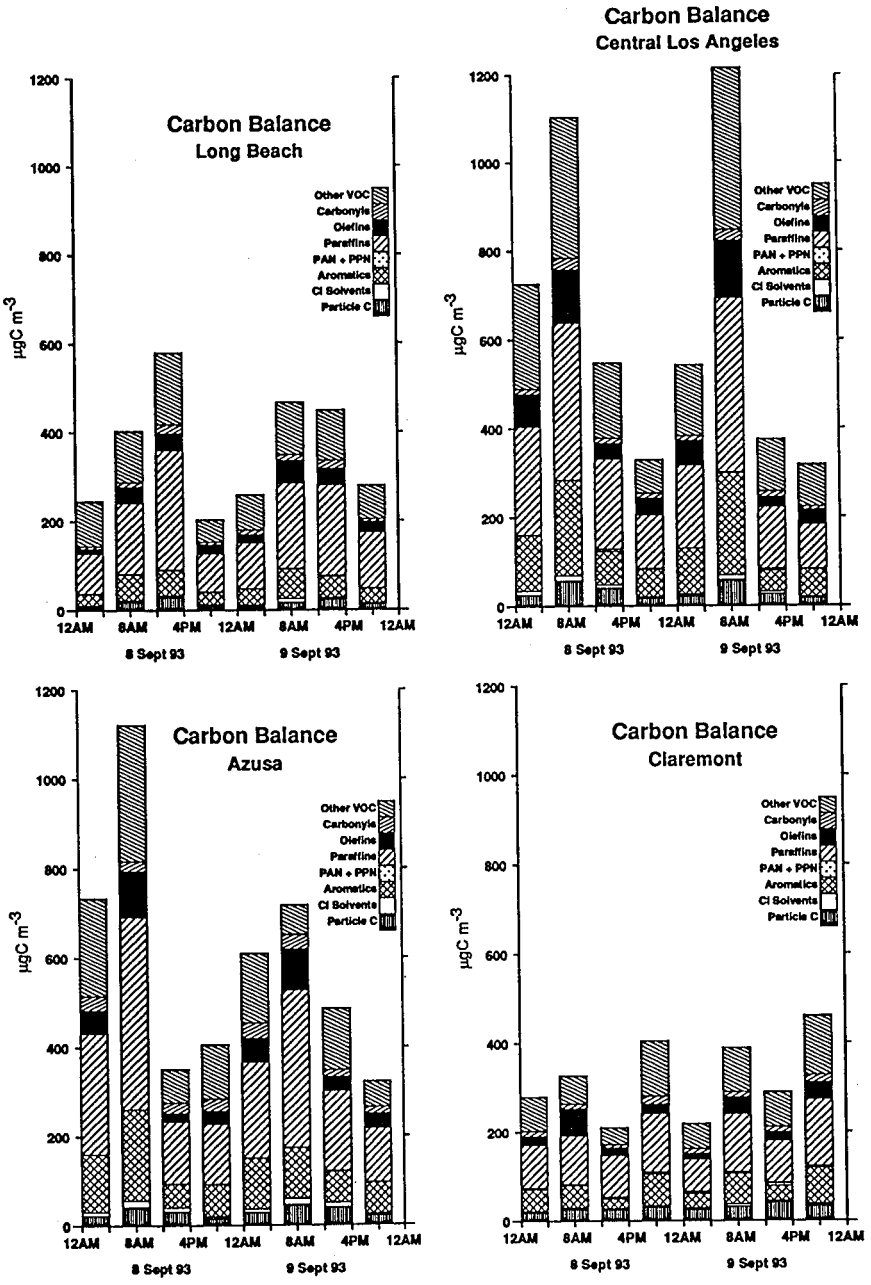

Figure 2.4:
Carbonaceous pollutant balance. Particulate carbon includes elemental plus organic carbon. The category labeled 'other VOC' consists of compounds in the vapor phase including organic acids, vapor phase compounds heavier than n-decane, and compounds that are unidentified because they are present in trace amounts.

traffic denisty is lower there than at Central Los Angeles, leading to lower morning concentrations at Claremont. During the afternoon, Claremont receives transported organic material that was emitted during the morning traffic peak in the more urbanized western portion of the air basin and that arrives at Claremont late in the day.

The diurnal variations of the major compound classes that contribute to total carbon concentrations also reveal information concerning the sources and fates of organic air contaminants. The secondary peroxyacyl nitrates are present at the highest concentrations in Claremont at the time of the ozone peak, consistent with their photochemical production. Carbonyls are present at the highest concentrations in Azusa; primary carbonyl compounds (e.g., primary formaldehyde and acetaldehyde contained in vehicle exhaust plus acetone and 2-butanone which are used as industrial solvents) and secondary carbonyl compounds formed by atmospheric chemical reactions combine at this downwind smog receptor site, which is also affected by local industrial sources. At all sites, the percentage contribution of aromatic hydrocarbons and olefins to total carbon decreases from the morning sampling to the early afternoon sampling period. On both sampling days, vapor-phase olefins decrease from 11% to 6% of the total carbon at the Central Los Angeles site between these two consecutive sampling periods, while vapor-phase aromatic hydrocarbons decrease from 21% to 14% of the total carbon on the first day, and from 20% to 13% on the second day between the morning and afternoon sampling periods. This is consistent with the selective reaction of the olefins and aromatic hydrocarbons with atmospheric oxidants during the late morning and afternoon photochemical smog period. The less reactive paraffins increase as a percentage of total carbon between the morning and early afternoon sampling periods on both days at the Central Los Angeles site.

As air parcels age certain volatile organic compounds that are directly emitted are converted to secondary organic aerosol consisting of polar compounds which condense as the low vapor pressure products of the gas-phase oxidation of volatile organic compounds [11,37-40,64,72,92-94]. One way to measure the extent of conversion via oxidation of volatile organic compounds to secondary organic aerosol is to calculate a gas-particle distribution factor for carbon-containing air pollutants [95]. Figure 2.5 shows the ratio of organic carbon in the particle phase to the total organic carbon defined as the sum of total organics in the vapor phase plus organic carbon in the particle phase. At Long Beach between 2.6-5.4% of the total organic carbon is found as particulate phase organics, with the lowest fraction during the middle of the night, and the highest values in the afternoon. At Central Los Angeles, a wider variation by time of day is observed; between 2.7 and 6.5% of the total organic carbon is found as organic aerosol. The highest fraction particulate organics also occurs at Central Los Angeles in the afternoon; lower fractions organic aerosol are observed overnight and during the morning traffic rush hours, indicating less aged air parcels at those times. In Azusa, a still wider variation between relatively fresh versus aged air parcels is evident with a minimum of 3.1% OC in the particulate phase during the first nighttime sampling period, and a maximum of 9.0% of the organic material in the particle phase during the afternoon photochemically active sampling period. The ratio of organic carbon in the particle phase to total organic carbon is highest overall in Claremont, varying between 6.1 and 12.5%, consistent with having the greatest degree of air parcel aging at the farthest downwind site. Further evidence of air parcel aging is seen in the ratio of the more reactive to less reactive gas-phase hydrocarbons. That ratio decreases progressively from higher values at coastal sites to lower values at inland smog receptor

sites. For example the ratio of 1,3-butadiene to benzene decreases from 0.086 at Long Beach to 0.065 at Central Los Angeles, 0.061 at Azusa, and 0.042 at Claremont. The picture that emerges from the present study is consistent with long-standing evidence that secondary organic aerosol accumulates with travel downwind over the air basin while primary organic vapors are depleted by chemical reaction, leading to increased ratios of particulate to total organic carbon over time.

2.2.2 Nitrogen-Containing Air Pollutants

A similar material balance on the nitrogen-containing air pollutants was constructed, as shown in Figure 2.6, in order to place organic nitrates in context relative to inorganic nitrogen-containing species. All ambient measurements were converted to an equivalent basis stated in terms of μg N m^{-3}. The nitrogen-containing pollutant present in highest concentrations is NO, which accounts for as much as 75% of the nitrogen containing pollutants measured at Central Los Angeles during the morning rush hour. NO concentrations at Central Los Angeles and elsewhere drop to below minimum reporting limits of 10 ppb during the afternoon sampling period. The fraction of the nitrogen-containing air pollutants that are present as NO is lowest at the farthest inland site, Claremont, never accounting for more than half of the nitrogen present in nitrogen-containing pollutants at anytime during this episode at that site. The sum of NO plus NO_2, designated NO_x, corresponds to as much as 92% of the total nitrogen-containing air pollutants measured at the Central Los Angeles site during the morning rush hour, and never less than 43% of the nitrogenous pollutants measured at that site. At the Claremont site, NO_x represents at most 85% of the nitrogen-containing air pollutants measured, with a minimum value of 12% NO_x during the after-

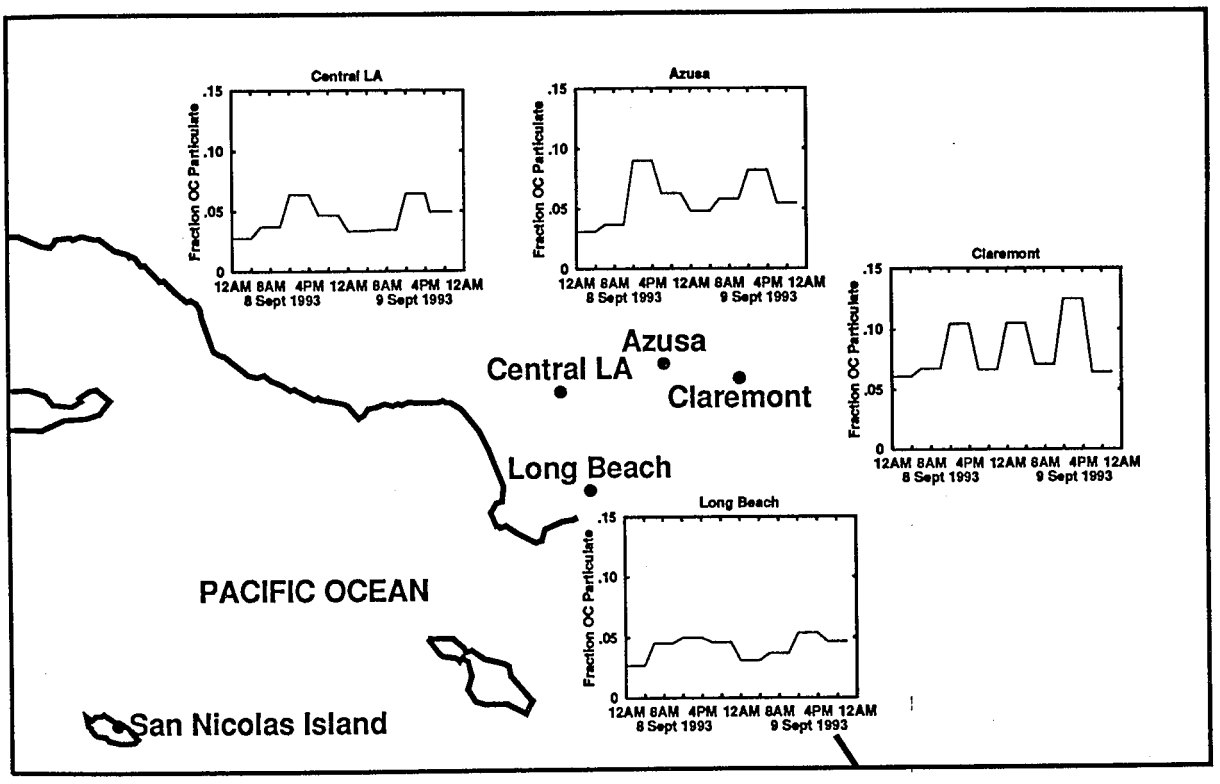

Figure 2.5:
Fraction organic carbon in the particle phase, measured as particulate organic carbon divided by the sum of total organics in the vapor phase plus particulate organic carbon.

noon air sampling period on the second day of this smog episode. That afternoon sample on the second day is dominated by the further reaction products of the oxidation of NO and NO_2, including aerosol nitrate, nitric acid and peroxyacyl nitrates. The secondary pollutants nitric acid and the peroxyacyl nitrates show the strong spatial and diurnal variations that are characteristic of photochemically-generated products.

The branching ratio between organic and inorganic nitrate was computed by taking the ratio of total organic nitrate (PAN+PPN) to total nitrate (PAN + PPN + HNO_3 + total particulate NO_3^-). Total particulate nitrate and ammonium measurements made using Teflon filters were adjusted for losses due to volatilization of fine particle NH_4NO_3 during sampling by first computing the difference between NO_3^- collected on fine particle nylon filters located downstream of a MgO coated diffusion denuder versus NO_3^- collected on fine particle Teflon filters and then adding a stiochiometrically equivalent ammount of both NH_4^+ and NO_3^- to the samples collected on all Teflon filters. As seen in Figure 2.7, the fraction of total nitrates that consists of PAN plus PPN averages 14.8% at Long Beach, 9.6% at Central Los Angeles, and 12.3% at Azusa, with higher values averaging 33.6% in Claremont. The absolute values of the nitric acid levels measured in Claremont in this study (range 0.9 to 24.9 ppb) are similar to levels observed in the area by previous studies [80,96-99]. However, the peroxyacyl nitrate levels during the Sept. 8-9, 1993, experiment are substantially lower than have been seen in earlier years during such smog episodes, thus yielding relatively low ratios of organic nitrates to total nitrate. During a study from 1989 to 1991, Grosjean and Bytnerowicz [99] found roughly equal levels of organic nitrate and inorganic nitrate at Tanbark Flats during the day (0600-1800 hours PDT). In Claremont during 1980, Grosjean [96] reported PAN / (PAN + inorganic NO_3^-) ratios that range

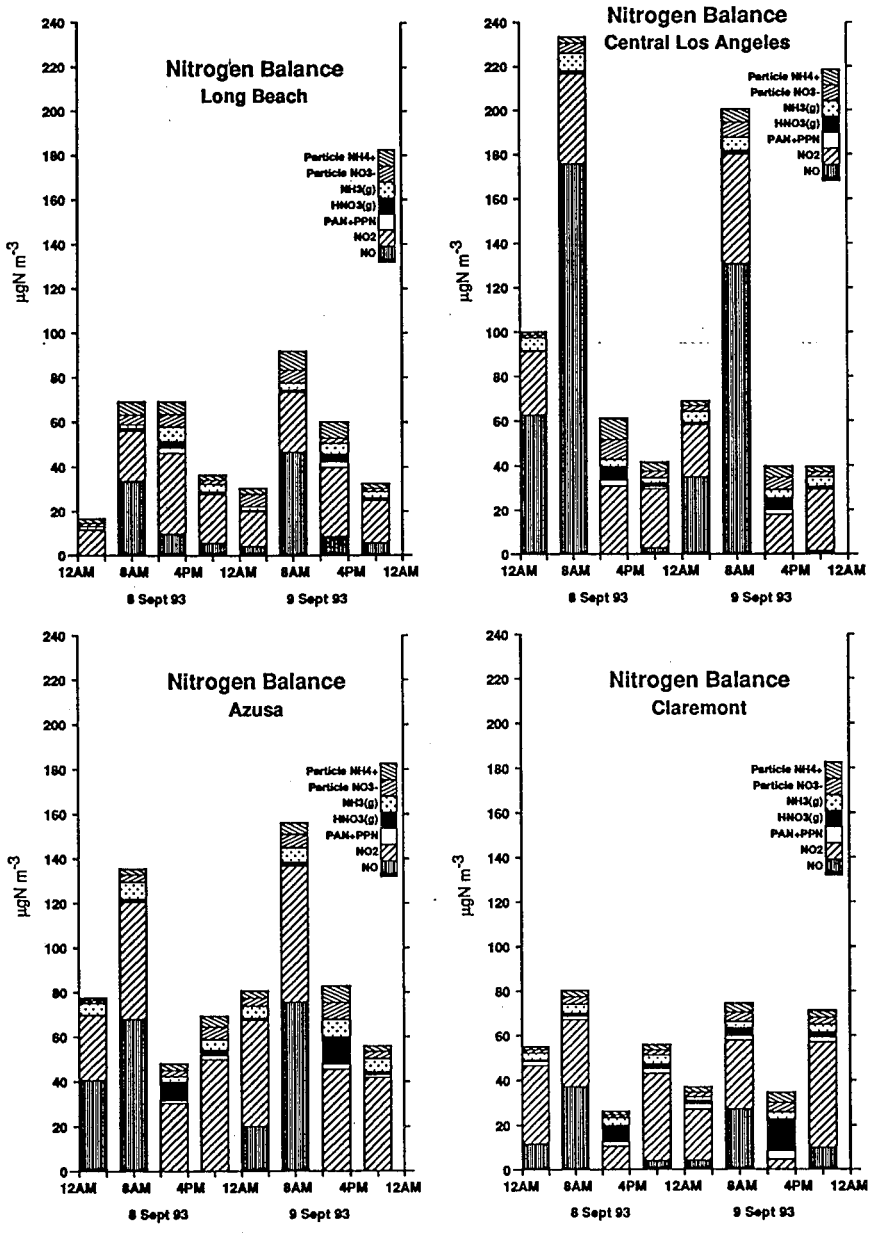

Figure 2.6:
Nitrogen-containing pollutant balance.

from 0.52 to 0.80 during the afternoon photochemical smog period. Data from the present study indicate a reduction in peroxyacyl nitrates compared to inorganic forms of nitrate, a result that could be due either to the very high temperature during the episode studied here or to the continued emphasis on ozone control strategies that are predicated on reduction of organic precursor pollutants.

The fraction of nitrogen-containing air pollutants present in the particle phase is shown in Figure 2.8. The relatively high fraction of the nitrogen found in the particle phase at Long Beach is due to coarse particle nitrates, that are probably formed by reaction between HNO_3 vapor and sea salt from the marine environment [82,100-103]. The highest fractions of pollutant-derived nitrogen in the particle phase are found during the afternoon sampling periods at Central Los Angeles on both days and in Claremont on the second day with peak particulate N fractions in the range 23.5 to 27.4%. The trends in secondary nitrate aerosol formation loosely track those of organic carbon in the particle phase.

2.2.3 Chlorine-Containing Air Pollutants

The sources of chlorine-containing pollutant emissions to the Southern California atmosphere include chlorofluorocarbons, volatile organic compounds containing chlorine from dry cleaning solvents and industrial degreasers [69,70], plus inorganic chloride from sea spray, wood burning, construction dust, motor vehicle exhaust, and geological sources [75]. Gas phase hydrochloric acid release to the atmosphere in Southern California has been linked to reactions of sea salt with NO_2 or HNO_3 [82,102-104]. To obtain a regional perspective on the distribution of chlorine between particle-phase chloride and gas-phase hydrochloric acid and chlorinated organics, the ratio of particulate chloride to

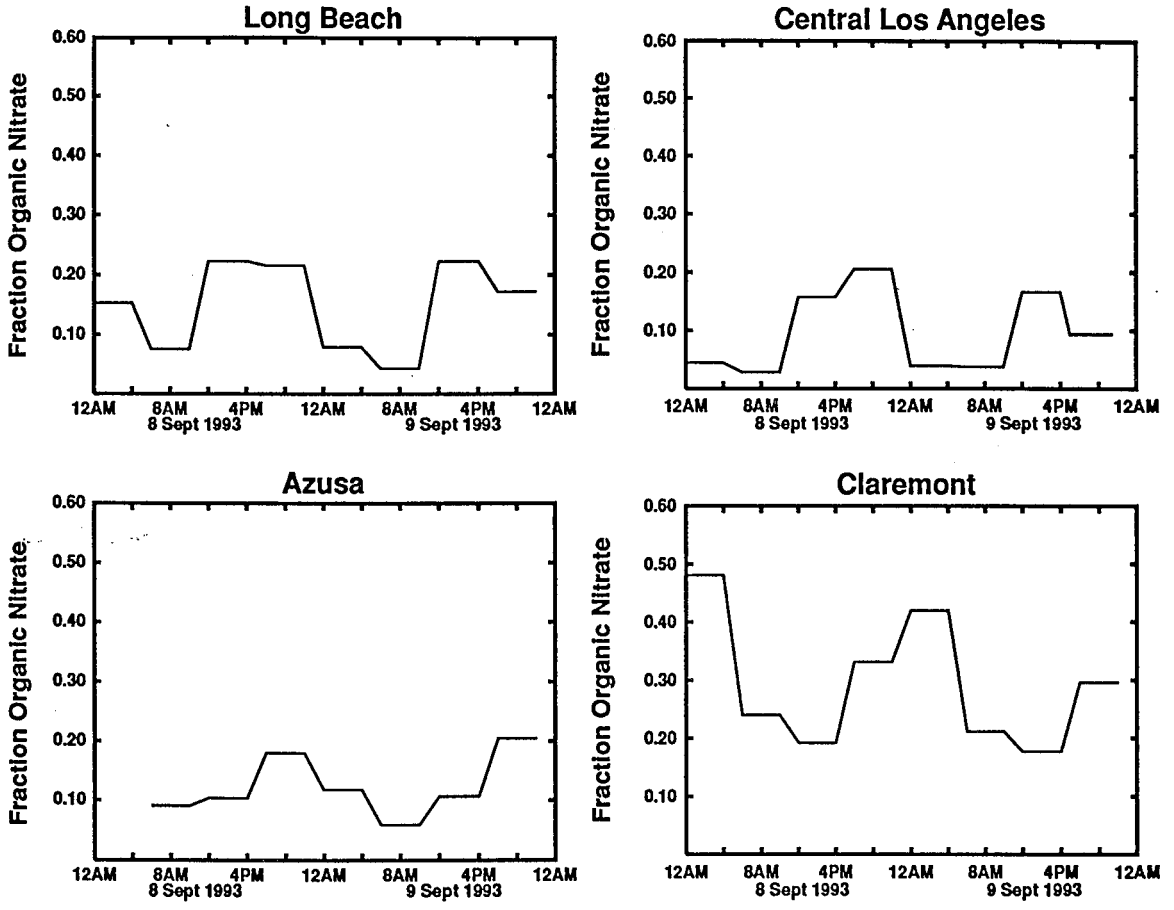

Figure 2.7:
Fraction organic nitrate measured as (PAN+PPN)/(PAN + PPN + particulate NO_3^- + HNO_3).

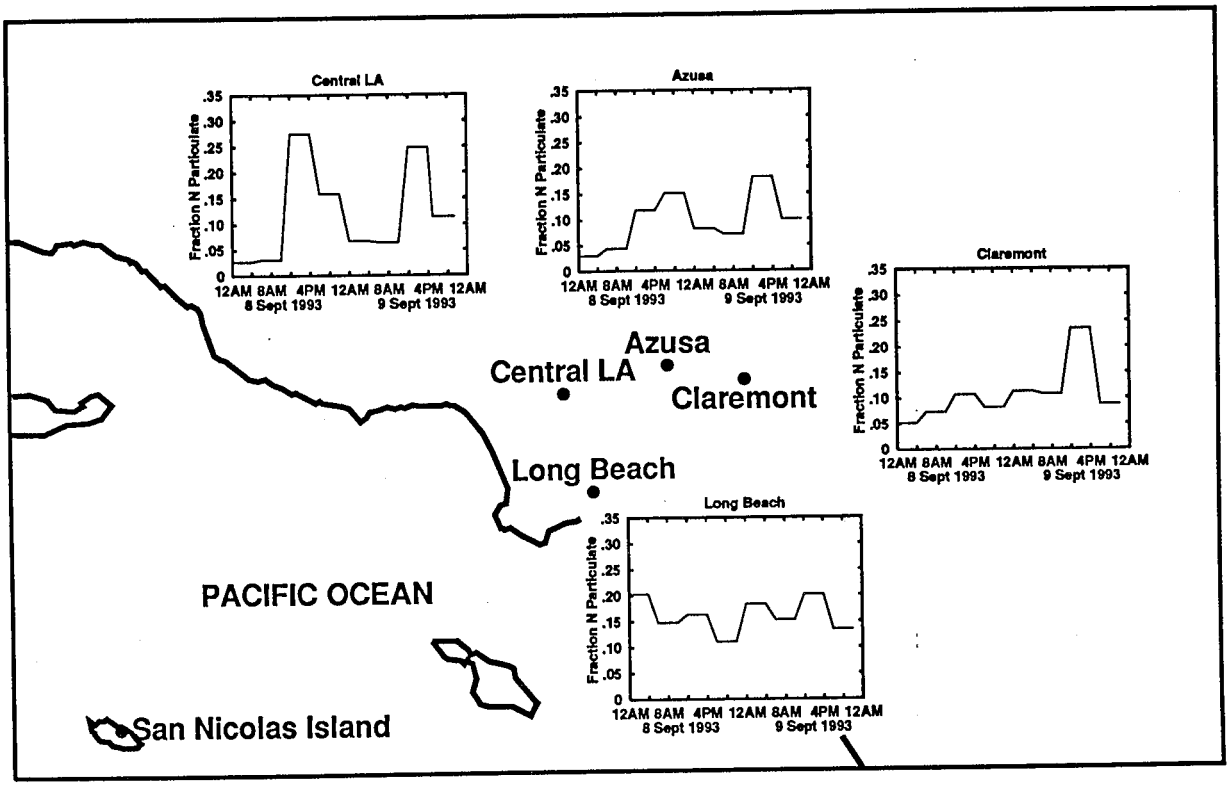

Figure 2.8:
Fraction nitrogen-containing pollutants present in the particle phase. Total particulate NO_3^- and NH_4^+ corrected for volatilization of NH_4NO_3 by comparison of nitrate data collected on fine particle nylon versus fine particle Teflon filters.

total chloride plus chlorine (total Cl) was calculated. As before, calculations were preceeded by converting all pollutant concentrations to an equivalent μg Cl m^{-3} basis. Particulate Cl^- was taken from total particle Teflon filters, except in cases where this value was below the detection limit of approximately 0.5 μg m^{-3}, in which case the fine particle nylon filter Cl^- was used which has a lower detection limit of approximately 0.25 μg m^{-3}. Hydrochloric acid concentrations were measured by the denuder difference method employing nylon filters (see reference 82); chlorine-containing organic compounds were measured by GC/ECD and GC/MS.

At Long Beach the fraction of Cl accounted for by organic compounds varied from 77% to 95% between sampling periods. As seen in Figure 2.9, the fraction of Cl in the particle phase at Long Beach shows behavior strikingly different from the fraction particulate organic carbon and fraction particulate nitrogen. The fraction particulate Cl at Long Beach shows a minimum in the afternoon, reflecting depletion by the reaction of sea salt with HNO_3 and NO_2 to form gas-phase hydrochloric acid during the peak photochemical smog period. This same behavior is seen at Central Los Angeles, where the particulate Cl concentration during the afternoon sample of the second day is below detection (i.e., below 0.25 μg Cl m^{-3}). At the inland sites, total Cl is still dominated by organic Cl: less than 6% of the Cl is present in inorganic compounds at Azusa, and less than 10% at Claremont. At Azusa, the fraction of the Cl in the particle phase is highest overnight, and again the data reflect loss of Cl from the particle phase during the photochemically active daytime periods. Little temporal variation in the fraction Cl in the particle phase is seen in Claremont; the fraction Cl in the particle phase is quite low at all times at Claremont suggesting that Claremont is located far enough inland that it consistently receives aerosol that has been transformed by exposure

to local photochemically-generated acid gases during this episode.

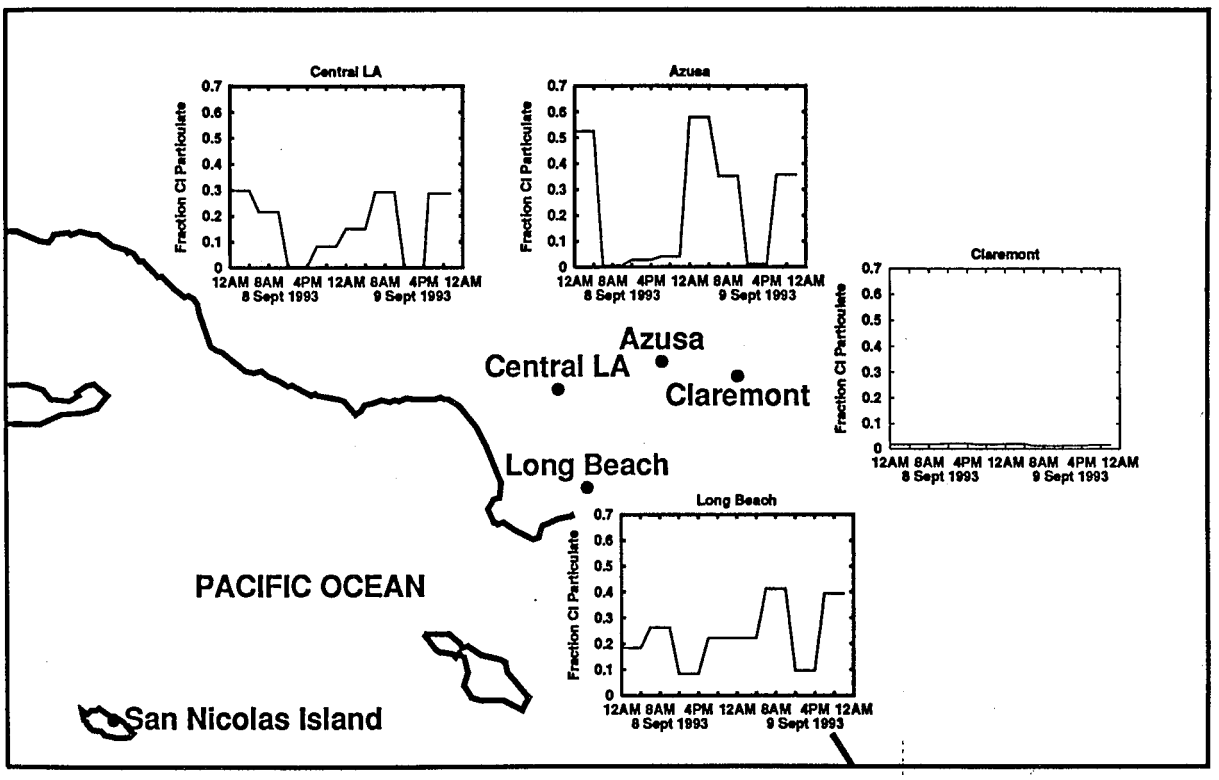

Figure 2.9:
Fraction particulate chloride measured as (particle Cl^-)/(particle Cl^- + HCl + volatile organic chlorine).

Bibliography

[1] A. J. Haagen-Smit. Chemistry and physiology of Los Angeles smog. *Industr. Engr. Chem.*, 44: 342-346, 1952.

[2] A. J. Haagen-Smit, C. E. Bradley and M. M. Fox. Ozone formation in photochemical oxidation of organic substances. *Industr. Engr. Chem.*, 45: 2086-2091, 1953.

[3] H. A. Gray, G. R. Cass, J. J. Huntzicker, E. K. Heyerdahl and J. A. Rau. Characterization of atmospheric organic and elemental carbon particle concentrations in Los Angeles. *Environ. Sci. Technol.*, 20: 580-589, 1986.

[4] W. F. Rogge, L. M. Hildemann, M. A. Mazurek, B. R. T. Simoneit and G. R. Cass. Quantification of urban organic aerosols at a molecular level: identification, abundance, and seasonal variation. *Atmos. Environ.*, 27A: 1309-1330, 1993.

[5] S. M. Larson and G. R. Cass. Characteristics of summer midday low-visability events in the Los Angeles area. *Environ. Sci. Technol.*, 23: 281-289, 1989.

[6] D. W. Dockery, C. A. Pope, X. Xu, J. D. Spengler, J.H. Ware, M. E. Fay, B. G. Ferris and F. E. Speizer. An association between air-pollution and mortality in Six United States cities. *N. Engl. J. Med.*, 329: 1753-1759, 1993.

[7] A. G. Russell and G. R. Cass. Verification of a mathematical-model for aerosol nitrate and nitric-acid formation and its use for control measure evaluation. *Atmos. Environ.*, 20: 2011-2025, 1986.

[8] C. Pilinis and J. H. Seinfeld. Continued development of a general equilibrium model for inorganic multicomponent atmospheric aerosols. *Atmos. Environ.*, 21: 2453-2466, 1987.

[9] C. Pilinis and J. H. Seinfeld. Development and evaluation of an Eularian photochemical gas-aerosol model. *Atmos. Environ.*, 22: 1985-2001, 1988.

[10] A. G. Russell, K. F. McCue and G. R. Cass. Mathematical modeling of the formation of nitrogen-containing air pollutants. 1. Evaluation of an Eularian photochemical model. *Environ. Sci. Technol.*, 22: 263-271, 1988.

[11] S. N. Pandis, R. A. Harley, G. R. Cass and J. H. Seinfeld. Secondary organic aerosol formation and transport. *Atmos. Environ.*, 26A: 2269-2282, 1992.

[12] S. N. Pandis, A. S. Wexler and J. H. Seinfeld. Secondary organic aerosol formation and transport-II. Predicting the ambient secondary organic aerosol size distribution. *Atmos. Environ.*, 27A: 2403-2416, 1993.

[13] W. F. Rogge, L. M. Hildemann, M. A. Mazurek, B. R. T. Simoneit and G. R. Cass. Mathematical modeling of atmospheric fine particle-associated primary organic compound concentrations. *J. Geophys. Res.*, 101: 19379-19394, 1996.

[14] G. J. McRae, W. R. Goodin and J. H. Seinfeld. Development of a second generation mathematical-model for urban air-pollution. 1. Model formulation. *Atmos. Environ.*, 16: 679-696, 1982.

[15] G. J. McRae and J. H. Seinfeld. Development of a second generation mathematical-model for urban air-pollution. 2. Model performance. *Atmos. Environ.*, 17: 501-522, 1983.

[16] S. Sillman, J. A. Logan and S. C. Wofsy. The sensitivity of ozone to nitrogen oxides and hydrocarbons in regional ozone formation. *J. Geophys. Res.*, 95: 1837-1851, 1990.

[17] R. A. Harley, A. G. Russell. G. J. McRae, G. R. Cass and J. H. Seinfeld. Photochemical modeling of the Southern California Air Quality Study. *Environ. Sci. Technol.*, 27: 378-388, 1993.

[18] R. A. Harley and G. R. Cass. Modeling the concentrations of gas-phase toxic organic air pollutants: direct emissions and atmospheric formation. *Environ. Sci. Technol.*, 28: 88-98, 1994.

[19] R. A. Harley and G. R. Cass. Modeling the atmospheric concentrations of individual volatile organic compounds. *Atmos. Environ.*, 29: 905-922, 1995.

[20] R. E. Neligan. Hydrocarbons in the Los Angeles atmosphere. *Arch. Environ. Health*, 5: 581-591, 1962.

[21] A. P. Altshuller and T. A. Bellar. Gas chromatographic analysis of hydrocarbons in the Los Angeles atmosphere. *J. Air Pollut. Control Assoc.*, 13: 81-87, 1963.

[22] E. R. Stephens and F. R. Burleson. Analysis of the atmosphere for light hydrocarbons. *J. Air Pollut. Control Assoc.*, 17: 147-153, 1967.

[23] W. A. Lonneman, S. L. Kopczynski, P. E. Darley and F. D. Sutterfield. Hydrocarbon composition of urban air pollution. *Environ. Sci. Technol.*, 8: 229-236, 1974.

[24] J. G. Calvert. Hydrocarbon involvement in photochemical smog formation in Los Angeles atmosphere. *Environ. Sci. Technol.*, 10: 256-262, 1976.

[25] C. E. Feigley and H. E. Jeffries. Analysis of processes affecting oxidant and precursors in the Los Angeles Reactive Pollutant Program Operation 33. *Atmos. Environ.*, 13: 1369-1384, 1979.

[26] A. P. Altshuller, W. A. Lonneman, F. D. Sutterfield and S. L. Kopczynski. Hydrocarbon composition of the atmosphere of the Los Angeles basin-1967. *Environ. Sci. Technol.*, 5: 1009-1016, 1971.

[27] H. Mayrsohn and J. H. Crabtree Source reconciliation of atmospheric hydrocarbons. *Atmos. Environ.*, 10: 137-143, 1976.

[28] H. Mayrsohn, J. H. Crabtree, M. Kuramoto, R. D. Sothern and S. H. Mano. Source reconciliation of atmospheric hydrocarbons-1974. *Atmos. Environ.*, 11: 189-192, 1977.

[29] D. Grosjean and K. Fung. Hydrocarbons and carbonyls in Los Angeles air. *J. Air Pollut. Control Assoc.*, 34: 537-543, 1984.

[30] W. P. L. Carter. Development of ozone reactivity scales for volatile organic compounds. *J. Air Waste Manage. Assoc.*, 44: 881-899, 1994.

[31] F. M. Bowman, C. Pilinis and J. H. Seinfeld. Ozone and aerosol productivity of reactive organics. *Atmos. Environ.*, 29: 579-589, 1995.

[32] D. Grosjean and J. H. Seinfeld. Parameterization of the formation potential of secondary organic aerosols. *Atmos. Environ.*, 23: 1733-1747, 1989.

[33] M. S. Miller, S. K. Friedlander and G. M. Hidy. A chemical element balance for the Pasadena aerosol. *J. Colloid Interface Sci.*, 39: 165-176, 1972.

[34] G. M. Hidy, B. R. Appel, R. J. Charlson, W. E. Clark, S. K. Friedlander, D. H. Hutchison, T. B. Smith, J. Suder, J. J. Weslowski and K. T. Whitby. Summary of the California Aerosol Characterization Experiment. *J. Air Pollut. Control Assoc.*, 25: 1106-1114, 1975.

[35] R. H. Hammerle and W. R. Pierson. Sources and elemental composition of aerosol in Pasadena, Calif. by energy-dispersive X-ray fluorescence. *Environ. Sci. Technol.*. 9: 1058-1068, 1975.

[36] B. R. Appel, E. L. Kothny, E. M. Hoffer, G. M. Hidy, G.M. and J. J. Wesolowski. Sulfate and nitrate from the California Aerosol Characterization Experiment (ACHEX). *Environ. Sci. Technol.*, 12: 418-425, 1978.

[37] R. J. O'Brien, J. R. Holmes and A. H. Bockian. Formation of photochemical aerosol from hydrocarbons. *Environ. Sci. Technol.*, 9: 568-576, 1975.

[38] D. Schuetzle, D. Cronn, A. L. Crittenden and R. J. Charlson. Molecular composition of secondary aerosol and its possible origin. *Environ. Sci.*

Technol., 9: 838-845, 1975.

[39] D. R. Cronn, R. J. Charlson, R. L. Knights, A. L. Crittenden and B. R. Appel. A survey of the molecular nature of primary and secondary components of particles in urban air by high-resolution mass spectrometry. *Atmos. Environ.*, 11: 929-937, 1977.

[40] B. R. Appel, E. M. Hoffer, E. L. Kothny, S. M. Wall, M. Haik and R. L. Knights. Analysis of carbonaceous material in Southern California atmospheric aerosols. 2. *Environ. Sci. Technol.*, 13: 98-104, 1979.

[41] A. H. Miguel and S. K. Friedlander. Distribution of benzo[a]pyrene and coronene with respect to particle size in Pasadena aerosols in the submicron range. *Atmos. Environ.*, 12: 2407-2413, 1978.

[42] D. Grosjean. Polycyclic aromatic-hydrocarbons in Los Angeles air from samples collected on Teflon, glass and quartz filters. *Atmos. Environ.*, 17: 2565-2573, 1983.

[43] D. Grosjean, K. Van Cauwenberghe, J. P. Schmid, P. E. Kelley and J. N. Pitts. Identification of C3-C10 aliphatic dicarboxylic acids in airborne particulate matter. *Environ. Sci. Technol.*, 12: 313-317, 1978.

[44] R. J. Gordon and R. J. Bryan. Patterns in airborne polynuclear hydrocarbon concentrations at four Los Angeles sites. *Environ. Sci. Technol.*, 7: 1050-240, 1973.

[45] I. R. Kaplan and R. J. Gordon. Non-fossil-fuel fine-particle organic carbon aerosols in Southern California determined during the Los Angeles

Aerosol Characterization and Source Apportionment Study. *Aerosol Sci. Technol.*, 21: 343-359, 1994.

[46] L. M. Hildemann, D. B. Klinedinst, G. A. Klouda, L. A. Currie and G. R. Cass. Sources of urban contemporary carbon aerosol. *Environ. Sci. Technol.*, 28: 1565-1576, 1994.

[47] M. P. Hannigan, G. R. Cass, A. L. Lafleur, J. P. Longwell and W. R. Thilly. Bacterial mutagenicity of urban organic aerosol sources in comparison to atmospheric samples. *Environ. Sci. Technol.*, 28: 2014-2024, 1994.

[48] L. M. Hildemann, G. R. Markowski and G. R. Cass. Chemical composition of emissions from urban sources of fine organic aerosol. *Environ. Sci. Technol.*, 25: 744-759, 1991.

[49] W. F. Rogge. "Molecular tracers for sources of atmospheric carbon particles: Measurements and model predictions" Ph.D. Dissertation, California Institute of Technology, Pasadena, CA, 1993.

[50] W. F. Rogge, L. M. Hildemann, M. A. Mazurek, B. R. T. Simoneit and G. R. Cass. Sources of fine organic aerosol. 1. Charbroilers and meat cooking operations" *Environ. Sci. Technol.*, 25: 1112-1125. 1991,

[51] W. F. Rogge, L. M. Hildemann, M. A. Mazurek, B. R. T. Simoneit and G. R. Cass. Sources of fine organic aerosol. 2. Noncatalyst and catalyst-equipped automobiles and heavy-duty diesel trucks. *Environ. Sci. Technol.*, 27: 636-651, 1993.

[52] W. F. Rogge, L. M. Hildemann, M. A. Mazurek, B. R. T. Simoneit and G. R. Cass. Sources of fine organic aerosol. 3. Road dust, tire

debris, and organometallic break lining dust- roads as sources and sinks. *Environ. Sci. Technol.*, 27: 1892-1904, 1993.

[53] W. F. Rogge, L. M. Hildemann, M. A. Mazurek, B. R. T. Simoneit and G. R. Cass. Sources of fine organic aerosol. 4. Particulate abrasion products from leaf surfaces of urban plants. *Environ. Sci. Technol.*, 27: 2700-2711, 1993.

[54] W. F. Rogge, L. M. Hildemann, M. A. Mazurek, B. R. T. Simoneit and G. R. Cass. Sources of fine organic aerosol. 5. Natural gas home appliances. *Environ. Sci. Technol.*, 27: 2736-2744, 1993.

[55] W. F. Rogge, L. M. Hildemann, M. A. Mazurek, B. R. T. Simoneit and G. R. Cass. Sources of fine organic aerosol. 6. Cigarette smoke in the urban atmosphere. *Environ. Sci. Technol.*, 28: 1375-1388, 1994.

[56] H. A. Gray and G. R. Cass. Source Contributions to Atmospheric Fine Carbon Particle Concentrations. *submitted for publication in Atmos. Environ.*, 1997.

[57] J. J. Schauer, W. F. Rogge, L. M. Hildemann, M. A. Mazurek, G. R. Cass and B. R. T. Simoneit. "Source Apportionment of Airborne Particulate Matter Using Organic Compounds as Tracers" *Atmos. Environ.*, 30: 3837-3855, 1996.

[58] P. A. Solomon, T. Fall, L. G. Salmon, G. R. Cass, H. A. Gray and A. Davidson. Chemical characteristics of PM10 aerosols collected in the Los Angeles area. *J. Air Pollut. Control Assoc.*, 39: 154-163, 1989.

[59] D. R. Lawson. "The Southern California Air Quality Study" *J. Air Waste Manage. Assoc.*, 40: 156-165, 1990.

[60] P. H. McMurry and X. G. Zhang. Size distributions of ambient organic and elemental carbon. *Aerosol Sci. Technol.*, 10: 430-437, 1989.

[61] T. Pickle, D. T. Allen and S. E. Pratsinis. Sources and size distributions of aliphatic and carbonyl carbon in Los Angeles aerosol. *Atmos. Environ.*, 24: 2221-2228, 1990.

[62] G. T. Wolff, M. S. Ruthkosky, D. P. Stroup and P. E. Korsog. A characterization of the principal PM10 species in Claremont (summer) and Long Beach (fall) during SCAQS. *Atmos. Environ.*, 25A: 2173-2186, 1991.

[63] D. T. Mylonas, D. T. Allen, S. H. Ehrman and S. E. Pratsinis. The sources and size distributions of organonitrates in the Los Angeles aerosol. *Atmos. Environ.*, 25A: 2855-2861, 1991.

[64] B. J. Turpin, J. J. Huntzicker, S. M. Larson and G. R. Cass. Los Angeles summer midday particulate carbon: primary and secondary aerosol. *Environ. Sci. Technol.*, 25: 1788-1793, 1991.

[65] J. C. Chow, J. G. Watson, E. M. Fujita, Z. Lu, D. R. Lawson and L. L. Ashbaugh. Temporal and spatial variations of PM2.5 and PM10 aerosol in the Southern California Air Quality Study. *Atmos. Environ.*, 28: 2061-2080, 1994.

[66] A. Eldering, G. R. Cass and K. C. Moon. An air monitoring network using continuous particle size distribution monitors: connecting pollutant properties to visibility via Mie scattering calculations. *Atmos. Environ.*, 28: 2733-2749, 1994.

[67] R. A. Rasmussen. SCAQS hydrocarbon collection and analyses (Part I). Report to the California Air Resources Board under contract A6-179-32, Biospherics Research Corp., Hillsboro, OR, 1990.

[68] F. W. Lurmann and H. H. Main. Analysis of the ambient VOC data collected in the Southern California Air Quality Study. Sonoma Technology, Inc., Santa Rosa, CA. Report to the California Air Resources Board under contract A832-130, 1992.

[69] R. A. Harley, M. P. Hannigan and G. R. Cass. Respeciation of organic gas emissions and the detection of excess unburned gasoline in the atmosphere. *Environ. Sci. Technol.*, 26: 2395-2408, 1992.

[70] E. M. Fujita, J. G. Watson, J. C. Chow and Z. Lu. Validation of the chemical mass balance receptor model applied to hydrocarbon source apportionment in the Southern California Air Quality Study. *Environ. Sci. Technol.*, 28: 1633-1649, 1994.

[71] J. G. Watson, J. C. Chow, Z. Lu, E. M. Fujita, D. H. Lowenthal, D. R. Lawson and L. L. Ashbaugh. Chemical mass balance source apportionment of PM10 during the Southern California Air Quality Study. *Aerosol Sci. Technol.*, 16: 1487-1500, 1994.

[72] B. J. Turpin and J. J. Huntzicker. Secondary formation of organic aerosol in the Los Angeles basin: a descriptive analysis of organic and elemental carbon concentrations. *Atmos. Environ.*, 25A: 207-215, 1991.

[73] W. John and G. Reischl. A cyclone for size-selective sampling of ambient air. *J. Air Pollut. Control Assoc.*, 30: 872-876, 1980.

[74] J. J. Huntzicker, R. L. Johnson, J. J. Shah and R. A. Cary. Analysis of organic and elemental carbon in ambient aerosols by a thermal-optical method" In *Particulate Carbon: Atmospheric Life Cycle*, G. T. Wolff and R. L. Klimisch Eds.; Plenum, New York, 1982.

[75] R. Cary. Speciation of aerosol carbon using the thermo-optical method, presented at the Third International Conference on Carbonaceous Particles in the Atmosphere, Berkeley, CA. 1987.

[76] B. R. Appel, S. M. Wall, Y. Tokiwa and M. Haik. Simultaneous nitric acid, particulate nitrate and acidity measurements in ambient air. *Atmos. Environ.*, 14: 549-554, 1980.

[77] C. W. Spicer, J. E. Howes, T. A. Bishop, L. H. Arnold and R. K. Stevens. Nitric acid measurement methods: an intercomparison. *Atmos. Environ.*, 16: 1487-1500, 1982.

[78] J. Forrest, D. J. Spandau, R. L. Tanner and L. Newman. Determination of atmospheric nitrate and nitric acid employing a diffusion denuder with a filter pack. *Atmos. Environ.*, 16: 1473-1485, 1982.

[79] R. W. Shaw, R. K. Stevens, J. Bowermaster, J. W. Tesch and E. Tew. Measurements of atmospheric nitrate and nitric acid: the denuder difference experiment. *Atmos. Environ.*, 16: 845-853, 1982.

[80] S. V. Hering *et al.* The nitric acid shootout: field comparision of measurement methods. *Atmos. Environ.*, 22: 1519-1539, 1988.

[81] P. A. Solomon, S. M. Larson, T. Fall and G. R. Cass. Basinwide nitric acid and related species concentrations observed during the Claremont

Nitrogen Species Comparision Study. *Atmos. Environ.*, 22: 1587-1594, 1988.

[82] A. Eldering, P. A. Solomon, L. G. Salmon, T. Fall and G. R. Cass. Hydrochloric acid: a regional perspective on concentrations and formation in the atmosphere of Southern California. *Atmos. Environ.*, 25A: 2091-2102, 1991.

[83] W. T. Bolleter, C. J. Bushman and P. W. Tidwell. Spectrophotometric determinations of ammonium as indophenol. *Anal. Chem.*, 33: 592-594, 1961.

[84] P. A. Solomon, J. L. Moyers and R. A. Fletcher. High-volume dichotomous virtual impactor for the fractionation and collection of particles according to aerodynamic size. *Aerosol Sci. Technol.*, 2: 455-464, 1983.

[85] M. A. Mazurek, B. R. T. Simoneit, G. R. Cass and H. A. Gray. Quantitative high-resolution gas chromatography and high-resolution gas chromatography/mass spectrometry analyses of carbonaceous fine aerosol particles. *Inter. J. Environ. Anal. Chem.*, 29: 119-139, 1987.

[86] K. E. Thrane and A. Mikalsen. High-volume sampling of airborne polycyclic aromatic hydrocarbons using glass fibre filters and polyurethane foam. *Atmos. Environ.*, 15: 909-918, 1981.

[87] C. D. Keller and T. F. Bidleman. Collection of airborne polycyclic aromatic hydrocarbons ond other organics with a glas fiber filter-polyurethane foam system. *Atmos. Environ.*, 18: 837-845, 1984.

[88] *Method for the determination of non-methane organic compounds in ambient air using cryogenic preconcentration and direct flame ioniza-*

tion detection, EPA-600/4-89-018. U.S. Environmental Protection Agency: Research Triangle Park, NC, 1988.

[89] E. Grosjean, D. Grosjean, M. P. Fraser and G. R. Cass. Air Quality Model Evaluation Data for Organics. 2. C_1 - C_{14} Carbonyls in Los Angeles Air. *Environ. Sci. Technol.*, 30: 2687-2703, 1996.

[90] E. Grosjean, D. Grosjean, M. P. Fraser and G. R. Cass. An Air Quality Model Evaluation Data Set for Organics. 3. Peroxyacetyl nitrate and peroxypropionyl nitrate in Los Angeles Air. *Environ. Sci. Technol.*, 30: 2704-2714, 1996.

[91] D. Wolfe, B. Weber, D. Wuertz, D. Welsh, D. Merritt, S. King, R. Fritz, K. Moran, M. Simon, A. Simon, J. Cogan, D. Littell and E. Measure. An overview of the Mobile Profiler System: preliminary results from field tests during the Los Angeles Free-Radical Study. *Bull. Amer. Meteor. Soc.*, 76: 523-534, 1995.

[92] S. K. Friedlander. Chemical element balances and identification of air pollution sources. *Environ. Sci. Technol.*, 7: 235-240, 1973.

[93] B. R. Appel, P. Colodny and J. J. Wesolowski. Analysis of carbonaceous materials in Southern California atmospheric aerosols. *Environ. Sci. Technol.*, 10: 359-363, 1976.

[94] National Research Council *Ozone and other photochemical oxidants*, National Academy Press: Washington DC, 1977.

[95] D. Grosjean and S. K. Friedlander. Gas-particle distribution factors for organic and other pollutants in the Los Angeles atmosphere. *J. Air Pollut. Control Assoc.*, 25: 1038-1044, 1975.

[96] D. Grosjean. Distribution of atmospheric nitrogenous pollutants at a Los-Angeles area smog receptor site. *Environ. Sci. Technol.*, 17: 13-19, 1983.

[97] A. G. Russell and G. R. Cass. Acquisition of regional air quality model validation data for nitrate, sulfate, ammonium ion and their precursors. *Atmos. Environ.*, 18: 1815-1827, 1984.

[98] P. A. Solomon, L. G. Salmon, T. Fall and G. R. Cass. Spatial and temporal distribution of atmospheric nitric acid and particulate nitrate concentrations in the Los Angeles area. *Environ. Sci. Technol.*, 26: 1594-1601, 1992.

[99] D. Grosjean and A. Bytnerowicz. Nitrogenous air pollutants at a Southern California mountain forest smog receptor site. *Atmos. Environ.*, 27A: 483-492, 1993.

[100] W. D. Green. Maritime and mixed maritime-continental aerosols along the coast of Southern California. *J. Geophys. Res.*, 77: 5152-5160, 1972.

[101] C. S. Martens, J. J. Wesolowski, R. C. Harriss and R. Kaifer. Chlorine loss from Puerto Rican and San Francisco Bay Area marine aerosols. *J. Geophys. Res.*, 78: 8778-8791, 1973.

[102] S. M. Wall, W. John and J. L. Ondo. Measurement of aerosol size distributions for nitrate and major ionic species. *Atmos. Environ.*, 22: 1649-1656, 1988.

[103] W. John, S. M. Wall and J. L. Ondo. A new method for nitric-acid and nitrate aerosol measurement using the dichotomous sampler. *Atmos.*

Environ., 22: 1627-1635, 1988.

[104] B. R. Appel, Y. Tokiwa, V. Povard and E. L. Kothny. The measurement of atmospheric hydrochloric-acid in Southern California. *Atmos. Environ.*, 25A: 525-527, 1991.

3 Carbonyl Compounds and Peroxyacyl Nitrates in Los Angeles Air

3.1 Introduction

Carbonyl compounds and peroxyacyl nitrates are important atmospheric contaminants present in photochemical smog. As products of the oxidation of volatile organic compounds in photochemical smog [1], they provide important benchmarks against which the predictions of mathematical models describing atmospheric chemistry can be verified. Primary emissions of carbonyl compounds to the atmosphere undergo photolysis reactions leading to radical production and ozone formation [2]. Both carbonyl compounds and peroxyacyl nitrates are recognized as eye irratants, and several carbonyl compounds are believed to be toxic air contaminants [3]. First identified in photochemical smog in Southern California [4], peroxyacetyl nitrate ($CH_3C(O)OONO_2$ or PAN) and peroxypropionyl nitrate ($CH_3CH_2C(O)OONO_2$ or PPN) are known to be secondary products of the reactions of organic gases with the oxides of nitrogen (NO_x). PAN is an eye irritant, a plant toxicant, and may be mutagenic or carcinogenic [5-11]. Since PAN and PPN are formed directly from nitrogen dioxide and organic radical species, they also act as important indicators of the accuracy of the organic chemistry included in urban airshed models.

As part of the larger effort designed to collect a comprehensive set of data

on the concentrations of organic air pollutants present in photochemical smog [12], the ambient concentrations of 23 carbonyls and two peroxyacyl nitrates have been measured in the Southern California atmosphere during a severe photochemical smog event. Carbonyl concentrations were measured at five sites in and around Los Angeles during a two day smog episode. Ambient concentrations of peroxyacyl nitrates were measured over a two week period at four urban Southern California sites. These data first will be used to describe the nature and extent of carbonyl and PAN-like air pollutants in Southern California. In a later section of this thesis, these data will be used to evaluate the performance of a comprehensive photochemical airshed model for organic air pollutants.

3.2 Experimental Methods

A detailed description of the methods used to determine the ambient concentrations of carbonyl compounds and peroxyacyl nitrates are described elsewhere [13-14], and will be briefly summarized here.

3.2.1 Carbonyl Compounds

Sampling for carbonyl compounds employed collection on 2,4-dinitrophenylhydrazine (DNPH) impregnated cartridges. Carbonyl compounds undergo a selective reaction with the DNPH to form a corresponding dinitrophenylhydrazone, a stable, non-volatile product which binds the carbonyl for later analysis. Ambient samplers used C_{18} cartridges (SepPak cartridges, Millipore Corp.) coated with a solution of purified DNPH in acetonitrile. These cartridges were allowed to dry in carbonyl-free air before being sealed with Teflon tape, placed in solvent-washed aluminum foil and sealed in glass jars.

At the sampling sites, cartridges were loaded into ambient samplers which

used calibrated flowmeters and vacuum gauges to measure the airflow over the DNPH cartridges. Ambient air was drawn directly into the cartridges to prevent loss of carbonyl compounds to inlet lines. After each four-hour sampling period, the DNPH cartridges were resealed with Teflon tape, wrapped in clean aluminum foil, and returned to the laboratory where they were placed in freezers at -21°C until analysis. The cartridges were extracted with 2 mL of HPLC-grade acetonitrile; compounds were separated by liquid chromatography and analyzed by ultraviolet-visible spectrometry and mass spectrometry.

Hydrazone compounds were identified by preparing reference standards from authentic carbonyl compounds and purified DNPH. These same reference standards were used to construct calibration curves describing absorbance relative to hydrazone concentration. The calibration curves showed a linear relationship between absorbance and concentration for all hydrazones studied except glyoxal. For glyoxal, a polynomial fit to the calibration curve was used. The concentration of hydrazone in solution was used to calculate ambient concentrations of the corresponding carbonyl compound using the volume of air sampled as measured by the sampler flowmeter and the volume of acetonitrile used for extraction.

Carbonyl concentrations were measured at five sites in the Los Angeles area: four urban sites and one background site upwind of urban Southern California. San Nicolas Island, located approximately 100 km south and west of the Southern California coastline, was chosen as a background site because typical summer weather patterns draw air from the near-coastal Pacific Ocean and advect these air parcels to the east across urban Southern California. The urban air sampling sites chosen included Long Beach, Central Los Angeles, Azusa and Claremont. The different sites are affected

by primary emissions from industrial sources (Long Beach), vehicle sources (Central Los Angeles), as well as transport of primary emissions to downwind smog receptor sites (Azusa and Claremont) characterized by high concentrations of the products of atmospheric chemical reactions. At the four urban sites, four-hour integrated samples were collected every six hours over the two day smog episode that occurred on Sept. 8-9, 1993. The sampling periods were chosen to represent air quality characteristic of different times of the day. For example, one sampling period from 0600 hours PDT to 1000 hours PDT was selected to capture air that is enriched in the primary emissions from the morning traffic peak, while afternoon samples collected from 1200 hours PDT to 1600 hours PDT were scheduled to observe peak levels of afternoon photochemical smog formation. At the offshore site with lower levels of atmospheric pollutants, sampling periods of upto 11-hours duration were used to collect enough organic material for detection and analysis of carbonyl compounds.

3.2.2 Peroxyacyl Nitrates

The concentrations of the peroxyacyl nitrates PAN and PPN were measured at the four urban sites from Aug. 29 to Sept. 13, 1993, at Long Beach, from Aug. 30 to Sept. 11, 1993, at Central Los Angeles, from Aug. 28 to Sept. 13, 1993, at Azusa and from Sept. 1-11, 1993, at Claremont. While PAN is of interest because it is a global reservoir for radical species and NO_x [15], this study of photochemical smog formation focused on the regional formation of peroxyacyl nitrates across urban Southern California. The ambient concentrations of PAN and PPN were measured every 30 minutes during the period of study by electron capture gas chromatography (EC-GC) [14]. Ambient air was continuously pumped through the input line into the sampling loop

inside the GC, and injected onto the GC column every 30 minutes.

The response of the EC-GC system to peroxyacyl nitrates was quantified using authentic standard compounds synthesized in the liquid phase. The liquid standard solutions were stored in diffusion vials, and the output of these vials was used in combination with dilution air to calibrate the EC-GC instruments. Calibration of the EC-GC also employed chemiluminescent NO_x monitors in which a surface converter is used to reduce organic forms of nitrate to NO, followed by measurement of the quantity of NO produced.

During sampling, verification of the GC column flow rates, detector attenuation, and GC temperature controls assured the quality of the data collected. At the Claremont and Central Los Angeles sites, data from the pre-study and post-study calibrations were in good agreement. At Long Beach and Azusa, the pre-study and post-study calibrations showed some change in the response of the instruments during the study, resulting in a need to correct the data collected. At Long Beach, the pre-study and post-study calibration curves were averaged to give a mean response curve. At Azusa, a colocated PAN analyzer was used adjust the calibration slopes during the study. More details are available elsewhere [14] describing the calibration of the EC-GC instruments.

3.3 Results

3.3.1 Carbonyls

Twenty-three different carbonyl compounds were identified in samples collected during this sampling program. These included the C_1 to C_{14} n-aliphatic aldehydes; the ketones acetone, 2-butanone, and cyclohexanone; the unsaturated aldehyde crotonaldehyde; the dicarbonyls glyoxal, methylglyoxal and 2,3-butanedione; and the aromatic aldehydes benzaldehyde and

m-tolualdehyde.

Total carbonyl concentrations measured in this study average 17.9 ppbV at the four urban sites, and 3.5 ppbV at San Nicolas Island, indicating that elevated carbonyl concentrations are characteristic of urban air pollution. Of the four urban sites, average total carbonyl concentrations were 11.8 ppbV at Long Beach, 15.7 ppbV at Central Los Angeles, 26.8 ppbV at Azusa, and 17.1 ppbV at Claremont. The fact that highest concentrations are seen at Azusa results from the superposition of the two sources of carbonyl compounds in the atmosphere, direct emissions from primary sources and secondary formation via atmospheric chemistry; both are important at Azusa while the peak concentrations are not seen at the Central Los Angeles site (center of primary emissions in the Southern California region) or at Claremont (furthest downwind site characterized by the highest concentrations of secondary products, including ozone and PAN). When the total carbonyl concentrations are averaged over all sites at any given time, the results show 15.5 ppbV of total carbonyls from 0000 hours PDT to 0400 hours PDT, 20.8 ppbV from 0600 hours to 1000 hours PDT, 19.8 ppbV of total carbonyls from 1200 hours to 1600 hours PDT and 15.3 ppbV from 1800 hours PDT to 2200 hours PDT. This suggests that both primary emissions and secondary formation are important since there is no obvious increase in concentrations between the time of the morning traffic peak and the time of the afternoon photochemical smog peak.

Figures 3.1 - 3.3 show time series plots of formaldehyde, acetaldehyde and acetone, respectively, at the four urban sites. These three carbonyl compounds are present at the highest levels of any of the other measured carbonyl compounds, and account for an average of 24%, 18% and 7%, respectively, of the total carbonyl compound concentrations (on a volume basis) mea-

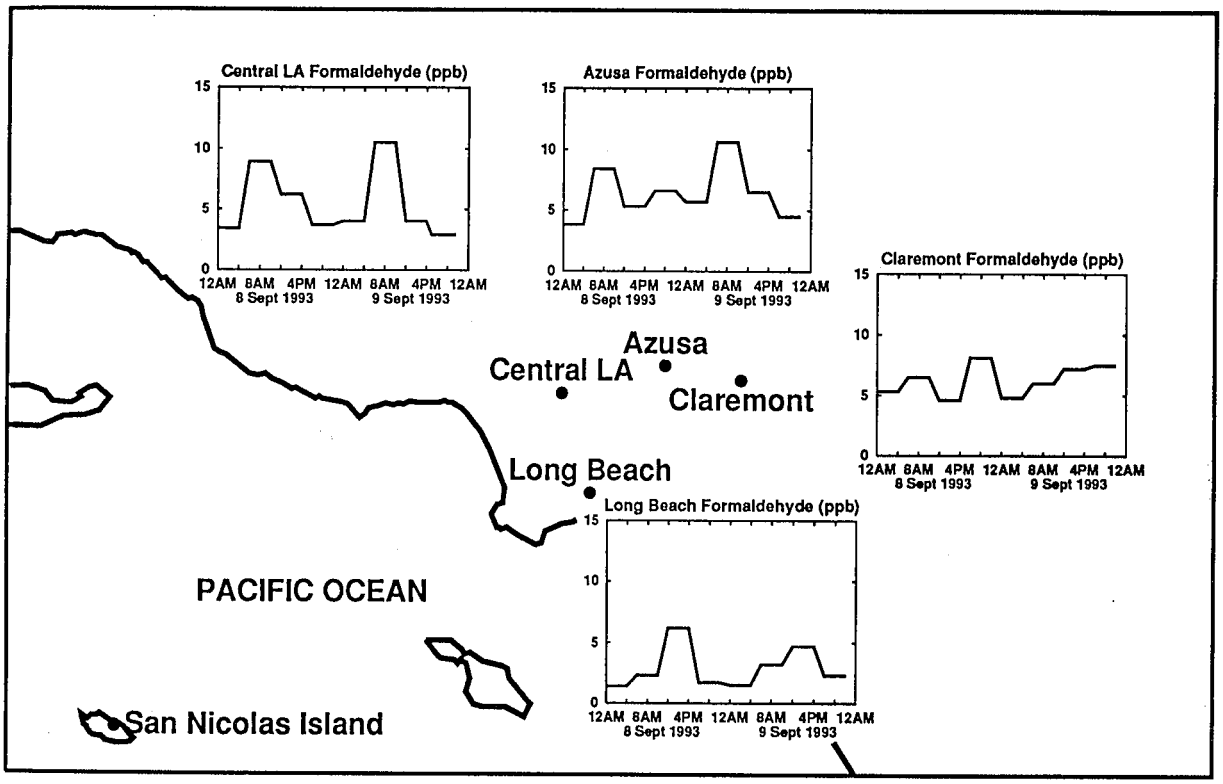

Figure 3.1:
Ambient concentrations of formaldehyde measured in Southern California Sept. 8-9, 1993.

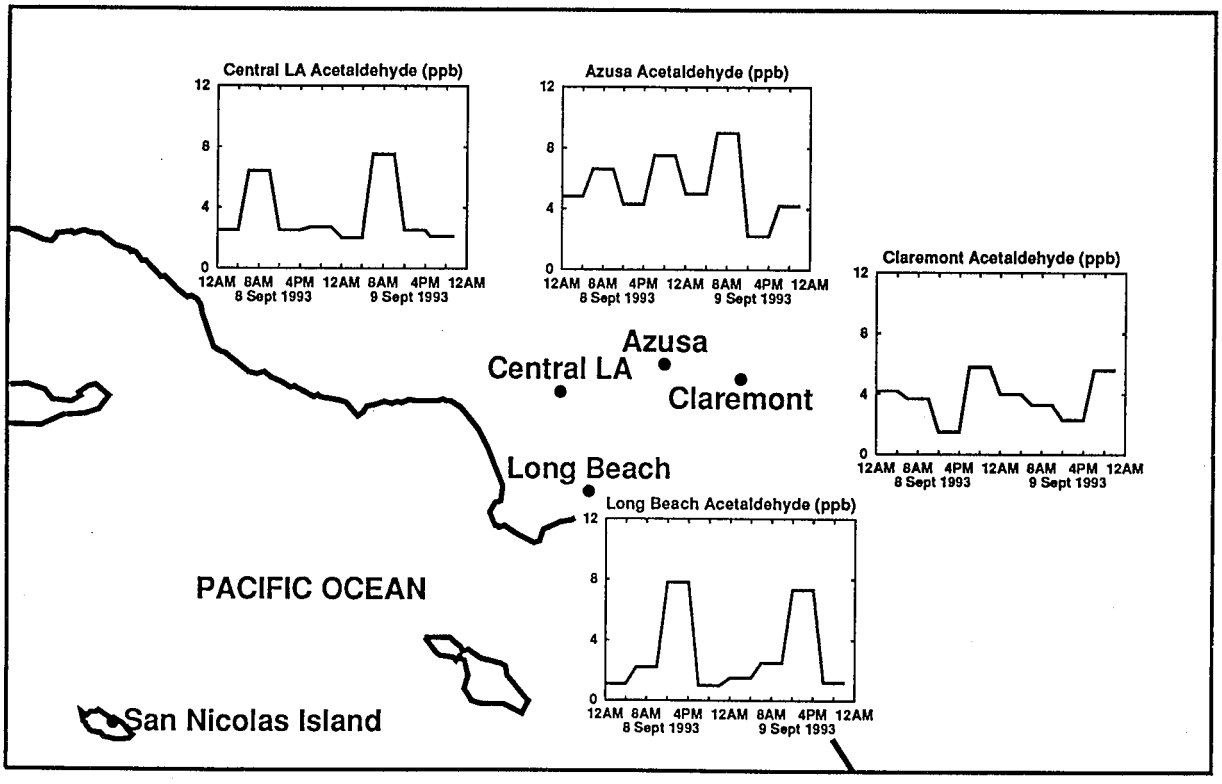

Figure 3.2:
Ambient concentrations of acetaldehyde measured in Southern California Sept. 8-9, 1993.

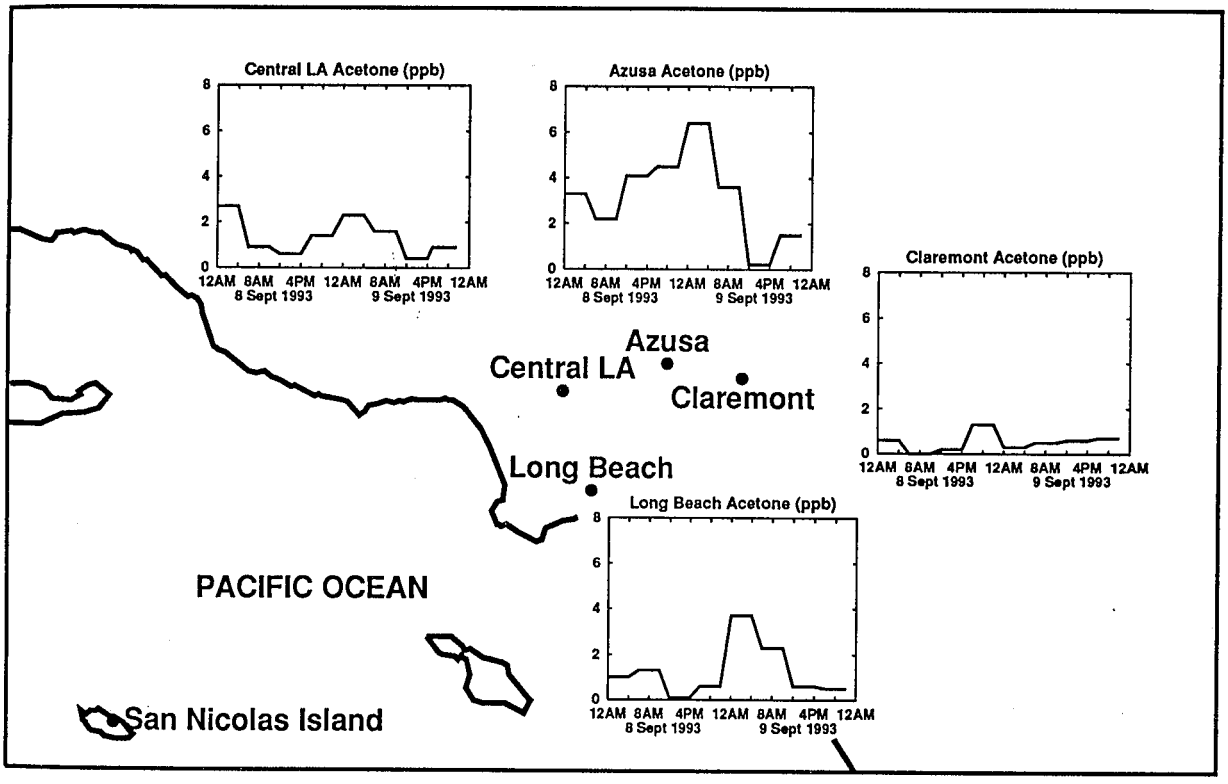

Figure 3.3:
Ambient concentrations of acetone measured in Southern California Sept. 8-9, 1993.

sured at the four urban sites. Indeed, for this reason, these three compounds are routinely measured in areas exceeding the National Ambient Air Quality Standard for ozone to assess their role in photochemical smog formation. Through comparison of the data from different sites, peak concentrations of formaldehyde and acetaldehyde are seen from 0600 to 1000 hours PDT in Central Los Angeles, reflecting emissions that occur during the morning traffic peaks. The highest concentrations seen at Claremont occur in the evening and night, reflecting arrival late in the day of secondary compounds transported to this site from upwind and also the effect of reduced mixing which commonly occurs during the nighttime in Southern California. The maximum concentrations at Long Beach occur in the afternoon sampling periods, suggesting either photochemical production or emissions from industrial sources during this sampling period. The highest concentrations of acetone are seen in the overnight samples at all sites suggesting the effect of either higher nighttime emissions or the effect of reduced mixing at night.

Urban concentrations of other carbonyl compounds are shown in Figure 3.4, including time series plots of crotonaldehyde, 2-butanone, benzaldehyde, cyclohexanone, glyoxal, n-hexanal, and methylglyoxal. The concentrations of some of these individual compounds, especially glyoxal, show strong indications of secondary formation with afternoon peaks in concentration and higher levels seen with downwind transport from the coast to inland smog receptor sites, which is consistent with laboratory studies showing that this dicarbonyl is a product of the oxidation of aromatic hydrocarbons [1].

Regional Background Carbonyl Concentrations

The total carbonyl concentrations measured at San Nicolas Island are much lower than urban concentations (3.5 ppbV at San Nicolas Island compared to

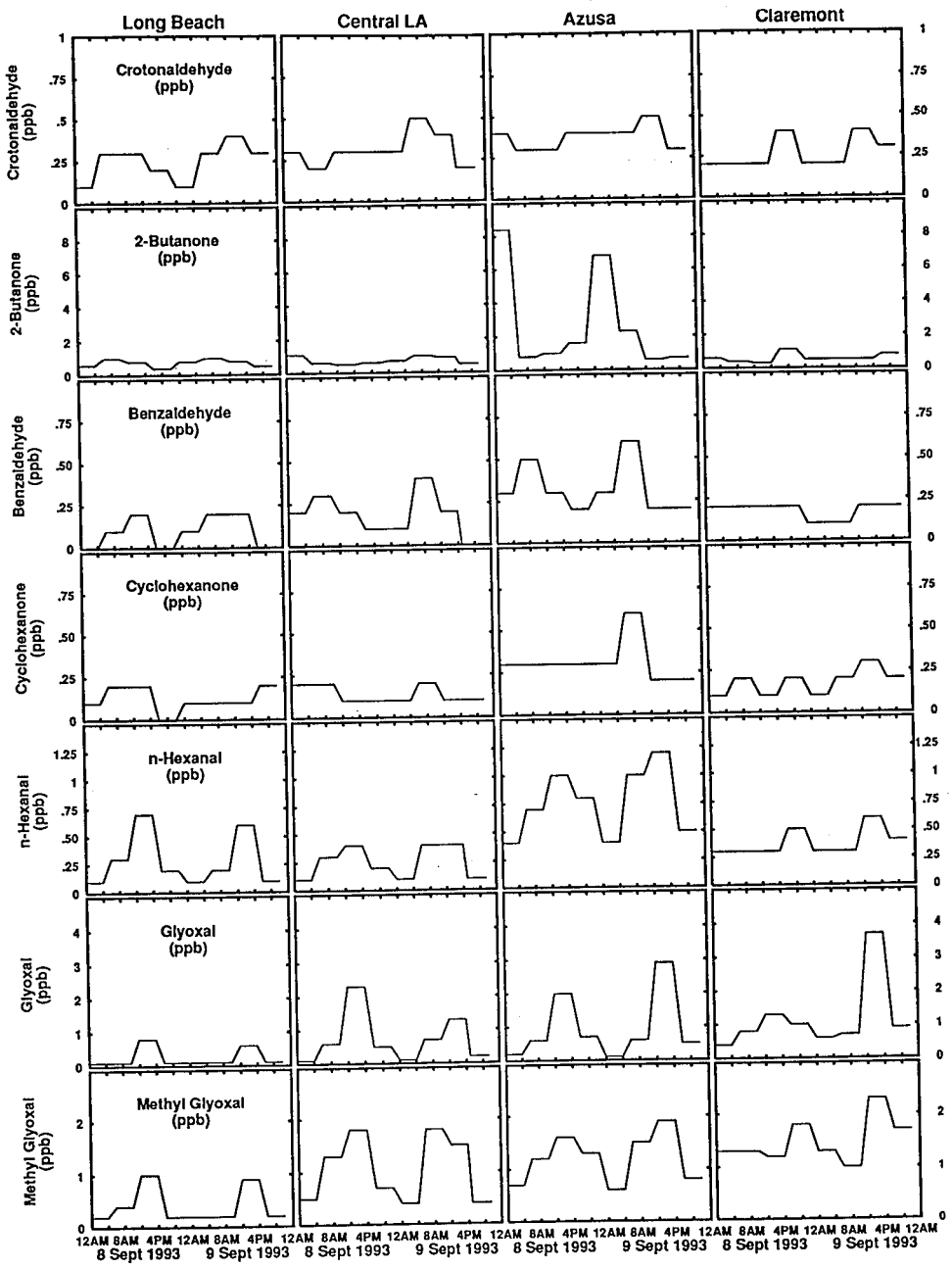

Figure 3.4:
Ambient concentrations of crotonaldehyde, 2-butanone, benzaldehyde, cyclohexanone, glyoxal, n-hexanal and methylglyoxal measured in Southern California September 8-9, 1993.

an urban average total carbonyl concentration of 17.9 ppbV). Carbonyls with similar concentrations at both urban sites and the background site include octanal with an urban to background ratio of 0.9, nonanal (1.6) and crotonaldehyde (1.1). Aliphatic aldehydes are expected products of the reaction of unsaturated fatty acids with ozone [16], and reaction of unsaturated fatty acids present in remote atmospheres [17] may represent a pathway for their formation in remote locations. Most carbonyls have an urban/background concentration ratio in Los Angeles that is much greater than unity, with the highest values of that ratio observed for 2-butanone (6.3), methylglyoxal (10.4), and glyoxal (15.6). Ambient concentrations of 2-butanone are dominated by industrial solvent emissions and methylglyoxal and glyoxal are secondary products of the oxidation of aromatic hydrocarbons emitted from anthropogenic sources.

Reaction of Carbonyl Compounds with the Hydroxyl Radical

Two main pathways exist for the removal of carbonyl compounds: reaction with the hydroxyl radical ($OH^{\cdot}$) and photolysis. While photolysis is an important pathway for reaction, the reaction with $OH^{\cdot}$ is the dominant removal process in polluted urban atmospheres [1]. This reaction between $OH^{\cdot}$ and carbonyl compounds provides an important source for organic radical species in the atmosphere, which in turn affects secondary formation of ozone. The three most common atmospheric carbonyl compounds (formaldehyde, acetaldehyde and acetone) are routinely measured at a few monitoring sites in areas exceeding the National Ambient Air Quality Standard for ozone. Figure 3.5 shows that those three commonly measured carbonyl compounds make up only a little more than half of the total carbonyl compound concentration measured at the four urban sites during this experiment. The

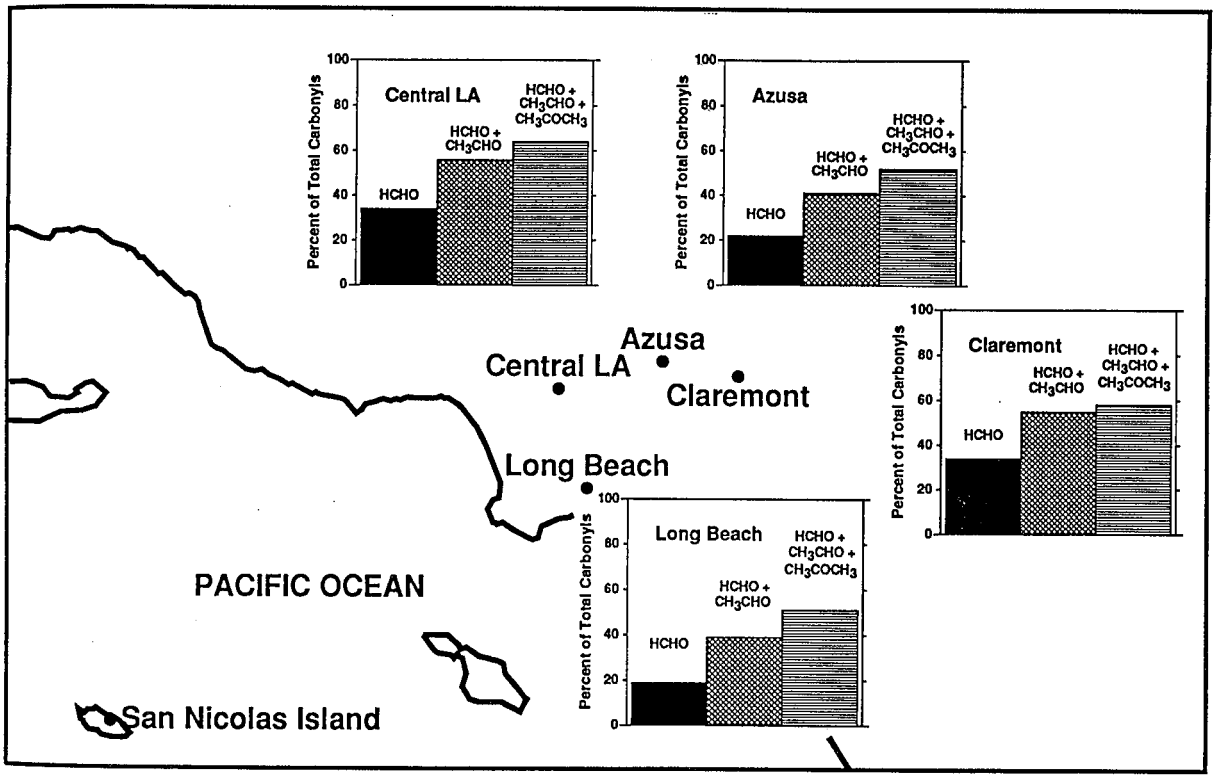

Figure 3.5:
Contribution of the three most common carbonyl compounds to atmospheric total carbonyl compound concentrations at the four urban sites studied.

contribution to atmospheric chemical reactivity due to the remaining higher molecular weight carbonyls has been largely overlooked.

To investigate the importance of the additional carbonyl compounds on atmospheric reactivity, urban-average ambient concentrations of the 23 carbonyls measured during these experiments were multiplied by the reaction rate of these compounds with $OH^{\cdot}$. This calculation produces an index showing the relative importance of the different carbonyl compounds in $OH^{\cdot}$ removal by carbonyls. Of the major carbonyl compound classes, aliphatic aldehydes contribute 81.6% of the reactivity of carbonyl compounds when judged by their reaction rate with the hydroxyl radical. Only 27.9% of the reactivity of the total carbonyls mixture in the Los Angeles atmosphere is contributed by formaldehyde and acetaldehyde, which together account for 42.3% of the total carbonyl concentration. Thus 53.7% of the reactivity of the carbonyl compounds as a whole is contributed by the higher molecular weight aliphatic aldehydes that are seldom measured. Both the relative concentration and the fraction of hydroxyl radical removal by the individual n-alkanal homologs is shown in Table 3.1 and in Figure 3.6.

Of these n-alkanals, nonanal is present at higher levels than alkanals other than formaldehyde and acetaldehyde. The elevated concentration of this homolog can be attributed to atmospheric formation from the reactions of ozone with unsaturated fatty acids [16] and 1-decene [18] as well as direct emissions of nonanal from meat-cooking operations [19].

3.3.2 Peroxyacyl Nitrates

PEROXYACETYL NITRATE

Ambient concentrations of PAN and PPN were measured at the four urban sites involved in this study. The highest concentration of PAN was measured

Table 3.1: Relative contribution of ambient carbonyls to removal of OH.

Carbonyl class and compound	Average urban conc. (ppb)	Carbonyl-OH reaction rate constant, 10^{-11} cm^3 $molec^{-1}$ s^{-1}	Product of urban concentration and reaction rate (s^{-1})	Percent total OH removal by carbonyls
Aliphatic Aldehydes				
formaldehyde	5.3±2.4(32)	0.98[b]	1.3	12.6
acetaldehyde	4.0±2.3(32)	1.58[b]	1.5	15.3
propanal	0.79±0.54(32)	1.96[b]	0.37	3.7
butanal	0.71±0.54(32)	2.35[b]	0.41	4.0
pentanal	0.41±0.54(32)	2.85[b]	0.29	2.8
hexanal	0.42±0.54(32)	3.04[c]	0.31	3.1
heptanal	0.64±0.54(19)	3.23[c]	0.51	5.0
octanal	0.53±0.54(5)	3.42[c]	0.44	4.4
nonanal	1.09±0.54(5)	3.61[c]	0.96	9.5
decanal	0.53±0.54(3)	3.80[c]	0.49	4.9
undecanal	0.29±0.54(2)	3.99[c]	0.28	2.8
dodecanal	0.33±0.02(3)	4.18[c]	0.34	3.3
tridecanal	0.34±0.04(2)	4.37[c]	0.36	3.6
tetradecanal	0.58(1)	4.56[c]	0.64	6.4
subtotal: C_1-C_{14} aldehydes	15.96		8.2	81.6
Ketones				
acetone	1.6±1.5(32)	0.023[b]	0.001	0.10
2-butanone	1.2±1.7(32)	0.115[b]	0.03	0.34
cyclohexanone	0.20±0.09(31)	0.60[c]	0.03	0.29
nopinone	0.34±0.29(6)	1.4[d]	0.12	1.2
subtotal: Ketones	3.34		0.18	1.9
Unsaturated Carbonyls				
acrolein	≤ 0.04(32)	1.99[b]	≤0.02	≤0.19
crotonaldehyde	0.30±0.10(32)	3.6[b]	0.26	2.6
methacrolein	≤0.08(32)	3.35[b]	≤0.07	≤0.65
methylvinylketone	≤0.08(32)	1.88[b]	≤0.04	≤0.36
4-acetyl-1-methylcyclohexane	0.12±0.09(2)	12.9[d]	0.37	3.7
subtotal: Unsaturated	0.42		≤0.76	≤7.6
Aromatics				
benzaldehyde	0.22±0.11(28)	1.29[b]	0.07	0.7
m-tolualdehyde	0.24±0.10(12)	3.0[c]	0.18	1.7
subtotal: Aromatics	0.42		0.24	2.4
Dicarbonyls				
glyoxal	0.78±0.85(32)	1.14[b]	0.22	2.2
methylglyoxal	1.04±0.61(32)	1.72[b]	0.44	4.3
subtotal: Dicarbonyls	1.82		0.65	6.5

[a] Mean±1 standard deviation of ambient concentrations measured at four urban locations Sept. 8-9, 1993; number of observations above detection limits given in parentheses. [b] From Atkinson (1990) Reference [1]. [c] No data, rate constant estimated from structure-reactivity considerations, see Grosjean, et al. (1996) Reference [13]. [d] From Atkinson and Aschmann (1993) Reference [20].

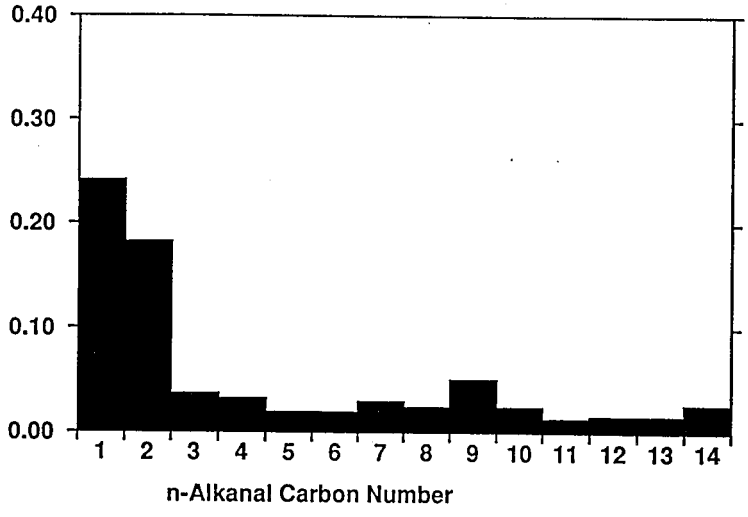

b) Percentage contribution to removal of hydroxyl radical

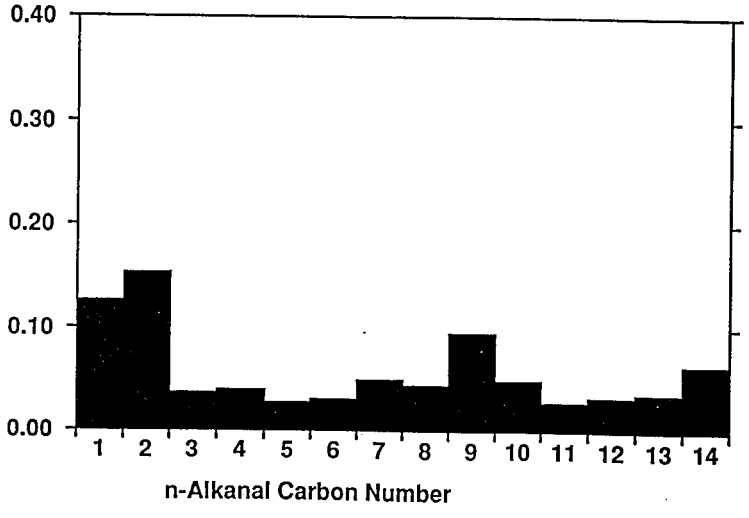

Figure 3.6:
Percentage contribution of n-alkanals to (a) ambient carbonyl concentration and (b) removal of hydroxyl radical by chemical reaction.

at Claremont (9.9 ppb) on September 9. At the other sites, the highest concentrations measured ranged from 5.5 ppb in Long Beach to 6.1 ppb in Azusa to 6.9 ppb in Central Los Angeles. The peak concentrations do not exactly follow the expected increase with downwind transport of a purely secondary compound. However, the average concentrations (the average of the concentrations $\geq$ the detection limit of 0.010 ppb $\pm$ one standard deviation) measured over the entire study period of approximately 2 weeks increase from 0.92$\pm$0.95 ppb at Long Beach, to 1.06$\pm$1.27 ppb in Central Los Angeles, to 1.76$\pm$1.33 ppb in Azusa and 2.99$\pm$1.64 ppb in Claremont. This concentration buildup is consistent with PAN formation during transport of air parcels to the inland smog receptor sites at the eastern end of the air basin result in higher average concentations of PAN in Claremont and Azusa, and may be a more accurate measure of the enviromental exposure to PAN.

The average diurnal variation of PAN concentrations measured over the entire study period is shown in Figure 3.7. Diurnal variations showed peak values during the early afternoon, and minimum values during the nighttime and early morning hours. Average peak concentrations increase from the western end of the basin (Long Beach and Central Los Angeles), which is the dominant source region of precursor hydrocarbons and NO_x in the air basin, to the downwind eastern end of the basin (Azusa and Claremont). The atmospheric concentation of PAN is determined by reactions leading to its formation and destruction, including:

$$CH_3CO_3^{\cdot} + NO_2 \rightleftharpoons CH_3(O)OONO_2 \quad (PAN) \tag{3.1}$$

$$CH_3CO_3^{\cdot} + NO \rightarrow CH_3^{\cdot} + CO_2 + NO_2 \tag{3.2}$$

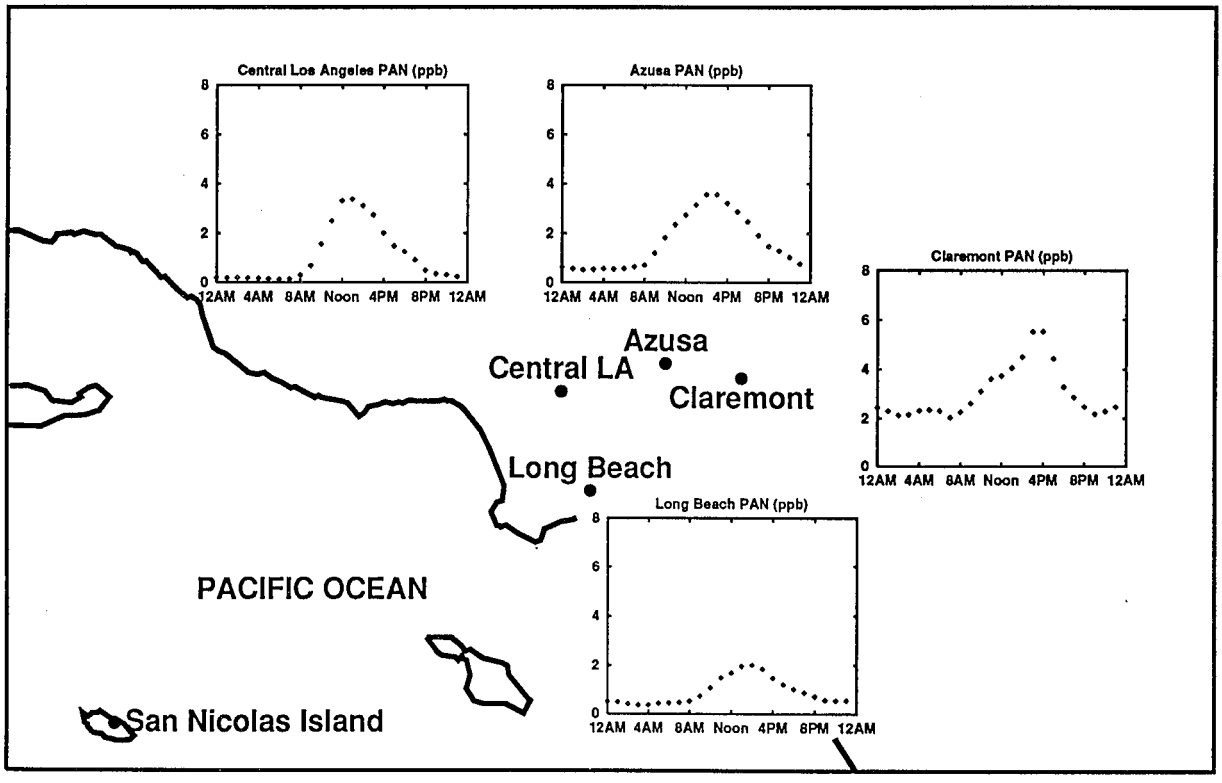

Figure 3.7:
Diurnal variation of PAN concentrations averaged at each of the four urban sites over the period Aug. 28 - Sept. 13, 1993.

$$CH_3^{\cdot} + O_2 \rightarrow CH_3CO_2^{\cdot} \tag{3.3}$$

$$CH_3CO_2^{\cdot} + NO \rightarrow CH_3O^{\cdot} + NO_2 \tag{3.4}$$

$$CH_3O^{\cdot} + O_2 \rightarrow HCHO + HO_2^{\cdot} \tag{3.5}$$

Peak concentrations during the photochemically active early afternoon with greatest sunlight intensity can be explained by the formation of PAN from the acetylperoxy radical and nitrogen dioxide (reaction 3.1). Figure 3.7 shows that the peak concentrations are shifted to later times at the inland sites compared to the two sites in the western portion of the air basin, the primary source region in Southern California. At Claremont, the nighttime levels of PAN do not decrease as significantly as at other sites. This occurs because of the lower primary emissions from motor vehicles in the Claremont area as compared to Central Los Angeles. Primary emissions of NO react with the acetylperoxy radical to form CO_2 and NO_2 and the acetyl radical (reaction 3.2), thereby reducing PAN formation.

The peak ambient PAN concentrations measured during this summer 1993 experiment are significantly lower than peak concentrations measured in previous years. For example, peak values of 30, 19, 16 and 13 ppb PAN were measured in Claremont, Anaheim, Long Beach and Central Los Angeles in the summer of 1987 [21]. The inorganic nitrate levels measured during this experiment are of a magnitude similar to those measured in previous studies [12]. The lower branching ratio between organic and inorganic nitrate formation that is apparent in the 1993 experimental data possibly results

from the fact that local air quality management plans have emphasized the control of hydrocarbon precursors to ozone formation [22].

Peroxypropionyl Nitrate

Concentations of peroxypropionyl nitrate (PPN) were measured at the four urban sites over the two week period of the experiment. The peak PPN concentrations at each of the sites measured during this period were 0.9 ppb, 1.0 ppb, 1.5 ppb, and 1.2 ppb in Long Beach, Central Los Angeles, Azusa and Claremont, respectively. The average PAN concentration over the entire two week period was 0.25±0.14 ppb (average of concentrations $\geq$ detection limit of 0.016 ppb ± one standard deviation) at Long Beach, 0.24±0.18 ppb at Central Los Angeles, 0.47±0.24 ppm at Azusa and 0.31±0.17 ppb at Claremont.

The average diurnal variation of PPN over the study period, shown in Figure 3.8 is similar to that of PAN, and indeed should be similar because both pollutants are produced by similar routes of formation. PPN is formed from the reaction of NO_2 with the higher molecular weight homologs of the acetylperoxy radical shown in reaction 3.1, in competition with reaction between those radicals and NO to form CH_3CHO, NO_2, CO_2 and $HO_2\cdot$ in a reaction sequence directly analogous to that shown for PAN.

Thermal Decomposition of Peroxyacyl Nitrates

The main mechanism of removal of PAN from the atmosphere is thermal decomposition, followed by reaction of the resulting acetylperoxy radical with NO. The back reaction of Equation 3.1 is dependant on temperature, while the forward reaction is dependant only on the concentration of the precursors. During the period of the Sept. 8-9, 1993, field experiment, a high-pressure system emerged over the South Coast Air Basin, inducing sunny

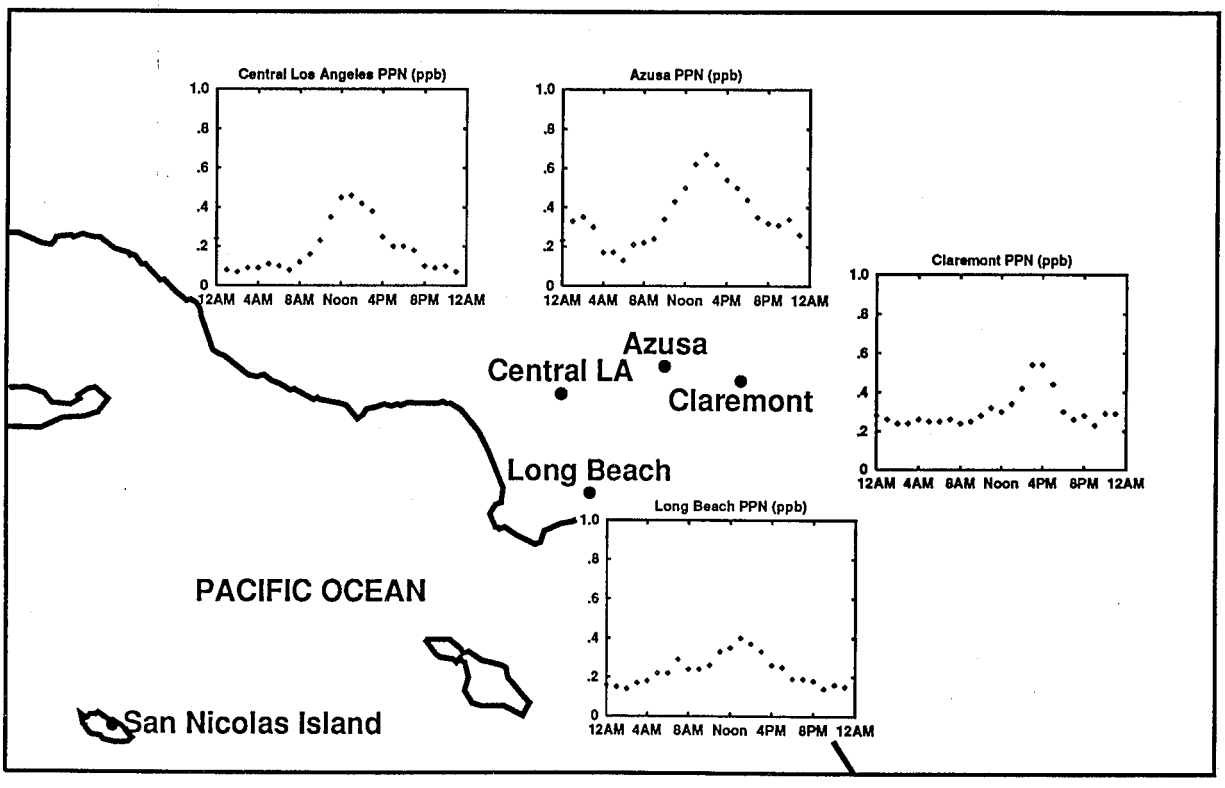

Figure 3.8:
Diurnal variation of PPN averaged at each of the four urban sites averaged from Aug 28 - Sept. 13, 1993.

hot weather and decreased mixing due to a very strong temperature inversion aloft. Ground level temperatures in the eastern end of the basin peaked at more than 40°C in Claremont on the second day of the smog episode (Sept. 9). The effect of these high temperatures on ambient concentrations of PAN was investigated through calculation of the extent of PAN thermal decomposition.

From the chemical reactions shown above, thermal decomposition of PAN can be calculated as [23-24]:

$$\frac{d(ln[PAN])}{dt} = \frac{k_{-1}k_2[NO]}{k_2[NO] + k_1[NO_2]} \tag{3.6}$$

where k_1 and k_{-1} are the reaction rates for the forward and back reactions shown in Equation 3.1, and k_2 is the reaction rate for Equation 3.2. The reaction rate k_{-1} is $2.25 \times 10^{16}\ e^{-13{,}573/T}$ (in units s^{-1}) and $k_2/k_1 = 1.95$, independant of temperature [23]. Using Equation 3.6, the quantity of PAN lost to thermal decomposition can be calculated using hourly NO, NO_2 and ambient temperature data during the severe smog episode of Sept. 8-9, 1993. Overall, the amount of PAN lost to thermal decomposition during the peak photochemical smog period of the day is comparable to the amount of PAN remaining in the atmosphere, as shown in Figure 3.9. This result is important because PAN decomposition releases NO_2 to the atmosphere thereby increasing the ratio of NO_2 to NO, which increases ozone formation.

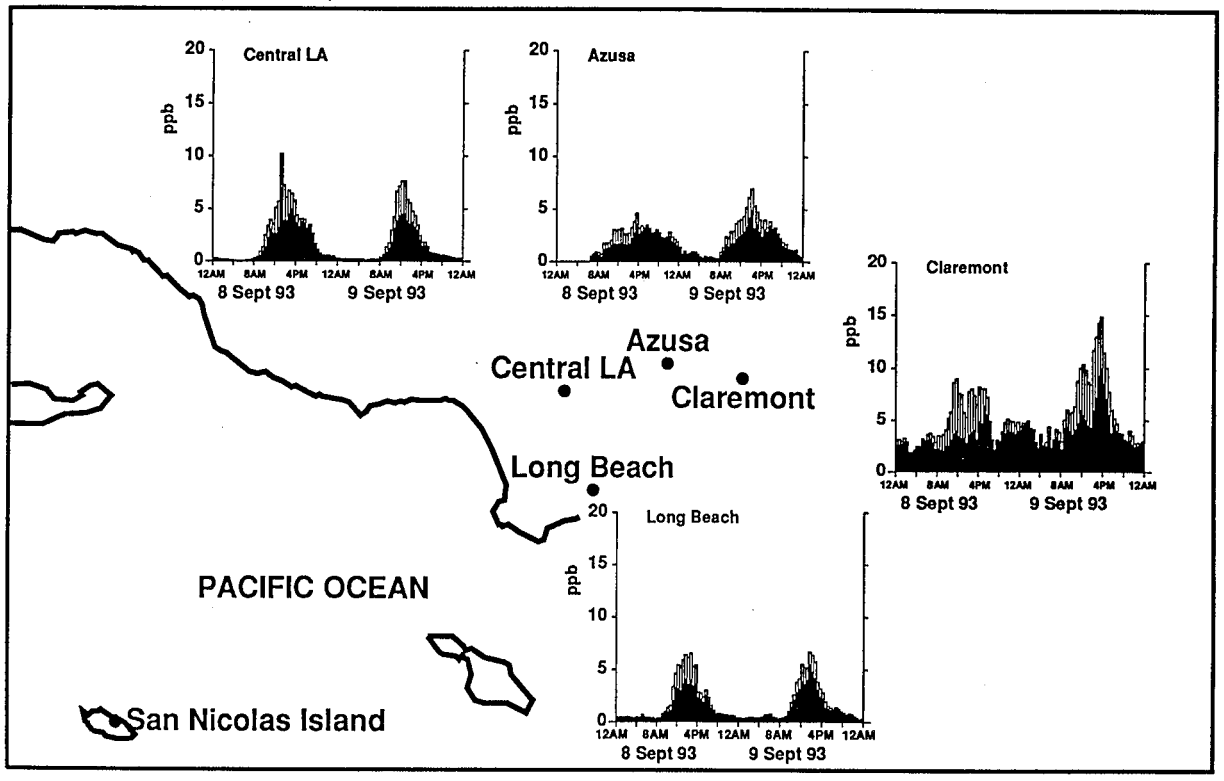

Figure 3.9:
Measured PAN concentrations Sept. 8-9, 1993 (solid bars); and PAN concentration calculated to be lost during that hour to thermal decomposition (open bars).

Bibliography

[1] R. Atkinson. Gas-phase tropospheric chemistry of organic compounds: a review. *Atmos. Environ.*, 24A: 1-41, 1990.

[2] National Research Council *Rethinking the Ozone Problem in Urban and Regional Air Pollution*, National Academy Press: Washington DC, 1991.

[3] National Research Council *Formaldehyde and Other Aldehydes*, National Academy Press: Washington DC, 1981.

[4] E. R. Stephens, P. L. Hanst, R. C. Doerr and W. E. Scott. Reactions of nitrogen dioxide and organic compounds in air. *Ind. Eng. Chem.*, 48: 1498-1504, 1956.

[5] E. R. Stephens. The formation, reactions and properties of peroxyacylnitrates (PANs) in photochemical air pollution. *Adv. Environ. Sci. Technol.*, 1: 119-146, 1969.

[6] J. B. Mudd. Reaction of peroxyacetylnitrate with glutathione. *J. Biol. Chem.*, 241: 4077-4080, 1966.

[7] O. C. Taylor. Importance of peroxyacetylnitrate as a phytotoxic air pollutant. *J. Air Pollut. Control Assoc.*, 19: 347-351, 1969.

[8] M. J. Peak and W. L. Belser. Some effects of the air pollutant, peroxyacetylnitrate, upon deoxyribonucleic acid and upon nucleic acid bases. *Atmos. Environ.*, 3: 385-397, 1969.

[9] J. E. Lovelock. PAN in the natural environment; its possible significance in the epidemiology of skin cancer. *Ambio*, 6: 131-133, 1977.

[10] P. J. Temple and O. C. Taylor. World-wide measurements of peroxyacetylnitrate (PAN) and implications for plant injury. *Atmos. Environ.*, 17: 1583-1587, 1983.

[11] T. E. Kleindienst, P. B. Shepson, D. F. Smit, E. E. Hudgens, C. M. Nero, L. T. Cupitt, J. J. Bufalini and L. D. Claxton. Comparison of mutagenic activities of several peroxyacylnitrates. *Environ. Mol. Mutagen.*, 16: 70-80; 1990.

[12] M. P. Fraser, D. Grosjean, E. Grosjean, R. A. Rasmussen and G. R. Cass. Air quality model evaluation data for organics. 1. Bulk chemical composition and gas/particle distribution factors. *Environ. Sci. Technol.*, 30: 1731-1743, 1996.

[13] E. Grosjean, D. Grosjean, M. P. Fraser and G. R. Cass. Air Quality Model Evaluation Data for Organics. 2. C_1 - C_{14} Carbonyls in Los Angeles Air. *Environ. Sci. Technol.*, 30: 2687-2703, 1996.

[14] E. Grosjean, D. Grosjean, M. P. Fraser and G. R. Cass. An Air Quality Model Evaluation Data Set for Organics. 3. Peroxyacetyl nitrate and peroxypropionyl nitrate in Los Angeles Air. *Environ. Sci. Technol.*, 30: 2704-2714, 1996.

[15] W. J. Moxim, H. Levy and P. S. Kasibhatla. Simulated global tropospheric PAN- its transport and impact on NOx. *J. Geophys. Res. Atmos.*, 101D: 12621-12638, 1996.

[16] K. Kawamura and R. B. Gagosian. Implications of ω-oxocarboxylic acids in the remote marine atmosphere for photo-oxidation of unsaturated fatty acids. *Nature*, 325: 330-332, 1987.

[17] B. R. T. Simoneit. Characterization of organic-constitutents in aerosols in relation to their origin and transport- a review. *Intern. J. Environ. Anal. Chem.*, 23: 207-237, 1986.

[18] E. Grosjean, D. Grosjean and J. H. Seinfeld. Atmospheric chemistry of 1-octene, 1-decene, and cyclohexene - gas-phase carbonyl and peroxyacyl nitrate products. *Environ. Sci. Technol.*, 30: 1038-1047, 1996.

[19] W. F. Rogge, L. M. Hildemann, M. A. Mazurek, B. R. T. Simoneit and G. R. Cass. Sources of fine organic aerosol. 1. Charbroilers and meat cooking operations. *Environ. Sci. Technol.*, 25: 1112-1125, 1991.

[20] R. Atkinson and S. M. Aschmann. Atmospheric chemisty of the monoterpene reaction-products nopinone, camphenilone, and 4-acetyl-1-methylcyclohexene. *J. Atmos. Chem.*, 16: 337-348, 1993.

[21] E. L. Williams and D. Grosjean. Southern California Air Quality Study- Peroxyacetylnitrate. *Atmos. Environ.*, 24: 2369-2377, 1990.

[22] *1997 Air Quality Management Plan*, South Coast Air Quality Management District: Diamond Bar, CA, 1996.

[23] E. C. Tuazon, W. P. L. Carter and R. Atkinson. Thermal-decomposition of peroxyacetylnitrate and reactions of acetyl peroxy-radicals with NO and NO2 over the temperature range 283-313K. *J. Phys. Chem.*, 95: 2434-2437, 1991.

[24] D. Grosjean, E. Grosjean and E. L. Williams. Thermal decomposition of PAN, PPN, and vinyl-PAN. *J. Air Waste Manage. Assoc.*, 44: 391-396, 1994.

4 C_2 to C_{36} Non-Aromatic Hydrocarbons

4.1 Introduction

The hydrocarbons present in urban atmospheres are important contributors to a number of different problems associated with air pollution. The lightest hydrocarbons react with the oxides of nitrogen to promote ozone formation [1]. The heaviest hydrocarbons form a considerable fraction of the fine aerosol particles ($d_p \leq 2.5\mu m$) [2,3], are easily inhalable [4], and have been linked to adverse health effects [5].

Hydrocarbons in the atmosphere exist as gaseous, semivolatile and particle-phase materials. Gaseous and particle-phase organic compounds traditionally have been studied separately. The purpose of this chapter is to describe the important features of the non-aromatic hydrocarbons that can be seen when they are measured simultaneously over the carbon number range from C_2 to C_{36} during a severe photochemical smog episode in Southern California. Individual compound classes studied include normal-, branched and cyclic alkanes, normal-, branched and cyclic alkenes, alkynes, monoterpenes, isoprenoids, tricyclic terpanes, triterpanes, diasteranes, and steranes. The

Reference: Fraser, M. P.; Cass, G. R.; Simoneit, B. R. T.; Rasmussen, R. A. Air Quality Model Evaluation Data for Organics. 4. C_2 to C_{36} Non-Aromatic Hydrocarbons. *Environ. Sci. Technol.*, **31**, 1997: 2356-2367.

methods used for making measurements of these compounds will be described. Descriptors that can be used to convey the main features of the hydrocarbon distribution across the entire range of carbon numbers studied will be developed. The concentrations and relative composition of the hydrocarbons present in regional background air upwind of the Los Angeles area will be contrasted with that measured within the city. Comparisons will be drawn between gaseous and particle-phase tracers of motor vehicle exhaust and changes in the hydrocarbon distribution in the Los Angeles atmosphere over the past decade will be examined. Ultimately, these data are intended for use in the evaluation of photochemical airshed models that simultaneously track both gas-phase and particle-phase organics.

4.2 Experimental Methods

4.2.1 Collection of Samples

During the summer of 1993, a field experiment was undertaken to measure the concentrations of as many individual organic compounds as possible in both the gas and particle phases simultaneously [6]. Samples of four-hour duration were collected at five sites in Southern California every six-hours over a 2-day photochemical smog event that occurred on September 8-9, 1993, to obtain time series data on the concentrations of individual organic compounds for use in evaluating air quality model performance. The sampling sites consisted of four stations within the greater Los Angeles urban area at Long Beach, Central Los Angeles, Azusa, and Claremont, plus a background site located upwind of the city at San Nicolas Island. The severity of the photochemical smog episode and the overall experimental design are more fully described by Fraser et al. [6].

The data reported here were collected from two samplers: a sampler using

internally electropolished stainless steel canisters to collect volatile organic compounds [7], and a high volume dichotomous virtual impactor [8] that was used to collect particulate and semivolatile organic compounds. Particle-phase organics were collected on pre-baked quartz fiber filters (QFFs; Pallflex 2500 QAO; 102 mm diameter), and semivolatile organics were collected on polyurethane foam (PUF) cartridges located downstream of the fine particle quartz fiber filter located in the high volume dichotomous sampler.

The 6-l stainless steel canisters used for organic gas sampling were shipped and deployed into the field under high vacuum, used to collect 4-h integrated samples, sealed and returned to the laboratory for analysis.

The quartz fiber filters were annealed at 550°C for at least 8-h before use to lower their carbon blank levels. Clean filters were sealed in annealed aluminum foil packages for storage and transportation prior to use. Particle sampling occurred for 4-h periods at a nominal flow rate of 350 lpm through the high volume dichotomous sampler, with 90% of that flow directed to the fine particle filter and PUF combination and 10% of that flow directed to the coarse particle filter. After sampling, filters were stored in annealed glass jars with solvent-rinsed Teflon lid liners, and sealed with Teflon tape. Samples were refrigerated immediately upon removal from the samplers, returned to the laboratory packed on ice within 12-h, where they were placed in freezers at -21°C until analyzed.

PUF plugs having a diameter of 7.6 cm were cut from commercially available polyurethane foam (density = 0.022 g cm^{-3}, ILD = 30). Five PUF plugs each 2.5 cm thick were stacked in series forming the 12.5 cm deep bed used to collect each sample. PUF plugs were cleaned by repeated washings in dichloromethane (DCM). Five 300 ml aliquots of distilled-in-glass grade DCM were used successively to clean each PUF plug segment by repeatedly

compressing the foam at least 50 times in clean glass jars. After the five washings, each PUF plug was allowed to dry. Each stack of 5 PUF segments was then compressed into a solvent-rinsed aluminum cartridge (6.3 cm diameter, 15.2 cm length) having 5.1 cm diameter flanges at each end that were temporarily sealed with Teflon caps. The PUF plugs were transported to the field in these housings, used to collect a sample, and then resealed with Teflon caps, refrigerated, and returned to the laboratory. Within the laboratory organic clean room, the PUF plugs were removed from the aluminum cartridges, placed in annealed glass jars with Teflon lid liners, and stored in a freezer at -21°C until analysis.

4.2.2 Analytical Methods

Individual vapor phase organic compounds collected in stainless steel canisters were analyzed by gas chromatography (GC) with flame ionization detection and by gas chromatography-mass spectrometry (GC-MS). The conditions for analysis for the two GC methods were similar. The GC-FID method used a Hewlett Packard model HP 5890A/3396A system. A J&W Scientific DB-1 column was used (60 m x 0.32 mm x 1.0 micron film thickness). The sample loading procedure froze out 500 ml of air directly onto a 15.2 x .3 cm stainless steel loop filled with 60-80 mesh glass beads in liquid O_2 (-183°C). Desorption was at 100°C in boiling water onto the head of the column held at -60°C for cryo-focusing. The GC temperature program was held for 5 minutes and then increased at 4°C/min to 200°C. Analog-digital data collection was done on the HP 3396A integrator and stored on a HP 9914B disc recorder.

The GC-MS method for volatile organic compounds used a similar DB-1 column but with a 0.25 mm ID in a Hewlett Packard mass selective detector

model HP 5970 MSD/9000/300 system. The sample loading procedure used 1-5 liters of air trapped on a multibed Tenax RA - Ambersorb - Charcoal trap used in a Dynatherm Analytical Instruments model 890 system. Sample desorption temperature was 300°C for 6 minutes with transfer of the sample to a freeze-out loop immersed in liquid N_2 (-196°C). The construction of the trap and the temperature transfer and column programs were the same as those used for the GC-FID analysis. The data were captured on a Hewlett Packard model HP 9000/300 computer and processed by the operating software in the HP 5970 MS ChemStation.

Identification and quantification of the VOC compounds were from known standards and the mass spectral library in the NIST/EPA/MSDC Mass Spectral Database Version 2. Primary calibrations of the working standards were done directly against the NIST SRM standards for benzene (tank #1805) and propane (tank #1665B).

Quartz fiber filters were extracted and analyzed for individual organic compounds following the procedures of Mazurek et al. [9], which will only be summarized here briefly. Before extraction, filters were spiked with a known amount of perdeuterated tetracosane ($\underline{n}$-$C_{24}D_{50}$) to monitor extraction efficiency. Each filter was extracted with two aliquots of hexane followed by three aliquots of 2:1 benzene:isopropanol; each aliquot consisted of 35 ml of solvent, and with each aliquot, the sample was sonicated for 10 minutes. The extracts were collected in a boiling flask after being filtered over glass wool. The extract was concentrated to 2-4 ml volume by rotary vacuum evaporation (37°C, 400-450 mm Hg), and then transferred into a conical vial. In this vial, the volume was further reduced under nitrogen blowdown to approximately 400 μl, with the volume of each of the aliquots being determined with a 500 μl syringe ($\pm$10 μl units).

The PUF plugs were spiked with a recovery suite of eight perdeuterated compounds to monitor extraction efficiency and loss during blowdown. The plugs were extracted three times successively with 250 ml DCM, and the extracts were combined in a boiling flask. Extraction included compressing the foam in the extraction solvent at least 50 times during each of the three extraction steps. All extracts were filtered over glass wool. The combined extract was concentrated to 2-4 ml volume by rotary vacuum distillation (30°C, 300-350 mm Hg). The total extract was transferred to a conical vial and concentrated to 500 μl volume by gentle nitrogen blowdown. The solutes were then transferred into benzene by adding 2.5 ml benzene and concentrating to approximately 300 μl. All aliquots were stored in a freezer at -21°C until analysis.

4.2.3 GC-MS Analysis

The particle filter sample extracts and PUF plug extracts were analyzed by GC-MS. The PUF extracts were analyzed on a Finnigan 4000 quadrupole gas chromatograph-mass spectrometer connected to an INCOS data acquisition system. The column used was a 0.32 mm internal diameter x 30 m DB-1701 capillary column (bonded phase 86% dimethyl, 14% cyanopropylphenyl polysiloxane, 0.25 μm film thickness; J&W Scientific, Rancho Cordova, CA). For analysis of the semivolatile organics collected on the PUF cartridges, the chromatographic conditions are: (1) sample injection into a splitless injection port at 300°C, (2) column isothermal hold at 40°C, (3) temperature ramp of 4°C min^{-1} to 100°C, (4) temperature ramp of 10°C min^{-1} to 275°C, (5) isothermal hold for 17.5 min. The mass spectrometer scanned from 50 to 500 Da once per second. Organic compounds were ionized by electron impact (EI) with an electron energy of 70 eV. 1-phenyldodecane was used as the co-

injection standard to monitor the response of the instrument. Quartz fiber filter extracts were analyzed on a Finnigan GCQ ion trap gas chromatograph-mass spectrometer. The same column, scan rate and range, and ionization technique were used as on the Finnigan 4000 system. For analysis of the particle-phase organics chromatographic conditions are: (1) sample injection into a splitless injection port at 300°C, (2) column isothermal hold at 65°C, (3) temperature ramp of 10°C min^{-1} to 275°C, (4) isothermal hold for 49 min. Before analysis, filter extracts were further concentrated to approximately 20 μl, with the extract volume being determined immediately before injection with a 25 μl syringe ($\pm$0.50 μl markings).

4.2.4 Compound Identification

Identification of compounds in the PUF and filter extracts was accomplished by a number of processes. First, authentic standards were used in compound identification for those hydrocarbons discussed in the present paper whenever possible. Those standards include: 11 $\underline{n}$-alkanes, pristane, 20R,5α(H),14α(H),17α(H)-cholestane, squalane, squalene, $\underline{n}$-pentadecylcyclohexane, and $\underline{n}$-heptadecylcyclohexane. Next, the retention times and fragmentation patterns of unknowns present in homologous series for which authentic standards exist for one or several members of the series were compared to authentic standards. Further, the fragmentation pattern of unknown compounds was compared to the National Institute of Standards and Technology (NIST) mass spectral reference library on the Finnigan 4000 data station, or the Wiley mass spectral reference library on the Finnigan GCQ.

4.2.5 Compound Quantification

Individual organic compounds were quantified by manually integrating the compound peaks present in the ion chromatograms. Relative ion counts were

converted to compound mass concentrations using response factors relating the ion counts of individual organic compounds to the ion counts of the known amount of the coinjection standard (1-phenyldodecane). These relative response factors were calculated by injection of authentic standards and the coinjection standard. Where no authentic standards were available, the relative response factors (RRFs) were estimated from authentic standards of related compounds (i.e., RRF for 20R,5α(H),14α(H),17α(H)-cholestane used to quantify all steranes). Correction for extraction and blowdown losses was accomplished using recovery standards ($\underline{n}$-$C_{24}D_{50}$ for filter samples; $\underline{n}$-$C_{15}D_{32}$ and $\underline{n}$-$C_{24}D_{50}$ for PUF samples). The blowdown losses for individual compounds relative to the blowdown loss of the deuterated recovery standards were measured by concentrating a known amount of the authentic standards and the recovery standards exactly as in the extractions, followed by quantification of the loss of the authentic standards relative to the deuterated recovery standards. The recoveries of perdeuterated compounds ranged from 21% to 110% and averaged 61% for the quartz fiber filter samples, and ranged from 42% to 98% and averaged 56% for the polyurethane foam samples. The quantities of organic compounds reported in the tables that follow include compensation for the losses that occur during extraction and blowdown. Ambient concentrations of the organic compounds were calculated from the mass concentrations in solution, the total volume of the extract, the volume of extract injected, the mass of the coinjection standard injected, relative instrument response factors, blowdown losses, and the volume of air sampled.

4.2.6 Quality Assurance

The integrity of the data collected was monitored through all stages of sample collection, extraction, and quantification. Procedural blanks for the quartz fiber filters and PUF plugs were analyzed by the same extraction/quantification techniques explained above. Contaminants present on the quartz fiber filters were found to be minor. The cleaned PUF plugs showed several residual contaminant peaks that originate from anti-oxidants and plasticizers used in the foam manufacturing. These contaminant peaks and 1,1'-biphenyl from the benzene solvent used were monitored in all samples and are excluded from the list of environmental pollutants. The estimated precision of compound quantification by GC-MS was obtained by repeated injection of the reference standards used. Error propagation calculations conducted on the errors from volume determination, compound integration and integration of internal standards led to an estimated precision of $\pm$ 20.5%. Independant estimates of accuracy via intercomparison of methods were not possible because there is no overlap of compounds identified in both the canister samples and polyurethane foam plug samples.

4.3 Results and Discussion

A material balance on the atmospheric non-aromatic hydrocarbon concentrations averaged over the 32 samples collected at four urban sites studied during this experiment is shown in Figure 4.1. Figure 4.1 is divided into major compound classes and summed over all C_2 - C_{36} species measured during the experiment. Of the total carbon contained in non-methane organic compounds measured in this experiment, 46% of the carbon could be attributed to non-aromatic hydrocarbons. The remaining carbon is contributed mostly by aromatic compounds, with vapor-phase concentrations dominating

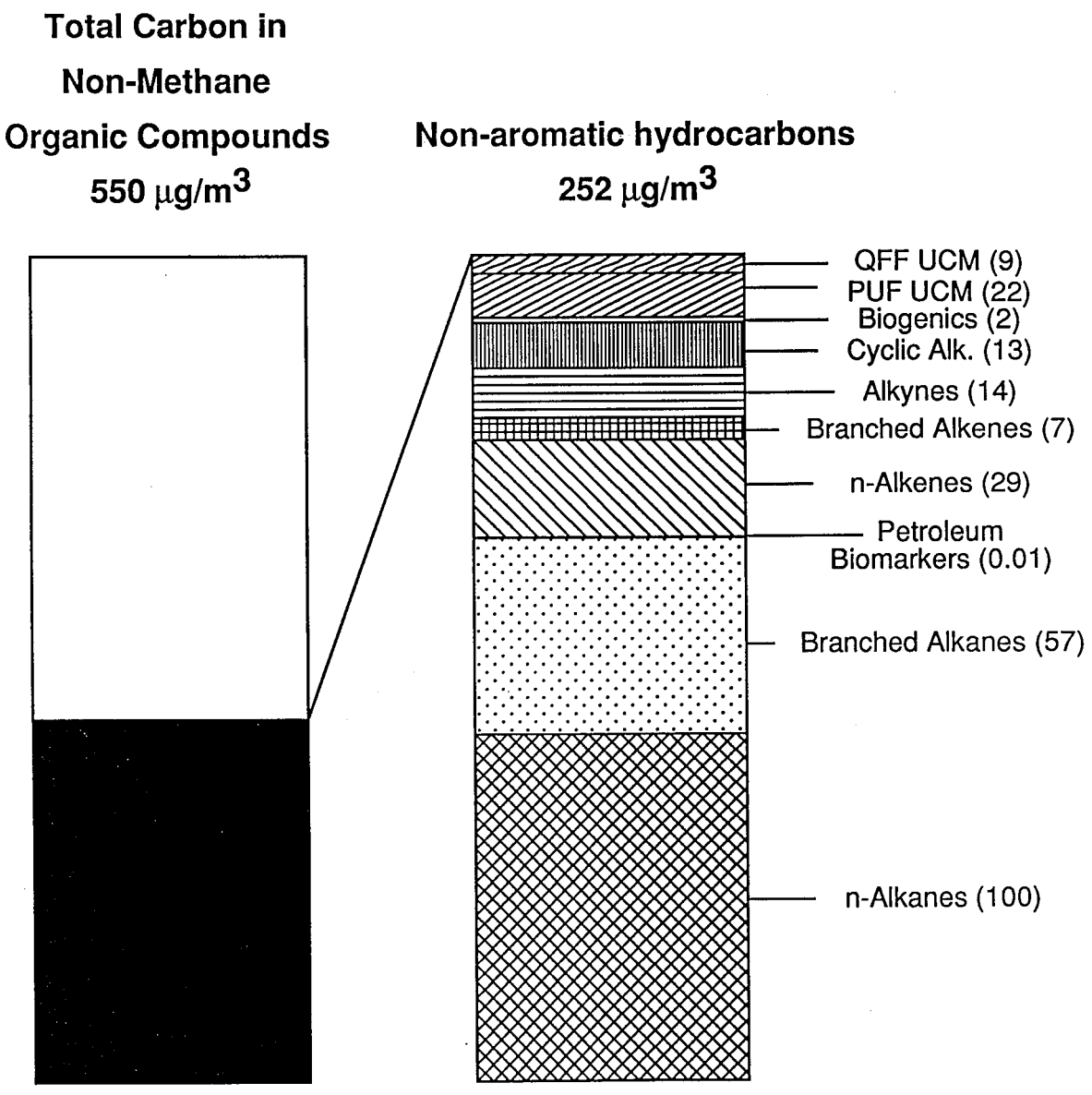

Figure 4.1:
A material balance on the atmospheric non-methane organic compounds over the range C_2-C_{36} showing the portion attributed to non-aromatic hydrocarbons. Compound classes are described in text. Concentrations represent an average over all samples taken at the four urban air monitoring sites in the Los Angeles area, September 8-9, 1993.

over particle-phase organics concentrations [6]. The non-aromatic compound classes observed include *n*-alkanes, branched alkanes, *n*-alkenes, branched alkenes, alkynes, identified cyclic compounds consisting of a mixture of simple and substituted cyclic alkanes and alkenes, biogenic hydrocarbons, petroleum biomarkers, plus unresolved higher molecular weight branched and naphthenic cyclic hydrocarbons that appear as a hump underlying the resolved organic compounds on GC traces of atmospheric samples (often called the unresolved complex mixture, UCM) [2]. An UCM was present in both the semivolatile organics samples collected on the polyurethane foam and in the particulate organics samples collected on the quartz fiber filters. The category labeled petroleum biomarkers includes triterpanes, steranes, tricyclic terpanes, and diasteranes. The mean concentrations measured at the four urban sites and the range of concentrations measured over 4-h sampling intervals for the individual organic compounds within each major compound class are given in Table 4.1.

4.3.1 n-Alkanes

Ambient concentrations were determined for the entire homologous series of 35 normal alkanes in the carbon number range of C_2 to C_{36}. Of those, the C_2 to C_{10} *n*-alkanes were quantified by GC-FID analysis of the VOC canister; the C_2 to C_{13} *n*-alkanes were quantified by GC-MS analysis of the VOC canister; the C_{14} to C_{28} *n*-alkanes present as vapor-phase organics were quantified from the PUF samples by GC-MS analysis; and the particulate *n*-alkanes from C_{18} to C_{36} were analyzed from the filter samples by GC-MS analysis. In reporting the data, the VOC canister data obtained by GC-FID analysis are used for the C_2 to C_{10} *n*-alkanes; the VOC canister data from the GC-MS analysis are used for the C_{11} to C_{13} *n*-alkanes; the PUF plug data

Table 4.1: Average (and range) of non-aromatic hydrocarbon concentrations measured at urban sites.

Compound and Class	Vapor phase organics by canister sampler ($\mu g/m^3$)	Vapor phase semi-volatile organics by PUF sampling (ng/m^3)	Fine Particulate Organics (ng/m^3)
n-Alkanes			
Ethane	20.14 (8.40-44.90)		
Propane	26.74 (9.30-78.40)		
n-Butane	16.45 (7.10-45.10)		
n-Pentane	18.75 (5.40-95.00)		
n-Hexane	6.66 (2.30-16.20)		
n-Heptane	3.75 (1.30-9.50)		
n-Octane	1.95 (0.70-4.60)		
n-Nonane	1.36 (0.40-3.30)		
n-Decane	2.11 (0.50-4.70)		
n-Undecane	1.47 (0.00-2.05)		
n-Dodecane	0.93 (0.00-1.37)		
n-Tridecane	0.31 (0.00-0.68)		
n-Tetradecane		14.99 (0.00-46.77)	
n-Pentadecane		37.47 (0.00-94.28)	
n-Hexadecane		64.23 (0.00-146.25)	
n-Heptadecane		155.14 (42.98-450.11)	
n-Octadecane		106.34 (45.39-294.07)	0.75 (0.00-2.91)
n-Nonadecane		87.89 (37.71-246.53)	0.99 (0.00-2.72)
n-Eicosane		77.47 (32.47-173.98)	1.80 (0.29-3.72)
n-Heneicosane		44.34 (18.31-100.23)	0.99 (0.12-2.69)
n-Docosane		29.07 (9.72-64.63)	0.83 (0.05-1.99)
n-Tricosane		19.72 (5.25-55.57)	2.28 (0.32-5.19)
n-Tetracosane		10.23 (2.38-29.61)	3.42 (0.51-8.35)
n-Pentacosane		7.29 (1.24-19.21)	3.49 (0.75-10.17)
n-Hexacosane		4.13 (1.17-8.40)	3.20 (0.54-8.23)
n-Heptacosane		1.39 (0.00-8.65)	3.66 (0.85-8.93)
n-Octacosane		0.14 (0.00-2.04)	2.30 (0.00-6.02)
n-Nonacosane			4.08 (0.68-12.31)
n-Triacontane			1.75 (0.00-6.78)
n-Hentriacontane			3.81 (0.00-14.47)
n-Dotriacontane			1.24 (0.00-5.81)
n-Tricontane			2.18 (0.00-8.65)
n-Tetracontane			1.07 (0.00-4.44)
n-Pentacontane			1.16 (0.00-6.85)
n-Hexacontane			0.37 (0.00-3.25)
Branched Alkanes			
i-Butane	8.10 (3.40-19.10)		
2,2-Dimethylpropane	0.00 (0.00-0.00)		
i-Pentane	33.48 (14.00-81.10)		
2,2-Dimethylbutane	0.90 (0.00-2.30)		
2,3-Dimethylbutane	2.98 (1.20-7.60)		
2-Methylpentane	10.66 (4.10-27.30)		
3-Methylpentane	6.88 (2.60-17.60)		
2,2-Dimethylpentane	0.15 (0.00-0.34)		
2,4-Dimethylpentane	2.47 (0.80- 6.50)		

Table 4.1 (continued): Non-aromatic hydrocarbons.

Compound and Class	Vapor phase organics by canister sampler ($\mu g/m^3$)	Vapor phase semi-volatile organics by PUF sampling (ng/m^3)	Fine Particulate Organics (ng/m^3)
Branched Alkanes(continued)			
3,3-Dimethylpentane	0.14 (0.00-0.68)		
2-Methylhexane	4.64 (1.60-11.80)		
2,3-Dimethylpentane	3.89 (1.40-10.80)		
3-Methylhexane	5.47 (2.00-12.50)		
2,2,4-Trimethylpentane	7.19 (2.00-18.70)		
2,5-Dimethylhexane	0.75 (0.00-3.90)		
2,4-Dimethylhexane	1.21 (0.00-4.10)		
2,3,4-Trimethylpentane	2.26 (0.70-6.20)		
2,3-Dimethylhexane	0.93 (0.00-2.50)		
2-Methylheptane	1.90 (0.70-4.60)		
3-Methylheptane+2-Ethylhexane	1.79 (0.40-5.20)		
2,2-Dimethylheptane	0.00 (0.00-0.00)		
2,2,4-Trimethylhexane	0.00 (0.00-0.00)		
2,4-Dimethylheptane	0.15 (0.00-1.02)		
2,6-Dimethylheptane	0.30 (0.00-1.37)		
3-Methyloctane	1.01 (0.00-2.39)		
2,6-Dimethyloctane	0.64 (0.00-2.05)		
2,6-Dimethylnonane	0.65 (0.00-1.02)		
Norpristane		49.83 (13.11-143.26)	
Pristane		116.03 (0.00-665.77)	
Phytane		109.65 (22.78-320.04)	
n-Alkenes			
Ethene (Ethylene)	15.80 (1.90-48.10)		
Propene	6.29 (0.80-19.00)		
1-Butene	1.02 (0.00-3.40)		
trans-2-Butene	0.75 (0.00-3.00)		
cis-2-Butene	0.55 (0.00-2.00)		
1-Pentene	1.00 (0.00-2.80)		
trans-2-Pentene	1.14 (0.00-3.80)		
cis-2-Pentene	0.64 (0.00-2.20)		
1-Hexene	0.40 (0.00-1.30)		
trans-2-Hexene	0.33 (0.00-1.60)		
cis-2-Hexene	0.14 (0.00-0.70)		
cis-3-Hexene	0.03 (0.00-0.34)		
Branched Alkenes			
i-Butene	2.35 (0.20-8.70)		
3-Methyl-1-butene	0.34 (0.00-1.10)		
2-Methyl-1-butene	1.13 (0.00-3.40)		
2-Methyl-2-butene	1.17 (0.00-4.30)		
4-Methyl-1-pentene	0.16 (0.00-0.90)		
trans-4-Methyl-2-pentene	0.13 (0.00-0.68)		
cis-3-Methyl-2-pentene	0.08 (0.00-0.34)		
cis-4-Methyl-2-pentene	0.00 (0.00-0.00)		
2-Methyl-1-pentene	0.29 (0.00-1.00)		
2-Methyl-2-pentene	0.00 (0.00-0.00)		
2,4,4-Trimethyl-1-pentene	0.93 (0.00-5.90)		
2,4,4-Trimethyl-2-pentene	0.00 (0.00-0.00)		

Table 4.1 (continued): Non-aromatic hydrocarbons.

Compound and Class	Vapor phase organics by canister sampler ($\mu g/m^3$)	Vapor phase semi-volatile organics by PUF sampling (ng/m^3)	Fine Particulate Organics (ng/m^3)
Diolefins			
1,3-Butadiene	0.81 (0.00-2.50)		
Alkynes			
Ethyne (Acetylene)	14.47 (2.50-40.90)		
Saturated Cyclic Hydrocarbons			
Cyclopentane	1.71 (0.60-3.80)		
Methylcyclopentane	6.20 (2.30-16.50)		
Cyclohexane	1.42 (0.60-3.20)		
Methylcyclohexane	5.00 (1.00-15.80)		
cis-1,3-Dimethylcyclopentane	0.36 (0.00-0.68)		
Ethylcyclohexane	0.00 (0.00-0.00)		
trans-1,3-Dimethylcyclopentane	0.37 (0.00-0.68)		
1,2,4-Trimethylcyclopentane	0.31 (0.00-0.68)		
1,2,3-Trimethylcyclopentane	0.15 (0.00-0.34)		
trans-1,4-Dimethylcyclohexane	0.48 (0.00-1.02)		
trans-1,3-Dimethylcyclohexane	0.09 (0.00-0.34)		
cis-1,3-Dimethylcyclohexane	0.13 (0.00-0.34)		
1,1,3-Trimethylcyclohexane	0.38 (0.00-0.68)		
1,2,4-Trimethylcyclohexane	0.30 (0.00-0.68)		
trans-1-Ethyl-4-methylcyclohexane	0.30 (0.00-0.68)		
cis-1-Ethyl-4-methylcyclohexane	0.35 (0.00-0.68)		
Propylcyclohexane	0.39 (0.00-0.68)		
Butylcyclohexane	0.29 (0.00-0.68)		
Nonylcyclohexane		7.40 (1.17-19.38)	
Decylcyclohexane		11.08 (2.74-32.62)	
Undecylcyclohexane		16.93 (5.61-55.88)	
Dodecylcyclohexane		17.37 (7.63-40.41)	
Tridecylcyclohexane		18.89 (7.34-34.97)	
Tetradecylcyclohexane		18.97 (9.81-37.20)	
Pentadecylcyclohexane		21.96 (5.88-33.07)	
Hexadecylcyclohexane		11.44 (3.25-20.89)	
Heptadecylcyclohexane		5.30 (0.71-9.54)	
Octadecylcyclohexane		1.56 (0.00-2.77)	
Unsaturated Cyclic Hydrocarbons			
Cyclopentene	0.28 (0.00-1.10)		
1-Methylcyclopentene	0.08 (0.00-0.34)		
Biogenic Hydrocarbons			
Isoprene	0.70 (0.00-4.50)		
α-Pinene	0.51 (0.00-1.71)		
d-Limonene	0.33 (0.00-1.02)		
Squalene		47.41 (9.62-124.25)	
Tricyclic Terpanes			
8β,13α-Dimethyl-14β-n-butylpodocarpane		3.91 (1.99-5.80)	
8β,13α-Dimethyl-14β-[3'-methylbutyl]podocarpane		1.96 (1.04-2.98)	

Table 4.1 (continued): Non-aromatic hydrocarbons.

Compound and Class	Vapor phase organics by canister sampler ($\mu g/m^3$)	Vapor phase semi-volatile organics by PUF sampling (ng/m^3)	Fine Particulate Organics (ng/m^3)
Diasteranes			
20S,13β(H),17α(H)-Diacholestane			0.29 (0.00-0.99)
20R,13β(H),17α(H)-Diacholestane			0.26 (0.00-0.95)
Hopanes			
22,29,30-Trisnorneohopane			0.60 (0.00-2.86)
22,29,30-Trisnorhopane			0.44 (0.00-1.63)
17α(H),21β(H)-29-Norhopane			1.09 (0.00-4.06)
18α(H)-29-Norneohopane			0.34 (0.00-1.33)
17α(H),21β(H)-Hopane			1.58 (0.00-6.14)
22S,17α(H),21β(H)-30-Homohopane			0.71 (0.00-2.91)
22R,17α(H),21β(H)-30-Homohopane			0.48 (0.00-1.97)
22S,17α(H),21β(H)-30-Bishomohopane			0.48 (0.00-1.77)
22R,17α(H),21β(H)-30-Bishomohopane			0.37 (0.00-1.68)
Steranes			
20R,5α(H),14β(H),17β(H)-Cholestane			0.31 (0.00-1.02)
20R,5α(H),14α(H),17α(H)-Cholestane			0.44 (0.00-1.24)
20R+S,5α(H),14β(H),17β(H)-Ergostane			0.53 (0.00-2.41)
20R+S,5α(H),14β(H),17β(H)-Sitostane			0.48 (0.00-1.67)

are used for C_{14} to C_{28} vapor-phase $\underline{n}$-alkanes; and the quartz fiber filter data are used for the C_{18} to C_{36} particle-phase $\underline{n}$-alkanes. In the cases where individual $\underline{n}$-alkanes were measured on both the PUF plugs and the quartz fiber filters, the data could be summed to give total ambient concentrations.

The vapor/particle partitioning of the eleven $\underline{n}$-alkanes which were measured on both the PUF and quartz fiber filter samples is shown in Figure 4.2a. The vapor/particle partitioning follows carbon number (and volatility), with the lower molecular weight (and more volatile) alkanes being found predominantly in the vapor phase.

Vapor/particle partitioning has been widely studied, resulting in mathematical models which describe the partitioning process [10-13]. The partitioning constant ($K_{i,opm}$) was calculated:

$$K_{i,opm} = \frac{P_i}{G_i \sum_k P_k} \tag{4.1}$$

where P_i and G_i (μg m^{-3}) are the atmospheric concentrations of an individual organic compound in the particle-phase and vapor-phase, respectively, and $\sum_k P_k$ is the total concentration of fine particulate organic compounds (μg m^{-3}) [6]. Observational data have shown that for urban particulate matter the partitioning constant can be related to the saturation vapor pressure over a liquid pool of the organic compound of interest, p_L^0, according to:

$$log K_{i,opm} = m_{r,opm} log p_L^0 + b_{r,opm} \tag{4.2}$$

To perform such a check on the *n*-alkane data from the present experiment, vapor pressures (in torr) were calculated according to the Antoine equation using ambient temperatures during sampling, with the constants for the individual alkanes calculated according to the work of Kadowaki [14]. The total fine particle organic compound concentration was estimated in the present study as 1.4 times the measured fine particle organic carbon. The regression equation based on all four-hour average samples from the four urban sites is given below $\pm$ one standard deviation:

$$log K_{i,opm} = (-1.10 \pm 0.03) log p_L^0 + (-6.83 \pm 0.37); n = 292, r = 0.90 \tag{4.3}$$

The nominal slope estimate is steeper than the value of -1.0 predicted from theory, most likely due to filter artifacts during sampling.

The possibility of penetration of semivolatile organics through the PUF plugs (breakthrough) was monitored on a test sample taken for this purpose during these experiments. The five consecutive foam plug sections used in

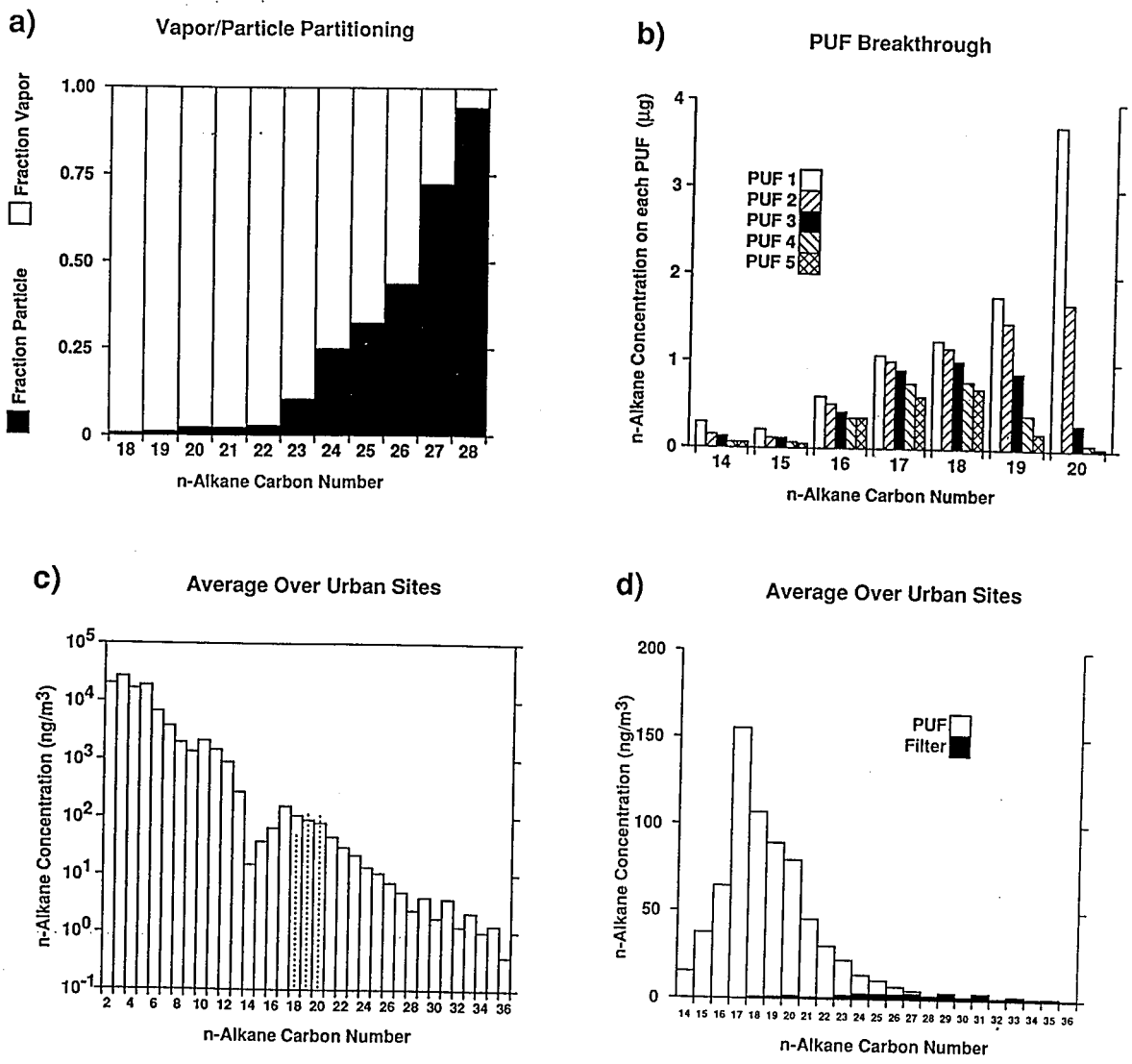

Figure 4.2:
Atmospheric concentrations and characteristics of the n-alkanes. (a): Vapor/particle partitioning of 11 n-alkanes measured in both the vapor and particle phases, averaged over all sampling periods at the four urban air monitoring sites. (b): Penetration of semivolatile n-alkanes through consecutive polyurethane foam plug sections. PUF1 was immediately downstream of the quartz fiber filter, PUF2 downstream of PUF1, etc. (c): Distribution according to carbon number of the n-alkanes concentrations averaged over all sampling periods at the four urban sites. Dashed lines at C_{18}, C_{19} and C_{20} show the concentrations of the isoprenoid alkanes norpristane, pristane, and phytane, respectively, for purposes of comparison of comparable molecular weight. (d): Comparison of vapor phase semivolatile n-alkanes to the particle phase n-alkanes.

sampling were divided, each plug was extracted separately, and the *n*-alkanes measured on each plug were quantified. Seven *n*-alkanes in the range from C_{14} to C_{20} were found on all five of the PUF plugs, as shown in Figure 4.2b. The data presented show the total *n*-alkane mass extracted from each of the five PUF plugs, with PUF1 being located immediately downstream the quartz fiber filter, PUF2 located downstream of PUF1, etc. Unlike the vapor/particle partitioning data shown in Figure 4.2a where the partitioning correlates directly with carbon number, breakthrough appears to depend on both the carbon number (volatility) and the ambient concentration of the alkane in question. The alkane mass on the last (5th) PUF plug is 9.1% of the mass collected on all PUF plugs for the C_{14} alkane; 9.2% for the C_{15} alkane; 15.7% for the C_{16} alkane; 13.7% for the C_{17} alkane; 14.1% for the C_{18} alkane; 3.9% for the C_{19} alkane; and 0.4% for the C_{20} alkane.

The distribution of the *n*-alkane concentrations according to carbon number averaged over all samples taken at the four urban sites (Long Beach, Central Los Angeles, Azusa, and Claremont) is shown on a log scale in Figure 4.2c. The abundance of the *n*-alkanes falls almost exponentially with increasing *n*-alkane carbon number. From C_{14} to C_{16}, the ambient concentration measured is lower than a linear extrapolation through the data (on a log scale), although the distribution of hydrocarbons in unrefined petroleum generally falls along a smooth curve [15]. The lower concentrations of the C_{14}-C_{16} *n*-alkanes may arise from the use of various processes at petroleum refineries to segregate hydrocarbons into different product streams and to crack higher molecular weight organics into molecules suited for blending into lighter and more valuable fuels, but a more likely explanation is that the brief dip in the relative atmospheric concentrations of the *n*-C_{14} - *n*-C_{16} alkanes may represent a reduced sampling efficiency for the PUF plugs for

the lowest molecular weight species captured by the PUFs. At high alkane carbon numbers, between the C_{29} to C_{35} alkanes, a sawtooth pattern is apparent in the data in Figure 4.2c, which reflects vascular plant wax inputs to the atmosphere that are enriched in the odd carbon number $\underline{n}$-alkanes [2,3].

In Figure 4.2d, the semivolatile vapor phase $\underline{n}$-alkanes measured on PUF cartridges and the particle phase $\underline{n}$-alkanes measured by filter sampling are compared on a linear scale. The most obvious feature of this figure is the dominance of $\underline{n}$-alkanes in the vapor phase collected on the PUF plugs. The distribution of gas phase $\underline{n}$-alkanes shows no obvious preference of even or odd carbon number homologs, suggesting that the alkanes in this range are from geologically mature sources (fossil fuels) [2]. Further, high concentrations of norpristane (2,6,10-trimethylpentadecane), pristane (2,6,10,14-tetramethylpentadecane) and phytane (2,6,10,14-tetramethylhexadecane) were measured during these experiments (see Table 4.1 and dashed lines in Figure 4.2c), which is consistent with fossil sources of carbon in the range of C_{16} to C_{20}, which is approximately the distillation range of diesel fuels [16]. In contrast the particulate alkanes present in the filter extracts show two groups of $\underline{n}$-alkanes having different characteristics: a lower molecular weight group with carbon number maxima at about $\underline{n}$-C_{25} having no carbon number preference (characteristic of petroleum) and a higher molecular weight group showing a strong odd carbon predominance, especially above $\underline{n}$-C_{29} (characteristic of recent biological origin, e.g., plant waxes). The dominant residual in the higher molecular weight group (odd $\underline{n}$-alkane most enriched over adjacent even $\underline{n}$-alkanes) is the C_{31} $\underline{n}$-alkane, consistent with results of leaf wax abrasion source testing for the Southern California area [17].

4.3.2 Alkenes

The most striking characteristic of the alkene compound class (in the range of two to eight carbons) is the strong diurnal variation. Averaged over all sampling periods at the four urban sites studied, the branched and normal alkenes comprise 14.7% of the non-aromatic hydrocarbons, but that ratio varies from a maximum 21.9% during the 6 a.m. - 10 a.m. morning traffic peak at Central Los Angeles on Sept. 9, 1993, to a minimum of 7.2% in the 12 noon - 4 p.m. afternoon period at Claremont on Sept. 9, 1993. Gas phase photochemical reactions deplete the reactive olefins during downwind transport with dramatic reductions between the morning conditions seen in areas of high traffic density versus the afternoon sampling periods at photochemical smog receptor sites like Claremont and Azusa [18,19]. This depletion was quantified for the individual olefins by computing the fractional depletion of the concentration of specific olefins as follows: the olefin to acetylene concentration ratio found in the 12 noon to 4 p.m. sample taken at Azusa on Sept. 8, 1993, was divided by the olefin to acetylene concentration ratio present in the 6 a.m. to 10 a.m. sample taken upwind of Azusa earlier that morning at Central Los Angeles. Olefin concentrations were normalized by the slow reacting motor vehicle exhaust tracer acetylene measured in the same sample to adjust for dilution with increased afternoon mixing depths. Olefins from gasoline evaporation that have a spatial distribution similar to vehicle traffic are included in this analysis, but biogenic olefins are excluded. The relative depletion of the olefins over transport from Central Los Angeles to Azusa is shown in Figure 4.3 as a function of each olefin's initial reaction rate with the hydroxyl radical. Reaction rates were available for 17 of the measured olefins [20]. This figure shows the depletion of the more reactive alkenes, with many alkenes being below detection limits in the afternoon sample.

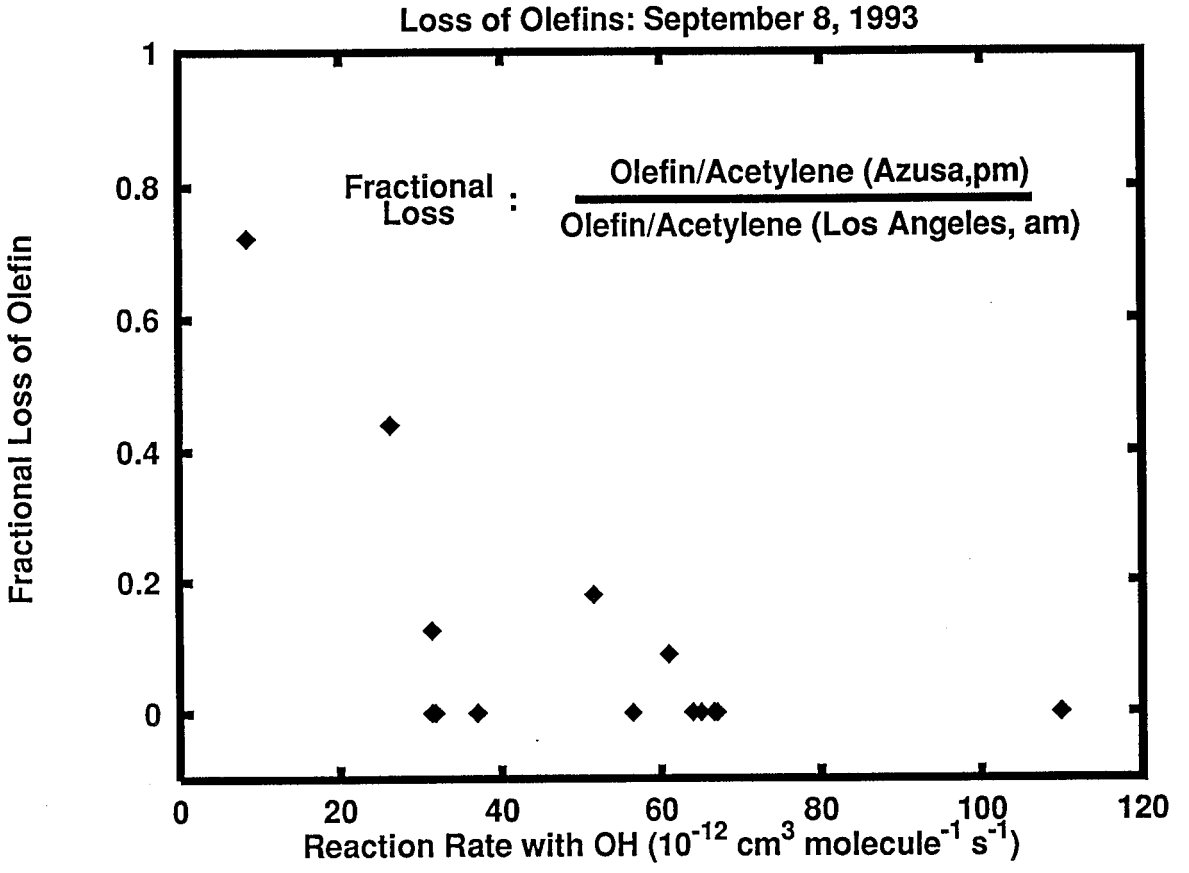

Figure 4.3:
Depletion of olefins between a morning sampling period in Central Los Angeles and an afternoon sampling period downwind at Azusa. All olefin concentrations are normalized by acetylene to correct for dilution by increased afternoon mixing depths. The depletion is plotted against olefin reaction rate with the hydroxyl radical.

4.3.3 Alkynes

The alkyne acetylene was quantified during this experiment. Acetylene in the Los Angeles atmosphere is due almost entirely to motor vehicle exhaust, with only small contributions from other sources [21]. Since acetylene is formed during combustion and is not present in gasoline, acetylene can be used to distinguish tailpipe emissions from sources of gasoline evaporation. The reaction rate of acetylene with the hydroxyl radical and ozone is slow compared to other volatile organic compounds of interest [20]. For these reasons, acetylene will be used to trace motor vehicle exhaust in this study.

4.3.4 Biogenic Hydrocarbons

Biogenic hydrocarbons measured in addition to the previously mentioned plant wax derived high molecular weight alkanes include squalene, isoprene, α-pinene, and d-limonene. Isoprene is emitted by plants only during daylight hours [22]. Isoprene concentrations measured during this study do indicate such a daytime source with average urban concentrations of 0.36 μg m^{-3} in the midnight to 4 a.m. samples, 0.70 μg m^{-3} in the 6 a.m. to 10 a.m. samples, 1.31 μg m^{-3} in the noon to 4 pm samples, and 0.41 μg m^{-3} in the 6 p.m. to 10 p.m. samples. Isoprene concentrations were highest in Claremont, consistent with previous investigations [23]. Monoterpenes are emitted from vegetation both during the day and night [22]. The monoterpenes α-pinene and d-limonene were detected in overnight and early morning samples in Central Los Angeles and Azusa. At Claremont α-pinene was the only monoterpene detected, and it was found in only one early morning sample, while at Long Beach d-limonene was the only monoterpene detected, again in only one early morning sample. That emissions of monoterpenes occur both day and night but that ambient concentrations are measurable only at night and during

early morning hours is consistent with destruction of these highly reactive substances during daylight photochemical smog periods.

4.3.5 Petroleum Biomarkers

Molecular markers are indicator compounds that can be utilized to trace the source of organic matter [24,25]. Such molecules have definitive chemical structures which can be related either directly or indirectly via a set of diagenetic or environmental changes to their source. These sources may be biogenic, geologic, or synthetic [24]. The biomarkers of utility for fingerprinting petroleum residues are comprised mainly of isoprenoid alkanes, triterpanes (hopanes), steranes, and the unresolved complex mixture (UCM) [26]. Considerable effort has been invested in identifying and quantifying petroleum biomarkers [2,27,28]. The petroleum biomarkers quantified during this study include hopanes, steranes, diasteranes, and tricyclic terpanes, as well as the isoprenoid alkanes (Table 4.1). While these compounds comprise only a small fraction of the organics mass in urban air pollution, the hopanes and steranes can be measured in motor vehicle exhaust and can be used as particle-phase tracers of the contribution of motor vehicle exhaust to ambient pollutant concentrations [2,29-31]. The diurnal variations of the sum of the hopanes plus steranes is shown in Figure 4.4. As expected, these vehicle exhaust tracers typically reach their highest concentrations during the morning traffic peak, particularly at Central Los Angeles.

4.3.6 Unresolved Complex Mixture

An unresolved complex mixture (UCM) of branched and cyclic hydrocarbons exists in ambient semivolatile vapor phase organics and particulate organics samples. The UCM appears as a hump on GC traces and underlies the hundreds of individual peaks that can be resolved chromatographically.

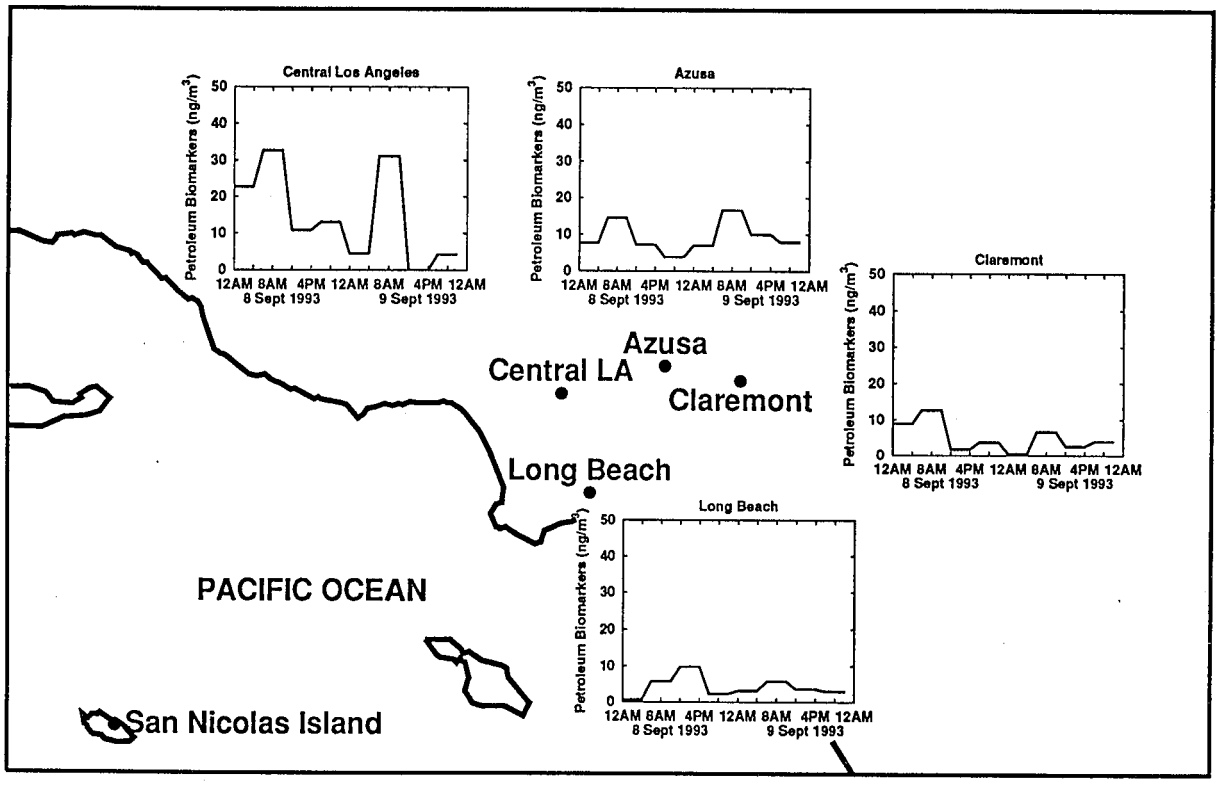

Figure 4.4:
Diurnal variation in the sum of the triterpanes (hopanes) and steranes used as vehicle exhaust tracers.

In this study, the quantities of organics present in two separate UCM humps were measured. The semivolatile organics samples collected on polyurethane foam contain an UCM having a peak concentration that elutes from the GC column between the elution points of the C_{17} and C_{18} $\underline{n}$-alkanes. The particulate organics samples collected on the quartz fiber filters contain an UCM having a concentration maximum between the elution points of the C_{25} and C_{26} $\underline{n}$-alkanes. The magnitude of each UCM was quantified in each sample by integrating the total ion current corresponding to the UCM hump over successive intervals defined by the elution points of the series of the $\underline{n}$-alkanes (see [32]). The response factor for the $\underline{n}$-C_n alkane was used to convert area counts to mass concentrations for all UCM counts falling between the elution points of the $\underline{n}$-C_n to $\underline{n}$-C_{n+1} alkane. Figure 4.5 shows a comparison of the concentration of branched, cyclic, and normal alkanes from the canister, PUF, and particulate matter filter samples. On the PUF and filter samples, the UCM is plotted for purposes of comparison. The organic compounds contained within the UCM are unresolved because the variations due to branching increase with molecular size, yielding so many isomers that complete separation becomes impossible. Figure 5 shows that for the larger molecules, the degree of branching increases until the UCM dominates over the normal isomers.

4.3.7 Regional Background Concentrations at San Nicolas Island

A knowledge of VOC concentrations upwind of the Los Angeles area is critical to the success of photochemical air quality modeling studies in Southern California because such measurements are needed to set the boundary conditions for inflows into the modeling region [33]. During the present experiments, measurements of volatile, semivolatile, and particle-phase organics

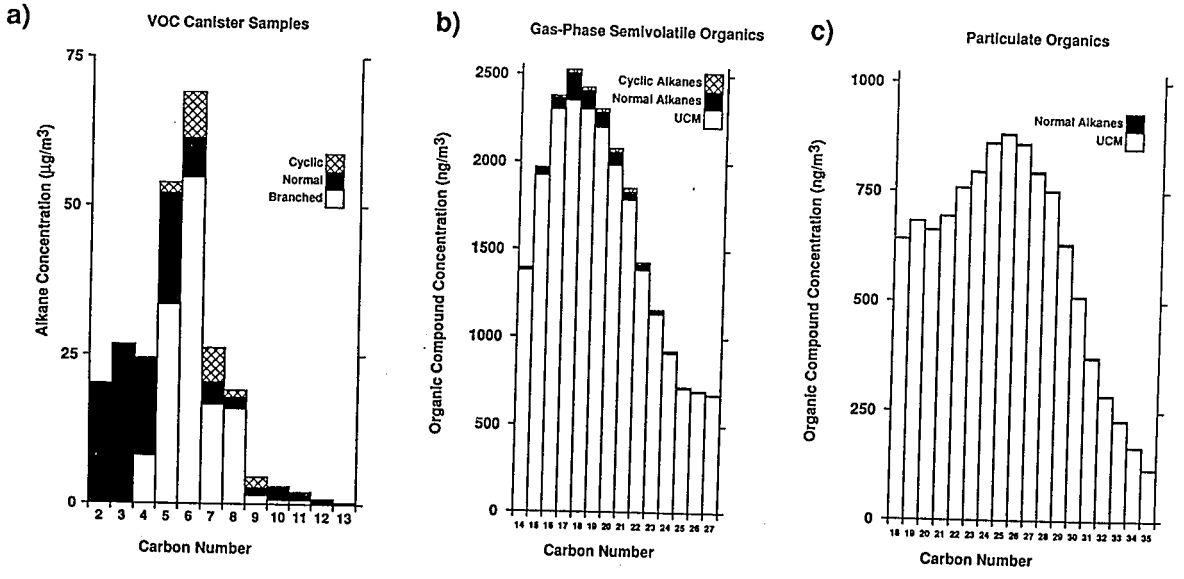

Figure 4.5:
Comparison of the branched, cyclic, and normal alkanes: (a) volatile organic compounds, (b) gas-phase semivolatile organic compounds collected on PUF cartridges, and (c) particle-phase organics. Branched and cyclic alkanes present as an unresolved complex mixture (UCM) on the PUF and particle-phase samples are shown for purposes of comparison, where the UCM mass concentrations graphed at carbon number C_n is that eluting between the elution points of the C_n and C_{n+1} $\underline{n}$-alkanes.

were made at San Nicolas Island, located approximately 100 km south and west of the Los Angeles area coastline (see location in Figure 4.4). In Table 4.2, the average concentrations and range of concentrations measured in the four samples collected at San Nicolas Island are given along with the ratios of the average concentrations at San Nicolas Island to the average concentrations at the urban air monitoring sites for those non-aromatic hydrocarbons that are above detection levels at San Nicolas Island.

The compounds measured at San Nicolas Island can be divided into separate classes representative of different source types. Squalene, a biogenic hydrocarbon that is an intermediate in the biosynthesis of steroids and triterpenoids is present at concentrations at San Nicolas Island that are nearly as high as within the Los Angeles urban area. The olefin 2,4,4-trimethyl-1-pentene also is present at considerable levels at San Nicolas Island, at 16% of urban concentrations. The source of this compound is at present unknown. A number of the intermediate molecular weight ($\underline{n}$-C_{20} - $\underline{n}$-C_{28}) $\underline{n}$-alkane homologs are present at San Nicolas Island at approximately 10% of their urban levels. Finally, the petroleum markers, pristane and phytane, and the slowly reacting auto exhaust tracer acetylene are found in the San Nicolas Island atmosphere at about 2% of their average concentration within the Los Angeles urban area. The highly reactive olefinic hydrocarbons emitted from motor vehicle exhaust, such as 1,3-butadiene, are below detection limits at San Nicolas Island. This suggests that the atmosphere at San Nicolas Island can be described as a mixture of biogenically derived organic compounds combined with aged, diluted petroleum hydrocarbons and their combustion products.

Table 4.2: Non-aromatic hydrocarbons: average (and range) of the San Nicolas Island concentrations and ratio of concentrations at San Nicolas Island to urban mean concentrations, Sept. 8-9, 1993.

Compound	San Nicolas Concentration ($\mu g\ m^{-3}$)	Ratio San Nicolas to Urban
Squalene	42.21 (21.10-51.46)	0.890
2,4,4-Trimethyl-1-pentene	0.15 (0.00-0.40)	0.161
n-Hexacosane	1.04 (0.36-1.89)	0.142
n-Pentacosane	1.24 (0.75-1.99)	0.115
n-Heptacosane	0.49 (0.00-1.28)	0.098
n-Eicosane	6.51 (4.54-10.00)	0.082
n-Tetradecane	1.16 (0.58-2.01)	0.077
n-Tetracosane	1.02 (0.63-1.58)	0.075
n-Docosane	2.04 (1.34-3.67)	0.068
3-Methylhexane	0.33 (0.00-0.80)	0.060
n-Tricosane	1.26 (0.90-1.66)	0.057
Ethane	1.03 (1.00-1.10)	0.051
2-Methylhexane	0.23 (0.00-0.50)	0.050
n-Octadecane	4.61 (3.57-7.06)	0.043
n-Pentadecane	1.46 (0.78-2.35)	0.039
n-Nonadecane	3.30 (2.26-4.37)	0.037
n-Hexadecane	2.13 (1.51-3.43)	0.037
i-Butene	0.08 (0.00-0.10)	0.034
n-Heneicosane	1.41 (1.00-2.02)	0.031
Pristane	3.35 (1.55-5.71)	0.029
n-Heptadecane	4.42 (2.94-7.80)	0.028
Phytane	2.64 (1.45-4.11)	0.024
Acetylene	0.28 (0.20-0.40)	0.019
Propane	0.48 (0.30-0.70)	0.018
n-Nonacosane	0.06 (0.00-0.12)	0.017
Propene	0.10 (0.10-0.10)	0.016
n-Octane	0.03 (0.00-0.10)	0.015
n-Octacosane	0.03 (0.00-0.05)	0.014
n-Butane	0.20 (0.20-0.20)	0.012
i-Butane	0.08 (0.00-0.10)	0.010
n-Hentriacontane	0.04 (0.00-0.06)	0.009
Ethene	0.13 (0.10-0.20)	0.008
n-Pentane	0.10 (0.10-0.10)	0.005
n-Hexane	0.03 (0.00-0.10)	0.005
i-Pentane	0.13 (0.10-0.20)	0.004
2-Methylpentane	0.03 (0.00-0.10)	0.003

4.3.8 Comparison of Potential Tracers for Motor Vehicle Exhaust

Previous studies of particle-phase organic compound emissions in the Los Angeles area show that petroleum biomarkers such as the hopanes and steranes can be used as nearly unique particle-phase tracers of motor vehicle exhaust [30,31]. The vapor phase organic compound acetylene likewise is attractive as a vehicle exhaust tracer because it is formed in combustion, reacts slowly in the atmosphere, is not present in gasoline itself so it cannot be confused with hydrocarbon evaporative emissions, and has few sources other than vehicle exhaust in the Los Angeles area [21]. The present study provides a unique opportunity to compare the concentrations of these particle-phase and gas-phase vehicle exhaust tracers. The Pearson correlation coefficient was computed between the sum of all particle-phase petroleum biomarkers concentrations (sum of hopanes and steranes) versus the acetylene concentration measured simultaneously at each urban sampling site over each period of observation (32 sample sets). As shown in Table 4.3, these alternative tracer concentrations track each other with a correlation coefficient of 0.82. A search was conducted to identify a compound present in the semivolatile organics samples that may serve an analogous purpose. The petroleum biomarker phytane would be expected to arise from motor vehicle exhaust in the same way as is the case for the hopanes and steranes, although further source test data and emission inventory data will be needed to confirm this. Table 4.3 shows that phytane concentrations also correlate about as well with acetylene and the particle-phase petroleum biomarkers concentrations as acetylene and the higher molecular weight particulate petroleum biomarkers correlate with each other.

Table 4.3: Pearson Correlation coefficients between gas-phase and particle-phase vehicle exhaust tracers.

Marker Number	1	2	3
(1) Acetylene	1.00	0.82	0.78
(2) Hopanes + Steranes	0.82	1.00	0.86
(3) Phytane	0.78	0.86	1.00

Marker Categories:

[1] Acetylene, a tracer for motor vehicle exhaust which is not present in petroleum or its dervitives.

[2] The hopanes + steranes category is a summation of the triterpanes (hopanes) and steranes listed in Table 4.1.

[3] Phytane (2,6,10,14-tetramethylhexadecane).

4.3.9 Long Term Trends in Hydrocarbon Concentrations

The present work represents the first thorough study of vapor phase organics concentrations published for the Los Angeles area since the Southern California Air Quality Study (SCAQS) was conducted in 1987. Similarly, the particle-phase organics data developed during the present experiments provide the first opportunity to view high molecular weight petroleum biomarker concentrations since the 1982 study reported by Rogge et al. [3]. Extensive pollution control efforts have been undertaken during the past decade that should have left their mark on the hydrocarbon composition of the Los Angeles atmosphere. Therefore, it is useful to compare the condition of the Los Angeles atmosphere during this 1993 smog episode to conditions present during comparable seasons of previous years. In Table 4.4, vapor phase non-aromatic hydrocarbons concentrations averaged over all urban sites studied during the Sept. 8-9, 1993, smog episode are compared to data taken during the Aug. 28, 1987, episode of the Southern California Air Quality Study. The SCAQS data are average values for Aug. 28, 1987, from eight sites in the Los Angeles Basin (Long Beach, Hawthorne, Central Los Angeles, Ana-

Table 4.4: Comparison of non-aromatic hydrocarbons to SCAQS data.

Compound	Average Concentration 28 August 1987 (SCAQS) (μg m^{-3})	Average Concentration 8-9 September 1993 (μg m^{-3})	Ratio 1993 to SCAQS
1-Butene	2.56	1.02	0.40
n-Butane	32.58	16.45	0.51
Cyclohexane	2.39	1.42	0.60
i-Butane	13.42	8.10	0.60
Propane	41.74	26.74	0.64
Isoprene	0.91	0.70	0.77
n-Heptane	4.66	3.75	0.80
Cyclopentane	2.05	1.71	0.84
3-Methylpentane	8.02	6.88	0.86
n-Hexane	7.73	6.66	0.86
i-Pentane	38.61	33.48	0.87
Methylcyclohexane	5.69	5.00	0.88
n-Octane	2.16	1.95	0.90
2-Methylpentane	11.66	10.66	0.92
Methylcyclopentane	6.71	6.20	0.92
3-Methylhexane	5.80	5.47	0.94
cis-2-Butene	0.57	0.55	0.97
2,3-Dimethylbutane	3.01	2.98	0.99
n-Nonane	1.36	1.36	1.00
Ethane	19.45	20.14	1.04
2,4-Dimethylpentane	2.33	2.47	1.06
n-Pentane	17.63	18.75	1.06
Ethene	14.78	15.80	1.07
2-Methylhexane	4.26	4.64	1.09
2,2-Dimethylbutane	0.80	0.90	1.13
Propene	5.40	6.29	1.16
2,2,4-Trimethylpentane	6.14	7.19	1.17
2,3-Dimethylpentane	3.30	3.89	1.18
1,3-Butadiene	0.68	0.81	1.19
Acetylene	11.60	14.47	1.24
trans-2-Butene	0.57	0.75	1.32

heim, Burbank, Azusa, Claremont, and Rubidoux) [22,34]. The averaging is done to represent an average concentration across the air basin. The four sites used during SCAQS and not sampled during 1993 are distributed in a fashion analogous to the four sites that were used (one near the coast, one approximately 20 km inland, one at a mid-basin smog receptor site, and one far downwind). These two episodes are closely matched by both season of the year and level of photochemical activity. The peak 1-h average ozone concentration of 0.29 ppm over the Sept. 8-9, 1993, episode occurred on Sept. 9, 1993, at Claremont, while the 1-h average ozone peak on Aug. 28, 1987, reached 0.29 ppm at Glendora, just slightly west of Claremont. Additionally, mixing depths were similar during the two experiments. Vertical temperature profiles measured at Claremont on September 9, 1993, indicate a mixing depth between 300 and 400 m at 1400 PST [35,36], compared to a mixing depth during the August 28, 1987, SCAQS experiment of 440 m at 1400 PST [37].

The most obvious feature of the VOC data shown in Table 4.4 is that many of the lightest blending components of gasoline (e.g., *n*-butane and i-butane) are considerably depleted in the 1993 Los Angeles atmosphere when compared with corresponding hydrocarbons measured in 1987. This reflects the reformulation of gasolines to remove the lightest components in order to comply with new regulations that further restrict the Reid vapor pressure of gasoline (RVP) [16]. The limit on the RVP of summer gasoline in 1987 was 9.0 PSI, and was reduced to 7.8 PSI in 1992. Additionally, cyclohexane is depleted in the 1993 atmosphere compared to 1987. One approach to reducing the benzene content of gasoline is the removal of cyclohexane and methylcyclopentane from petroleum feed stocks [38], and the lower 1993 ambient concentrations of these compounds when compared to 1987 may re-

flect ongoing efforts to reduce benzene in gasoline. Most of the remaining non-aromatic hydrocarbons present during the 1993 smog episode studied are found at ±20% of their concentrations observed during the 1987 episode; indeed if that were not the case, the ozone concentrations reached during the two smog episodes probably would not have been so similar. The high NO_x levels measured in the 1993 experiment [6] lead to lower NMHC to NO_x ratios than measured during the 1987 SCAQS experiments. Measured during the 0600-1000 PDT sampling period on September 8-9, 1993, this ratio ranged from 4.2 to 6.9 and averaging 5.4 for the four urban sites. The NMHC to NO_x ratio for these same four sites ranged from 7.5 to 8.8 during the summer SCAQS experiments, and averaged 8.1 during a similar time of day (0700-0800 PDT) [19].

The hopanes and steranes are petroleum biomarkers that are found in the particulate matter emissions from motor vehicles [30]. They can be used to trace particle emissions from vehicles in Los Angeles where it can be shown that vehicle exhaust dominates the local emissions of such compounds [31]. In Table 4.5 the hopanes and steranes concentrations present at Central Los Angeles during the September 1993 experiment reported here are compared to the September 1982 monthly average hopane and steranes concentrations at Central Los Angeles contained in the data base compiled by Rogge et al. [3]. The 1993 data do not show decreased hopanes and steranes concentrations when compared with those of a decade earlier. Source test data show that catalyst equipped autos have greatly decreased hopanes, steranes and organic aerosol mass emission rates when compared to earlier non-catalyst equipped autos [30,32]. With vehicle turnover replacing older pre-catalyst cars with catalyst-equipped vehicles, one would be expected to reduced concentrations of particulate organic tracers for vehicle exhaust aerosol. However

Table 4.5: Average concentrations of petroleum biomarkers at Central Los Angeles in September 1982 and 1993.

Compound	September 1982 Concentrations	8-9 September 1993 Concentrations	Ratio 1993 to 1982
22,29,30-Trisnorneohopane	0.57	0.60	1.0
17α(H),21β(H)-29-Norhopane	0.92	1.09	1.2
17α(H),21β(H)-Hopane	1.80	1.58	0.9
22S,17α(H),21β(H)-30-Homohopane	0.80	0.71	0.9
22R,17α(H),21β(H)-30-Homohopane	0.61	0.48	0.8
22S,17α(H),21β(H)-30-Bishomohopane	0.39	0.48	1.2
22R,17α(H),21β(H)-30-Bishomohopane	0.29	0.37	1.3
20R,5α(H),14α(H),17α(H)-Cholestane	0.27	0.31	1.2
20R+S,5α(H),14β(H),17β(H)-Ergostane	0.47	0.53	1.1
20R+S,5α(H),14β(H),17β(H)-Sitostane	0.61	0.48	0.8

this trend is not observed in the ambient data.

Bibliography

[1] National Research Council *Rethinking the Ozone Problem in Urban and Regional Air Pollution*, National Academy Press: Washington DC, 1991.

[2] B. R. T. Simoneit. "Characterization of organic-constitutents in aerosols in relation to their origin and transport- a review" *Intern. J. Environ. Anal. Chem.*, 23: 207-237, 1986.

[3] W. F. Rogge, L. M. Hildemann, M. A. Mazurek, B. R. T. Simoneit and G. R. Cass. Quantification of urban organic aerosols at a molecular level: identification, abundance, and seasonal variation. *Atmos. Environ.*, 27A: 1309-1330, 1993.

[4] T. I. Chan and M. Lippmann. Experimental measurements and empirical modelling of the regional deposition of inhaled particles in humans. *Am. Ind. Hyg. Assoc. J.*, 41: 399-409, 1980.

[5] D. W. Dockery, C. A. Pope, X. Xu, J. D. Spengler, J.H. Ware, M. E. Fay, B. G. Ferris and F. E. Speizer. An association between air-pollution and mortality in Six United States cities. *N. Engl. J. Med.*, 329: 1753-1759, 1993.

[6] M. P. Fraser, D. Grosjean, E. Grosjean, R. A. Rasmussen and G. R. Cass. Air quality model evaluation data for organics. 1. Bulk chemical composition and gas/particle distribution factors. *Environ. Sci. Technol.*, 30: 1731-1743, 1996.

[7] R. A. Rasmussen. SCAQS hydrocarbon collection and analysis. Report to the California Air Resources Board under contract A6-179-32; Biospherics Research Corp.: Hillsboro, OR, 1990.

[8] P. A. Solomon, J. L. Moyers and R. A. Fletcher. High-volume dichotomous virtual impactor for the fractionation and collection of particles according to aerodynamic size. *Aerosol Sci. Technol.*, 2: 455-464, 1983.

[9] M. A. Mazurek, B. R. T. Simoneit, G. R. Cass and H. A. Gray. Quantitative high-resolution gas chromatography and high-resolution gas chromatography/mass spectrometry analyses of carbonaceous fine aerosol particles. *Inter. J. Environ. Anal. Chem.*, 29: 119-139, 1987.

[10] C. E. Junge. Basic considerations about trace constituents in the atmosphere as related to the fate of global pollutants. In *Fate of Pollutants in Air and Water Environments*, Part I; Wiley: New York, 1977.

[11] J. F. Pankow and T. F. Bidleman. Interdependance of the slopes and intercepts from log-log correlations of measured gas-particle partitioning and vapor pressure-I. Theory and analysis of available data. *Atmos. Environ.*, 26A: 1071-1080, 1992.

[12] J. F. Pankow. An absorption model of gas/particle partitioning of organic compounds in the atmosphere. *Atmos. Environ.*, 28: 185-188, 1994.

[13] C. Liang and J. F. Pankow. Gas/particle partitioning of organic compounds to environmental tabacco smoke: partition coefficient measurements by desorption and comparison to urban particulate material. *Environ. Sci. Technol.*, 30: 2800-2805, 1996.

[14] S. Kadowaki. Characterization of carbonaceous aerosols in the Nagoya urban area. 2. Behavior and origin of particulate n-alkanes. *Environ. Sci. Technol.*, 28: 129-135, 1994.

[15] R. P. Philp. Oil-oil and oil-source rock correlations: techniques. In *Organic Geochemistry*, Engel, M.H.; Macko, S.A. Eds.; Plenum Press: New York, 1993.

[16] J. H. Gary and G. E. Handwerk. *Petroleum Refining*, 2nd ed.; Marcel Dekker: New York, 1984.

[17] W. F. Rogge, L. M. Hildemann, M. A. Mazurek, B. R. T. Simoneit and G. R. Cass. Sources of fine organic aerosol. 4. Particulate abrasion products from leaf surfaces of urban plants. *Environ. Sci. Technol.*, 27: 2700-2711, 1993.

[18] J. G. Calvert. Hydrocarbon involvement in photochemical smog formation in Los Angeles atmosphere" *Environ. Sci. Technol.*, 10: 256-262, 1975.

[19] E. M. Fujita, B. E. Croes, C. L. Bennett, D. R. Lawson, F. W. Lurmann, M. M. Main. Comparison of emission inventory and ambient concentration ratios of CO, NMOG, and NO_x in California's South Coast Air Basin. *J. Air Waste Manage. Assoc.*, 42: 264-276, 1992.

[20] R. Atkinson. Gas-phase tropospheric chemistry of organic compounds: a review. *Atmos. Environ.*, 24A: 1-41, 1990.

[21] R. A. Harley, M. P. Hannigan and G. R. Cass. Respeciation of organic gas emissions and the detection of excess unburned gasoline in the atmosphere. *Environ. Sci. Technol.*, 26: 2395-2408, 1992.

[22] R. A. Rasmussen. Isoprene: identification as a forest-type emission to the atmosphere. *Environ. Sci. Technol.*, 4: 667-671, 1970.

[23] F. W. Lurmann and H. H. Main. Analysis of the ambient VOC data collected in the Southern California Air Quality Study. Report to the California Air Resources Board under contract A832-130; Sonoma Technology, Inc.: Santa Rosa, CA, 1992.

[24] B. R. T. Simoneit. In *Chemical Oceanograhy*, 2nd ed.; J. P. Riley and R. Chester, Eds.; Academic Press: New York, 1978.

[25] B. R. T. Simoneit. In *Proc. Symp. Marine Chem. into the Eighties*, J. A. J. Thompson and W. D. Jamieson, Eds.; Nat. Res. Council of Canada: Ottawa, 1982.

[26] K. E. Peters and J. M. Moldowan. *The Biomarker Guide*. Prentice-Hall: Englewood Cliffs, NJ, 1993.

[27] R. B. Johns, Ed. *Biological Markers in Sedimentary Record*, Elsevier: Amsterdam, 1986.

[28] B. R. T. Simoneit. In *Biological Markers in the Sedimentary Record*, R. B. Johns, Ed.; Elsevier: Amsterdam, 1986.

[29] B. R. T. Simoneit and M. A. Mazurek. "Organic tracers in ambient aerosols and rain" *Aerosol Sci. Technol.*, 10: 267-291, 1989.

[30] W. F. Rogge, L. M. Hildemann, M. A. Mazurek, B. R. T. Simoneit and G. R. Cass. Sources of fine organic aerosol. 2. Noncatalyst and catalyst-equipped automobiles and heavy-duty diesel trucks. *Environ. Sci. Technol.*, 27: 636-651, 1993.

[31] J. J. Schauer, W. F. Rogge, L. M. Hildemann, M. A. Mazurek, G. R. Cass and B. R. T. Simoneit. Source Apportionment of Airborne Particulate Matter Using Organic Compounds as Tracers *Atmos. Environ.*, 30: 3837-3855, 1996.

[32] L. M. Hildemann, M. A. Mazurek, G. R. Cass and B. R. T. Simoneit. Quantitative characterization of urban sources of organic aerosol by high-resolution gas chromatography. *Environ. Sci. Technol.*, 25: 1311-1325, 1991.

[33] D. A. Winner, G. R. Cass and R. A. Harley. Effect of alternative boundary conditions on predicted ozone control strategy performance: a case study in the Los Angeles area. *Atmos. Environ.*, 29: 3451-3464, 1995.

[34] R. A. Harley and G. R. Cass. Modeling the atmospheric concentrations of individual volatile organic compounds. *Atmos. Environ.*, 29: 905-922, 1995.

[35] A. Lashgari. California Air Resources Board, Sacramento, CA, personal communication, 1997.

[36] D. Wolfe, B. Weber, D. Wuertz, D. Welsh, D. Merritt, S. King, R. Fritz, K. Moran, M. Simon, A. Simon, J. Cogan, D. Littell and E. Measure. An overview of the Mobile Profiler System: preliminary results from field tests during the Los Angeles Free-Radical Study. *Bull. Amer. Meteor. Soc.*, 76: 523-534, 1995.

[37] R. A. Harley, A. G. Russell, G. J. McRae, G. R. Cass and J. H. Seinfeld. Photochemical modeling of the Southern California Air Quality Study.

Environ. Sci. Technol., 27: 378-388, 1993.

[38] J. A. Anabtawi, S. A. Ali M .A. Ali. Impact of gasoline and diesel specifications on the refining industry. *Energy Sources*, 18: 203-214, 1996.

5 Non-polar and Semi-polar Aromatic Compounds

5.1 Introduction

Aromatic compounds constitute one of the most important classes of air pollutants in urban atmospheres. Single-ring aromatic compounds are a main component of both gasoline and many industrial solvents and thus are present in large concentrations in urban air. These volatile aromatic compounds undergo gas-phase chemical reactions, leading to ozone formation and to secondary organic aerosol growth [1,2]. Single-ring compounds such as benzene, and heavier multiple-ring polycyclic aromatic compounds present both in the vapor phase and in urban particulate matter have been studied as human carcinogens and mutagens [3,4].

While aromatic compounds are present both in the vapor phase and in the particle phase, low molecular weight gas-phase aromatic compounds traditionally have been studied separately from the heavier polycyclic aromatic compounds, which partition between the vapor and particle phases. The purpose of this paper is to describe the important features of non-polar and semi-polar aromatic air pollutants across the entire range from C_6 to C_{22} which encompasses the gas-phase, semivolatile and particle-phase aromatics. This will be done within the context of an experiment conducted in Southern California that was designed to acquire time series data for use in the evaluation of comprehensive photochemical airshed models for the prediction of individual organic compound concentrations (e.g., see reference 5). Previous

portions of this work describe the bulk properties of the gas/aerosol mixture [6], and the concentrations of carbonyls [7], peroxyacyl nitrates [8], and non-aromatic hydrocarbons [9] during the same photochemical smog episode. In the present chapter we present results for non-polar and semi-polar aromatic compounds; aromatic acids also are present and are to be discussed in a separate chapter on atmospheric organic acids [10].

5.2 Experimental Methods

5.2.1 Collection of Samples

A field experiment was undertaken in the Los Angeles area during the summer of 1993 to investigate the ambient concentrations of as many individual organic compounds in the vapor and particle phases as possible. Additional details of the field sampling experiment have been reported previously [6].

The data given here were collected by two separate samplers: an internally electropolished stainless steel canister sampler for measuring volatile organic compounds, and a high volume dichotomous virtual impactor combined with a polyurethane foam (PUF) cartridge used to collect particle-phase and semivolatile organic compounds. Data were collected over four-hour sampling intervals that were centered within consecutive six-hour periods during the two-day smog episode of Sept. 8-9, 1993, at the four urban sites and one offshore island site shown in Figure 5.1. The short sampling periods were employed to monitor the diurnal variations in pollutant levels, as well as to minimize possible sampling losses due to volatilization and chemical reaction of material sampled onto filters. Ozone concentrations peaked at a 1-h average value of 0.29 ppm at Claremont on September 9, marking the highest ozone concentration event in that year.

Internally electropolished stainless steel canisters were used to sample

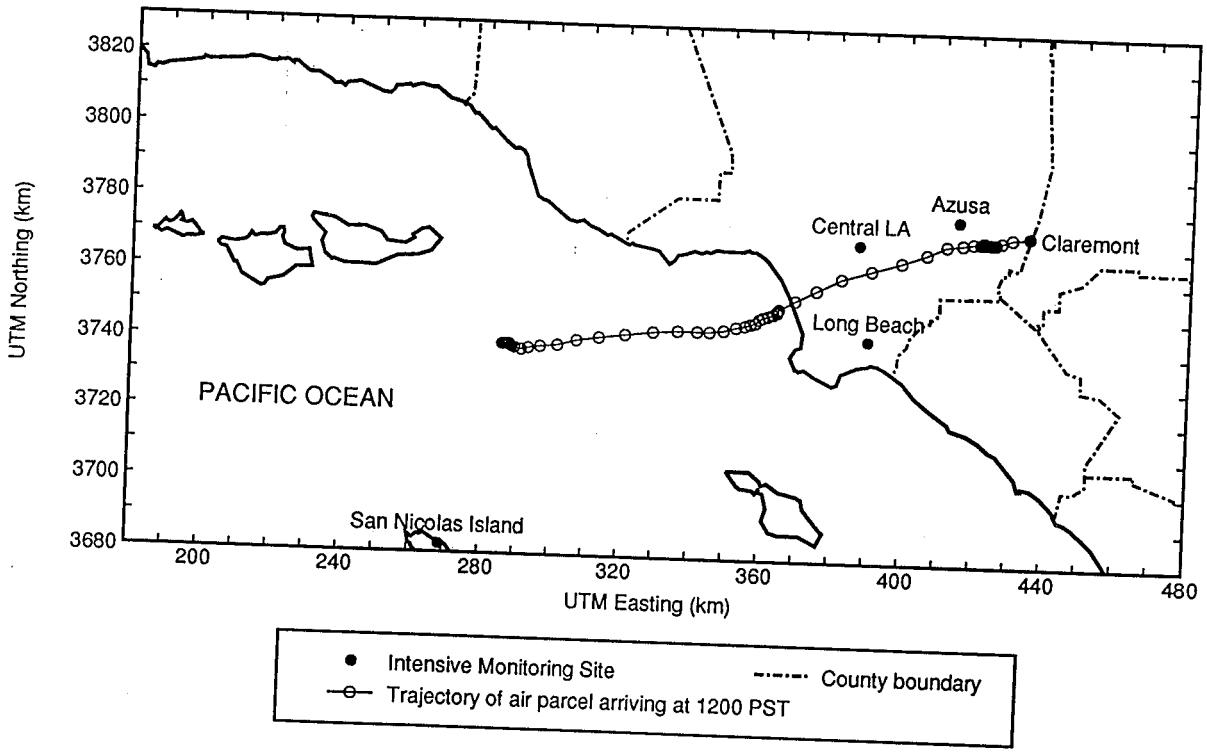

Figure 5.1:
A trajectory showing air parcel arriving at Claremont at 1200 hours PST, September 9, 1993, with each circle representing the position of the air parcel at a previous hour.

volatile organic compounds. These 6-L stainless steel canisters were shipped and deployed to the field under high vacuum, used to collect 4-h integrated samples of volatile organic compounds (VOCs), sealed and returned to the laboratory for analysis.

Fine particle organic compounds were collected at a flow rate of nominally 320 lpm on quartz fiber filters (QFFs: Pallflex 2500 QAO; 102 mm diameter) using a high volume dichotomous virtual impactor [11]. Semivolatile organic compounds were collected at the same flow rate on polyurethane foam (PUF) cartridges located downstream of the fine particle filter of the high volume dichotomous sampler. The quartz fiber filters were annealed at 550°C for at least 8-h before use to lower their carbon blank. Clean filters were transported to the field in annealed aluminum foil packages. PUF plugs (diameter = 7.6 cm) were cut from commercially available polyurethane foam (density = 0.022 g cm^{-3}; Indentation Load Deflection (or ILD) = 30). Five individual plugs (2.5 cm thick) were stacked within an aluminum cartridge to give a total depth of 12.5 cm for each sample collected. The foam plugs were cleaned before use by repeated washings in distilled-in-glass grade dichloromethane (DCM). After sampling, filters were stored in annealed glass jars, and sealed with Teflon tape, and PUF cartridges were sealed with Teflon end caps. Both filter samples and PUF cartridges were refrigerated after removal from the samplers, returned to the laboratory within 12-h, where they were frozen at -21°C until extracted and analyzed.

5.2.2 Analytical Methods

Individual organic compounds were measured by gas chromatography (GC) with flame ionization detection, as well as by gas chromatography-mass spectrometry (GC-MS). The analytical procedures and chromatography condi-

tions are described in great detail elsewhere [9], and will only be summarized here.

Vapor phase organics collected in stainless steel canisters were analyzed using a Hewlett Packard model HP 5890A/3396A GC-FID system. A J&W Scientific DB-1 column (60 m × 0.32 mm i.d. × 1.0 μm film thickness) column was used. Organic material from 500 ml of air was frozen onto glass beads that had been cooled to -183°C by liquid O_2. The organic compounds were desorbed at 100°C and focused onto the column held at -60°C. The GC temperature ramp was held there for 5 min and then increased at 4°C min^{-1} to 200°C.

The VOC canister samples were also analyzed by GC-MS using a Hewlett Packard model HP 5970 MSD/9000/300 mass sensitive detector system. The sample loading procedure trapped 1-5 liters of air on a multibed Tenax TA-Ambersorb-Charcoal trap used in a Dynatherm Analytical Instruments model 890 system. The sample was desorbed at 300°C for 6 min onto glass beads held in liquid N_2 (-196°C). The column focusing and temperature ramp were the same as in the GC-FID procedures. A similar DB-1 column but with a 0.25 mm internal diameter was used in the GC-MS system.

Before extraction, particle filter samples were spiked with a known amount of perdeuterated tetracosane (n-$C_{24}D_{50}$), used to calculate extraction recovery. Two aliquots of hexane, and three aliquots of 2:1 benzene:isopropanol of 35 ml each were used for consecutive extraction steps. The solvent aliquots were added successively to the sample, sonicated for 10 min, then the extracts were removed, filtered through glass wool, and combined in a boiling flask. The extracts were concentrated to between 2 and 4 ml by vacuum aspiration at 35-37°C under reduced pressure. Extracts were transferred into conical vials, and then blown down under a gentle stream of ultra pure nitrogen to

a final volume of approximately 400 μl.

Semivolatile organics samples collected on PUF plugs were spiked with a suite of eight perdeuterated compounds to monitor extraction efficiency and losses during blowdown, ranging in volatility between n-decane and n-tetracosane. The plugs were extracted three times with 250 ml each of DCM, and the extracts were combined in a boiling flask. The volumes were reduced to 2-4 ml by rotary vacuum distillation (30°C under reduced pressure). The concentrated extracts were then transferred to conical vials (15 ml) and further concentrated to approximately 500 μl under gentle nitrogen blowdown. Benzene (2.5 ml) was added to transfer the solutes into that solvent, and then the sample was reconcentrated to a final volume of approximately 300 μl.

After final concentration, both the filter extracts and PUF extracts were divided into two aliquots, with the volume of each aliquot determined with a dedicated 500 μl syringe ($\pm$10 μl markings). One aliquot of each pair was derivatized with diazomethane to convert organic acids to their methyl ester analogs, and aromatic alcohols to their methoxy analogs. Analysis of the underivitized sample in each pair showed none of the aromatic methoxy compounds. After derivatization, the samples were reconcentrated before analysis. All extract aliquots were frozen at -21°C in the dark when in storage.

The particle-phase and semivolatile vapor-phase organics samples were analyzed by GC-MS. All samples were analyzed on a Finnigan 4000 quadrupole gas chromatograph-mass spectrometer. Further information concerning trace organics in the particle phase was obtained using a Finnigan GCQ ion trap gas chromatograph-mass spectrometer after concentrating the aliquots to approximately 20 μl. All analyses used a 30 m DB-1701 capillary column (0.32

mm ID for the Finnigan 4000, 0.25 mm ID for the Finnigan GCQ). For the particle-phase organics, the temperature ramp was as follows: (1) injection into a splitless injection port at 300°C; (2) column isothermal hold at 65°C for 10 min; (3) temperature ramp to 275°C at a rate of 10°C min^{-1}; (4) isothermal hold for 49 min. The temperature ramp for semivolatile-phase organics from the polyurethane foam samples was: (1) injection into a splitless injection port at 300°C; (2) column isothermal hold at 40°C for 10 min; (3) temperature ramp to 100°C at a rate of 4°C min^{-1}; (3) temperature ramp to 275°C at a rate of 10°C min^{-1}; (4) isothermal hold for 17.5 min. For all sample injections, the mass spectrometer scanned from 50 to 500 da once per second, using electron impact ionization at 70 eV. A coinjection standard (1-phenyldodecane) was used to calibrate and monitor the response of the instrument.

5.2.3 Compound Identification

Identification of the VOC compounds was performed by reference to authentic standards and the mass spectral library in the NIST/EPA/MSDC Mass Spectral Database Version 2.

Authentic standards were used for identification of particle phase and semivolatile organics whenever possible. Standards available to us included: acenaphthene, acenaphthylene, anthracene, anthracene-9,10-dione, benz[a]-anthracene, benz[a]anthracene-7,12-dione, benz[de]anthracen-7-one, benzo-[a]pyrene, benzo[b]fluoranthene, benzo[ghi]perylene, benzo[k]fluoranthene, benzyl alcohol, chrysene, coronene, cyclopenta[cd]pyrene, dibenzofuran, dibenzothiophene, 2,6-dimethylnaphthalene, 3,6-dimethylphenanthrene, 2,4-dimethylphenol, 2,6-dimethylphenol, 3,5-dinitrophenol, 1-ethylnaphthalene, 4-ethylphenol, fluoranthene, fluorene, 9H-fluoren-9-one, indan-1-one, indeno[1,2,3-

cd]pyrene, 1(3H)-isobenzofuranone, 2-methylanthracene-9,10-dione, 1-methylnaphthalene, 2-methylnaphthalene, 1-methylphenanthrene, 2-methylphenanthrene, 2-methylphenol, 3-methylphenol, 4-methylphenol, naphthalene, nitrobenzene, 3-nitrobiphenyl, 1-nitronaphthalene, 2-nitronaphthalene, 2-nitrophenol, 4-nitrophenol, perylene, phenalen-9-one, phenanthrene, 9-phenanthrol, phthalan, pyrene, 2,3,5-trimethylphenol, triphenylene, and xanthone. Aromatic alcohols were measured as their methoxy analogs after derivitization by diazomethane. When no standard compounds were available, the retention times and fragmentation patterns of unknowns present were compared to authentic standards of related compounds and established retention indeces [12,13]. Further, the fragmentation patterns of unknown compounds were compared to the National Institute of Standards and Technology (NIST) or Wiley mass spectral reference libraries.

5.2.4 Compound Quantification

Quantification of the VOC compounds from the stainless steel canisters was accomplished using primary calibrations of working standards against NIST SRM standards for benzene (tank #1805) and propane (tank #1665B).

Individual organic compounds from the filter and polyurethane foam extracts were quantified by manually integrating the compound peaks present in the ion chromatograms. The relative ion counts from this integration were converted to compound mass using response factors that relate the ion counts of the compound of interest to the ion counts of the known amount of the coinjection standard. The relative response factors were calculated from injections of authentic standards and the coinjection standard. Where no authentic standards were available, the relative response factors were estimated from the authentic standard of a related compound (i.e., response

factor for benz[de]anthracen-7-one was used for cyclopenta[cd]pyrenone).

In some cases, various isomers of particular organic compounds were encountered. When both the mass spectra and the retention times of authentic standards matched unknowns, exact identification was possible (i.e., 9-phenanthrol). In other cases, the mass spectra match but the retention times did not match. In these cases, the fragmentation pattern and relative retention time were used to confirm the functionality of the compound but not the exact isomer. For example, authentic 3,5-dinitrophenol was used to confirm the dinitrophenol functionality, and ruled out the 3,5- substitution pattern since the retention times did not match exactly.

Corrections for extraction and blowdown losses were accomplished by spiking both filter and PUF samples using perdeuterated recovery standards, and through experiments relating the loss for individual organic compounds relative to the loss for the perdeuterated standards, as described by Mazurek et al. [14]. The ambient concentrations presented in this paper include corrections for such blowdown and extraction losses.

5.2.5 PUF Breakthrough

To monitor PUF breakthrough during this experiment, a test sample was collected before the field program began. This sample was collected in Azusa from 12 noon to 4 p.m. to obtain an upper estimate of the extent of compound breakthrough from the sampling train due to the high summertime temperatures in Southern California. The data presented in Table 5.1 show the mass of aromatic compounds measured on each of the five individual PUF plugs when extracted separately. The data show that naphthalene breaks through the sampling train completely, whereas the heavier PAH (including the 178 and 202 MW PAH) are completely trapped. For this reason the data for

naphthalene and the methyl naphthalenes used throughout this discussion (e.g., Figure 5.2) are from the analysis of the VOC canister samples, not the PUF cartridges. This may lead to an underestimation of the ambient concentrations of the methylnaphthalenes, as comparison between sampling methods suggests that canister sampling for these compounds shows lower concentration than other sampling techniques [15]. Indeed, the ratio between naphthalene and methylnaphthalene concentrations reported here indicates lower concentrations of methylnaphthalenes compared to other similar studies [16]. Estimates of the concentrations of C2, C3, and C4-substituted naphthalenes have been made after correction based on use of the PUF breakthrough data. Exponential decay curves were fit to the PUF breakthrough data, and the concentrations of C2, C3, and C4-substituted naphthalenes were estimated by integrating under these breakthrough curves.

5.2.6 Quality Assurance

Efforts were taken to ensure the integrity of the data collected through all stages of sample collection, extraction, and quantification. Calibrated flow meters were used to measure the air flow through the samplers before and after each sampling period. Samples were refrigerated after collection, and returned to the laboratory, where they were placed in freezers in the dark at -21°C. The extraction grade solvents were distilled-in-glass, and were checked for purity before use. All glassware used in extraction and sample storage was annealed at 550°C for at least 8-h before use; all parts of the solvent transfer lines were solvent rinsed in extraction grade solvents. Procedural blanks for the quartz fiber filters and PUF plugs were analyzed by the same extraction/quantification techniques explained above, and contaminants present on the quartz fiber filters were found to be minor. Residual contaminant peaks

Table 5.1:
Breakthrough experiment. Fraction mass measured on each PUF plug relative to the first plug in the sampling train.

Compound	PUF1	PUF2	PUF3	PUF4	PUF5
Chrysene/Triphenylene	1.00	trace	N.D.	N.D.	N.D.
Benz[a]anthracene	1.00	trace	N.D.	N.D.	N.D.
Cyclopenta[cd]pyrene	1.00	N.D.	N.D.	N.D.	N.D.
Benzo[ghi]fluoranthene	1.00	trace	N.D.	N.D.	N.D.
Pyrene	1.00	0.07	0.01	0.01	0.01
Fluoranthene	1.00	0.06	0.01	0.01	0.01
Phenanthrene	1.00	0.33	0.06	0.02	0.02
Fluorene	1.00	0.91	0.75	0.49	0.41
Dibenzofuran	1.00	1.03	0.86	0.76	0.68
C4-Substituted Naphthalene	1.00	0.52	0.51	0.19	0.19
C3-Substituted Naphthalene	1.00	0.94	0.94	0.47	0.48
C2-Substituted Naphthalene	1.00	0.74	0.76	0.76	0.53
1-Methyl Naphthalene†	1.00	0.92	0.86	0.70	0.63
2-Methyl Naphthalene†	1.00	0.90	0.86	0.68	0.60
Naphthalene†	1.00	1.04	1.00	0.84	0.93

N.D.- None detected
trace- Trace levels seen, but not large enough to quantify
†- Compounds for which PUF collection is not intended (VOC canister data available)

that originate from anti-oxidants and plasticizers used in the foam manufacturing were found on the cleaned PUF plugs. These contaminant peaks and biphenyl and phenol from the benzene solvent used were present in all samples but are excluded from the list of environmental pollutants. The estimated accuracy of compound quantification by GC-MS was obtained by repeated injection of the reference standards used. This error was combined with standard accuracies in volume determinations, and error propagation calculations conducted on these errors led to an estimated precision (one standard deviation) of $\pm$ 20%.

5.3 Results and Discussion

Non-polar and semi-polar aromatic compounds identified and quantified at the four urban sites shown in Figure 5.1 during this experiment are listed in Table 5.2. In addition to those observed, others were present but not reported because of uncertainties associated with identification or quantification of the compounds. For example, phenol and biphenyl were measured but not reported because of contamination from solvents used in extraction. Also, coronene was identified to be present but was not quantified because its very high molecular weight taxed the capabilities of the GC-MS system used.

Among the aromatic compounds, the single-ring aromatic hydrocarbons measured by stainless steel VOC canister collection make up most of the mass of air pollutants. The single-ring compounds include benzene, a known toxic compound. Semivolatile organic compounds collected on polyurethane foam include aromatic hydrocarbons, nitro-substituted aromatics, oxygenated aromatics, and sulfur-substituted aromatics. These include mutagenic compounds, including cyclopenta[cd]pyrene, measured both in the vapor phase and particle phase. Heavier, particle-phase aromatic compounds measured

Table 5.2: Average (and range) of urban ambient concentrations of aromatic compounds measured in Southern California over the period Sept. 8-9, 1993.

Compound	Vapor phase organics by canister sampler ($\mu g/m^3$)	Vapor phase semi-volatile organics by PUF sampling (ng/m^3)	Fine particulate organics (ng/m^3)
Aromatic Hydrocarbons			
Benzene	12.9 (3.2-37.2)		
Toluene	30.8 (9.8-85.7)		
Ethylbenzene	5.2 (0.9-14.5)		
m-Xylene + p-Xylene	17.4 (1.8-53.0)		
Styrene	0.9 (0.0-12.9)		
o-Xylene	6.6 (1.7-19.2)		
i-Propylbenzene	0.3 (0.0-1.9)		
n-Propylbenzene	1.4 (0.0-3.8)		
p-Ethyltoluene	4.4 (0.0-13.4)		
m-Ethyltoluene	2.4 (0.0-6.9)		
1,3,5-Trimethylbenzene	2.8 (0.0-7.3)		
o-Ethyltoluene	1.9 (0.0-5.7)		
1,2,4-Trimethylbenzene	6.8 (0.0-20.3)		
p-Cymene	0.8 (0.0-2.9)		
1,2,3-Trimethylbenzene	2.0 (0.0-6.5)		
2,3-Dihydro-1H-indene (Indane)	0.9 (0.0-3.2)		
2,3-Dihydro-1-methyl-1H-indene	0.5 (0.0-2.0)		
2,3-Dihydro-4-methyl-1H-indene	0.8 (0.0-3.0)		
2,3-Dihydro-4,7-dimethyl-1H-indene	0.04 (0.0-0.6)		
Naphthalene	6.0 (0.0-22.6)		
2-Methylnaphthalene	0.2 (0.0-1.5)		
1-Methylnaphthalene	0.1 (0.0-1.3)		
C2 Naphthalenes		*approx. 400*	
C3 Naphthalenes		*approx. 300*	
C4 Naphthalenes		*approx. 150*	
Acenaphthylene		15.61 (0.37-80.27)	
Fluorene		29.77 (1.12-87.69)	
C1 Fluorenes		15.06 (0.44-40.12)	
C2 Fluorenes		14.13 (0.39-36.43)	
Phenanthrene		50.34 (3.59-140.03)	
Anthracene		3.04 (0.00-15.33)	
C1 Phenanthrenes		17.71 (1.11-57.83)	
C1 Anthracene		0.70 (0.00-4.03)	
C2 substituted MW 178 PAHs		10.32 (0.58-31.98)	
C3 substituted MW 178 PAHs		3.32 (0.00-15.98)	
C4 substituted MW 178 PAHs		0.53 (0.00-1.73)	
Fluoranthene		9.78 (0.68-27.98)	0.07 (0.00-0.26)
Acephenanthrylene		0.75 (0.00-4.47)	0.02 (0.00-0.05)
Pyrene		7.23 (0.65-26.32)	0.07 (0.00-0.26)
C1 substituted MW 202 PAHs		2.04 (0.07-8.91)	0.07 (0.00-0.36)
C2 substituted MW 202 PAHs			0.03 (0.00-0.32)
Benzo[ghi]fluoranthene		0.90 (0.00-5.02)	0.20 (0.00-0.97)
Cyclopenta[cd]pyrene		0.26 (0.00-1.72)	0.14 (0.00-1.02)
Benz[a]anthracene		0.10 (0.00-1.29)	0.15 (0.00-1.09)
Chrysene/Triphenylene		0.44 (0.00-1.70)	0.34 (0.00-1.62)
C1 substituted MW 226 PAHs			0.14 (0.00-0.97)
C1 substituted MW 228 PAHs			0.34 (0.00-2.16)
C2 substituted MW 228 PAHs			0.09 (0.00-0.46)

Table 5.2 (continued): Average (and range) of urban ambient concentrations of aromatic compounds.

Compound	Vapor phase organics by canister sampler ($\mu g/m^3$)	Vapor phase semi-volatile organics by PUF sampling (ng/m^3)	Fine particulate organics (ng/m^3)
Benzo[k]fluoranthene			0.22 (0.00-1.07)
Benz[e]acephenanthrylene			0.20 (0.00-1.00)
Benzo[j]fluoranthene			0.02 (0.00-0.10)
Benzo[e]pyrene			0.22 (0.02-1.00)
Benzo[a]pyrene			0.14 (0.00-0.80)
Perylene			0.05 (0.00-0.51)
Methyl substituted MW 252 PAHs			0.10 (0.00-0.88)
Indeno[1,2,3-cd]fluoranthene			0.10 (0.00-0.46)
Indeno[1,2,3-cd]pyrene			0.29 (0.02-1.38)
Benzo[ghi]perylene			0.77 (0.03-4.23)
Oxygenated Aromatics			
Indanone		33.34 (6.26-91.02)	
Phthalan		3.64 (0.00-10.35)	
Phthalide (Isobenzofuranone)		191.28 (62.48-461.69)	
Dibenzofuran		19.99 (1.65-56.58)	
Benzyl alcohol		30.50 (2.67-143.97)	
o-Cresol		46.77 (0.54-384.86)	
m+p-Cresol		90.53 (6.36-542.61)	
Dimethyl Phenols		110.26 (3.86-885.48)	
9-Phenanthrol		41.14 (3.94-157.98)	
Fluoren-9-one		4.10 (0.10-14.11)	0.29 (0.00-1.04)
Phenalen-9-one		0.71 (0.19-1.62)	0.53 (0.00-2.23)
Anthracene-9,10-dione		2.52 (0.41-6.41)	0.36 (0.00-1.14)
Methylanthracene-9,10-dione			0.09 (0.00-0.24)
Benz[de]anthracen-7-one			0.20 (0.00-1.00)
Benz[a]anthracene-7,12-dione			0.09 (0.00-0.31)
Cyclopenta[def]phenanthrone			0.05 (0.00-0.14)
1,8-Naphthalic Anhydride			0.41 (0.00-1.65)
Benzo[cd]pyren-6-one			0.54 (0.00-2.47)
Nitrated Aromatics			
Nitrobenzene		12.77 (0.90-45.66)	
4-Nitrophenol		102.12 (0.00-409.04)	
Dinitrophenol		42.36 (0.00-207.20)	
Dihydroxynitrobenzene			1.62 (0.03-10.52)
1-Nitronaphthalene		12.94 (0.00-32.96)	
2-Nitronaphthalene		5.34 (0.00-21.20)	
3-Nitrobiphenyl		13.43 (0.00-36.35)	
Other substitutions			
p-Dichlorobenzene	0.6 (0.0-2.1)		
Benzothiazole		18.04 (0.48-56.24)	
Dibenzothiophene		6.34 (0.20-14.28)	

on the quartz fiber filters include oxygenated aromatics and polycyclic aromatic hydrocarbons. While these particle-phase polycyclic aromatic compounds are present at lower ambient concentrations than the volatile aromatic compounds, they include important atmospheric carcinogens such as benzo[a]pyrene [17], and potential tracers for vehicle exhaust, such as benzo-[ghi]perylene [18-20]. The ambient concentrations of three other aromatic compounds, including sulfur- and chloro- substituted compounds are listed in Table 5.2. One of these, benzothiazole, is used as a vulcanization accelerator in compounding rubber products and is found in source emissions from tire tread attrition [21]. p-Dichlorobenzene is used as an insecticidal fumigant, and is an intermediate in the production of plastics for electronics components.

5.3.1 Distribution of the Number of Aromatic Rings

From single ring compounds (such as benzene and toluene) to heavier polycyclic aromatic hydrocarbons, we see a general trend of decreasing ambient concentrations with increasing number of rings, similar to a trend that we have reported for non-aromatic compounds of progressively increasing carbon number [9], specifically the normal alkanes. The trend toward decreasing ambient concentrations of normal alkanes with increasing carbon number can be attributed to their similar distribution in crude petroleum [9]. Aromatics likewise are present in declining concentration with increasing carbon number in petroleum products such as diesel fuel [22], so that emissions of unburned fuel could contribute to the observed atmospheric pattern. But more importantly, when mono-aromatics and PAH are synthesized in combustion, larger molecules are both more difficult to form in the first place and once formed are more readily removed by conversion into soot, thereby also leading to

declining concentrations with increasing carbon number [23].

Figure 5.2 shows the gas-phase and particle-phase ambient concentrations for a number of PAH. This is done to stress the importance of including the gas-phase compounds in an analysis of PAH. The gas-phase PAH concentrations are much higher than the particle phase concentrations for the lower molecular weight members of this series, and include important mutagenic compounds, such as cyclopenta[cd]pyrene. These results are consistent with previous reports of Yamasaki et al. [24] which report roughly equal concentrations of MW 228 PAH in the vapor and particle phases. However, both sets of measurements are succeptable to partitioning artifacts which overestimate the fraction of PAH in the vapor phase.

5.3.2 Temporal and Spatial Distribution of Ambient Concentrations

Ambient concentration data collected during this experiment can be used to study the temporal and spatial distribution of aromatic compound concentrations. Examples of the ambient concentrations of benzene, cyclopenta-[cd]pyrene, benzo[a]pyrene, 3-nitrobiphenyl, and dinitrophenol measured at individual urban sites during the two-day smog episode are given in Figure 5.3. The graphs in Figure 5.3 are organized according to distance from the coastline, and when viewed alongside the map of Figure 5.1 can be used to visualize the characteristic temporal and spatial distribution of key aromatic compounds. The vapor-phase mono-aromatic hydrocarbons analyzed in this experiment (e.g., benzene), as well as the ordinary PAH, including the two given in Figure 5.3, show peak concentrations at the Central Los Angeles sampling site. This is consistent with the high density of motor vehicles and stationary sources in the region. Also, ambient concentrations of aromatic

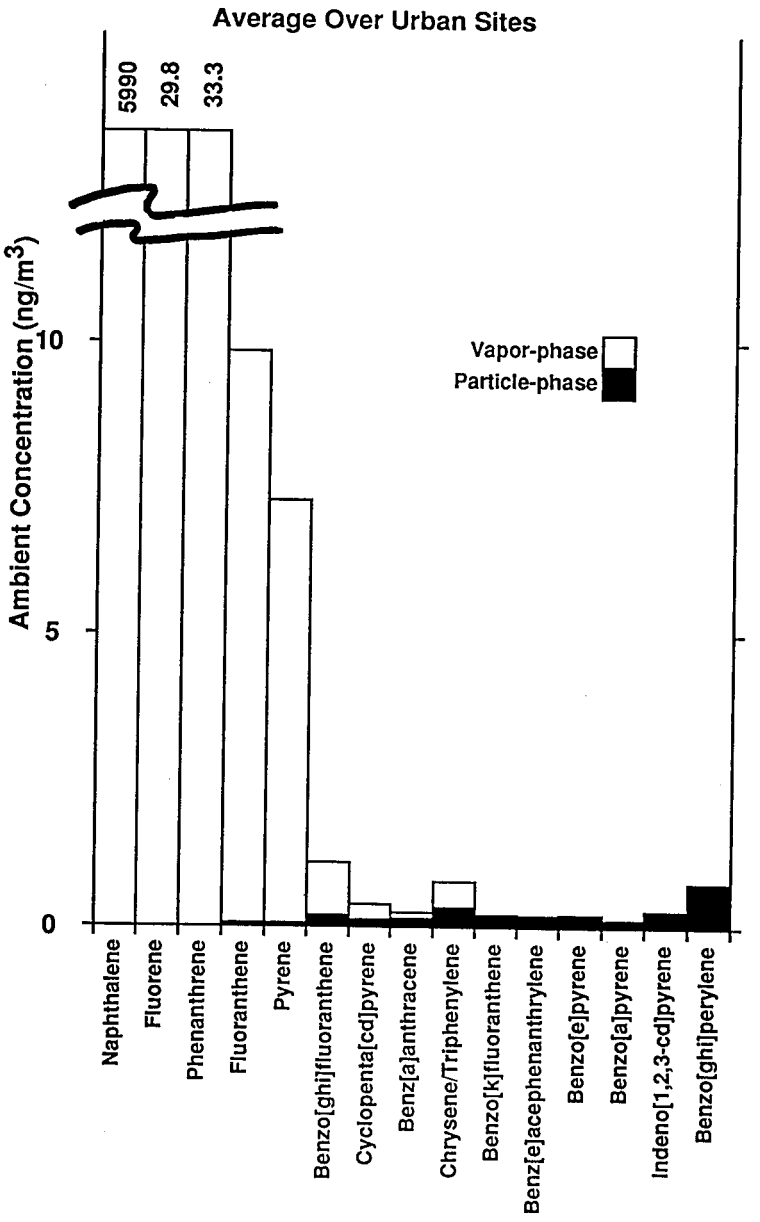

Figure 5.2:
The gas-phase and particle-phase concentrations of a number of PAH measured during this experiment.

hydrocarbons peaked during the morning sampling period (6 a.m. - 10 a.m.), coincident with the morning traffic rush hours. The ambient concentrations of mono-aromatic vapors and ordinary PAH are lower at the inland sampling sites at Azusa and Claremont, especially for the reactive aromatics [25, 26].

Figure 5.3 also shows the concentrations of 3-nitrobiphenyl and dinitrophenol measured during this experiment. These nitrated aromatics are present at higher concentrations at the inland sites (Azusa and Claremont) and their concentrations build up during the day, a characteristic shared by most of the nitro-substituted aromatics and a number of oxy-substituted aromatic compounds. Since the data appear to describe the decline of the concentrations of primary aromatics with distance away from Central Los Angeles coupled with the formation of secondary reaction products, further analyses were conducted to explore the apparent relative rates of depletion of the primary species and formation of the secondary reaction products.

5.3.3 Aromatic Compounds Depleted by Atmospheric Chemical Reactions

Wind speed and direction information collected at the South Coast Air Quality Management District's network of ambient air quality monitoring sites was used to calculate transport times for air parcels from the time that they cross the coastline of Southern California until they arrive at Claremont during this episode. Backward trajectories from Claremont were calculated from gridded windfields that in turn were prepared by interpolation of the wind observations by the method of Goodin et al. [27]. All such trajectories pass over the coastline near Hawthorne and are advected inland south of Central Los Angeles. These trajectories encounter overnight air stagnation, as wind speeds decrease during the night and early morning hours. Transport times

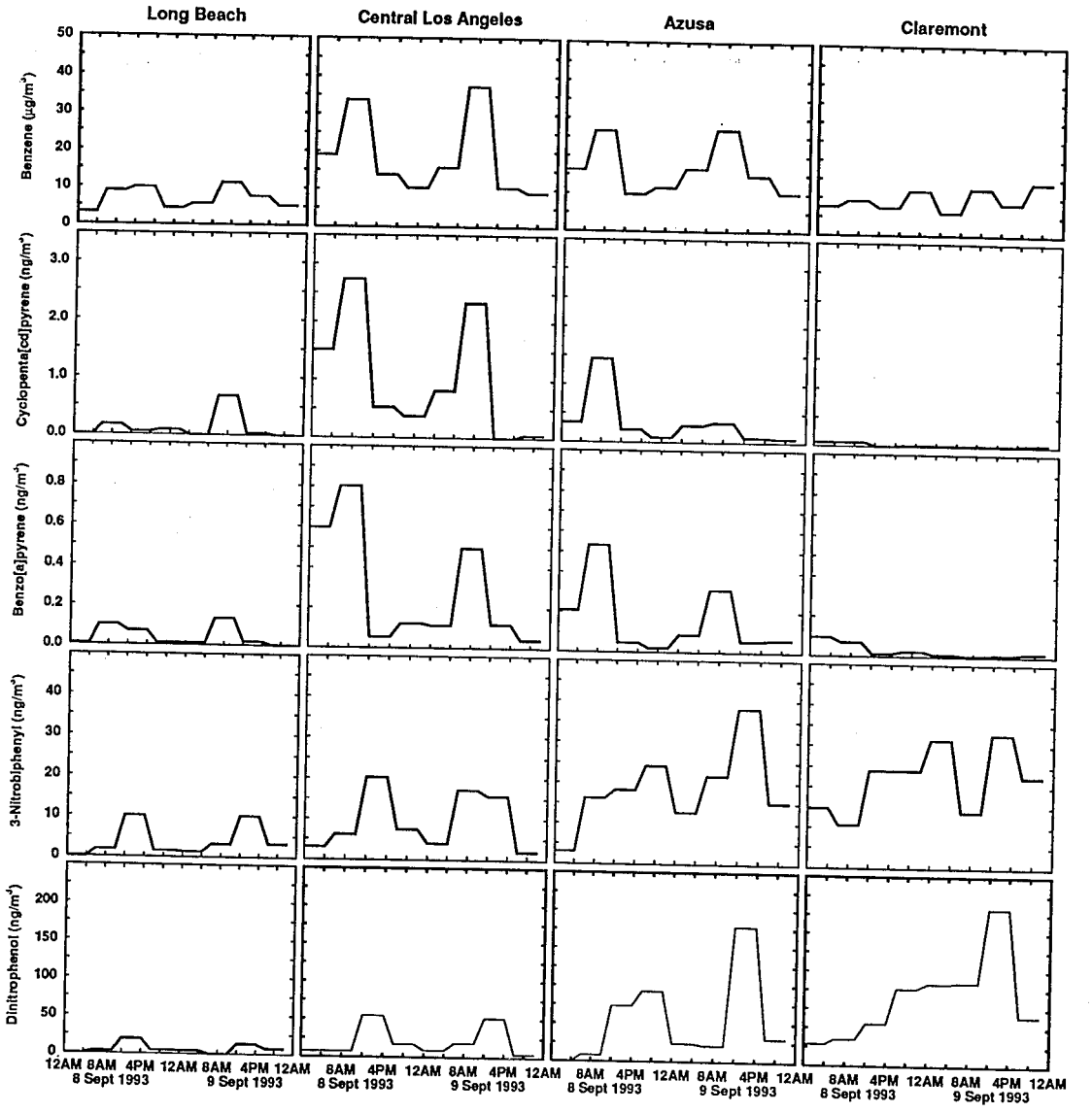

Figure 5.3:
The ambient concentrations of benzene, cyclopenta[cd]pyrene, benzo[a]pyrene, 3-nitrobiphenyl and dinitrophenol measured over the two day period of this experiment.

from the coast to Claremont are all greater than 24 hours. An example of one of the trajectories arriving at Claremont at Noon PST on the second day of the experiment (Sept. 9, 1993) is shown in Figure 5.1, with each circle representing the location of the air parcel at a previous hour.

Table 5.3 shows two-day average ambient concentrations as a function of site, and as a function of the time of day for a number of aromatic hydrocarbons. The peak concentrations are observed at Central Los Angeles and ambient concentrations decrease with inland advection to Claremont. A number of atmospheric processes act to lower the concentration of these primary organic contaminants as they are transported downwind. Radiative heating increases the depth of the mixed layer adjacent to the ground as the day progresses thereby diluting the emissions. Gas-phase chemical reactions deplete the more reactive compounds as they are transported downwind. The diurnal variation of the concentration of these pollutants shows the effects of these same processes. Photochemical reactions combined with increased mixing depths during the afternoon cause the lowest ambient concentrations of the primary aromatic hydrocarbons to be observed during the 12 noon - 4 p.m. sampling period. In addition to atmospheric chemical reaction, loss of PAH can occur by reaction after material is collected on the filter face during the 4-h sampling period. The most reactive aromatic compounds (e.g., 1,2,4-trimethylbenzene or benzo[a]pyrene) [25, 28] show the greatest relative depletion, exhibited through their exaggerated diurnal variation between morning and afternoon sampling periods, as well as their more rapid decline in relative concentration over transport from Los Angeles to Claremont. These findings are consistent with laboratory investigations, which show short atmospheric lifetimes (less than one day) for gas-phase PAH succeptable to attack by the hydroxyl radical [4], or particle-phase PAH exposed

Table 5.3: Ambient concentrations of selected example aromatic hydrocarbons measured in Southern California over the period Sept. 8-9, 1993, averaged at specific air sampling sites and by time of day.

	Samples at all times aggregated by sampling site				Samples at all urban sites aggregated by time of day			
Vapor Phase Aromatic Hydrocarbons(μg m^{-3})	Long Beach	Central LA	Azusa	Claremont	12 am–4 am	6 am–10 am	12 pm–4 pm	6 pm–10 pm
Benzene	7.0	18.7	16.6	9.6	11.2	20.7	10.2	9.5
Toluene	16.6	43.6	42.0	21.1	28.4	49.3	22.9	22.8
o-Xylene	3.6	9.6	9.0	4.0	6.4	11.0	4.0	5.0
1,2,4-Trimethylbenzene	3.9	10.1	9.7	3.6	7.3	11.8	2.9	5.3
Semivolatile and Particulate PAHs (ng m^{-3})								
Acenaphthylene	9.89	34.68	13.80	4.00	24.14	25.84	1.99	10.39
Phenanthrene	33.3	89.6	49.5	29.1	46.2	65.1	49.1	40.8
Anthracene	0.90	4.74	1.73	0.94	3.59	6.07	0.71	1.80
Pyrene	5.17	13.87	6.48	3.69	5.93	11.80	6.17	5.29
Cyclopenta[cd]pyrene	0.14	1.04	0.36	0.03	0.39	0.97	0.12	0.09
Benzo[a]pyrene	0.05	0.29	0.17	0.03	0.14	0.31	0.05	0.03
Benzo[ghi]perylene	0.32	1.36	1.12	0.22	0.73	1.56	0.37	0.36

to sunlight [29].

Table 5.4 shows the ratio formed when the ambient concentrations of various classes of aromatic compounds measured at Claremont are divided by the concentrations observed at Central Los Angeles. Benzene is a relatively slowly reacting organic compound, and the decline in benzene ambient concentrations between Central Los Angeles and Claremont is due to the greater primary emission rates near Central Los Angeles, combined with the effect of increased mixing depths in inland valleys that act to dilute benzene concentrations during downwind transport from Central Los Angeles toward Claremont. Benzene is not expected to undergo significant chemical reaction

in the time required for transport from Central Los Angeles to Claremont, and comparison of the relative concentration of benzene to that of other aromatics during cross-basin transport can be used to judge the relative importance of dilution versus chemical reaction in determining aromatics concentrations. The further and progressive decline in the Claremont/Los Angeles concentration ratio for the remaining aromatic hydrocarbons clearly shows an increase in depletion due to reaction rates that increase as the number of aromatic rings increases and further shows that as these gas-phase aromatic compounds become more substituted, their reaction rates typically increase. This behavior is consistent with laboratory measurements of the rate of reaction of the hydroxyl radical with various volatile organic compounds. The OH reaction rates with the xylenes exceed that with toluene which in turn exceeds that with benzene [25, 26]. The OH reaction rate with 2,3- dimethylnaphthalene exceeds that with the mono-methylnaphthalenes which in turn exceed that with naphthalene [25, 26]. From Table 4, this generalization appears to be true for heavier gas-phase aromatic compounds as well. That the depletion ratio further suggests more rapid reaction rates with increasing number of aromatic rings is also consistent with laboratory data on the reaction rates of gas-phase PAH with the hydroxyl radical [25]. Particle-phase PAH show signs of atmospheric chemical reaction, with cyclopenta-[cd]pyrene, benzo[a]pyrene, and benz[a]anthracene showing the most rapid depletion, which is consistent with laboratory studies which rank benz[a]-anthracene and benzo[a]pyrene among the most reactive particle-phase PAH, followed by benzo[ghi]perylene, benzo[b]fluoranthene, chrysene/triphenylene, indeno[1,2,3-cd]pyrene, and benzo[k]fluoranthene [29].

The difference in atmospheric reaction rates of the different PAH is also apparent when comparing their ambient concentrations as a function of time

Table 5.4: Ratio of two-day average ambient aromatic hydrocarbon concentrations at Claremont to Central Los Angeles, showing the effect of depletion due to increased reaction rate with increasing extent of substitution.

	Compound	Ratio Claremont to Central Los Angeles
1 ring		
	Benzene	0.51
	C1-substituted Benzene	0.48
	C2-substituted Benzenes	0.40
	C3-substituted Benzenes	0.37
2 rings		
	Naphthalene	0.42
	C1-substituted Naphthalenes	0.39
	C2-substituted Naphthalenes	0.30
	C3-substituted Naphthalenes	0.20
3 rings		
	Phenanthrene	0.35
	Anthracene	0.20
	C1-substituted Phenanthrenes and Anthracenes	0.28
	C2-substituted Phenanthrenes and Anthracenes	0.24
	C3-substituted Phenanthrenes and Anthracenes	0.23
4 rings		
	MW 202 PAHs	0.29
	C1-substituted MW 202 PAHs	0.10
	C2-substituted MW 202 PAHs	0.09
5 rings		
	Cyclopenta[cd]pyrene	0.03
	Benz[a]anthracene	0.09
	Chrysene/Triphenylene	0.22
	Benzo[k]fluoranthene	0.21
	Benzo[a]pyrene	0.11
6 rings		
	Indeno[1,2,3-cd]pyrene	0.20
	Benzo[ghi]perylene	0.19

of day. For example, the relative reaction rates of phenanthrene and anthracene can be investigated through examination of changes in the concentration ratio between these two similar PAH over the course of the day. Differences exist among published data for the reaction rates of the hydroxyl radical with anthracene relative to phenanthrene. One study reports that anthracene reacts four times more rapidly with the hydroxyl radical than phenanthrene [30], while a second study reports roughly equal reaction rates for the hydroxyl radical with phenanthrene and anthracene [31]. Additionally, evidence that anthracene reacts with ozone has also been reported [32]. The ambient data show that anthracene appears to undergo more rapid reaction in the atmosphere than phenanthrene (see Table 5.4). Whether this difference is due to more rapid reaction of anthracene with the hydroxyl radical when compared to phenanthrene or the reaction of anthracene with ozone is uncertain. Calculating the ratio of anthracene to phenanthrene, averaged over all urban sampling sites on both days of the experiment, peak values are observed in samples from morning sampling periods (6 a.m. - 10 a.m. PDT), with anthracene levels equalling 9% of the phenanthrene levels. This corresponds to the time of day when the peak in fresh emissions from vehicle traffic occurs during the morning commute to work. During the next sampling period (noon - 4 p.m. PDT), anthracene levels fall to less than 1% of the phenanthrene levels. The apparent reason for this drop is more rapid reaction of anthracene with photochemical oxidants produced during daytime smog formation cycle. This ratio then increases during the 6 p.m. - 10 p.m. sampling periods to 4%, and to 8% during the 12 midnight to 4 a.m. sampling periods, as primary sources emit PAH overnight into a photochemically inactive atmosphere.

5.3.4 Aromatic Compounds Formed by Atmospheric Chemical Reactions

A number of the nitrated and oxygenated aromatic compounds measured during this experiment on the polyurethane foam and particle filters showed characteristics that point toward secondary formation via atmospheric chemical reactions. These include the nitrated aromatic compounds 1-nitronaphthalene, 2-nitronaphthalene, 3-nitrobiphenyl, and dinitrophenol, as well as certain oxygenated aromatics (e.g., cyclopenta[cd]phenanthrone). Table 5.5 shows the ambient concentrations of several example compounds averaged over all sampling periods at each of the four urban sites. The ambient concentrations of these compounds increase progressively with distance inland from the coastline. It is fairly clear that such compounds are probably produced at least in part by photochemical reactions as air parcels are advected inland. This is because the primary emissions source strength is highest near Central Los Angeles and downwind transport would otherwise be expected to reduce the concentrations of those pollutants that are emitted directly from primary sources. The results in Table 5.5 are also consistent with reports of secondary formation of the nitro-arenes in the Southern California atmosphere [4, 16], laboratory studies showing formation of these compounds [33,34], and reports of increasing 1,8-naphthalic anhydride concentrations as wood smoke is exposed to sunlight [35].

Other compounds show signs of secondary formation that become apparent when the diurnal variation of ambient concentrations is considered. Examples of such compounds are given in Table 5.6. When the ambient concentration of a compound increases during the afternoon photochemical smog period (12 noon - 4 p.m.) despite the increased dilution during this period due to increased inversion base height, then it is likely that that pollutant is

Table 5.5: Average of ambient concentrations (ng m^{-3}) of several example aromatic compounds measured in Southern California over the period September 8-9, 1993, which show signs of secondary formation based on a trend toward increasing concentration at the downwind sites.

Compound	Long Beach	Central LA	Azusa	Claremont
1-Nitronaphthalene	4.69	10.7	19.9	16.4
2-Nitronaphthalene	1.34	3.81	8.13	8.11
3-Nitrobiphenyl	3.88	9.47	18.7	21.8
Dinitrophenol	6.44	21.1	53.4	88.6
Naphthalic Anhydride	0.10	0.36	0.32	0.85
Cyclopenta[cd]phenanthrone	0.02	0.05	0.07	0.09

being produced by photochemical reactions. While some of the oxy-PAH and nitro-PAH increase in ambient concentration as air parcels are advected inland (for example, fluorenone and 2-nitronaphthalene), others do not. For example, dihydroxynitrobenzene concentrations averaged over all sites at each time period and averaged over all times at each site are shown in Figure 5.4a and b, respectively. The diurnal variations show peak concentrations during the 12 noon - 4 p.m. sampling period, which generally indicates atmospheric chemical formation. However, concentrations of dihydroxynitrobenzene are seen to peak strongly at Central Los Angeles, rather than at areas farther downwind. This suggests that either dihydroxynitrobenzene is formed very rapidly by atmospheric chemical reactions such that peak concentrations appear near the source of primary precursor emissions at Central Los Angeles, and/or that it is depleted rapidly by atmospheric chemical reactions such that concentrations do not build up in downwind areas.

A complete list of the compounds studied here that show signs of formation by chemical reaction by their spatial distribution (increasing concentrations with inland advection) include fluoren-9-one, indanone, 1-nitronaphthalene, 2-nitronaphthalene, 3-nitrobiphenyl, nitrobenzene, 4-nitrophenol,

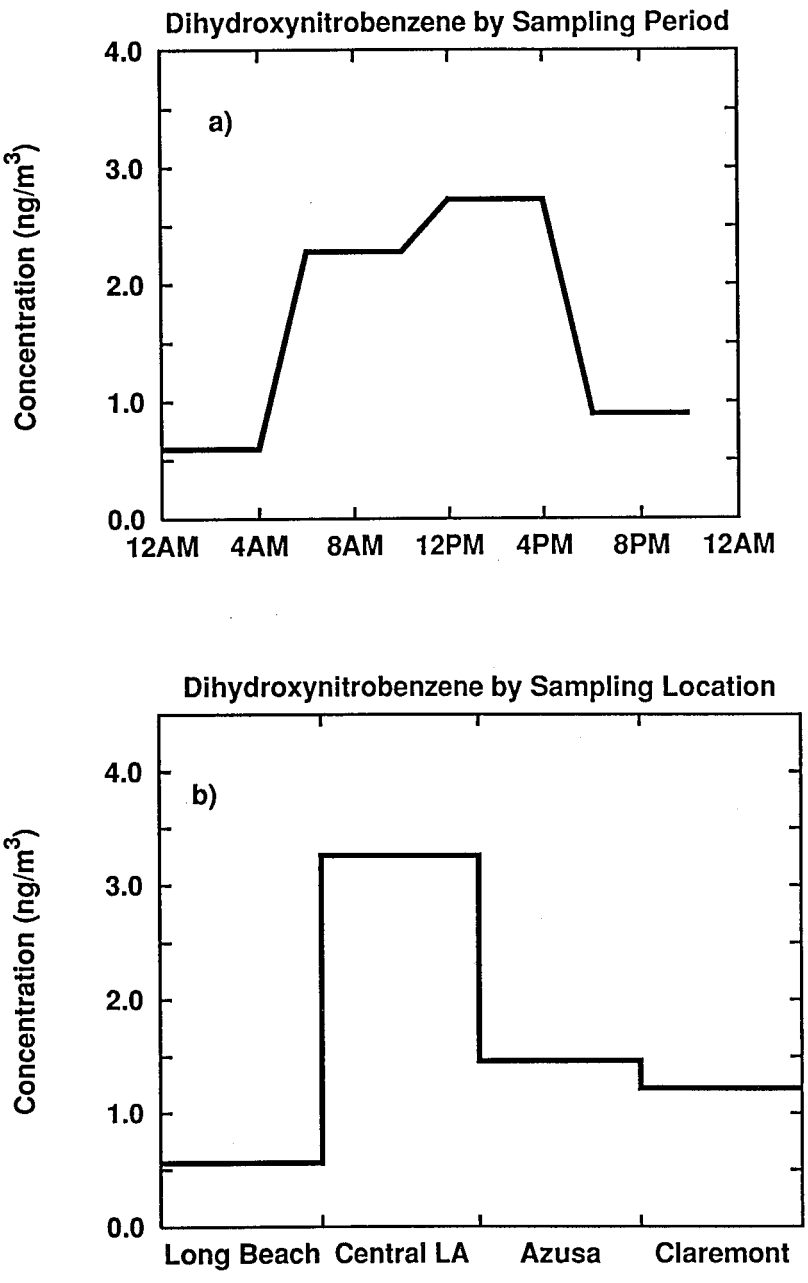

Figure 5.4:
Dihydroxynitrobenzene concentrations averaged over (a) all sites at each time period, and (b) all times at each site.

Table 5.6: Average of ambient concentrations (ng m^{-3}) of several example aromatic compounds measured in Southern California over the period Sept. 8-9, 1993, which show signs of secondary formation based on a diurnal variation that peaks during the afternoon peak photochemical smog period

	Samples at all times aggregated by sampling site				Samples at all urban sites aggregated by time of day			
Compound	Long Beach	Central LA	Azusa	Claremont	12 am–4 am	6 am–10 am	12 pm–4 pm	6 pm–10 pm
Fluoren-9-one	0.46	0.73	8.08	8.31	3.43	4.28	5.15	4.96
2-Nitronaphthalene	1.34	3.81	8.13	8.11	3.42	3.57	7.97	6.43
Anthracene-9,10-dione	1.56	3.52	3.30	3.15	1.79	2.96	4.18	2.96
Nitrobenzene	4.45	8.99	16.98	20.74	5.41	10.6	18.0	17.0
4-Nitrophenol	26.2	86.0	158	139	32.5	45.4	199	132
Dinitrophenol	6.44	21.1	53.4	88.6	22.4	25.2	81.6	40.3
Dihydroxynitrobenzene	0.56	3.26	1.46	1.22	0.60	2.28	2.74	0.90
3-Nitrobiphenyl	3.88	9.47	18.7	21.8	8.77	11.3	21.1	12.5

dinitrophenol, cyclopenta[cd]phenanthrone, and 1,8-naphthalic anhydride. In addition to those listed above, anthracene-9,10-dione and dihydroxynitrobenzene show signs of secondary formation according to their diurnal variation (afternoon concentration peaks). Not all of the oxygenated aromatic compounds display the behavior characteristic of secondary formation. These include benz[de]anthracen-7-one, benz[a]anthracene-7,12-dione, phenalen-9-one, benzo[cd]pyren-6-one, phthalan, benzyl alcohol, dibenzofuran, phenanthrol, phthalide, o-cresol, m+p-cresol, and the dimethyl phenols. While oxygenated aromatics can be produced by atmospheric oxidation of precursor hydrocarbons, the ambient concentrations of these aromatics appear to be dominated by direct emissions from primary sources. In the case of benz[de]anthracen-7-one, benz[a]anthracene-7,12-dione and benzo[cd]pyren-6-one, all of these compounds are emitted from known primary sources at

rates consistent with their atmospheric concentrations in the Los Angeles atmosphere [36,37]. Further the mono-oygenated aromatic ketones would be difficult to produce by atmospheric chemical reactions because the necessary precursor PAH are both thermodynamically unstable and are not found in the atmosphere.

Secondary formation of nitrobenzene via nitration of benzene is expected to be slow considering the long atmospheric lifetime of benzene. However, the atmospheric concentrations observed include direct emissions [38] in addition to atmospheric formation. Any atmospheric formation is likely the result of the very high levels of nitrogen dioxide present during the current study [6]. Primary emissions of cresols also have been reported from automobiles and cigarette smoke [39,40], and the spatial and temporal distribution of the ambient data in the present study imply that the primary sources may be more important than secondary formation of these compounds.

5.3.5 Regional Background Concentrations at San Nicolas Island

To understand the regional background atmosphere upwind of Southern California, measurements of volatile, semivolatile, and particle-phase organic compounds were made at San Nicolas Island, 100 km south and west of the Southern California coast (see location in Figure 5.1). This knowledge is important to the success of photochemical modeling studies in Southern California. Table 5.7 lists the average concentrations (and range of concentrations) measured at San Nicolas Island, along with a comparison between average urban concentrations and average upwind concentrations. A number of other compounds (including benzo[ghi]perylene, cyclopenta[cd]pyrene, and methyl-PAH) were observed, but at concentrations too low to be accurately quantified.

Table 5.7: Average ambient concentrations of aromatic compounds measured at San Nicolas Island over the period Sept. 8-9, 1993.

Compound	San Nicolas Island Average	Average Urban Concentration	Ratio San Nicolas Island to Urban
Cyclopenta[cd]phenanthrone	0.02 ng/m^3	0.05 ng/m^3	0.3
Phthalide	32.5 ng/m^3	192. ng/m^3	0.2
Chrysene/Triphenylene	0.14 ng/m^3	0.78 ng/m^3	0.2
Anthracene	0.32 ng/m^3	3.04 ng/m^3	0.1
Anthracene-9,10-dione	0.22 ng/m^3	2.72 ng/m^3	0.08
Phenanthrene	3.74 ng/m^3	50.3 ng/m^3	0.07
Dibenzofuran	1.26 ng/m^3	20.1 ng/m^3	0.06
Fluoranthene	0.51 ng/m^3	9.78 ng/m^3	0.05
Pyrene	0.27 ng/m^3	7.23 ng/m^3	0.04
Dibenzothiophene	0.26 ng/m^3	6.34 ng/m^3	0.04
Fluorene	1.17 ng/m^3	29.8 ng/m^3	0.04
1,8-Naphthalic anhydride	0.02 ng/m^3	0.41 ng/m^3	0.03
Phenalene-9-one	0.02 ng/m^3	0.53 ng/m^3	0.03
9-Phenanthrol	0.92 ng/m^3	41.1 ng/m^3	0.02
Benzene	0.3 μg/m^3	12.9 μg/m^3	0.02
Fluorene-9-one	0.07 ng/m^3	4.39 ng/m^3	0.02
Benzothiozole	0.14 ng/m^3	18.0 ng/m^3	0.01
Phthalan	0.03 ng/m^3	3.64 ng/m^3	0.01
o-Cresol	0.27 ng/m^3	46.8 ng/m^3	0.01
m+p-Cresol	0.83 ng/m^3	90.6 ng/m^3	0.01
Toluene	0.2 μg/m^3	30.8 μg/m^3	0.01

In general, the most prominant compounds are oxygenated aromatics, including cyclopenta[cd]pyrenone, phthalide, and anthracene-9,10-dione. A few PAH are present at less than 20% of their urban concentrations, including chyrsene/triphenylene, anthracene and phenanthrene. The primary gas-phase mono-aromatics (e.g., toluene and benzene) are present at only 1-2% of their urban concentrations. This implies that San Nicolas Island can be viewed as receiving diluted, aged air parcels consistent with long distance transport.

5.3.6 Historical Trends

To investigate the effectiveness of emission control programs implemented to date, ambient concentrations of aromatic compounds measured during this field experiment can be compared to reported ambient concentrations from earlier sampling programs in the Los Angeles area.

In the particle phase, benzo[a]pyrene levels in Los Angeles show a decline from 30 ng m^{-3} collected in Central Los Angeles during the period October 1952 to June 1953 [41]; to 1.6 ng m^{-3} collected in Central Los Angeles in February 1958 and June 1959 [42]; to 1.1 ng m^{-3} collected at Central Los Angeles from June 1971 to June 1972 [43]; to 0.72 ng m^{-3} collected in Pasadena during October 1976 - March 1977 [44]; to 0.54 ng m^{-3} (mean of winter and summer averaged concentrations) measured from August 1981 to February 1982 at seven sites in Southern California [45]; to 0.46 ng m^{-3} collected from January 1982 - December 1982 at Central Los Angeles [46, 47]. While the current sampling program that was conducted during the summer will understate the annual average benzo[a]pyrene concentrations, a comparison to the historial long-term average values can be constructed based on the ratios between summertime and annual average concentrations (when available), which are 0.31 for 1958; 0.59 for 1976; 0.26 for 1981-1982; and 0.33 for 1982. Using a ratio between annual average and summertime concentrations and the average benzo[a]pyrene concentration at Central Los Angeles of 0.3 ng m^{-3} during the present experiments, we estimate a long-term average concentration of benzo[a]pyrene of the same magnitude as sampling conducted in 1981 and 1982.

A review of historical trends in volatile aromatic compounds [48] shows a similar trend of dramatic decrease by a factor of 5-10 from the early 1960's to the late 1970's and early 1980's, after which ambient concentrations of

benzene and toluene appear to level off. The Aug. 27-29, 1987, epsiode of the Southern California Air Quality Study provides an interesting comparison to the results of the present experiment because ozone concentrations reached similar levels both during the 1987 and 1993 experiments. During Aug. 28, 1987, ambient concentrations of benzene and toluene averaged 12.9 μg m^{-3} and 36.4 μg m^{-3}, respectively, over eight sites in the Los Angeles area [5]. These concentrations are almost identical to the urban average benzene concentration of 12.9 μg m^{-3} and toluene concentration of 30.8 μg m^{-3} measured during the present 1993 experiments.

The present experiments were undertaken after the summer Reid vapor pressure (RVP) reformulation of gasoline but before the introduction of California Phase II reformulated gasoline. Earlier discussions in this work [9] document the effect of the RVP restrictions imposed in the summer on the reduction of C4 hydrocarbons in the Los Angeles atmosphere. California Phase II reformulated gasoline, introduced in 1996 following the present experiments, restricted the benzene content of gasoline to 0.8%, and aromatic compounds to 22%, by volume. The present experiments thus form a baseline against which data taken in subsequent years can be compared to judge the effect of California Phase II reformulated gasoline on the atmospheric concentrations of aromatic compounds.

Bibliography

[1] National Research Council *Rethinking the Ozone Problem in Urban and Regional Air Pollution*, National Academy Press: Washington DC, 1991.

[2] J. R. Odum, T. Hoffmann, F. Bowman, D. Collins, R. C. Flagan and J. H. Seinfeld. Gas/particle partitioning and secondary organic aerosol yields. *Environ. Sci. Technol.*, 30: 2580-2585, 1996.

[3] National Research Council *Polycyclic Aromatic Hydrocarbons: Evaluation of Sources and Effects*, National Academy Press: Washington DC, 1983.

[4] R. Atkinson and J. Arey. Atmospheric chemistry of gas-phase polycyclic aromatic hydrocarbons: formation of atmospheric mutagens. *Environ. Health Perspect.*, 102: 117-126, 1994.

[5] R. A. Harley and G. R. Cass. Modeling the atmospheric concentrations of individual volatile organic compounds. *Atmos. Environ.*, 29: 905-922, 1995.

[6] M. P. Fraser, D. Grosjean, E. Grosjean, R. A. Rasmussen and G. R. Cass. Air quality model evaluation data for organics. 1. Bulk chemical composition and gas/particle distribution factors. *Environ. Sci. Technol.*, 30: 1731-1743, 1996.

[7] E. Grosjean, D. Grosjean, M. P. Fraser and G. R. Cass. Air Quality Model Evaluation Data for Organics. 2. C_1 - C_{14} Carbonyls in Los Angeles Air. *Environ. Sci. Technol.*, 30: 2687-2703, 1996.

[8] E. Grosjean, D. Grosjean, M. P. Fraser and G. R. Cass. An Air Quality Model Evaluation Data Set for Organics. 3. Peroxyacetyl nitrate and peroxypropionyl nitrate in Los Angeles Air. *Environ. Sci. Technol.*, 30: 2704-2714, 1996.

[9] M. P. Fraser, G. R. Cass, R. A. Rasmussen and B. R. T. Simoneit. Air quality model evaluation data for organics. 4. C_2 to C_{36} non-aromatic hydrocarbons. *Environ. Sci. Technol.*, 31: 2356-2367, 1997.

[10] M. P. Fraser, G. R. Cass and B. R. T. Simoneit. Air quality model evaluation data for organics. 6. Aromatic and aliphatic organic acids. *in preparation*, 1997.

[11] P. A. Solomon, J. L. Moyers and R. A. Fletcher. High-volume dichotomous virtual impactor for the fractionation and collection of particles according to aerodynamic size. *Aerosol Sci. Technol.*, 2: 455-464, 1983.

[12] M. L. Lee, D. L. Vassilaros, C. M. White and M. Novotny. Retention indicies for programmed-temperature capillary-column gas chromatography of polycyclic aromatic hydrocarbons. *Anal. Chem.*, 51: 768-774, 1979.

[13] J. König, E. Balfanz, W. Funcke and T. Romanowksi. Determination of oxygenated polycyclic aromatic hydrocarbons in airborne particulate matter by capillary gas chromatography and gas chromatography/mass spectrometry. *Anal. Chem.*, 55: 599-603, 1983.

[14] M. A. Mazurek, B. R. T. Simoneit, G. R. Cass and H. A. Gray. Quantitative high-resolution gas chromatography and high-resolution gas chromatography/mass spectrometry analyses of carbonaceous fine aerosol particles. *Inter. J. Environ. Anal. Chem.*, 29: 119-139, 1987.

[15] B. Zielinska, J. C. Sagebill, G. Harshfield, A. W. Gertler and W. R. Pierson. Volatile organic compounds up to C20 emitted from motor vehicles; measurement methods. *Atmos. Environ.*, 30: 2269-2286, 1996.

[16] J. Arey, R. Atkinson, B. Zielinska and P. A. McElroy. Diurnal concentrations of volatile polycyclic aromatic hydrocarbons and nitroarenes during a photochemical air pollution episode in Glendora, California. *Environ. Sci. Technol.*, 23: 321-327, 1989.

[17] IARC Monographs: Diesel and gasoline engine exhaust and some nitroarenes. World Health Organization, International Agency for Research on Cancer: Lyon, France, 1989.

[18] A. H. Miguel and P. A. P. Pereira. Benzo[k]fluoranthene, benzo[ghi]perylene and indeno[1,2,3-cd]pyrene- new tracers of automotive emissions in receptor modeling. *Aerosol Sci. Technol.*, 10: 292-295, 1989.

[19] C. K. Li and R. M. Kamens. The use of polycyclic aromatic hydrocarbons as source signatures in receptor modeling. *Atmos. Environ.*, 27A: 523-532, 1993.

[20] C. Venkataraman and S. K. Friedlander. Source resolution of fine particulate polycyclic aromatic hydrocarbons using a receptor model modified for reactivity. *J. Air & Waste Manage. Assoc.*, 44: 1103-1108, 1994.

[21] W. F. Rogge, L. M. Hildemann, M. A. Mazurek, B. R. T. Simoneit and G. R. Cass. Sources of fine organic aerosol. 3. Road dust, tire debris, and organometallic break lining dust- roads as sources and sinks. *Environ. Sci. Technol.*, 27: 1892-1904, 1993.

[22] P. T. Williams, K. D. Bartle and G. E. Andrews. The relation between polycyclic aromatic-compounds in diesel fuels and exhaust particulates. *Fuel*, 65: 1150-1158, 1986.

[23] J. B. Howard. Carbon addition and oxidation reactions in heterogeneous combustion and soot formation, presented at the 23rd Symposium (International) on Combustion, The Combustion Institute; Pittsburgh, PA. 1990.

[24] H. Yamasaki, K. Kuwata and H. Miyamoto. Effects of ambient temperature on aspects of airborne polycyclic aromatic hydrocarbons. *Environ. Sci. Technol.*, 16: 189-194, 1982.

[25] R. Atkinson. Kinetics and mechanisms of the gas-phase reactions of the hydroxyl radical with organic compounds. *J. Phys. Chem. Ref. Data Monograph*, 1: 1-246, 1989.

[26] R. Atkinson. Gas-phase tropospheric chemistry of organic compounds: a review. *Atmos. Environ.*, 24A: 1-41, 1990.

[27] W. R. Goodin, G. J. McRae and J. H. Seinfeld. A comparison of interpolation methods for sparce data: application of wind and concentration fields. *J. Appl. Metorol.*, 18: 761-771. 1979.

[28] T. Nielsen. The decay of benzo[a]pyrene and cyclopenta[cd]pyrene in the atmosphere. *Atmos. Environ.*, 22: 2249-2254, 1988.

[29] R. M. Kamens, J. Guo, J. N. Fulcher and D. A. Bell. Influence of humidity, sunlight, and temperature on the daytime decay of polycyclic hydrocarbons on atmospheric soot particles. *Environ. Sci. Technol.*, 22: 103-108, 1988.

[30] H. W. Biermann, H. MacLeod, R. Atkinson, A. W. Winer and J. N. Pitts. Kinetics of the gas-phase reactions of the hydroxyl radical with naphthalene, phenanthrene, and anthracene. *Environ. Sci. Technol.*, 19: 244-248, 1985.

[31] R. S. C. Kwok, W. P. Harger, J. Arey and R. Atkinson. Reactions of gas-phase phenanthrene under simulated atmospheric conditions. *Environ. Sci. Technol.*, 28: 521-527, 1994.

[32] E. S. C. Kwok, R. Atkinson and J. Arey. Kinetics of the gas-phase reactions of indan, indene, fluorene, and 9.10-dihydroxyanthracene with OH radicals, NO_3 radicals and O_3. *Int. J. Chem. Kinet.*, 29: 299-309, 1997.

[33] R. Aktinson, S. M. Aschmann and J. Arey. Reactions of OH and NO3 radicals with phenol, cresols and 2-nitrophenol at 296±2K. *Environ. Sci. Technol.*, 26: 1397-1403, 1992.

[34] R. Atkinson, J. Arey, B. Zielinska and S. M. Aschmann. Kinetics and nitro-products of the gas-phase OH and NO_3 radical-initiated reactoins of naphthalene-d8, fluoranthene-d10 and pyrene. *Int. J. Chem. Kinet.*, 22: 999-1014, 1990.

[35] R. M. Kamens, H. Karam, J. Guo, J. M. Perry and L. Stockburger.

The behavior of oxygenated polycyclic aromatic hydrocarbons on atmospheric soot particles. *Environ. Sci. Technol.*, 23: 801-806, 1989.

[36] W. F. Rogge, L. M. Hildemann, M. A. Mazurek, B. R. T. Simoneit and G. R. Cass. Mathematical modeling of atmospheric fine particle-associated primary organic compound concentrations. *J. Geophys. Res.*, 101: 19379-19394, 1996.

[37] M. P. Fraser, G. R. Cass and B. R. T. Simoneit. Gas-phase and particle-phase organic compounds emitted from motor vehicle traffic in a Los Angeles roadway tunnel. *submitted to Environ. Sci. Technol.*, 1997.

[38] K. Kuwata, M. Uebori and Y. Yamazaki. Reversed-phase liquid chromatographic determination of phenols in auto exhaust and tobacco smoke as p-nitrobenzeneazophenol derivatives. *Anal. Chem.*, 53: 1531-1534, 1981.

[39] P. A. Mulawa and S. H. Cadle. Measurement of phenols in automobile exhaust. *Anal. Lett.*, 14: 671-687, 1981.

[40] P. Kotin, H. L. Falk, P. Mader and M. Thomas. Aromatic hydrocarbons 1. Presence in the Los Angeles atmosphere and the carcinogenicity of atmospheric extracts. *AMA Arch. Ind. Hyd. Occ. Med.*, 9: 153-163, 1954.

[41] E. Sawicki, T. R. Hauser, W. C. Elbert, F. T. Fox and J. E. Meeker. Polynuclear aromatic hydrocarbon composition of the atmosphere in some large American cities. *Amer. Ind. Hyg. Assoc. J.*, 23: 137-144, 1962.

[42] R. J. Gordon and R. J. Bryan. Patterns in airborne polynuclear hydrocarbon concentrations at four Los Angeles sites. *Environ. Sci. Technol.*, 7: 1050-1053, 1973.

[43] A. H. Miguel and S. K. Friedlander. Distribution of benzo[a]pyrene and coronene with respect to particle size in Pasadena aerosols in the submicron range. *Atmos. Environ.*, 12: 2407-2413, 1978.

[44] D. Grosjean. Polycyclic aromatic hydrocarbons in Los Angeles air from samples collected on Teflon, glass and quartz filters. *Atmos. Environ.*, 17: 2565-2573, 1983.

[45] W. F. Rogge, L. M. Hildemann, M. A. Mazurek, B. R. T. Simoneit and G. R. Cass. Quantification of urban organic aerosols at a molecular level: identification, abundance, and seasonal variation. *Atmos. Environ.*, 27A: 1309-1330, 1993.

[46] W. F. Rogge. "Molecular tracers for sources of atmospheric carbon particles: Measurements and model predictions" Ph.D. Dissertation, California Institute of Technology, Pasadena, CA, 1993.

[47] H. B. Singh, L. J. Salas, B. K. Cantrell and R. M. Redmond. Distribution of aromatic hydrocarbons in the ambient air *Atmos. Environ.*, 19: 1911-1919, 1985.

6 Organic Acids in the Los Angeles Atmosphere

6.1 Introduction

Much of the research on carboxylic acids concentrations in the atmosphere has focused on the water soluble low molecular weight acids, including formic and acetic acids [1, 2, 3, 4, 5, 6]. These acids are present in the gas-phase, partition into aqueous aerosol droplets, and thus are important to the chemistry of fog water and cloud droplets. The present research instead focuses on the higher molecular weight acids which are not as water soluble. While present at lower ambient concentrations, these compounds partition between the vapor phase and organic particulate matter. Higher molecular weight acids constitute the most abundant class of organic compounds found in fine particulate matter in the urban atmosphere [7], and are thus of interest because of the need to reduce fine particulate matter concentrations in order to attain compliance with the recently adopted National Ambient Air Quality Standard for fine particles [8].

Organic acids are relatively stable in the atmosphere, with removal dominated by wet and dry deposition processes [9, 10]. They are emitted to the atmosphere directly from natural and anthropogenic primary sources, and also are produced by secondary formation from gas-phase hydrocarbons and certain oxygenated species via atmospheric chemical reactions [11].

Previous studies of the Southern California atmosphere show that aliphatic dicarboxylic acids display a diurnal variation that indicates secondary for-

mation due to atmospheric chemical reactions [11, 12]. Oxidation of cyclic olefins and diolefins is suggested as one possible formation route. Analysis of particulate matter collected during 1982 in Southern California shows that both aliphatic dicarboxylic acids and aromatic polycarboxylic acids display similar spatial and seasonal characteristics, suggesting that atmospheric formation may be the main source of aromatic polycarboxylic acids in the atmosphere as well [7]. In a study of urban particulate matter in Tokyo, Kawamura and Ikushima [13] report that C_2 - C_4 aliphatic diacids are present at higher concentrations during summer months, and they show that positive correlations exist between total dicarboxylic acid concentrations (normalized by total aerosol carbon) and oxidant concentrations, again suggesting that the diacids are produced by reactions that occur in photochemical smog. However, the highest molecular weight aliphatic diacids (C_6 - C_{10}) showed high concentrations in both summer and winter samples in Tokyo [13], leading to the question of whether the same routes of emission and atmospheric chemical reaction govern the ambient concentrations of different individual compounds within this compound class. The role of primary emissions of both aliphatic and aromatic diacids was investigated in the Los Angeles area [14]. Analysis of exhaust samples from gasoline and diesel engines showed ratios between the aliphatic and aromatic diacids that are similar to those seen in the urban atmosphere, which along with the high overall emission rates measured in that study suggest that direct emissions from motor vehicles might be an important contributor to the atmospheric concentrations of dicarboxylic acids [14, 15].

The present study reports experimental results that describe the ambient concentrations of 49 organic acids in the Los Angeles atmosphere. These data have been collected as part of a larger study of vapor-phase, semi-volatile and

particle-phase organic compounds [16]. Some of the questions raised above concerning the importance of primary emissions versus secondary formation of higher molecular weight organic acids will be addressed through statistical analyses of the spatial and diurnal variations in the ambient concentrations of individual acids when compared to the ambient concentrations of other classes of organic compounds whose ambient concentrations are known to be governed by primary emissions or by secondary formation due to atmospheric chemical reactions.

6.2 Experimental Methods

6.2.1 Collection of Samples

Samples were collected during the summer of 1993 at five sites in and around Southern California as part of an effort to measure the ambient concentrations of as many particle-phase, semivolatile, and vapor-phase organic compounds as possible for use in the evaluation of an airshed model that tracks the ambient concentrations of individual organic compounds. Four-hour integrated samples centered within consecutive six-hour intervals were collected over a two-day photochemical smog episode on Sept. 8-9, 1993. Meterological conditions during the experiment exhibited the low mixing depths and stagnant transport conditions that occur during the summer months in Southern California, leading to peak ozone concentrations approaching 0.3 ppm.

A complete description of the experiment, including the samplers deployed, sample preparation, extraction techniques, and organic compound quantification methods is presented elsewhere [16, 17]; only brief summaries will be given here. Organic acids were collected using two separate samplers: a high-volume dichotomous sampler [18] that employs quartz fiber filters

(QFFs) followed by polyurethane foam (PUF) cartridges to trap particle and vapor-phase organic compounds, plus a low-volume particulate matter sampler in which potassium hydroxide impregnated glass fiber filters, were placed in stacked filter holders downstream of Teflon particle prefilters. The high volume dichotomous sampler filters and PUF cartridges were employed to collect particle phase and high molecular weight vapor-phase organic acids, respectively, while the KOH impregnated filters deployed with the low-volume sampler were used to measure the higher concentration low-molecular weight gas-phase acids. The samples collected by the quartz fiber filters and PUF cartridges are discussed here, while the analysis of the KOH impregnated filter samples being undertaken separately by other methods.

The quartz fiber filters used to collect particle-phase organics (Pallflex QAO 2500) were baked at 550°C for a least 8-h before use to reduce their contaminant blank values. These filters were stored in prebaked aluminum foil packets for transportation to the field experiment. After sampling, the filters were placed in prebaked glass jars, sealed with Teflon lined lids, and returned to the laboratory where they were stored at -21°C until analysis.

Polyurethane foam plugs (density = 0.022 g cm^{-3}, ILD = 30) were cleaned by repeated washings in dichloromethane (DCM). Each PUF cartridge consisted of a bed of 7.6 cm diameter foam segments 12.5 cm deep packed within an aluminum housing. Each PUF cartridge was sealed with Teflon film, deployed into the field for sampling, resealed, returned to the laboratory, where the foam was transferred into precleaned glass jars with Teflon lined lids, and frozen until analysis.

6.2.2 Analytical Methods

The samples were extracted from the collection media, concentrated and analyzed by gas chromatography-mass spectrometry (GC-MS) using a Finnigan 4000 system accompanied by a NOVA-4C data station. A complete description of the extraction and analysis techniques has been given previously [19, 17], and will only be summarized here.

Before extraction, samples were spiked with the following perdeuterated compounds to monitor extraction efficiency and loss in the concentration steps: for the PUF samples, n-decane(D12), n-pentadecane(D32), n-tetracontane(D50), benzoic acid(D5), phenol(D5), hexanoic acid(D11), decanoic acid(D29); for filter samples, n-tetracontane(D50). After extraction and concentration to approximately 400 μl, each filter and polyurethane foam extract was divided into two aliquots. One of these aliquots was derivitized with diazomethane to convert carboxylic acids into their methyl ester analogs for quantification by GC-MS. All carboxylic acids were quantified as their methyl ester derivatives. Analysis of the underivitized samples did not show the methyl esters of interest, removing the possibility that the actual airborne pollutants measured were originally present as the organic methyl esters.

The GC-MS technique employed J&W Scientific DB1701 columns (30 m $\times$ 0.32 mm internal diameter; bonded phase 86% dimethyl, 14% cyanopropylphenyl polysiloxane; J&W Scientific, Rancho Cordova, CA). Response of the GC-MS instrument was monitored through use of 1-phenyldodecane as a co-injection standard that accompanied the injection of each sample. Compound identification and quantification was accomplished by comparison to authentic standards when available. Authentic standards used for quantification include benzoic acid, 2-methyl benzoic acid, 3-methyl benzoic acid, 4-methyl benzoic acid, 2,3-dimethyl benzoic acid, 2,4-dimethyl benzoic acid,

2,5-dimethyl benzoic acid, 2,6-dimethyl benzoic acid, 3,4-dimethyl benzoic acid, 3,5-dimethyl benzoic acid, dehydroabietic acid, 7-oxodehydroabietic acid, 1,2-benzenedicarboxylic acid, 1,3-benzenedicarboxylic acid, 1,4-benzenedicarboxylic acid, 4-methyl-1,2-benzenedicarboxylic acid, 1,2,3-benzenetricarboxylic acid, 1,2,4-benzenetricarboxylic acid, 1,3,5-benzenetricarboxylic acid, 1,2,4,5-benzenetetracarboxylic acid, propanedioic acid, butanedioic acid, butenedioic acid, methyl-butanedioic acid, pentanedioic acid, hexanedioic acid, octanedioic acid, nonanedioic acid, n-octanoic acid, n-decanoic acid, n-dodecanoic acid, n-tetradecanoic acid, n-hexadecanoic acid, n-hexadecenoic acid, n-octadecanoic acid, n-octadecenoic acid, n-eicosanoic acid, and n-docasonoic acid. Unknown compounds were identified by comparison to the NIST/EPA mass spectral data libraries and fundamental interpretation of the mass fragmentation patterns. When authentic standards were not available, the response of the instrument to similar compounds was used to estimate the response factor, and also to support the probable identification of the compound.

Analysis of field and laboratory blanks taken during this sampling program revealed traces of normal alkanoic acids on both quartz fiber filters and polyurethane foam cartridges, and phthalic acid on the quartz fiber filters. In some cases, especially for hexadecanoic acid and octadecanoic acid measured on the polyurethane foam, blank levels were of the same order of magnitude as the ambient measurements. For this reason, the data for normal alkanoic acids collected on polyurethane foam are suspect and are not reported. In the other cases where blank levels were a small fraction of the ambient concentrations measured, blank values were subtracted from the reported atmospheric concentrations.

Corrections for extraction efficiency and blowdown losses were calculated

by quantifying the perdeuterated recovery standard spikes, and relating the losses of these recovery spikes to individual organic compound losses. The relationship between losses of perdeuterated recovery standard spikes and target organic compounds was calculated by spiking known quantities of both recovery standards and authentic organic compound standards onto filter and PUF media and then extracting and concentrating according to the analytical methods used to extract the ambient samples. The ambient concentrations reported here include these corrections for recovery and extraction efficiencies. Recovery during extraction and blowdown ranged from 21% to 110% between samples and averaged 61% for all quartz fiber filter samples; and ranged from 42% to 98% between samples and averaged 56% for the samples collected from the polyurethane foam plugs.

6.3 Results and Discussion

The ambient concentrations of 27 alkanoic, 2 alkenoic and 20 aromatic acids, including polycarboxylic acids, were measured during this experiment. The average and range of their concentrations are listed in Table 6.1 for all samples taken at the four urban sites.

6.3.1 n-Alkanoic and n-Alkenoic Acids

Seventeen n-alkanoic acids and two n-alkenoic acids were measured during this experiment. In addition to the particle-phase alkanoic acids, vapor-phase alkanoic acids were measured but are not reported because of the relatively high n-alkanoic acids background values on the polyurethane foam plugs used for sample collection. The main particle phase atmospheric alkanoic acids are stearic (C_{16}) and palmitic (C_{18}) acids. These compounds are emitted from numerous sources, including meat cooking operations [20, 21], vegetative

Table 6.1: Average (and range) of urban ambient concentrations of high molecular weight carboxylic acids measured at four urban sites in Southern California over the period Sept. 8-9, 1993.

Compound	Vapor phase semi-volatile organics by PUF sampling (ng/m^3)	Fine particulate organics (ng/m^3)
n-Alkanoic acids		
n-octanoic acid	nr	2.4 (0.9-4.8)
n-nonanoic acid	nr	4.9 (2.0-11.7)
n-decanoic acid	nr	3.2 (1.7-5.3)
n-undecanoic acid	nr	3.1 (0.0-18.7)
n-dodecanoic acid	nr	12.1 (3.4-33.8)
n-tridecanoic acid	nr	4.4 (1.2-7.7)
n-tetradecanoic acid	nr	22.1 (7.7-50.8)
n-pentadecanoic acid	nr	8.7 (1.5-27.4)
n-hexadecanoic acid (palmitic acid)	nr	72.6 (10.2-196.7)
n-heptadecanoic acid	nr	3.2 (0.5-13.9)
n-octadecanoic acid (stearic acid)	nr	33.8 (4.9-99.3)
n-nonadecanoic acid	nr	1.7 (0.0-7.0)
n-eicosanoic acid	nr	3.6 (0.0-12.1)
n-heneicosanoic acid	nr	0.9 (0.0-4.3)
n-docosanoic acid	nr	2.6 (0.0-8.7)
n-tricosanoic acid	nr	1.0 (0.0-6.6)
n-tetracosanoic acid	nr	2.6 (0.0-6.3)
n-Alkenoic acids		
n-hexadecenoic acid	nr	2.9 (0.0-7.7)
n-octadecenoic acid	nr	7.7 (0.0-34.2)
Alkanedioic acids		
propanedioic acid		38.6 (0.3-473.5)
butanedioic acid		58.5 (0.5-440.1)
methylbutanedioic acid		13.8 (0.2-115.8)
pentanedioic acid		20.4 (1.9-195.8)
hexanedioic acid		7.5 (0.0-24.1)
octanedioic acid		1.4 (0.2-2.0)
nonanedioic acid		2.9 (0.3-7.0)
Benzene carboxylic acids		
benzoic acid	299.7 (41.5-962.2)	
2-methylbenzoic acid	10.2 (0.7-35.7)	
3-methylbenzoic acid	75.0 (3.7-322.8)	
4-methylbenzoic acid	57.8 (4.3-253.8)	
2,4-dimethylbenzoic acid	21.6 (2.0-91.8)	
2,5-dimethylbenzoic acid	25.8 (4.9-84.5)	
2,6-dimethylbenzoic acid	6.1 (1.4-20.2)	
3,4-dimethylbenzoic acid	52.2 (5.8-188.4)	
3,5-dimethylbenzoic acid	52.0 (4.9-277.8)	

Table 6.1(continued): Organic acid concentrations.

Compound	Vapor phase semi-volatile organics by PUF sampling (ng/m^3)	Fine particulate organics (ng/m^3)
Benzoic carboxylic acids(continued):		
1,2-benzenedicarboxylic acid		80.2 (4.1-242.4)
1,3-benzenedicarboxylic acid		4.9 (0.3-12.9)
1,4-benzenedicarboxylic acid		5.4 (0.9-17.2)
4-methyl-1,2-benzenedicarboxylic acid		54.1 (1.2-262.8)
1,2,3-benzenetricarboxylic acid		14.8 (0.7-74.5)
1,2,4-benzenetricarboxylic acid		18.9 (2.0-52.7)
1,3,5-benzenetricarboxylic acid		0.3 (0.0-0.9)
1,2,4,5-benzenetetracarboxylic acid		1.0 (0.0-5.1)
Resin acids		
Dehydroabietic acid		0.5 (0.0-3.4)
Oxodehydroabietic acid		$\leq$0.1 (0.0-0.1)
Polycarboxylic aromatic acids		
2,6-naphthalenedicarboxylic acid		2.4 (0.5-6.3)

nr: not reported; see text.

detritus [22], fossil fuel combustion [23] and others. Given that alkanoic acids are emitted from numerous sources, an effort will be undertaken later in the present study to infer the most important sources by examining the extent to which changes in the n-alkanoic acids concentrations track the ambient concentrations of other compounds (e.g., the petroleum biomarkers) that act as nearly unique tracers for the presence of the effluent from specific sources (e.g., motor vehicle traffic) in the atmosphere [24, 25].

6.3.2 Alkanoic and Aromatic Diacids

The concentrations of eight alkanedioic acids were measured during this experiment. These compounds, found entirely in the particle phase, were measured at levels similar to the ambient concentrations of the eight aromatic diacids also quantified during this experiment. The concentrations of aromatic diacids were dominated by 1,2-benzenedicarboxylic acid and 4-methyl-1,2-benzenedicarboxylic acid. These compounds, known by their common names phthalic acid and 4-methyl phthalic acid, are widely used as plasticizers. Phthalic acid is ubiquitous and was measured on the blank filters used during this sampling program despite extensive efforts undertaken to control contamination; the ambient levels reported here include appropriate blank corrections.

Benzene polycarboxylic acids measured in this experiment include diacids, triacids and one tetraacid. These compounds, listed in Table 6.1, show a definite preference to the 1,2 substitution pattern. 1,2-benzenedicarboxylic acid (phthalic acid) is commonly used as a plasticizer in the production of plastics. However, high concentrations of other similar compounds, including 4-methyl-1,2-benzenedicarboxylic acid, 1,2,3-benzenetricarboxylic acid and 1,2,4-benzenetricarboxylic acid, imply that there may be sources other than

Table 6.2:
Average of ambient concentrations (ng m^{-3}) of several benzene polycarboxylic acids measured in Southern California over the period Sept. 8-9 1993.

	Samples at all times aggregated by sampling site				Samples at all urban sites aggregated by time of day			
Compound	Long Beach	Central LA	Azusa	Claremont	12 am–4 am	6 am–10 am	12 pm–4 pm	6 pm–10 pm
1,2 Benzenedicarboxylic Acid	37.6	81.3	71.7	130.4	51.7	101.3	112.5	45.7
1,3 Benzenedicarboxylic Acid	4.3	8.0	4.3	5.4	3.6	9.5	4.8	3.6
4-Methyl-1,2-Benzenedicarboxylic Acid	18.2	42.2	46.8	109.0	38.3	87.4	61.2	25.3
1,2,4-Benzenetricarboxylic Acid	12.4	22.3	13.3	27.7	15.6	25.7	17.2	14.6
1,3,5-Benzenetricarboxylic Acid	0.2	0.3	0.3	0.5	0.3	0.5	0.3	0.3
1,2,4,5-Benzenetetracarboxylic Acid	0.9	2.0	0.3	0.9	0.7	1.4	1.0	0.7

the off-gassing of plasticizers from plastics.

The spatial and temporal distribution of the ambient concentrations of these benzene polycarboxylic acids implies that both primary emissions and secondary formation may be important in governing their ambient concentrations. Table 6.2 shows the ambient concentrations of these compounds at different sites and also during different times of the day. In nearly all cases, the highest overall ambient concentrations of benzene carboxylic acids are seen at the furthest inland site, Claremont. This pattern is typical of those compounds that are formed by atmospheric chemical reactions. However, the highest short-term average concentrations typically occur during the time of the morning traffic peak, which is a pattern that is characteristic of many primary pollutants emitted from motor vehicle traffic. Measurements of vehicular emissions made in the Van Nuys tunnel in Los Angeles show that all of the compounds listed in Table 6.2 are among the primary pollutants

emitted from motor vehicle traffic [26]. Thus the atmospheric behavior of the benzene polycarboxylic acids is consistent with both previous studies that have associated dicarboxylic acids with primary emissions from motor vehicles [14, 26] and secondary formation by atmospheric chemical reactions [12, 7].

While it appears that both primary emissions and secondary formation are important for this class of compounds, compounds with carboxylic acid groups in the 1,2- positions tend more toward the characteristics associated with secondary formation than is the case for compounds with other substitution patterns, such as 1,3-benzenedicarboxylic acid. For example, 1,2-benzenedicarboxylic acid displays its highest concentrations at Claremont, the furthest inland site, and also shows a general trend of increasing concentration with advection inland. Further, it reaches its highest concentration in the middle of the afternoon peak photochemical smog period, in contrast to 1,3-benzenedicarboxylic acid concentrations which peak at Central Los Angeles at the time of the morning traffic rush hours. One source of compounds with a 1,2-substitution pattern is the oxidation of polycyclic aromatic compounds, for example naphthalene, to give an aromatic diacid with the 1,2-substitution pattern. This oxidation pathway has been reported in studies of the phototransformation of naphthalene adsorbed onto fly ash and other solids [27], as well as the photooxidation of benz[a]anthracene [28]. A more complete analysis of the important processes that contribute to atmospheric concentrations will be discussed later along with statistical analysis of the ambient database collected during this experiment.

6.3.3 Benzoic, Methylbenzoic and Dimethylbenzoic Acids

The two-day concentration distribution at the four urban sites studied for benzoic acid, the toluic acids (methyl benzoic acids) and dimethyl benzoic acids is shown in Figure 6.1. Also shown in Figure 6.1 is the site-by-site distribution of aromatic alcohols, including the sum of the three cresol isomers and sum of the methyl cresols [29]. The very different shape of these distributions leads to the conclusion that the ambient concentrations of the alcohols are dominated by local emission sources or very rapid atmospheric reactions close to primary sources and that the ambient concentrations of the benzoic acids are dominated by build-up due to atmospheric reactions during downwind transport. Peak cresol concentrations in Central Los Angeles may represent high local emissions of precursor aromatic compounds and then rapid reaction to form high concentrations of secondary aromatic alcohols close to the source location. However, sampling inside a local roadway tunnel shows high direct emissions of cresols from motor vehicle traffic, consistent with the explanation that the concentration pattern shown in Figure 6.1, is dominated by direct emissions of cresols rather than atmospheric formation [29, 26]. Additionally, benzoic acid emissions from vehicles were measured during the Van Nuys tunnel experiment, although at much lower levels than the cresols [26]. The higher concentrations of benzoic acid in the atmosphere when compared to the cresols suggests that secondary formation dominates the ambient concentrations of benzoic acid. The ambient distribution of benzoic acid suggests formation by atmospheric chemical reactions, consistent with recent reports of benzoic acid production from the olefin-ozone reaction involving styrene [30]. Using average styrene concentrations of 0.9μg m^{-3} [29], an average ozone concentration of 50 ppb, along with the reaction rate of styrene with ozone [31], the fraction of styrene which

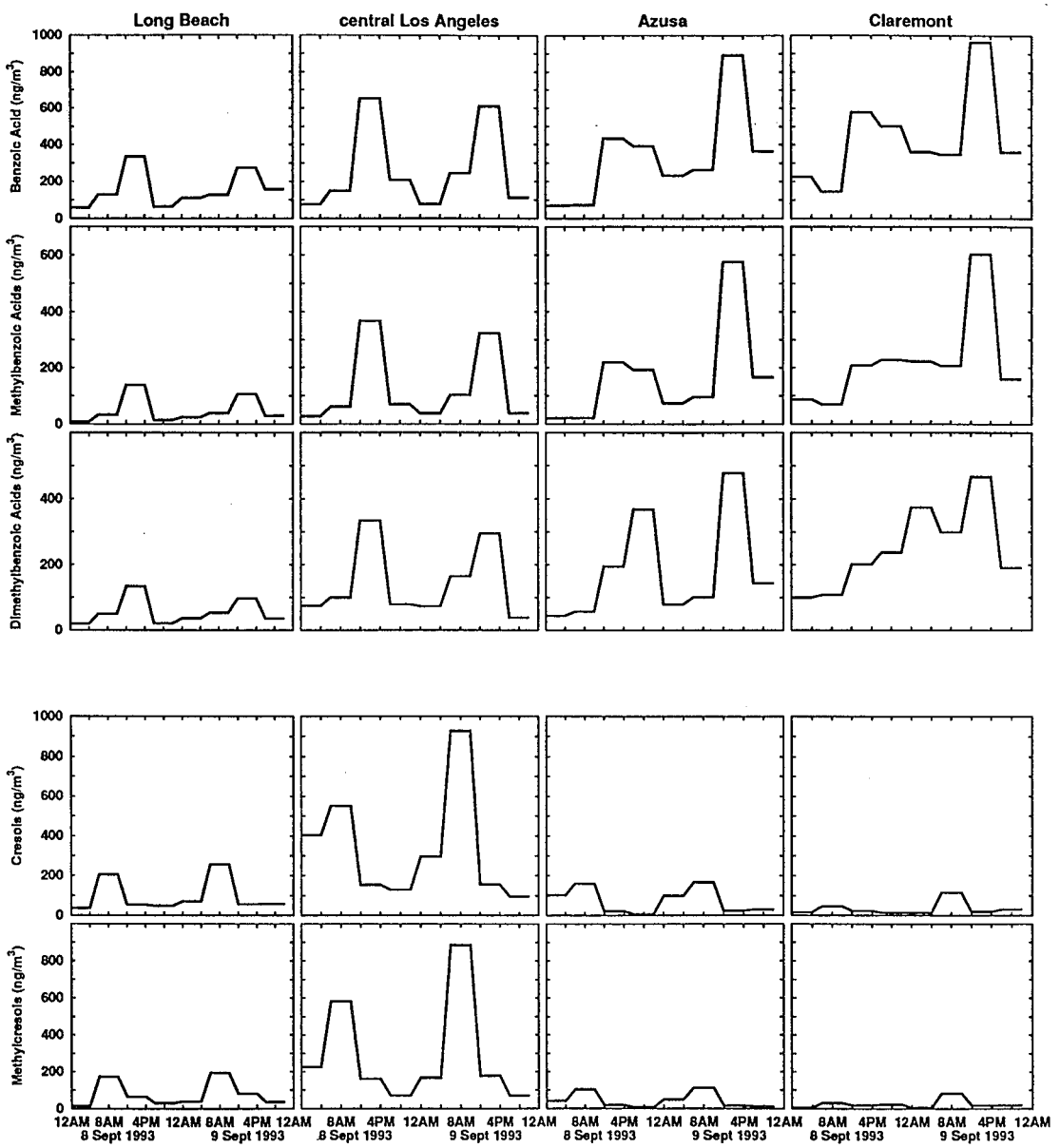

Figure 6.1:
The two-day concentration distributions of benzoic acid, the sum of the methylbenzoic acids, the sum of the dimethylbenzoic acids, the sum of the cresol isomers, and the sum of methylcresol isomers.

reacts with ozone to form benzaldehyde [30], and assuming that the other product of the ozone-olefin reaction is benzoic acid [32], the ozone-styrene reaction alone can explain the observed benzoic acid concentrations within an 8 hour reaction time, significantly shorter than the transport time of air parcels across the South Coast Air Basin during these experiments.

6.3.4 Dehydroabietic and Oxodehydroabietic Acids

Dehydroabietic acid and oxodehydroabietic acid are resin acids commonly found among the emissions from combustion of coniferous trees [33]. Dehydroabietic acid is also found in tire wear particles [34] from the addition of resinous material to affect the physical properties of the tire rubber. The ambient concentrations of dehydroabietic acid range from 0.16 ng m^{-3} at Long Beach to 0.48 ng m^{-3} at Central Los Angeles. The peak concentrations are observed at Central Los Angeles, coincident with the highest density of primary emission sources in the center of the Southern California urban area. Concentrations decrease with advection inland, dropping to 0.35 ng m^{-3} at Azusa and 0.30 ng m^{-3} at Claremont. Trace concentrations of oxodehydroabietic acid, an oxidation product of dehydroabietic acid contributed both by primary emissions sources plus secondary formation, are found.

6.3.5 Organic Acids Concentrations at San Nicolas Island

Octanoic acid, nonanoic acid and certain aliphatic dicarboxylic acids are present at the upwind background site (San Nicolas Island) at levels comparable to averages across the four urban sites. Table 6.3 shows the ratio of the average ambient concentration of each organic acid at San Nicolas Island to its average concentration at the four urban sites. Fatty acids as a compound class are known to be enriched in the surface microlayer of the ocean, including both the normal saturated acids and mono-unsaturated acids [35]. These

Table 6.3:
Average (and range) of ambient concentrations of carboxylic acids measured at San Nicolas Island and the ratio between average concentrations at San Nicolas Island and four urban sampling sites.

Compound	Concentration at San Nicolas Island (ng m^{-3})	Ratio San Nicolas to urban average concentrations
octanoic acid	4.56 (1.63-9.04)	1.87
nonanoic acid	4.13 (2.02-5.98)	0.84
butanedioic acid	44.29 (18.67-59.81)	0.76
hexanedioic acid	3.43 (0.37-6.00)	0.46
propanedioic acid	17.10 (5.32-30.12)	0.44
butenedioic acid	0.07 (0.05-0.09)	0.26
pentanedioic acid	5.29 (1.87-6.75)	0.26
decanoic acid	0.75 (0.58-0.99)	0.23
octanedioic acid	0.24 (0.12-0.32)	0.22
methybutanedioic acid	2.72 (1.09-3.71)	0.20
nonanedioic acid	0.41 (0.14-0.58)	0.14
1,3,5-benzenetricarboxylic acid	0.05 (0.03-0.05)	0.13
tetradecanoic acid	2.21 (0.24-3.13)	0.10
dodecanoic acid	1.14 (0.31-2.31)	0.09
1,2-benzenedicarboxylic acid	6.78 (1.70-13.04)	0.08
benzoic acid	23.65 (15.88-31.33)	0.08
pentadecanoic acid	0.58 (0.00-1.46)	0.07
hexadecanoic acid	4.22 (0.00-7.04)	0.06
1,2,4-benzenetricarboxylic acid	0.48 (0.09-0.85)	0.03
1,4-benzenedicarboxylic acid	0.09 (0.05-0.12)	0.02
4-methyl-1,2-benzenedicarboxylic acid	0.97 (0.29-1.80)	0.02
dehydroabietic acid	0.02 (0.00-0.02)	0.02
heptadecanoic acid	0.07 (0.00-0.24)	0.02
octadecanoic acid	0.54 (0.00-1.94)	0.02
3,4-dimethyl benzoic acid	0.63 (0.39-0.75)	0.01
1,3-benzenedicarboxylic acid	0.09 (0.07-0.10)	0.01
o-toluic acid	0.12 (0.00-0.22)	0.01
p-toluic acid	0.53 (0.03-0.97)	0.01
tridecanoic acid	0.05 (0.00-0.14)	0.01
2,5-dimethyl benzoic acid	0.27 (0.00-1.11)	0.01
m-toluic acid	0.53 (0.24-0.92)	0.01
1,2,3-benzenetricarboxylic acid	0.10 (0.00-0.24)	0.01
octadecenoic acid	0.07 (0.03-0.12)	0.01
3,5-dimethyl benzoic acid	0.32 (0.00-0.60)	0.01

compounds are among those detected at high concentrations at San Nicolas Island. Aliphatic dicarboxylic acids are relatively stable compounds in the atmosphere and are thought to be derived from photochemical reactions [11]. They have been used as model compounds to investigate organic compound effects on aerosol behavior in cloud droplet nucleation [36]. Their presence at concentrations at San Nicolas Island that are similar to the concentrations seen in the Southern California urban atmosphere suggests that these compounds emanate from marine sources, or that their ambient concentrations are affected by long-range transport or natural sources of either the acids or their hydrocarbon precursors rather than just local anthropogenic emissions to the Southern California atmosphere. Aromatic acids, including benzoic acids and benzene polycarboxylic acids are found at relatively low concentrations at San Nicolas Island, consistent with urban emissions as the dominant source of these compounds or the precursor gases that react to form these compounds.

Nonanoic Acid, Nonanedioic Acid and Octadecenoic Acid

Nonanoic and nonanedioic acid are known to come from the oxidation of cis-9-octadecenoic (oleic) acid [37]. Elevated ambient concentrations of the two C_9 acids have been attributed to this pathway. In the present experiments, ambient concentrations of these three compounds have been studied simultaneously in a severely oxidizing atmosphere, and the concentration changes observed for these compounds during transport across the air basin can be used to better understand this chemical reaction process.

The ambient concentrations averaged over different sites in the basin are shown in Table 6.4. Air parcel transport from the coastline of Southern California to Claremont during the current study required roughly two days

Table 6.4: Comparison of site distributions of nonanoic, nonanedioic and oleic acids.

Compound	San Nicolas Island	Long Beach	Central LA	Azusa	Claremont
Nonanoic Acid	4.1	3.4	6.3	4.8	5.4
Nonanedioic Acid	0.3	2.0	2.7	3.6	3.2
Oleic (C18:1) Acid	0.07	2.4	12.6	10.2	5.4

time. During this transport process, there is no sharp increase in concentrations of nonanoic acid or nonanedioic acid. However, concentrations of oleic acid peak at Central Los Angeles, consistent with this area being the center of primary emissions in the basin, and decline with advection toward the inland valley. The ratio of concentrations of the expected reaction products (nonanedioic acid and nonanoic acid) to the parent compound (oleic acid) shifts to higher proportions of reaction products at the inland sites. Therefore, it appears that atmospheric oxidation of oleic acid may be an important pathway to form either nonanoic or nonanedioic acid over transport times of less than a few days.

6.4 Statistical Comparison of Ambient Concentrations

Pearson correlation coefficients between the ambient concentrations of organic acids and other atmospheric organic compounds were calculated to investigate possible common sources and similar atmospheric loss processes. The SPSS statistical package was used to perform these calculations. The data at all four urban monitoring stations and all sampling times were pooled yielding 32 observations on each contaminant. In some cases, the concentrations of closely related compounds are summed to create a concentration variable that represents an entire compound class. For example, the con-

Table 6.5: Pearson correlation coefficients between the ambient concentrations of organic acids and other compounds based on observations at all urban sites and times during the Sept. 8-9, 1993, Southern California field experiments.

	1	2	3	4	5	6	7	8	9	10	11	12	13
1	1.00	0.41	0.70*	0.40	-0.05	0.74*	0.37	0.84*	0.50*	0.36	0.27	0.13	0.52*
2	0.41	1.00	0.74*	0.59*	-0.01	0.41	0.27	0.40	-0.11	0.21	0.41	0.83*	-0.02
3	0.70*	0.74*	1.00	0.66*	0.01	0.60*	0.48*	0.62*	0.21	0.40	0.40	0.51*	0.22
4	0.40	0.59*	0.66*	1.00	0.09	0.09	0.46*	0.27	0.10	0.04	0.12	0.35	0.12
5	-0.05	-0.01	0.01	0.09	1.00	-0.15	0.53*	0.00	0.06	-0.24	-0.36	-0.25	-0.07
6	0.74*	0.41	0.60*	0.09	-0.15	1.00	0.03	0.65*	0.29	0.27	0.29	0.15	0.33
7	0.37	0.27	0.48*	0.46*	0.53*	0.03	1.00	0.41	0.21	-0.05	-0.17	0.01	0.13
8	0.84*	0.40	0.62*	0.27	0.00	0.65*	0.42	1.00	0.52*	0.48*	0.29	0.23	0.59*
9	0.50*	-0.11	0.21	0.10	0.06	0.29	0.21	0.52*	1.00	0.50*	0.38	-0.20	0.92*
10	0.36	0.21	0.30	0.04	-0.24	0.27	-0.05	0.48*	0.50*	1.00	0.68*	0.36	0.49*
11	0.27	0.41	0.40	0.12	-0.36	0.29	-0.17	0.30	0.38	0.68*	1.00	0.61*	0.44
12	0.13	0.83*	0.51*	0.35	-0.25	0.15	0.01	0.23	-0.20	0.37	0.61*	1.00	-0.05
13	0.52*	-0.02	0.22	0.12	-0.07	0.33	0.13	0.59*	0.92*	0.50*	0.44	-0.05	1.00

[1] 1,2-Benzenedicarboxylic acid
[2] Sum 1,3+1,4-Benzenedicarboxylic acids
[3] Sum Benzenetricarboxylic acids
[4] 1,2,4,5-Benzenetetracarboxylic acid
[5] Butanedioic acid
[6] Butenedioic acid
[7] Hexanedioic acid
[8] Octanedioic acid
[9] Benzoic acid
[10] Palmitic acid
[11] Stearic acid
[12] Petroleum biomarkers
[13] Glyoxal

* Statistically significant correlation with greater than 95% probability based on sample size of 32 observations on each variable.

centrations of 1,3-benzenedicarboxylic acid and 1,4-benzendicarboxylic acid are summed because these two compounds are highly correlated. Also, the ambient concentrations of the petroleum biomarkers, including the hopanes and steranes, are summed in this analysis. The ambient concentrations of these petroleum biomarkers have been used successfully to track the direct emissions from motor vehicles in the Los Angeles atmosphere [25, 38]. The ambient concentration of glyoxal [39] is included in this analysis as a possible marker for the extent of secondary formation by atmospheric chemical reactions. The results of these calculations are summarized in Table 6.5.

The data in Table 6.5 show a high correlation (r=0.83) between the ambient concentrations of petroleum biomarkers and the sum of 1,3-benzenedicarboxylic and 1,4-benzenedicarboxylic acids concentrations, but not between the petroleum biomarkers and 1,2-benzenedicarboxylic acid concentrations. This is consistent with the belief that 1,3- and 1,4-benzenedicarboxylic acid concentrations are dominated by primary emissions from motor vehicles, while other pathways dominate the ambient concentration of 1,2-benzenedicarboxylic acid. The ambient concentrations of the benzenetricarboxylic acids are more weakly correlated with the concentrations of the petroleum biomarkers than is the case for 1,3- and 1,4-benzenedicarboxylic acids, while the benzenetetracarboxylic acid concentrations are not correlated to a significant degree with the petroleum biomarker concentrations. The petroleum biomarker concentrations also are weakly but significantly correlated with the ambient concentration of stearic acid.

Ambient concentrations of 1,2-benzenedicarboxylic acid (phthalic acid) are highly correlated with the concentrations of 4-methyl-1,2-benzenedicarboxylic acid (not shown in Table 6.5), but not with other isomers of the benzenedicarboxylic acids family. Phthalic acid levels are correlated with

concentrations of benzenetricarboxylic acids, butanedioic acid, octanedioic acid, benzoic acid, and glyoxal, suggesting strongly that phthalic acid is being produced by atmospheric chemical reactions.

For alkanoic and alkenoic dicarboxylic acids, several groupings of correlated compounds emerge. First, the C_3 to C_5 alkanoic diacids are highly correlated with each other (not shown); and the correlation between butanedioic acid and the other compounds shown in Table 6.5 is representative of the ambient variations of the other compounds in the group of C_3 to C_5 alkanoic diacids. Changes in the ambient concentrations of these compounds do not closely track the ambient concentrations of any other compounds included in this analysis, except for the next higher member of the alkanoic diacids series, hexanedioic acid. Butenedioic acid shows a very different behavior, and is not correlated with the ambient concentrations of butanedioic acid. High correlation coefficients are found between butenedioic acid and phthalic acid, benzenetricarboxylic acids, and octanedioic acid all of which are thought to be produced by atmospheric chemical reactions as discussed above. Nonanedioic acid and octanedioic acid are well correlated (not shown), and Table 6.5 uses the correlation of octanedioic acid with other compounds to represent this compound group. Similar to the observed trend for butenedioic acid, octanedioic acid shows a high correlation with the concentrations of phthalic acid and benzenetricarboxylic acid. Octanedioic acid concentrations also correlate significantly with compounds produced by atmospheric chemical reactions, such as glyoxal and benzoic acid. Finally octanedioic acid is correlated with the concentrations of palmitic acid. Falling between the two groupings of alkanoic diacids just described, hexanedioic acid appears weakly but not significantly correlated with the lower molecular weight C_3 to C_5 alkanoic diacids.

Benzoic acid concentrations are highly correlated with the toluic and dimethylbenzoic acids, and are used in Table 6.5 as a surrogate for all of these compounds. This group of compounds is highly correlated with glyoxal, suggesting that secondary formation dominates ambient concentrations of these compounds. Benzoic acid is also correlated with phthalic acid, octanedioic acid, and palmitic acid.

Stearic acid and palmitic acid are correlated with each other, as might be expected given that they are both emitted in large quantities from meat cooking operations [20]. Stearic acid concentrations also are correlated with the concentrations of petroleum biomarkers indicating an association with vehicle traffic, consistent with the observation that steric acid was emitted from some aspect of vehicle traffic during the 1993 Van Nuys tunnel experiments [26]. Palmitic acid is correlated with the concentrations of octanedioic acid, glyoxal, and benzoic acid, while stearic acid is not significantly correlated with the concentrations of these compounds.

Overall, this analysis shows that the ambient concentrations of the different organic acids should not be assumed to be governed by the same formation routes. The concentration patterns of some compounds, including benzoic acids, phthalic acid and octanedioic acids, is consistent with secondary formation playing a important role. Benzenedicarboxylic acids excluding phthalic acid are highly correlated with the concentrations of petroleum biomarkers suggesting that primary emissions from motor vehicles dominate the observed ambient concentrations. Butanedioic acid and other low molecular weight aliphatic dicarboxylic acids are correlated with each other but do not appear correlated with any other compounds included in this analysis. These low molecular weight aliphatic dicarboxylic acids also are present in relatively high concentrations in the air at San Nicolas Island, and thus

their concentrations within the Los Angeles area may be influenced by long distance transport of polluted air or production from natural background hydrocarbons.

Bibliography

[1] D. Grosjean. Organic acids in Southern California air: ambient concentrations, mobile source emissions, in situ formation and removal processes. *Environ. Sci. Technol.*, 23:1506–1514, 1989.

[2] H. Puxbaum, C. Rosenberg, M. Gregori, C. Lanzerstorfer, E. Ober, and W. Winiwarter. Atmospheric concentrations of formic and acetic-acid and related compounds in eastern and northern Austria. *Atmos. Environ.*, 22:2841–2850, 1988.

[3] R. W. Talbot, K. M. Beecher, R. C. Harriss, and W. R. Cofer. Atmospheric geochemistry of formic and acetic-acids at a mid-latitude temperate site. *J. Geophys. Res.*, 93:1638–1652, 1988.

[4] W. R. Hartmann, M. Santana, M. Hermoso, M. O. Andreae, and E. Sanhueze. Diurnal cycles of formic and acetic-acids in the northern part of the Guyana Shield, Venezuela. *J. Atmos. Chem.*, 13:63–72, 1991.

[5] R. B. Norton. Measurements of gas-phase formic and acetic acids at the Mauna-Loa, observatory, Hawaii during the Mauna-Loa Observatory Photochemistry Experiment 1988. *J. Geophys. Res.*, 97:10389–10393, 1992.

[6] C. G. Nolte, P. A. Solomon, T. Fall, L. G. Salmon, and G. R. Cass. Seasonal and spatial characteristics of formic and acetic acids concen-

trations in the southern California atmosphere. *Environ. Sci. Technol.*, 31:2547–2553, 1997.

[7] W. F. Rogge, L. M. Hildemann, M. A. Mazurek, G. R. Cass, and B. R. T. Simoneit. Quantification of urban organic aerosols at a molecular level: identification, abundance and seasonal variation. *Atmos. Environ.*, 27A:1309–1330, 1993.

[8] Air quality criteria for particulate matter. US Environmental Protection Agency, Research Triangle Park, NC, 1996. EPA-600/P-95/AF-CF.

[9] A. Chebbi and P. Carlier. Carboxylic acids in the troposphere, occurrence, sources and sinks: a review. *Atmos. Environ.*, 30:4233–4249, 1996.

[10] K. Kawamura, S. Steinberg, and I. R. Kaplan. Concentrations of monocarboxylic and dicarboxylic acids and aldehydes in Southern California wet precipitation: Comparision of urban and nonurban samples and compositional changes during scavenging. *Atmos. Environ.*, 30:1035–1052, 1996.

[11] D. Grosjean. Aerosols. In *Ozone and other photochemical oxidants*, National Academy of Sciences, Washington, D.C., 1977.

[12] D. Grosjean, K. VanCauwenerghe, J. P. Schmid, P. E. Kelley, and J. N. Pitts. Identification of C_3 – C_{10} aliphatic dicarboxylic acids in airborne particulate matter. *Environ. Sci. Technol.*, 12:313–317, 1978.

[13] K. Kawamura and K. Ikushima. Seasonal changes in the distribution of dicarboxylic acids in the urban atmosphere. *Environ. Sci. Technol.*, 27:2227–2235, 1993.

[14] K. Kawamura and I. R. Kaplan. Motor vehicle exhaust as a primary source of dicarboxylic acids in Los Angeles ambient air. *Environ. Sci. Technol.*, 21:105–110, 1987.

[15] B. R. T. Simoneit and M. A. Mazurek. Organic tracers in ambient aerosols and rain. *Aerosol Sci. Technol.*, 10:267–291, 1989.

[16] M. P. Fraser, D. Grosjean, E. Grosjean, R. A. Rasmussen, and G. R. Cass. Air quality model evaluation data for organics. 1. Bulk chemical composition and gas/particle distribution factors. *Environ. Sci. Technol.*, 30:1731–1743, 1996.

[17] M. P. Fraser, G. R. Cass, B. R. T. Simoneit, and R. A. Rasmussen. Air quality model evaluation data for organics. 4. C2-C36 non-aromatic hydrocarbons. *Environ. Sci. Technol.*, 31:2356–2367, 1997c.

[18] P. A. Solomon, J. L. Moyers, and R. A. Fletcher. High-volume dichotomous virtual impactor for the fractionation and collection of particles according to aerodynamic size. *Aerosol Sci. Technol.*, 2:455–464, 1983.

[19] M. A. Mazurek, G. R. Cass, and B. R. T. Simoneit. Interpretation of high-resolution gas chromatography and high-resolution gas chromatography/mass spectrometry data acquired from atmospheric organic aerosol samples. *Aerosol Sci. Technol.*, 10:408–420, 1989.

[20] W. F. Rogge, L. M. Hildemann, M. A. Mazurek, G. R. Cass, and B. R. T. Simoneit. Sources of fine organic aerosol 1. Charbroilers and meat cooking operations. *Environ. Sci. Technol.*, 27:1112–1125, 1991.

[21] J. J. Schauer, M. J. Kleeman, G. R. Cass, and B. R. T. Simoneit. Measurement of emissions from air pollution sources. 1.C1 through C29 or-

ganic compounds from meat charbroiling. *to be submitted to Environ. Sci. Technol.*, 1997.

[22] W. F. Rogge, L. M. Hildemann, M. A. Mazurek, G. R. Cass, and B. R. T. Simoneit. Sources of fine organic aerosol 4. Particulate abrasion products from leaf surfaces of urban plants. *Environ. Sci. Technol.*, 27:2700–2711, 1993.

[23] B. R. T. Simoneit. Characterization of organic-constitutents in aerosols in relation to their origin and transport- a review. *Intern. J. Environ. Anal. Chem.*, 23:207–237, 1986.

[24] B. R. T. Simoneit. Application of molecular marker analysis to vehicular exhaust for source reconciliations. *Intern. J. Environ. Anal. Chem.*, 22:203–233, 1985.

[25] J. J. Schauer, W. F. Rogge, L. M. Hildemann, M. A. Mazurek, G. R. Cass, and B. R. T. Simoneit. Source apportionment of airborne particulate matter using organic compounds as tracers. *Atmos. Environ.*, 30:3837–3855, 1996.

[26] M. P. Fraser, G. R. Cass, and B. R. T. Simoneit. Gas-phase and particle-phase organic compounds emitted from motor vehicle traffic in a Los Angeles highway tunnel. *submitted for publication in Environ. Sci. Technol.*, 1997a.

[27] C. Guillard, H. Delprat, C. Hoang Van, and P. Pichat. Laboratory studies of the rates and products of the phototransformations of naphthalene adsorbed on samples of titanium dioxide, ferric oxide, muscovite and fly ash. *J. Atmos. Chem.*, 16:47–59, 1993.

[28] M. Jang and S. R. McDow. Products of benz[a]anthracene photodegradation in the presence of known organic constituents of atmospheric aerosols. *Environ. Sci. Technol.*, 31:1046–1053, 1997.

[29] M. P. Fraser, G. R. Cass, B. R. T. Simoneit, and R.A. Rasmussen. Air quality model evaluation data for organics. 5. C6-C22 non-polar and semi-polar aromatic hydrocarbons. *submitted for publication in Environ. Sci. Technol.*, 1997b.

[30] E. Grosjean and D. Grosjean. Carbonyl products of the gas-phase reaction of ozone with 1-alkenes. *Atmos. Environ.*, 30:4107–4113, 1996.

[31] R. A. Harley and G. R. Cass. Modeling the concentrations of gas-phase toxic organic air pollutants: direct emissions and atmospheric formation. *Environ. Sci. Technol.*, 28:88–98, 1993.

[32] J. H. Seinfeld. *Atmospheric Chemistry and Physics of Air Pollution.* John Wiley and Sons, New York, 1986.

[33] L. J. Standley and B. R. T. Simoneit. Characterization of extractable plant wax, resin and thermally matured components in smoke particles from prescribed burns. *Environ. Sci. Technol.*, 21:163–169, 1987.

[34] W. F. Rogge, L. M. Hildemann, M. A. Mazurek, G. R. Cass, and B. R. T. Simoneit. Sources of fine organic aerosol 3. Road dust, tire debris and organometallic brake lining dust: roads as sources and sinks. *Environ. Sci. Technol.*, 27:1892–1904, 1993.

[35] R. A. Duce, J. G. Quinn, C. E. Olney, S. R. Piotrowicz, B. J. Ray, and T. L. Wade. Enrichment of heavy metals and organic compounds

in the surface microlayer of Narragansett Bay, Rhode Island. *Science*, 176:161–163, 1972.

[36] M. L. Schulman, M. C. Jacobson, R. J. Charlson, R. E. Synovec, and T. E. Young. Dissolution behavior and surface tension effects of organic compounds in nucleating cloud droplets. *Geophys. Res. Lett.*, 23:277–280, 1996.

[37] K. Kawamura and R. B. Gagosian. Implications of ω-oxocarboxylic acids in the remote marine atmosphere for photo-oxidation of unsaturated fatty acids. *Nature*, 325:330–332, 1987.

[38] W. F. Rogge, L. M. Hildemann, M. A. Mazurek, G. R. Cass, and B. R. T. Simoneit. Mathematical modeling of atmospheric fine particle-associated primary organic compound concentrations. *J. Geophys. Res.*, 101:19373–19394, 1996.

[39] E. Grosjean, D. Grosjean, M. P. Fraser, and G. R. Cass. Air quality model evaluation data for organics. 2. C_1 – C_{14} carbonyls in Los Angeles air. *Environ. Sci. Technol.*, 30:2687–2703, 1996.

7 Gas-phase and Particle-phase Compounds Emitted from Motor Vehicle Traffic

7.1 Introduction

In order to understand the contribution of motor vehicles to air pollution, accurate characterization of vehicular emissions is needed. Ideally, this characterization should reflect the vehicle emissions as they occur under actual operation on the highway. Further, the chemical complexity of these emissions should be fully described. Conventional emissions inventories that state the volatile organic compound (VOC) and particulate matter (PM) emissions from vehicles often provide only a lumped representation of the hundreds of organic compounds that are actually present in vehicular emissions. Individual VOCs can have dramatically different chemical reactivity with respect to ozone formation [2], while some VOCs (e.g., formaldehyde and benzene) are toxic air contaminants, as are certain particle-phase species (e.g., specific polycyclic aromatic hydrocarbons) [3]. Other specific VOCs (e.g., many aromatics) are secondary aerosol precursors [4], and with the exception of a few studies (e.g., refs. 5-7) semi-volatile organics in the molecular weight range above C_{10} or C_{12} are seldom measured at all.

The purpose of this paper is to report a comprehensive characterization of the individual organic species emitted from motor vehicles. Individual vapor phase, semi-volatile, and particle phase organics are characterized simultane-

ously over the range of molecular weights from C_1 to C_{33}. Measurements are made of the emissions from over 7,000 motor vehicles under actual operation on a Los Angeles-area surface street as they pass through a highway tunnel. This experiment was conducted in conjunction with a comprehensive characterization of VOC, semi-volatile and particle phase organic compounds in Los Angeles ambient air in order to provide model evaluation data for use in testing photochemical airshed models that simultaneously track both gas-phase and particle-phase organic compounds [8-12].

Measurements made in Los Angeles are of particular importance. The Los Angeles area experiences the nation's worst photochemical smog problem and highest fine particle concentrations [13-14]. The existence of these problems indirectly drives much of the air pollution control program for the nation as a whole. While some measurements made in highway tunnels in the eastern states show emissions that are reasonably close to those expected given current emission inventory calculations [15], both experiments conducted in tunnels and remote sensing studies in California suggest that governmental emissions inventories historically have underestimated the actual VOC and CO emissions from the vehicle fleet operated in Los Angeles. In 1987, measurements made in Los Angeles in the Van Nuys tunnel suggested that the hot running CO and VOC exhaust emissions rates from in-use motor vehicles were approximately three times greater than those present in then-current governmental emissions inventory calculations [16-17]. Subsequent remote sensing studies showed that high-emitting vehicles amounting to only ten percent of the vehicle fleet are responsible for about 55 percent of the total CO emissions [18], and that cars and trucks that are more than 10 years old account for 58% of the total CO emissions [1]. More recent studies of vehicular emissions in tunnels in Northern California continue to show that the ratio

of pollutant concentrations in the emissions from vehicles in actual use still differ from those predicted by governmental emissions inventories [19]. Since air quality modeling emissions inventories for Los Angeles must continue to be corrected to reflect real-world emissions rates, it becomes very important to continue to monitor emissions from the Los Angeles in-use vehicle fleet through local experiments conducted in highway tunnels.

7.2 Experimental Methods

7.2.1 Sampling Sites

Samples were collected at the Van Nuys tunnel, where Sherman Way, a major east-west thoroughfare with three lanes of traffic in each direction, passes under the runway of the Van Nuys Airport. Samples were collected on September 21, 1993, from 0600 hours to 1000 hours PDT, during the morning traffic peak. Opposing traffic flow in the tunnel is separated by a wall; eight open doorways through this wall exist at regular intervals between the two portals. Samples were collected at a traffic turn-out in the east-bound bore of the tunnel 147 meters from the traffic entrance and 75 meters from the exit of the tunnel. A second set of sampling equipment was sited outdoors directly above the location where the roadway enters the tunnel in order to measure the urban background pollutant concentrations already present in air entering the tunnel. A video camera was placed at the traffic turn-out within the tunnel to record the vehicles as they passed the sampling site. Vehicle counts, distributions by vehicle age and vehicle type, and estimates of vehicle speeds were obtained from the video tapes. Vehicle speed was estimated by timing vehicles over a known distance in the tunnel. The video tapes were processed by an expert traffic analyst who determined the distribution of vehicles by age and type.

7.2.2 Sample Collection and Analysis

The methods used to collect and analyze samples taken at the Van Nuys tunnel are the same as previously described for ambient atmospheric samples collected during the series of experiments of which this tunnel study forms a part [8-12], and thus only will be briefly summarized here.

Internally electropolished stainless steel canisters were used to collect volatile organic compounds. The 6-l canisters were deployed to the field under high vacuum and used to collect both 4-h integrated and instantaneous grab samples. The concentrations of CO_2, CO, CH_4, individual organic compounds and SF_6 were determined by a number of techniques including GC-MS, GC-FID (flame ionization detection), and GC-ECD (electron capture detection).

Aldehydes and other carbonyls were measured by collection on DNPH impregnated C_{18} Sepak cartridges. Carbonyl compounds trapped as their dinitrophenylhydrazones were extracted and analyzed by liquid chromatrography [9].

High volume dichotomous virtual impactors [20] were used to obtain enough organic material over the short sampling period to measure individual organic compounds in the particle and vapor phases. Fine particle collection occured on 102 mm diameter pre-fired quartz fiber filters (Pallflex 2500 QAO). Directly downstream of the fine particle filter on the high volume dichotomous sampler, polyurethane foam (PUF) cartridges were used to collect semi-volatile organic compounds. GC-MS techniques were used to identify and quantify compounds from both the filter and polyurethane foam samples. A detailed description of the PUF materials and the extraction and analysis methods for both the filter and PUF samples by GC-MS are given elsewhere [11-12].

Low volume particulate matter samplers were used to support the measurements needed to construct a material balance on the chemical composition of fine particles in the tunnel. Fine particles and total airborne particulate matter samples were collected by filtration along with certain inorganic gas-phase species that can be measured on chemically reactive filters. Fine particulate samples were collected downstream of a Teflon-coated AIHL cyclone separator [21]. At the 34.7 lpm flow rate used during this experiment, the AIHL cyclone removed particles with a diameter larger than 1.6 μm. Samples were collected at flow rates of 10 and 5 lpm on two 47 mm diameter Teflon filters (Gelman Teflo) and at a flow rate of 10 lpm on one 47 mm diameter quartz fiber filter (Pallflex 2500 QAO) operated in parallel downstream of the cyclone separator. Particulate mass concentrations were measured gravimetrically by repeated weighings of the Teflon filters at 22°C and 50% RH using a Mettler Model M-55-A mechanical microbalance. The fine particle samples collected on one Teflon filter of each set were analyzed by X-ray fluorescence for 38 trace metals. Organic and elemental carbon concentrations were determined from the quartz fiber filters by the method of Birch and Cary [22]. The quartz fiber filters (QFFs) were baked before use for at least six-hours at 550°C to lower their carbon blanks. The denuder difference method employing two nylon filters (Gelman Nylasorb) operated downstream of the fine particle cyclone and cyclone/denuder combination, respectively, at a flow rate of 5 lpm each was used to measure gas phase nitric and hydrochloric acids and fine particle nitrate and chloride [23-24]. Extracts from the nylon filters and from the second fine particle Teflon filter of each set were analyzed by ion chromatography to measure nitrate, chloride and sulfate concentrations. Additionally, atomic absorption spectrophotometry was used to measure particulate sodium and magnesium concentrations.

Particle-phase ammonium ion collected on Teflon filters and gas-phase ammonia collected on oxalic acid impregnated glass fiber filters downstream of a Teflon pre-filter were measured by an indophenol colorimetric procedure [25]. Ammonia emissions within the tunnel were found to be unexpectedly high, and are reported in a separate chapter where they can be discussed at length [26].

The integrity of the data was monitored through the collection, extraction and analysis of the samples. Contaminants measured on field and laboratory blanks were excluded from the statement of emitted compounds. The normal carboxylic acids blank values measured on the polyurethane foam cartridges were present at a significant fraction of the ambient loadings; therefore, the ambient concentrations of these compounds could not be calculated and the data are not included in this study. In all other cases, the blank levels were low compared to ambient concentrations, and the data presented here include these blank corrections.

7.2.3 Calculation of Emission Rates

Emission factors for traffic within a tunnel can be calculated per unit of fuel consumed [1], or per vehicle-kilometer-traveled [16,27]. The method based on fuel consumption is particularly convenient for use in a tunnel study. In that case, the increase of CO_2, CO, organic gases plus organic particulate matter within the tunnel directly matches the amount of carbon that was present in the fuel consumed, and emissions factors for each pollutant species per unit fuel consumed can be computed based on a carbon balance in the tunnel. Emissions rates computed per unit fuel burned based on this carbon balance are highly accurate; they are insensitive to uncertainties in air flow rates through the tunnel and are insensitive to the effect of any small air

exchange between adjacent bores of the tunnel. Emission factors based on vehicle-kilometers-traveled require measurement of the volumetric air flow rate through the tunnel as well as traffic flows within the tunnel. Given that information, pollutant concentrations can be converted into mass fluxes per vehicle. The volumetric air flow rate through the Van Nuys tunnel was measured by release of a known quantity of sulfur hexafluoride (SF_6) at the entrance of the tunnel for a 29 minute period during the four-hour experiment. The SF_6 concentration then was determined in two stainless steel canisters used to measure volatile organic compounds inside the tunnel; the primary canister sampled for the entire 240 minute tunnel study experiment thereby capturing within it SF_6 released during the entire 29 min tracer experiment, while a secondary canister was instantaeously filled during the SF_6 release period to obtain one measure of the variability of the instantaeous dilution rate. The SF_6 tracer experiment gave volumetric flow rates through the east-bound bore of the tunnel of 157 m^3 sec^{-1} for the instantaneous grab sample, and 133 m^3 sec^{-1} for the 29 min integrated sample, values that are essentially equal within experimental errors. The mechanical ventilation system at the Van Nuys tunnel was not in use, but the traffic flow in the tunnel drives a piston flow of air from the entrance of the tunnel to the exit, and these volumetric flow rates imply a traffic-driven wind inside the tunnel of approximately 2.3 m s^{-1}, consistent with observations made at the site. Given these dilution rate data, the fleet average fuel economy can be calculated since the total carbon in the exhaust, the length of the tunnel between the entrance and the sampling site, and traffic flows are known.

The range of dilution rate values suggests an additional uncertainty of about 20% in the translation of emissions per unit fuel burned into fuel economy and mass emissions per vehicle km driven. Thus fuel economy and

emissions rates per km driven should both be considered to be best estimate values while data given per unit fuel burned are the primary results of this experiment. The fuel-based inventory negates the uncertainties in air flow by relating pollutants in the tunnel to total carbon in the tunnel. Further, recent studies have shown that fuel consumption-based emission rates are less affected by driving conditions (e.g., uphill versus downhill) than is the case for inventories based on vehicle-distance-traveled [15].

7.3 Results

The traffic through the tunnel was characterized from review of video tapes of the experiment. A total of 7060 vehicles were counted, 256 were identified as pre-catalyst light duty vehicles (107 pre-catalyst light-duty vans and trucks and 149 pre-catalyst automobiles), 4546 were identified as catalyst-equipped automobiles, and 1936 were identified as catalyst-equipped light-duty trucks and vans. The age distribution for these light-duty vehicles is shown in Figure 1. Additionally, 12 diesel-powered light-duty vehicles, 277 heavy-duty vehicles, and 33 motorcycles were viewed on the video tapes. Of the 277 heavy-duty vehicles, 186 were identified as diesel-powered and 91 were identified as gasoline-powered. The light-duty vehicle counts in Figure 7.1 show a decrease with increasing vehicle age, except for an excess of vehicles from model years between 1980 and 1983. The mean model year for gasoline-powered light duty vehicles was 1986.4. The average light-duty vehicle being driven through the Van Nuys tunnel was more than 7 years old during this experiment, older than the vehicle fleets typically seen in tunnel studies elsewhere [15,19], but very similar to the general distribution of vehicle traffic in Los Angeles as a whole [1]. Since the 1990 model year there has been a significant increase in the fraction of the vehicle traffic contributed by light

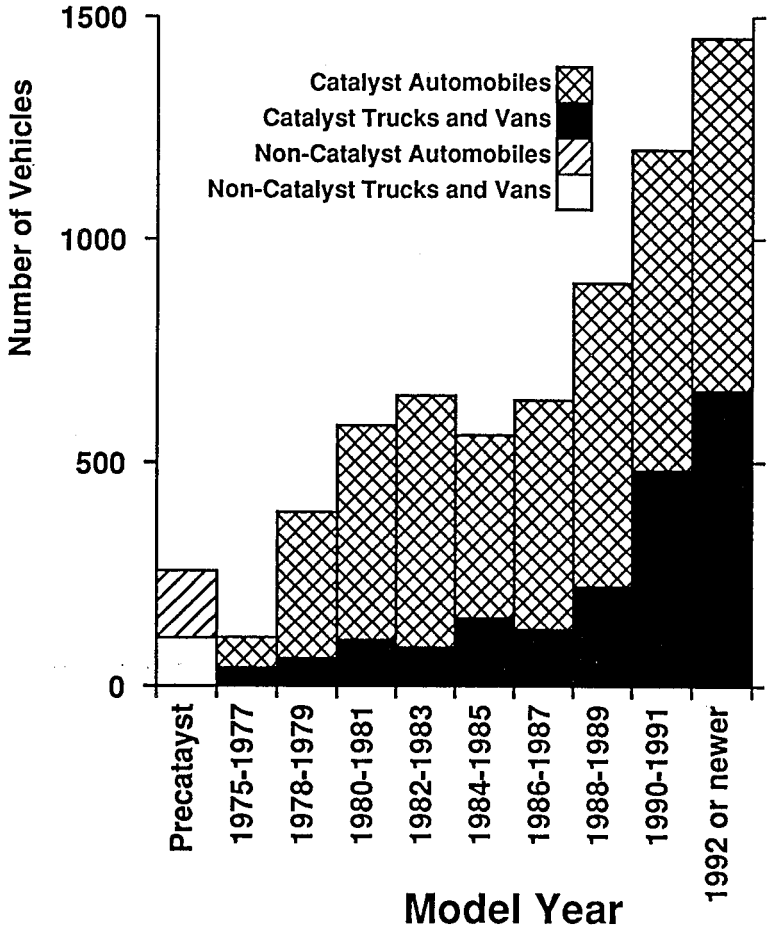

Figure 7.1:
Model year distribution of light-duty vehicles passing through the Van Nuys tunnel, 0600-1000 hours PDT, September 21, 1993.

trucks (a category which includes mini-vans and sport utility vehicles). The average vehicle speed in the tunnel was approximately 64 km hr^{-1} (40 mi hr^{-1}).

Using the dilution rate calculated from the SF_6 release, the vehicle counts, the total carbon measured in the exhaust (difference between in-tunnel and outdoor samplers), and average fuel parameters, the fleet-average fuel economy was calculated to be 6.3 km l^{-1} (14.7 mi $gallon^{-1}$) of gasoline-equivalent fuel. Using the distribution of vehicle ages and types and urban driving cycle fuel efficiency data for different vehicle types and ages [28-29], the fleet average fuel efficiency expected according to U.S. EPA fuel economy data would have been much higher, 8.6 km l^{-1} (20.2 mi $gallon^{-1}$). EPA fuel economy values are believed to be about 20% higher than actual fuel economy on the road [30], thereby indicating an expected fuel economy in actual use of 6.9 km l^{-1} (16.2 mi $gallon^{-1}$). The remaining small difference between calculated and measured fuel economy suggests that the vehicles are running with richer fuel/air mixtures or under heavier load than the EPA database would suggest.

7.3.1 Carbon Monoxide and Organic Vapor Emissions

The emission rates for carbon monoxide and total non-methane organic compounds (NMOC) are given in Table 7.1. Carbon monoxide emission rates (130 g l^{-1} or 20.8 g km^{-1}) and NMOC emission rates (9.1 g l^{-1} or 1.5 g km^{-1}) from the vehicle fleet in the Van Nuys tunnel are higher than reported for recent studies in highway tunnels in other cities. In the San Francisco Bay area, 1994 emission rates of 4.2 g l^{-1} for NMOC and 78.2 g l^{-1} for CO have been reported in the Caldecott tunnel [19]. In 1992, experiments conducted in the Ft. McHenry tunnel near Baltimore showed emission rates of 4.0 g

Table 7.1: Emission rates for non-methane hydrocarbons and carbon monoxide.

Pollutant	Fuel-based emission inventory	Emissions based on vehicle-kilometers-travelled
	gram per liter	gram per km
CO	130	20.8
NMOC	9.1	1.5

km^{-1} for CO and 0.4 g km^{-1} for NMOC [15]. The results of the present 1993 measurements in the Van Nuys tunnel are similar to values reported in the Van Nuys tunnel during the 1987 Southern California Air Quality Study, which were 13.1 g CO km^{-1} and 1.7 g HC km^{-1} [31]. CO emissions in the Van Nuys tunnel in September 1993 amounting to 130 g l^{-1} are within the range 108±25 g l^{-1} CO estimated for the hot stabilized exhaust emissions rate for the Los Angeles vehicle fleet in 1991 based on roadside remote sensing data [1]. While the emissions rates measured in the Van Nuys tunnel in September 1993 are high, it is unlikely that this is due to experimental error. The emissions rates per unit of fuel burned are easily measured from a carbon balance that is insensitive to air flow and mixing conditions in the tunnel, and those emissions rates per unit fuel burned, while high, are within the range observed by roadside remote sensing studies of Los Angeles vehicle traffic in the early 1990's.

Comparison to EMFAC Model

The EMFAC computer code is maintained by the California Air Resources Board (CARB) as the offical method for translating vehicle surveillance and test data into emission rate estimates for vehicle fleets in California. Emis-

Table 7.2: Vehicle fleet average emission rates predicted by the EMFAC-7G model at the temperature observed during the 1993 Van Nuys tunnel study.

		Emission Rate (grams per km)		
Case	Speed (mph)	Total HC†	CO	NO_x
Baseline EMFAC-7G	30	0.61	6.75	0.95
	40	0.43	5.27	1.05
	50	0.36	5.08	1.38
EMFAC-7G with Modified	30	0.62	15.56	1.05
Speed/Cycle Corrections	40	0.51	16.02	1.09
	50	0.47	15.76	1.18
EMFAC-7G with Modified	30	0.71	16.79	1.28
Speed/Cycle Corrections	40	0.59	17.29	1.33
and Grade Correction	50	0.54	17.01	1.43

† Includes exhaust and running loss hydrocarbons.

sion rates from the EMFAC model (version 7G) were computed by the staff of Sierra Research [32] for conditions expected if the 1993 vehicle fleet in Los Angeles were observed to travel through the Van Nuys tunnel. These results are shown in Table 7.2. The model first was used to represent warmed-up vehicle operation at speeds of 30, 40, and 50 mph at the nominal temperature in the tunnel (referred to as the baseline values in Table 7.2). In addition to these baseline EMFAC model calculations made by exercising the model according to CARB guidelines, other caclulations were performed that account for alternative assumptions regarding speed, driving cycle and grade corrections. The speed and driving cycle corrections are based on a limited test program conducted by Sierra Research to investigate the effect of vehicle speed on emissions under a variety of driving conditions [32]. The corrections used to account for driving cycle and grade increase predicted emission rates for organic gases and especially carbon monoxide significantly. While the corrections for carbon monoxide raise emission rates predicted by the

Table 7.3: Ambient concentrations of major contributors to fine[a] particulate matter inside and outside the tunnel.

Component	Tunnel Concentration $\mu g\ m^{-3}$	Background Concentration $\mu g\ m^{-3}$	Emissions in Tunnel $mg\ l^{-1}$	$mg\ km^{-1}$
Elemental Carbon	11.1 ±1.01	1.0 ±0.47	117.5±13.02	18.7±2.07
Organic Compounds[b]	21.7 ±1.41	9.6 ±1.02	141.4±20.34	22.5±3.23
SiO_2	1.0 ±0.09	0.9 ±0.07	1.2±1.33	0.2±0.21
Al_2O_3	0.4 ±0.08	0.6 ±0.08	0.0±1.32	0.0±0.21
SO_4^{2-}	7.4 ±0.21	7.4 ±0.21	0.0±3.47	0.0±0.55
Cl^-	0.8 ±0.13	trace	9.2±1.52	1.5±0.24
Mg^{2+}	0.6 ±0.08	0.1 ±0.01	5.1±0.94	0.8±0.15
Na^+	1.0 ±0.06	0.4 ±0.02	7.6±0.74	1.2±0.12
NO_3^-	10.8 ±0.42	5.5 ±0.21	61.9±5.49	9.8±0.87
NH_4^+	4.3 ±0.19	2.5 ±0.11	21.0±2.57	3.3±0.41
Other trace metals	6.2±1.33	7.0±1.37	0.0±22.32	0.0±3.54
Sum of Components	65.3±2.26	35.0±1.80	354.1±33.8	56.2±5.36
Gravimetric Mass	68.2±5.2	26.2±1.8	490.9±64.3	77.9±10.2

[a] Fine PM measured includes all particluate matter with $d_p \leq 1.6\ \mu m$. [b] Organic compound mass estimated as 1.4 × OC determined by thermal evolution and combustion analysis.

EMFAC model to within 20% of observed emission rates (which is within the error bounds of the tunnel dilution measurements as discussed earlier), hydrocarbons are still underpredicted by more than a factor of 2. Remaining factors other than poor vehicle condition that could account for a portion of the excess emissions in the tunnel include the possibility that not all vehicles were fully warmed-up before entering the tunnel.

7.3.2 Particle Emissions

The ambient concentrations of the fine particle species measured inside and outside the tunnel are listed in Table 7.3. Reasonable agreement is seen between the mass concentrations determined by gravimetric weighings of Teflon filters versus the sum of the individual chemical species measured. Based on the difference between the ambient concentrations of particulate matter and

gas-phase carbonaceous pollutants inside and outside the tunnel and the vehicle counts in the tunnel, the apparent fine particle emission rate from the vehicle traffic is calculated to be 491±65 mg l^{-1} (77.9±10.3 mg km^{-1}). The largest contributors to increased particle concentrations within the tunnel are organic compounds (141±20 mg l^{-1}; 22.5±3.2 mg km^{-1}), elemental carbon (118±13 mg l^{-1}; 18.7±2.1 mg km^{-1}) and ammonium nitrate (summing to 83±6 mg l^{-1}; 13.1±1.0 mg km^{-1}). To the best of our knowledge, ammonium nitrate is not emitted directly from vehicle exhaust. Source test data show only traces of particulate nitrate from the vehicle tailpipe [33]. Instead, substantial amounts of gas-phase NO_x are emitted, accompanied by 384 mg l^{-1} (61 mg km^{-1}) of gaseous ammonia during this experiment [26]. These ammonia emissions are consistent with the performance of 3-way catalyst-equipped vehicles that are running rich [34]. The high primary ammonia emissions then apparently lead to formation of fine particle ammonium nitrate inside the tunnel. If the secondary nitrate formed is subtracted from the particle levels in the tunnel, the estimated primary fine particle emission rate in the tunnel equals 271 (sum of species method) to 408 mg l^{-1} (gravimetric mass difference method); or 43.1 to 64.8 mg km^{-1}.

Fine particle emissions from vehicles include primary tailpipe particles from incomplete combustion in the engine, as well as tire dust, brake dust, and re-entrained road dust. Road dust deposited on urban streets includes soil dust, organic material from vegetation, and deposited particulate emissions from vehicles, including tire dust and brake lining wear debris; dust from all these sources is continually deposited onto and reentrained from street surfaces by passing vehicle traffic [35]. The importance of fugitive soil dust entrained from the road surface under the conditions of the tunnel study compared to tailpipe emissions can be judged by comparing the within-tunnel

and outdoor concentrations of the inorganic elements aluminum and silicon that are used to track the soil dust component of road dust [36]. X-ray fluorescence analysis of the fine particle samples shows that the levels of these two inorganic species are virtually identical inside and outside the tunnel, showing that fine particle soil dust resuspended by the vehicle traffic inside this particular tunnel is small. Organic chemical tracers, to be discussed shortly, can be used to set an upper bound on fine particle plant fragments and tire dust emissions within the tunnel.

7.3.3 Emissions of Individual Organic Compounds

Table 7.4 lists the emission rates of 221 organic compounds that are emitted from the vehicle fleet in the tunnel.

Vapor-phase emissions measured by VOC canister and DNPH cartridge samplers are given in mg per liter of fuel consumed and mg per vehicle-km-traveled. Vapor-phase, semi-volatile, and particle-phase organic compound emissions measured from PUF and filter samples are given in μg per liter of fuel burned and μg per km driven. These emissions are grouped according to organic compound functionality, with the emission rates stated separately for vapor-phase, semi-volatile, and particle-phase compounds. The emissions profile for the tunnel includes 64 aromatic hydrocarbons, 19 aromatic organic acids and 18 separate substituted aromatics, 31 normal alkanes, 23 branched alkanes, 16 cyclic alkanes, 17 petroleum biomarkers, 15 alkenes, 8 carbonyl compounds, 9 aliphatic organic acids, and the gasoline additive MTBE. These compound classes emitted from the vehicle fleet are measured in the VOC canister sampler and DNPH cartridges in amounts of 3.2 g l^{-1} of gasoline-equivalent fuel consumed for aromatics, 2.9 g l^{-1} for alkanes, 1.9 g l^{-1} for alkenes, 0.3 g l^{-1} for the carbonyls, and 0.2 g l^{-1} for MTBE. This corresponds

Table 7.4: Emission rates for individual organic compounds.

Compound	Volatile Organic Compound Emission Rates		Vapor-Phase Semi-Volatile Emission Rates		Particulate Organic Compound Emission Rates	
	mg l^{-1}	mg km^{-1}	μg l^{-1}	μg km^{-1}	μg l^{-1}	μg km^{-1}
n-Alkanes						
Ethane	119	18.9				
Propane	47	7.5				
n-Butane	146	23.2				
n-Pentane	230	36.5				
n-Hexane	135	21.4				
n-Heptane	89	14.1				
n-Octane	39	6.2				
n-Nonane	22	3.5				
n-Decane	11	1.7				
n-Undecane	19	3.0				
n-Dodecane	9	1.4				
n-Tetradecane			415.8	66.0		
n-Pentadecane			585.7	92.9		
n-Hexadecane			2051.0	325.5		
n-Heptadecane			2084.4	330.9	34.1	5.4
n-Octadecane			1661.8	263.7	55.6	8.8
n-Nonadecane			1298.8	206.0	60.5	9.6
n-Eicosane			745.1	118.3	48.9	7.8
n-Heneicosane			420.5	66.8	113.8	18.1
n-Docosane			199.0	31.6	123.9	19.7
n-Tricosane			91.0	14.5	164.5	26.1
n-Tetracosane			19.6	3.1	229.2	36.3
n-Pentacosane			19.2	3.1	158.4	25.1
n-Hexacosane			7.0	1.1	146.7	23.3
n-Heptacosane			2.9	0.5	104.0	16.5
n-Octacosane			0.8	0.2	77.6	12.4
n-Nonacosane					128.3	20.4
n-Triacontane					82.2	13.0
n-Hentriacontane					93.4	14.8
n-Dotriacontane					48.4	7.7
n-Tritriacontane					33.7	5.4
Branched Alkanes						
2-Methylpropane	14	2.2				
2-Methylbutane	564	89.5				
2-Methylpentane	242	38.4				
3-Methylpentane	153	24.3				
2,3-Dimethylbutane	68	10.8				
2-Methylhexane	111	17.6				
3-Methylhexane	119	18.9				
2,2-Dimethylpentane	5	0.8				
2,4-Dimethylpentane	70	11.1				
2,3-Dimethylpentane	122	19.4				
3,3-Dimethylpentane	5	0.8				
2-Methylheptane	47	7.5				
3-Methylheptane	60	9.6				
2,3-Dimethylhexane	28	4.4				
2,4-Dimethylhexane	45	7.1				

Table 7.4 (continued): Emission rates for individual organic compounds.

Compound	Volatile Organic Compound Emission Rates		Vapor-Phase Semi-Volatile Emission Rates		Particulate Organic Compound Emission Rates	
	mg l^{-1}	mg km^{-1}	μg l^{-1}	μg km^{-1}	μg l^{-1}	μg km^{-1}
Branched Alkanes: continued						
2,5-Dimethylhexane	41	6.5				
2,2,4-Trimethylpentane	208	33.0				
2,3,4-Trimethylpentane	76	12.1				
2,4-Dimethylheptane	5	0.8				
2,6-Dimethylheptane	5	0.8				
Norpristane			997.8	158.4		
Pristane			1675.6	266.0		
Phytane			1649.3	261.8		
Cyclic Alkanes						
Cyclopentane	14	2.2				
Cyclohexane	10	1.6				
Methylcyclohexane	23	3.7				
Methylcyclopentane	9	1.4				
Ethylcyclohexane	4	0.6				
1-Ethyl-4-methylcyclohexane	8	1.3				
Nonylcyclohexane			29.6	4.7		
Decylcyclohexane			91.9	14.6		
Undecylcyclohexane			102.6	16.3		
Dodecylcyclohexane			95.0	15.1		
Tridecylcyclohexane			72.1	11.4		
Tetradecylcyclohexane			81.0	12.9		
Pentadecylcyclohexane			91.8	14.6		
Hexadecylcyclohexane			47.7	7.6		
Heptadecylcyclohexane			20.5	3.3		
Octadecylcyclohexane			4.4	0.7		
Unresolved Complex Mixture(UCM)			231,000	36,700	113,000	17,900
Petroleum Biomarkers						
8β,13α-Dimethyl-14β-<u>n</u>-butylpodocarpane			35.2	5.5		
8β,13α-Dimethyl-14β-[3'-methylbutyl]podocarpane			16.5	2.6		
20S,13β(H),17α(H)-Diacholestane					11.2	1.8
20R,13β(H),17α(H)-Diacholestane					8.2	1.3
20R,5α(H),14β(H),17β(H)-Cholestane					11.4	1.8
20R,5α(H),14α(H),17α(H)-Cholestane					17.6	2.8
20R+S,5α(H),14β(H),17β(H)-Ergostane					22.3	3.6
20R+S,5α(H),14β(H),17β(H)-Sitostane					21.4	3.4
22,29,30-Trisnorneohopane					28.0	4.4
22,29,30-Trisnorhopane					18.1	2.9
17α(H),21β(H)-29-Norhopane					54.6	8.6
18α(H)-29-Norneohopane					15.6	2.4
17α(H),21β(H)-Hopane					82.0	13.0
22S,17α(H),21β(H)-30-Homohopane					34.7	5.5
22R,17α(H),21β(H)-30-Homohopane					23.3	3.7
22S,17α(H),21β(H)-30-Bishomohopane					21.8	3.4
22R,17α(H),21β(H)-30-Bishomohopane					14.0	2.3
Gasoline Additives						
MTBE	155	24.6				

Table 7.4 (continued): Emission rates for individual organic compounds.

Compound	Volatile Organic Compound Emission Rates		Vapor-Phase Semi-Volatile Emission Rates		Particulate Organic Compound Emission Rates	
	mg l^{-1}	mg km^{-1}	μg l^{-1}	μg km^{-1}	μg l^{-1}	μg km^{-1}
Alkenes						
Ethene	637	101.1				
Acetylene	486	77.1				
Propene	292	46.3				
cis-2-Butene	27	4.3				
trans-2-Butene	37	5.9				
2-Methylpropene	187	29.7				
1-Pentene	27	4.3				
cis-2-Pentene	21	3.3				
trans-2-Pentene	40	6.3				
3-Methyl-1-butene	10	1.6				
2-Methyl-2-butene	50	7.9				
2-Methyl-1-butene	35	5.6				
Cyclopentene	6	1.0				
1-Hexene	13	2.1				
2-Hexenes	4	0.6				
Aromatic Hydrocarbons						
Benzene	382	60.3				
Toluene	748	118.7				
Ethylbenzene	143	22.7				
n-Propylbenzene	34	5.4				
i-Propylbenzene	11	1.7				
o-Xylene	200	31.7				
m/p-Xylene	557	88.4				
o-Ethyltoluene	56	8.9				
m-Ethyltoluene	67	10.6				
p-Ethyltoluene	149	23.7				
1,2,3-Trimethylbenzene	84	13.3				
1,2,4-Trimethylbenzene	219	34.8				
1,3,5-Trimethylbenzene	77	12.2				
Indane	40	6.3				
1-Methylindane	28	4.4				
4-Methylindane	45	7.1				
4,7-Dimethylindane	7	1.1				
Naphthalene	326	51.7				
2-Methylnaphthalene	31	4.9				
1-Methylnaphthalene	25	4.0				
C2-substituted Naphthalenes			7778.0	1234.6		
C3-substituted Naphthalenes			3508.7	557.0		
C4-substituted Naphthalenes			1544.9	245.2		
Acenaphthylene			1949.5	309.4		
Fluorene			651.2	103.3		
C1-substituted Fluorenes			364.8	57.9		
C2-substituted Fluorenes			358.1	56.9		
C3-substituted Fluorenes			173.9	27.5		

Table 7.4 (continued): Emission rates for individual organic compounds.

Compound	Volatile Organic Compound Emission Rates		Vapor-Phase Semi-Volatile Emission Rates		Particulate Organic Compound Emission Rates	
	mg l^{-1}	mg km^{-1}	μg l^{-1}	μg km^{-1}	μg l^{-1}	μg km^{-1}
Aromatic Hydrocarbons: continued						
Phenanthrene			2456.1	389.9		
Anthracene			367.9	58.4		
C1-substituted Phenanthrenes			632.3	100.4		
C1-substituted Anthracenes			97.8	15.5		
C2-substituted MW 178 PAHs			385.7	61.3		
C3-substituted MW 178 PAHs			80.5	12.7		
C4-substituted MW 178 PAHs			11.6	1.8		
Fluoranthene			390.5	61.9	3.6	0.5
Acephenanthrylene			117.7	18.7	1.1	0.2
Pyrene			512.3	81.3	6.2	1.0
C1-substituted MW 202 PAHs			159.3	25.3	7.8	1.3
C2-substituted MW 202 PAHs			28.7	4.6	5.9	1.0
C3-substituted MW 202 PAHs					4.9	0.8
C4-substituted MW 202 PAHs					2.0	0.3
Benzo[ghi]fluoranthene			70.9	11.2	19.7	3.1
Cyclopenta[cd]pyrene			95.7	15.2	34.7	5.5
Benz[a]anthracene			15.5	2.4	20.9	3.3
Chrysene/Triphenylene			18.7	2.9	23.8	3.7
C1-substituted MW 226 PAHs					21.7	3.4
C1-substituted MW 228 PAHs					39.9	6.4
C2-substituted MW 228 PAHs					17.9	2.8
C3-substituted MW 228 PAHs					9.1	1.5
Benzo[k]fluoranthene					15.8	2.4
Benz[e]acephenanthrylene					16.1	2.6
Benzo[j]fluoranthene					4.9	0.8
Benzo[e]pyrene					21.7	3.4
Benzo[a]pyrene					18.3	2.9
Perylene					3.9	0.7
C1-substituted MW 252 PAHs					19.6	3.1
C2-substituted MW 252 PAHs					6.7	1.1
Indeno[123-cd]fluoranthene					10.4	1.6
Indeno[123-cd]pyrene					30.6	4.9
Benzo[ghi]perylene					102.2	16.3
Substituted and Heteroatom Aromatics						
Nitrobenzene			83.5	13.2		
Benzyl alcohol			1618.1	256.9		
o-Cresol			756.6	120.1		
m+p-Cresol			4449.1	706.3		
C2-substituted Phenols			1973.1	313.1		
9-Phenanthrol			205.7	32.6		
Indanone			670.3	106.4		
Phthalan			17.6	2.8		
Phthalide			365.9	58.0		
Fluoren-9-one			138.9	22.0	2.4	0.3
Dibenzothiophene			55.3	8.8	8.8	1.5
Benzothiazole			209.1	33.3	33.3	5.2
Dibenzofuran			187.3	29.7	29.7	4.7

Table 7.4 (continued): Emission rates for individual organic compounds.

Compound	Volatile Organic Compound Emission Rates		Vapor-Phase Semi-Volatile Emission Rates		Particulate Organic Compound Emission Rates	
	mg l^{-1}	mg km^{-1}	μg l^{-1}	μg km^{-1}	μg l^{-1}	μg km^{-1}
Functional Aromatics: continued						
Antracene-9,10-dione			9.0	1.4	6.0	1.0
Phenalen-9-one			1.6	0.3	32.6	5.2
Benz[de]anthracen-7-one					7.8	1.2
Benz[a]anthracene-7,12-dione					2.0	0.3
Benzo[cd]pyren-6-one					33.1	5.3
Carbonyl Compounds						
Formaldehyde	128	20.3				
Acetaldehyde	29	4.6				
Hexanal	5	0.8				
Nonanal	7	1.1				
2-Butanone	38	6.0				
Crotonaldehyde	20	3.2				
Benzaldehyde	20	3.2				
Methylglyoxal	27	4.3				
Aromatic Acids						
Benzoic acid			144.1	22.9		
2-Methylbenzoic acid			6.7	1.1		
3-Methylbenzoic acid			77.8	12.3		
4-Methylbenzoic acid			67.0	10.6		
2,6-Dimethylbenzoic acid			21.7	3.4		
2,5-Dimethylbenzoic acid			121.0	19.2		
2,4-Dimethylbenzoic acid			43.5	6.9		
3,5-Dimethylbenzoic acid			55.2	8.8		
3,4-Dimethylbenzoic acid			26.8	4.3		
Naphthoic acid			18.5	2.9		
Dehydroabietic acid					5.7	0.9
1,2-Benzenedicarboxylic acid					347.8	55.2
1,3-Benzenedicarboxylic acid					96.6	15.3
1,4-Benzenedicarboxylic acid					83.1	13.2
4-Methyl-1,2-benzenedicarboxylic acid					129.5	20.6
1,2,4-Benzenetricarboxylic acid					172.6	27.4
1,2,3-Benzenetricarboxylic acid					22.0	3.5
1,3,5-Benzenetricarboxylic acid					3.4	0.5
1,2,4,5-Benzenetetracarboxylic acid					6.1	1.0
Alkanoic Acids						
Palmitic acid					302.7	48.0
Stearic acid					185.8	29.5
Propanedioic acid					8.6	1.4
Butanedioic acid					59.7	9.5
Methylbutanedioic acid					14.4	2.3
Methylbutenedioic acid					25.5	4.0
Pentanedioic acid					20.6	3.2
Hexanedioic acid					4.6	0.7
Nonanedioic acid					5.8	0.9

to an emission rate of 8.5 g l^{-1} of identified compounds, leaving 0.6 g l^{-1} of total non-methane organic compounds from the canister sampler that are not identified at the single compound level. Semi-volatile organic compounds identified after collection on the polyurethane foam but not from the canister sampler contribute less than 0.3 g l^{-1} to the organic gases.

Normal Alkanes

In addition to the low molecular weight n-alkanes present in gasoline and diesel fuel which are expected in the tunnel, emissions of particulate n-alkanes that are characteristic of plant waxes are also apparent. This plant wax signature is evident in the form of higher emission rates of odd-carbon number high molecular weight n-alkanes such as nonacosane (n-C_{29}) and hentriacontane (n-C_{31}) relative to even carbon number alkanes of similar molecular weight, and can be compared to the dominance of the odd-carbon number homologues in aerosol particles emitted from leaf surfaces in the Southern California area [37, 38]. The excess of the C_{29} - C_{31} odd-carbon number n-alkanes seen within the tunnel over the smooth distribution of n-alkanes seen in crude oil [39] can be attributed to plant waxes entrained into the atmosphere from road dust [35]. The amount by which the calculated emission rate, E_p, of the n-C_{29} alkane exceeds the n-C_{29} alkane contribution from petroleum provides one indication of the quantity of plant wax-containing particles in the tunnel atmosphere, and is calculated as:

$$\Delta E_p(n-C_{29})_{attributable\ to\ plant\ waxes} = E_p(n-C_{29})_{total} - \frac{E_p(n-C_{30}) + E_p(n-C_{28})}{2} \tag{7.1}$$

and a similar equation can be written for that portion of the emissions of the n-C_{31} alkane that are attributable to plant waxes using the emission rates

of the n-C_{30} and the n-C_{32} alkanes. Using these techniques, the calculated emissions of excess n-C_{29} and n-C_{31} attributable to plant waxes are 7.9 and 4.7 μg per vehicle-km-traveled, respectively. Using the emission rates of these compounds attributable to plant waxes and the composition of plant fragment particles shed from leaves in Southern California [36], a rough estimate can be made of the emission rate of vegetative detritus within the tunnel that is created as tires pass over plant material on the road bed [37]. The calculations show a range of contribution to particulate matter emissions in the tunnel due to plant fragments of 0.5 to 1.4 mg per vehicle-km-traveled, which is less than 2% of the gain in fine particle concentration in the tunnel.

Branched and Cyclic Alkanes

Two separate categories of branched and cyclic alkanes are apparent in the data presented in Table 7.4. High emission rates of low molecular weight alkanes (in the carbon number range from roughly C_5 to C_8) can be attributed to the presence of these compounds in gasoline. An additional class of semi-volatile branched and cyclic parafins (in the carbon number range from roughly C_{18} to C_{22}) are emitted at a lower rate and can be attributed to the presence of these compounds in diesel fuels [40]. In addition to these resolved branched and cyclic hydrocarbons, the emissions from vehicles contain unresolved branched and cyclic compounds, commonly called the unresolved complex mixture (UCM) [39]. The UCM is characteristic of petroleum and appears as a hump on GC traces underlying the resolved peaks of individual compounds. Large UCM humps are present in the polyurethane foam samples and the particulate matter samples collected inside the tunnel, accounting for 230 mg l^{-1} of semi-volatile vapor-phase organics and 113 mg l^{-1} of particulate organics emissions. The UCM measured in the particle phase

corresponds to approximately 80% of the total organic compound mass measured by combustion analysis of the particle samples.

Petroleum Biomarkers

Petroleum biomarkers are molecular fossils present in petroleum that reflect chemical structures originating from the microorganisms from which the petroleum deposits formed. These unique chemical structures can be used to trace the source of the organic matter from which the petroleum deposits were formed and also can be used to trace the presence of petroleum residues in the environment [41]. Rogge et al. [42] and Schauer et al. [36] show that these petroleum biomarkers can be used to trace motor vehicle exhaust contributions to airborne particulate matter in the Southern California atmosphere. Listed in Table 7.4 are the emission rates of 17 individual petroleum biomarkers seen in both the particulate matter and semi-volatile organics samples.

Alkenes

The emission rates for 15 alkenes are given in Table 7.4. These compounds are among the most reactive in atmosphere, leading to ozone formation [43], and for this reason fleet-average alkene emission rates are of considerable interest.

In Figure 7.2, the emission rates of volatile organic compounds within the tunnel are compared to the composition of the average gasoline sold in Southern California during the summer of 1995. The open bars represent the emission rate of the volatile organic compounds, and the crosses represent the weight percentage of that compound in gasoline. The gasoline sample was blended to represent a market share weighted average of the product of the six largest gasoline vendors in the Los Angeles area, and was analyzed by

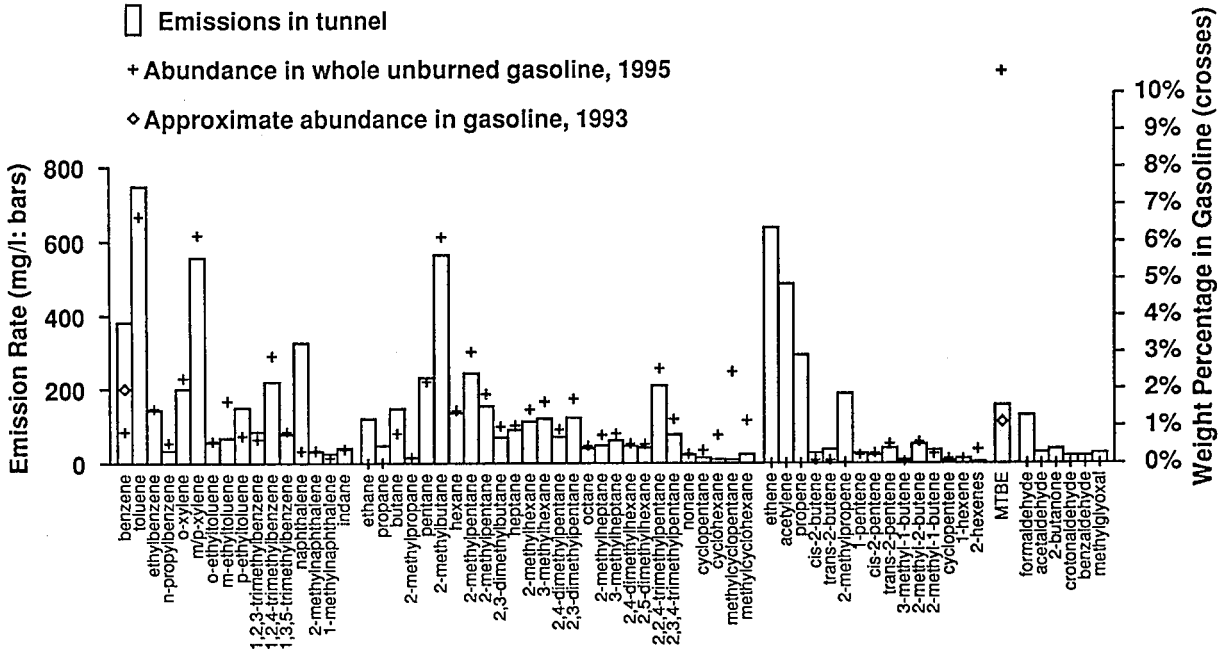

Figure 7.2:
Comparision of the emissions rates of identified organic compounds within the Van Nuys tunnel in September 1993 (bars) to the weight percentage of each compound in Southern California gasoline (cosses=1995 summer gasoline, diamonds=correction to conditions in summer 1993.)

gas chromatography to determine its chemical composition. While these two graphs need not necessarily track each other, there is a clear correlation for many organic compounds between the compound concentrations in gasoline and the relative compound emissions rates from the vehicle fleet inside the tunnel. During the interval between the summer 1993 tunnel study and the date of collection of the 1995 composite gasoline sample, new regulations mandated an increase in the oxygen content of gasoline from approximately 0.2% before the mandate (tunnel sample) to a minimum of 2% (gasoline sample), while reducing benzene in gasoline from approximately 2% to a maximum of 1%. Two percent oxygen in the fuel can be achieved by raising the MTBE content of gasoline to 11% by weight. The approximate levels of benzene and the oxygenated organic MTBE in Southern California gasoline in 1993 before the latest reformulation are shown by the diamond symbols in Figure 7.2. From Figure 7.2, it is clear that those compounds for which the open bar substantially exceeds the corresponding cross are produced in the combustion process inside the engine. These include the light olefins, aldehydes, a portion of the benzene and possibly naphthalene.

Aromatic Hydrocarbons

Concern over the mutagenic and carcinogenic potential of aromatic hydrocarbons has lead to efforts to understand their formation and atmospheric chemistry. The emission rates of 64 aromatic hydrocarbons measured in the vapor and particle phases are listed in Table 7.4. Aromatic compounds are present in trace amounts in petroleum products, including diesel fuel [44]. Survival of these fuel components [45], as well as build-up of smaller molecules to form polycyclic aromatic hydrocarbons (PAHs) during high-temperature combustion, and dealkylation of substituted aromatic compounds present in

fuel, all are mechanisms important in the emission of PAHs from vehicles.

Synthesis (build-up) of aromatic compounds from radical species during combustion will favor unsubstituted aromatic compounds over their alkylated homologs. Thus an increase in unsubstituted over substituted aromatics relative to the composition of fuel should be diagnositic for the presence of benzene and naphthalene formed in combustion. This is clearly the case for benzene, as seen in Figure 7.2. Since the methyl-substituted naphthalenes in the tunnel samples are present at about their expected abundance relative to the composition of the gasoline pool, it appears that naphthalene is being synthesized in combustion as well.

Substituted Aromatic Compounds

Substituted aromatic compounds, including one nitro-aromatic and a variety of oxygenated aromatics are present in the emissions from vehicles in the Van Nuys tunnel. The most prominent aromatic alcohols measured in vehicle exhaust include phenol, the cresols, and C2-substituted phenols. Although phenol was detected in the Van Nuys tunnel, its concentration is not reported in Table 7.4 because of interference from its presence as one of the few contaminants in the benzene solvent used in extraction and concentration of the PUF samples. Cresols are commonly viewed as atmospheric reaction products of OH attack on toluene, which is one of the first steps in one aromatic oxidation pathway leading to secondary organic aerosol formation. The presence of significant direct emissions of cresols from vehicle exhaust means that it is possible for some aromatics to bypass the initial atmospheric attack of OH on toluene, thereby bypassing one of the rate limiting steps in the oxidation pathway toward formation of secondary organic aerosol from aromatic precursors. Analysis of the spatial distribution of

cresols in the Los Angeles area atmosphere implies that primary emissions of these compounds dominate their atmospheric concentrations [12]. For that reason, atmospheric oxidation of directly emitted cresols should be viewed as a potentially important competitor to atmospheric toluene oxidation as a source of secondary organic aerosol. Direct emissions of vapor-phase cresols are seldom included in the vapor-phase organics profiles used to represent vehicle emissions within photochemical airshed models because as semi-volatile compounds they are seldom measured even though their presence in vehicle exhaust has been reported previously [46].

The emissions rates of aromatic ketones, including mono-ketones and di-ketones, were measured within the Van Nuys tunnel. Diketones in the atmosphere can come in part from atmospheric oxidation of primary aromatic hydrocarbons [47]. The particular mono-ketones measured in the tunnel when found in the atmosphere are expected to be due entirely to primary emissions, because the precursor hydrocabons for these compounds are not detected in the atmosphere (e.g., the three-ring hydrocarbon structure that would constitute a precursor to phenalen-9-one).

Carbonyl Compounds

In a manner similar to the formation of light olefins and some unsubstituted aromatic compounds, Figure 7.2 shows that a variety of carbonyls are formed during combustion. Methylglyoxal which is one of the principal end-products of atmospheric aromatics oxidation also is found in the direct emissions from motor vehicles, as shown in Table 7.4.

Alkanoic Acids

High molecular weight normal alkanoic acids, especially stearic (C_{18}) and palmitic (C_{16}) acids, are ubiquitous in atmospheric samples [48]. Overall,

the concentrations for most alkanoic acid homologs are about equal inside and outside the tunnel (within the error bounds on the quantification procedure) with palmitic and stearic acids being the only homologs which appear at substantially elevated concentrations inside the tunnel. High molecular weight n-alkanoic acids have been reported in the tailpipe emissions from vehicular sources [42,49], as well as in tire dust, brake lining wear dust and paved road dust [35]. Palmitic and stearic acids contributed over 50% of the mass concentration of the 27 n-alkanoic acids measured in road dust [35], with roughly twice the levels of palmitic acid when compared to stearic acid, a ratio very similar to that seen during the Van Nuys tunnel experiment. Additionally, the relative concentration ratio within the tunnel between these two acids and the two normal alkane homologs attributed to plant waxes is similar to the concentration ratios seen in road dust samples collected in Los Angeles [35]. In previously reported measurements of catalyst-equipped automobile exhaust composition [42], stearic and palmitic acids account for less than 15% of the total n-alkanoic acid emissions from the automobile tailpipe, with roughly four times as much palmitic acid as stearic acid. In heavy-duty diesel truck exhaust, these two homologs account for less than 20% of the total n-alkanoic acid emissions, with roughly twice as much palmitic as stearic acid [42]. Stearic acids are a blending component that is added to tire rubber during manufacturing [35]. In one tire dust sample analyzed to date, palmitic acid contributed 40% and stearic acid contributed 50% of the emissions of the n-alkanoic acids class [35]. In brake lining wear particle samples analyzed to date, these two homologs together contribute about 30% of the emissions of n-alkanoic acids, with roughly equal contributions [35]. Given the many contributing sources, it is not surprising that palmitic and stearic acids concentrations are elevated within the Van Nuys tunnel. Their rel-

ative distribution in the tunnel is similar to that seen in the atmosphere [50], and indeed dry deposition of atmospheric aerosols may contribute these compounds to the roadway surface where they are reentrained into the atmosphere by vehicular traffic.

Aromatic Organic Acids

Emission rates for aromatic acids, including benzene carboxylic acids, benzene dicarboxylic acids, benzene tricarboxylic acids, and benzene tetracarboxylic acids are listed in Table 7.4. Previous reports have implicated vehicle traffic as a source of gas-phase benzoic acid [51] and particle-phase 1,2-benzenedicarboxylic acid and methyl-1,2-benzenedicarboxylic acid [49,52] to which we now add another 16 related compounds. Particle-phase polyfunctional acids in the Los Angeles atmosphere show spatial and seasonal trends that indicate significant formation by secondary reactions in the atmosphere involving gaseous precursors [50]. It now appears that modeling of polyfunctional aromatic acids concentrations in the atmosphere will require consideration of both primary emissions and atmospheric photochemical oxidation processes.

The resin acid derivative dehydroabietic acid was quantified in the particle phase both inside and outside the tunnel. The particle-phase emission rate for this compound is calculated as 1.5 μg per vehicle-km-traveled. This resin acid has been quantified in wood smoke [53], tire dust and road dust particles [35]. The presence of dehydroabietic acid in tire dust is probably due to the practice of adding conifer resins to the tire batch as an extender and softener. The source of dehydroabietic acid in road dust particles is most likely either from tire dust deposited onto the road or alternatively from the debris of coniferous plants ground up by passing traffic as part of the paved road dust

mixture. Since woodsmoke is not a significant emission source during the summer in the Los Angeles area [36], an upper limit on the contribution of tire dust to the fine particle emission rate from vehicles and road dust can be estimated based on the ratio of dehydroabietic acid in tire dust to the emission rate of this compound inside the tunnel. Source test data for tire dust in Southern California show 7970 μg of dehydroabietic acid per gram of tire dust sampled [35]. On this basis, tire dust is estimated to contribute no more than 0.2 mg of fine particles per vehicle-km-traveled in the tunnel.

7.4 Discussion

The CO and vapor-phase organic compounds emissions rates of 130 g CO and 9.1 g VOC per liter of gasoline-equivalent fuel burned that were measured in 1993 in the Van Nuys tunnel were found to be higher than represented by governmental emissions inventories (e.g., EMFAC 7G basecase) but are within the range of the 108$\pm$25 g l^{-1} CO reported by roadside remote sensing studies in Los Angeles [1]. The detailed organic compound measurements made in the tunnel can be used to explore the possible cause of the higher VOC emission rates. One possibility is that an unusually large amount of unburned gasoline is either being emitted from the tailpipe or is leaking from vehicle fuel systems. Since the exhaust from properly functioning automobiles contains a large portion of unburned fuel components in any case, further enrichment has to be judged as an excess above the typical blend of burned and unburned exhaust hydrocarbons that is seen in laboratory-based tailpipe tests conducted on the vehicle fleets used for tracking compliance with emissions control regulations. As a rough approximation, we consider that the hydrocarbon composition of emissions in the tunnel is a linear combination of the auto exhaust characteristics seen in laboratory-based source

tests plus an extra increment due to unburned whole gasoline. For each VOC species measured, both in the tunnel and present in the source test data base, an expression is written:

$$C_{i_{tunnel}} = \alpha C_{i_{tailpipe}} + (1-\alpha) C_{i_{fuel}} + \delta(\alpha)_i \qquad (7.2)$$

where the C_i indicate the weight percent of species i in the tunnel, auto exhaust source test profile, and fuel composition data sets, and $\delta(\alpha)_i$ is the residual discrepancy between the tunnel data and a linear combination of the source profiles at a particular value of the unknown constant α. Using all VOC species appearing in the tunnel (except for benzene, butanes and MTBE that have been affected by gasoline reformulation), plus the 1995 gasoline sample described in Figure 7.2, and several auto source test data bases, the value of α that minimizes the sum of the squared residual discrepancies was computed for several different automobile exhaust profiles. When the catalyst-equipped automobile exhaust profile of Harley et al. [53] is used to describe the vehicle tailpipe, the best estimate is that the tunnel atmosphere is dominated by auto tailpipe exhaust (α=0.97). When either the Exh801a vehicle profile published by Fujita et al. [54] or the non-catalyst auto exhaust profile of Harley et al. [53] are used, the best estimate is that the tunnel atmosphere is about 74-75% traditional tailpipe emissions plus 25-26% additional unburned gasoline (which of course could be either leaking from the fuel systems or coming from the tailpipes of poorly maintained cars). There is a very shallow minimum in the best choice of α, and thus a wide range of exhaust and fuel mixtures nearly reproduce the tunnel result.

The comprehensive vapor-phase organics data collected in the present study make it possible to explore the differences in the photochemical reac-

tivity of the VOC emissions in the tunnel that would be estimated from the traditional VOC canister catch alone versus that seen when the additional species captured on the polyurethane foam and DNPH cartridge are added. The emission rates for the individual vapor-phase organic compounds were scaled according to their incremental reactivities on Carter's maximum incremental reactivity scale [2]. Using this scale, and summing contributions to reactivity for the individual organic compounds, the VOC canister sample accounted for 94% of the total reactivity measured by summing the VOC canister plus DNPH cartridge plus polyurethane foam sample for those compounds with known reactivity. Of those compounds not included in the VOC canister analysis, contributions from aldehydes and aromatic compounds contributed most of the additional reactivity.

The detailed information on fine particle composition in the tunnel likewise exposes interesting features of the emissions in the tunnel. The particles in this tunnel atmosphere during this particular experiment are almost entirely due to tailpipe emissions plus secondary ammonium nitrate formation. That is clear because the silicon, aluminum, dehydroabietic acid, and high molecular weight odd carbon number alkanes concentrations set upper limits of a few tenths of a mg km^{-1} on the fine particle road dust, tire dust and vegetative detritus that could be produced as fugitive emissions from the vehicle traffic, as explained earlier. The soot (EC) levels in the tunnel are higher than we initially expected relative to fine particle organics, but side calculations show that both the organic carbon and elemental carbon emission rates are within the range that could be achieved by this mix of vehicles, depending on the diesel engine technology used in the small fraction of the vehicles in the tunnel that have diesel engines. Knowing the organic chemical signature of a largely tailpipe emissions-dominated vehicle fleet, and particu-

larly its petroleum biomarker content, it will be possible in future work to set an upper limit on the amount of primary tailpipe fine particulate matter that is present in the Los Angeles urban atmosphere by using organic molecular tracer techniques [36].

Bibliography

[1] B. C. Singer and R. A. Harley. A fuel-based motor vehicle emission inventory. *J. Air & Waste Manage. Assoc.*, 46: 581-593, 1996.

[2] W. P. L. Carter. Development of ozone reactivity scales for volatile organic compounds. *J. Air & Waste Manage. Assoc.*, 44: 881-899, 1994.

[3] IARC Monographs: Evaluation of carcinogenic risks to humans- diesel and gasoline engine exhausts and some nitroarenes. World Health Organization, International Agency for Research on Cancer: Lyon, France, 1989.

[4] J. R. Odum, T. P. W. Jungkamp, R. J. Griffin, H. J. L. Forstner, R. C. Flagan and J. H. Seinfeld. Aromatics, reformulated gasoline and atmospheric organic aerosol formation. *Environ. Sci. Technol.*, 31: 1890-1897, 1997.

[5] D. H. Lowenthal, B. Zielinska, J. C. Chow, J. G. Watson, M. Gautam, D. H. Ferguson, G. R. Neuroth and K. D. Stevens. Characterization of heavy-duty diesel vehicle emissions. *Atmos. Environ.*, 28: 731-743, 1994.

[6] J. C. Sagebiel, B. Zielinska, W. R. Pierson and A. W. Gertler. Real-world emissions and calculated reactivities of organic species from motor vehicles. *Atmos. Environ.*, 30: 2287-2296, 1996.

[7] B. Zielinska and K. K. Fung. The composition and concentration of hydrocarbons in the range of C2 to C18 emitted from motor-vehicles. *Sci. Tot. Environ.*, 147: 281-288, 1994.

[8] M. P. Fraser, D. Grosjean, E. Grosjean, R. A. Rasmussen and G. R. Cass. Air quality model evaluation data for organics. 1. Bulk chemical composition and gas/particle distribution factors. *Environ. Sci. Technol.*, 30: 1731-1743, 1996.

[9] E. Grosjean, D. Grosjean, M. P. Fraser and G. R. Cass. Air Quality Model Evaluation Data for Organics. 2. C_1 - C_{14} Carbonyls in Los Angeles Air. *Environ. Sci. Technol.*, 30: 2687-2703, 1996.

[10] E. Grosjean, D. Grosjean, M. P. Fraser and G. R. Cass. An Air Quality Model Evaluation Data Set for Organics. 3. Peroxyacetyl nitrate and peroxypropionyl nitrate in Los Angeles Air. *Environ. Sci. Technol.*, 30: 2704-2714, 1996.

[11] M. P. Fraser, G. R. Cass, R. A. Rasmussen and B. R. T. Simoneit. Air quality model evaluation data for organics. 4. C_2 to C_{36} non-aromatic hydrocarbons. *Environ. Sci. Technol.*, 31: 2356-2367, 1997.

[12] M. P. Fraser, G. R. Cass, B. R. T. Simoneit and R. A. Rassmussen. Air quality model evaluation data for organics. 5. C6-C22 non-polar and semi-polar aromatic hydrocarbons" *submitted to Environ. Sci. Technol.*, 1997.

[13] National Research Council *Rethinking the Ozone Problem in Urban and Regional Air Pollution*, National Academy Press: Washington DC, 1991.

[14] C. Christoforou, L. G. Salmon, M. P. Hannigan, P. A. Solomon and G. R. Cass. Trends in fine particle concentration and chemical composition in Southern California. *submitted to J. Air Waste Manage. Assoc.*, 1997.

[15] W. R. Pierson, A. W. Gertler, N. F. Robinson, J. C. Sagebiel, B. Zielinska, G. A. Bishop, D. H. Stedman, R. B. Zweidinger and W. D. Ray. Real-world automotive emissions-summary of studies in the Fort McHenry and Tuscarora Mountain Tunnels. *Atmos. Environ.*, 30: 2233-2256, 1996.

[16] M. N. Ingalls. On-Road Vehicle Emission Factors from Measurements in a Los Angeles Area Tunnel. Proceedings of the Air & Waste Management Association 82nd Annual Meeting, Anaheim, CA, 1989.

[17] R. A. Harley, A. G. Russell, G. J. McRae, G. R. Cass and J. H. Seinfeld. Photochemical modeling of the Southern California Air Quality Study. *Environ. Sci. Technol.*, 27: 378-388, 1993.

[18] D. R. Lawson, P. J. Groblicki, D. H. Stedman, G. A. Bishop and P. L. Guenther. Emissions from in-use motor vehicles in Los Angeles: a pilot study of remote sensing and the inspection and maintenance program. *J. Air & Waste Manage. Assoc.*, 40: 1096-1105, 1990.

[19] T. W. Kirchstetter, B. C. Singer, R. A. Harley, G. R. Kendall and W. Chan. Impact of oxygenated gasoline use on California light-duty vehicle emissions. *Environ. Sci. Technol.*, 30: 661-670, 1996.

[20] P. A. Solomon, J. L. Moyers and R. A. Fletcher. High-volume dichotomous virtual impactor for the fractionation and collection of particles

according to aerodynamic size. *Aerosol Sci. Technol.*, 2: 455-464, 1983.

[21] W. John and G. Reischl. A cyclone for size-selective sampling of ambient air. *J. Air Pollut. Control Assoc.*, 30: 872-876, 1980.

[22] M. E. Birch and R. A. Cary. Elemental carbon-based method for monitoring occupational exposures to particulate diesel exhaust. *Aerosol Sci. Technol.*, 25: 221-241, 1996.

[23] P. A. Solomon, S. M. Larson, T. Fall and G. R. Cass. Basinwide nitric acid and related species concentrations observed during the Claremont Nitrogen Species Comparision Study. *Atmos. Environ.*, 22: 1587-1594, 1988.

[24] A. Eldering, P. A. Solomon, L. G. Salmon, T. Fall and G. R. Cass. Hydrochloric acid: a regional perspective on concentrations and formation in the atmosphere of Southern California. *Atmos. Environ.*, 25A: 2091-2102, 1991.

[25] W. T. Bolleter, C. J. Bushman and P. W. Tidwell. Spectrophotometric determinations of ammonium as indophenol. *Anal. Chem.*, 33: 592-594, 1961.

[26] M. P. Fraser and G. R. Cass. Detection of excess ammonia emissions from in-use vehicles and the implications for fine particle control. *submitted for publication in Environ. Sci. Technol.*, 1997.

[27] T. Y. Chang, S. W. Modzelewski, J. M. Norbeck and W. R. Pierson. Tunnel air quality and vehicle emissions. *Atmos. Environ.*, 15: 1011-1016, 1981.

[28] J. D. Murrell, K. H. Hellman and R. M. Heavenrich. Light-duty automotive technology and fuel economy trends through 1993. EPA/AA/TDG-93/01. Office of Mobile Sources, U.S. Environmental Protection Agency: Ann Arbor, MI 1993.

[29] Compilation of air pollution emission factors. Volume 2: Mobile Sources; EPA/AP-42. Office of Mobile Sources, U.S. Environmental Protection Agency: Ann Arbor, MI 1985.

[30] M. Mintz, A. D. Vyas and L. A. Conley. "Differences between EPA-test and in-use fuel economy: are the correction factors correct?" *Transportation Res. Record*, 1416: 124-130, 1993.

[31] W. R. Pierson, A. W. Gertler and R. L. Bradow. Comparison of the SCAQS tunnel study with other on-road vehicle emission data. *J. Air & Waste Manage. Assoc.*, 40: 1495-1504, 1990.

[32] P. Heirigs and L. Caretto. Sierra Research, Sacramento, CA; personal communication, 1997.

[33] L. M. Hildemann, G. R. Markowski and G. R. Cass. Chemical composition of emissions from urban sources of fine organic aerosol. *Environ. Sci. Technol.*, 25: 744-759, 1991.

[34] S. H. Cadle and P. A. Mulawa. Low molecular weight aliphatic amines in exhaust from catalyst-equipped cars. *Environ. Sci. Technol.*, 14: 718-723, 1980.

[35] W. F. Rogge, L. M. Hildemann, M. A. Mazurek, B. R. T. Simoneit and G. R. Cass. Sources of fine organic aerosol. 3. Road dust, tire

debris, and organometallic break lining dust- roads as sources and sinks. *Environ. Sci. Technol.*, 27: 1892-1904, 1993.

[36] J. J. Schauer, W. F. Rogge, L. M. Hildemann, M. A. Mazurek, G. R. Cass and B. R. T. Simoneit. Source Apportionment of Airborne Particulate Matter Using Organic Compounds as Tracers *Atmos. Environ.*, 30: 3837-3855, 1996.

[37] W. F. Rogge, L. M. Hildemann, M. A. Mazurek, B. R. T. Simoneit and G. R. Cass. Sources of fine organic aerosol. 4. Particulate abrasion products from leaf surfaces of urban plants. *Environ. Sci. Technol.*, 27: 2700-2711, 1993.

[38] L. M. Hildemann, W. F. Rogge, G. R. Cass, M. A. Mazurek and B. R. T. Simoneit. Contribution of primary aerosol emissions from vegetation-derived sources to fine particle concentrations in Los Angeles. *J. Geophys. Res.*, 101: 19541-19549, 1996.

[39] B. R. T. Simoneit. Characterization of organic-constitutents in aerosols in relation to their origin. *Intern. J. Environ. Anal. Chem.*, 23: 207-237, 1986.

[40] B. Zielinska, J. C. Sagebill, G. Harshfield, A. W. Gertler and W. R. Pierson. Volatile organic compounds up to C20 emitted from motor vehicles; measurement methods. *Atmos. Environ.*, 30: 2269-2286, 1996.

[41] K. E. Peters and J. M. Moldowan. *The Biomarker Guide*, Prentice-Hall: Englewood Cliffs, NJ, 1993.

[42] W. F. Rogge, L. M. Hildemann, M. A. Mazurek, B. R. T. Simoneit and G. R. Cass. Sources of fine organic aerosol. 2. Noncatalyst and

catalyst-equipped automobiles and heavy-duty diesel trucks. *Environ. Sci. Technol.*, 27: 636-651, 1993.

[43] R. Atkinson. Gas-phase tropospheric chemistry of organic compounds: a review. *Atmos. Environ.*, 24A: 1-41, 1990.

[44] P. T. Williams, K. D. Bartle and G. E. Andrews. The relation between polycyclic aromatic-compounds in diesel fuels and exhaust particulates. *Fuel*, 65: 1150-1158, 1986.

[45] P. J. Tancell, M. M. Rhead, R. D. Pemberton and J. Braven. Survival of polycyclic aromatic-hydrocarbons during diesel combustion. *Environ. Sci. Technol.*, 29: 2871-2876, 1995.

[46] P. A. Mulawa and S. H. Cadle. Measurement of phenols in automobile exhaust. *Anal. Lett.*, 14: 671-687, 1981.

[47] M. Jang and S. R. McDow. Products of benz[a]anthracene photodegradation in the presence of known organic-constituents of atmospheric aerosols. *Environ. Sci. Technol.*, 31: 1046-1053, 1997.

[48] B. R. T. Simoneit and M. A. Mazurek. Organic matter of the troposphere-II. Natural background of biogenic lipid matter in aerosols over the rural western United States. *Atmos. Environ.*, 16: 2139-2159, 1982.

[49] B. R. T. Simoneit. Application of molecular marker analysis to vehicle exhaust for source reconciliations. *Intern. J. Environ. Anal. Chem.*, 23: 203-233, 1985.

[50] W. F. Rogge, L. M. Hildemann, M. A. Mazurek, B. R. T. Simoneit and G. R. Cass. Quantification of urban organic aerosols at a molec-

ular level: identification, abundance, and seasonal variation. *Atmos. Environ.*, 27A: 1309-1330, 1993.

[51] K. Kawamura, L. L. Ng and I. R. Kaplan. Determination of organic acids (C1-C10) in the atmosphere, motor exhausts, and engine oils. *Environ. Sci. Technol.*, 19: 1082-1086, 1985.

[52] K. Kawamura and I. R. Kaplan. Motor exhaust emissions as a primary source for dicarboxylic acids in Los Angeles ambient air. *Environ. Sci. Technol.*, 21: 105-110, 1987.

[53] W. F. Rogge, L. M. Hildemann, M. A. Mazurek. B. R. T. Simoneit and G. R. Cass. Sources of fine organic aerosol. 9. Pine, oak and synthetic log combustion in a residential fireplace. *accepted for publication in Environ. Sci. Technol.*, 1997.

[54] R. A. Harley, M. P. Hannigan and G. R. Cass. Respeciation of organic gas emissions and the detection of excess unburned gasoline in that atmosphere. *Environ. Sci. Technol.*, 26: 2395-2408, 1992.

[55] E. M. Fujita, J. C. Watson, J. C. Chow and Z. Lu. Validation of the chemical mass balance receptor model applied to hydrocarbon source apportionment in the Southern California Air Quality Study. *Environ. Sci. Technol.*, 28: 1633-1649, 1994.

8 Detection of Excess Ammonia Emissions from In-Use Vehicles

Introduction

Ammonia emissions to the atmosphere arise from a great many sources including decay of livestock waste [1-5], use of chemical fertilizers [6-10], emissions from sewage treatment plants, and biological processes in soils [11-15]. Ammonia also is emitted in small amounts from most combustion processes. Pre-catalyst cars, for example, emit ammonia at a low rate [16-18], and accounted for only about 3.3 tons day^{-1} of the total of 150 tons day^{-1} of NH_3 emissions in the South Coast Air Basin (SoCAB) that surrounds Los Angeles in 1974 prior to the introduction of catalyst-equipped cars [19].

A large number of reports in recent years show that the actual hydrocarbon vapor and CO emissions from the motor vehicle fleet in Los Angeles are higher than that intended under the Clean Air Act provisions designed to achieve compliance with air quality standards for ozone and CO. Remote sensing of the vehicle exhaust composition applied to many thousands of individual cars has shown that emissions of CO from the vehicle fleet are increased substantially by a small fraction of very high emitting vehicles, and that in-use vehicle emissions are often much higher than the standards imposed on new vehicles [20, 21]. Measurements made in the Van Nuys highway tunnel in Los Angeles in 1987 by Ingalls et al. [22] likewise show that fleet-average hydrocarbon and CO emissions at that time were approximately two to three times higher than predicted by then-current regulatory

computer-based models that track the emissions expected given the introduction of catalyst-equipped autos into the Southern California vehicle fleet. For this reason, atmospheric models that predict ozone formation in the Los Angeles area commonly use hydrocarbon and CO emissions inventory data for motor vehicles that have been scaled upward by a factor of two to three times the values previously expected from the motor vehicle fleet [23].

The excess hydrocarbon and CO emissions from in-use catalyst-equipped motor vehicles strongly suggests that many cars in Los Angeles are running with rich air/fuel mixtures. That in turn raises the possibility that the local ammonia emissions from three-way catalytic converters within the in-use motor vehicle fleet likewise could be much higher than expected for properly operating vehicles tested under the customary Federal Test Procedure urban driving cycle. It is known that malfunctioning three-way catalyst-equipped cars unintentionally can manufacture ammonia when they are running rich [18], and it is also possible that driving conditions other than those envisioned by the Federal Test Procedure may lead to fuel-rich operation as well. In a recent aerosol modeling study of southern California, Lurmann et al. [24] find significant underpredictions of gas-phase ammonia (predicting 19 ppb NH_3 compared to 29 ppb observed) which motivates the search for further ammonia emissions in southern California.

Excess ammonia emissions from the vehicle fleet could pose a serious problem for air quality control in Los Angeles because ammonia emissions react in the atmosphere with the nitric acid produced in photochemical smog to yield fine particle ammonium nitrate [19, 25-27]. The Los Angeles area already experiences the highest fine particle concentrations in the United States. Light scattering by fine particles is the cause of the well-known Los Angeles visibility problem [28-30], and aerosol nitrate concentrations often

dominate the fine particle concentrations on the worst days of the year [31-33].

In order to determine whether or not excess ammonia emissions are being released to the atmosphere in large quantities from three-way catalyst-equipped automobiles and light trucks in Los Angeles, measurements of ammonia emissions from a fleet of more than 7000 vehicles were made in a Los Angeles highway tunnel. The purpose of this paper is to report the results of that experiment and to discuss the implications for air pollution control in the Los Angeles area.

Experimental Methods

Collection of Samples

Measurements of motor vehicle exhaust were made within the Van Nuys tunnel, where Sherman Way, a major east-west thoroughfare with three lanes of traffic in each direction, passes under the runway of the Van Nuys Airport. Samples were collected on Tuesday, September 21, 1993, from 0600 to 1000 hours PDT during the morning traffic peak. In the tunnel, the traffic flow in opposite directions is separated by a wall, with eight open doorways in that wall that allow minimal access between the two bores of the tunnel. Samples were collected in the east-bound tunnel at a traffic turn-out, 147 meters from the tunnel entrance, and 75 meters from the tunnel exit. A second set of sampling equipment was located on the tarmac of the airport, directly above the site where the roadway enters the tunnel. A video camera was used at the traffic turn-out within the tunnel to record the vehicles as they passed the sampling site. Vehicle counts, distributions by vehicle age and vehicle type, and estimates of vehicle speeds were obtained from this videotape. Vehicle speed was estimated by timing the images of vehicles passing over a known

distance in the tunnel from the videotape. At no point in the videotapes did traffic conditions cause congestion in the tunnel, and vehicle speeds were generally uniform over the length of the experiment. Each vehicle viewed on the video tape was assigned to a vehicle class, and all light-duty vehicles were further assigned to a model year by an acknowledged expert in the field of vehicle identification.

Measurement Methods

The sampling methods used during the Van Nuys tunnel experiment are the same as those used for atmospheric sampling by Fraser et al. [34] and will only be briefly summarized here.

Low volume particulate matter samplers were used to collect fine ($d_p \leq 1.6\ \mu m$) and total airborne particulate matter and certain inorganic gas-phase species. Measurements of gas-phase ammonia and particle-phase ammonium ion were accomplished by use of open-faced stacked filter systems in which particulate matter is first collected on a Teflon pre-filter followed by collection of gas-phase ammonia on oxalic acid impregnated glass fiber backup filters. These filters were extracted in distilled-deionized water, and the aqueous ammonium concentrations were measured by an indophenol colorimetric procedure [35].

To measure fuel consumption inside the tunnel based on the amount of carbon-containing fuel burned, internally electropolished stainless steel canisters were used to collect gas-phase air pollutants. The 6-l canisters were deployed to the field under high vacuum, and used to collect both 4-h integrated and instantaneous grab samples both inside and outside the tunnel. Gas chromatography with flame ionization detection (GC-FID) was used to determine the concentrations of methane, carbon monoxide, carbon dioxide,

and total non-methane volatile organic compounds [36]. Sulfur hexafluoride (released as an artificial tracer in order to determine dilution inside the tunnel) was measured by gas chromatography with electron capture detection (GC-ECD).

Calculation of Emission Rates

To measure vehicle emissions per unit of fuel consumed, pollutant concentrations outside the tunnel first are subtracted from those inside the tunnel in order to calculate the increment to total carbon concentrations due to vehicle exhaust inside the tunnel. The total carbon concentration increase inside the tunnel is directly related to fuel consumption and the ratio of individual pollutants to this total carbon concentration increase can be used directly to calculate emissions per unit of fuel burned using fuel carbon content and density. Fuel-specific emission rate calculations in the present paper are based on the density and carbon content of gasoline, as only 2.8% of the vehicles within the tunnel were diesel-powered. The carbon weight fraction of gasoline is taken to be 0.87 and the density of gasoline is taken to be 750 g l^{-1} in these calculations. The oxygen content in southern California gasoline at the time of this experiment is approximately 0.2% by weight. Translation of these emissions rates per unit of fuel burned into emission factors based on vehicle-miles travelled requires measurement of the dilution of vehicle exhaust inside the tunnel as well as traffic flows through the tunnel. Because the Van Nuys tunnel studied here is short relative to its cross-sectional area (length to cross-sectional area of one bore yields a ratio of approximately 3 m^{-1}), the fuel consumption-based emission factor is preferred because it eliminates any possible uncertainties in measuring the extent of vehicle exhaust dilution within the tunnel, including uncertainties due to the effect

of any air exchange through the openings between the two sections of the tunnel in which traffic flows in opposite directions.

Volumetric Air Flow Rate through the Tunnel

The volumetric air flow rate through the tunnel was measured by releasing 1.8 grams of sulfur hexafluoride (SF_6) at the entrance of the tunnel for 29 minutes of the four-hour sampling period. By analogy to to turbulent fluid flow through a pipe, the tracer is expected to be well mixed across the tunnel bore well before the air flow reaches the sampling location. SF_6 was then measured in two stainless steel canisters used to collect volatile organic compounds inside the tunnel; the primary canister sampled for the entire 240 minute experiment and thus contained within it a sample collected over the duration of the entire SF_6 release. A second canister was filled instantaneously during the SF_6 release period to measure the degree of short-term departure from the long-term average dilution rate. From the rate of SF_6 release and the resulting concentration far down the tunnel, it is possible to calculate the outside air flow rate through the tunnel. The mechanical ventilation system within the Van Nuys tunnel was not in use during this experiment. Instead, the traffic in the tunnel creates a piston flow of air through the tunnel from its entrance to the exit. Given data on air volumes flowing through the tunnel, vehicle fleet average fuel efficiency can be calculated since the total carbon concentration increment inside the tunnel then can be converted to a total carbon flux, and vehicle counts and distances traveled are also known. Given data on vehicle fuel economy (km l^{-1}) and emission rates per unit fuel burned (mg l^{-1}), it is then possible to calculate emissions rates per vehicle km traveled.

Table 8.1: Gas-phase concentrations measured inside and outside the Van Nuys tunnel.

Pollutant	units	Background concentration	Tunnel concentration
CO	ppmV	0.8	10.7
CO_2	ppmV	365	468
Methane	ppmV	2.0	2.0
Non-Methane Hydrocarbons ($\leq C_{10}$)	ppbC	302	1927
Other Organics (TO12 - NMHC)	ppbC	72	328
SF_6	pptV	5.8	160
Ammonia	$\mu g\ m^{-3}$	1.9	34

Results and Discussion

The traffic volume and the distribution of vehicle types and ages flowing through the tunnel were scored by viewing the video tape of the experiment by an acknowledged expert in the field. A total of 7060 vehicles were counted, including 4546 catalyst-equipped automobiles, 256 pre-catalyst gasoline-powered automobiles and light-duty trucks, 12 diesel-powered automobiles, 1936 catalyst-equipped light trucks and vans, 91 heavy-duty gasoline-powered trucks, 186 heavy-duty diesel trucks, and 33 motorcycles. The distribution of gasoline-powered light-duty vehicles as a function of model year is shown in Figure 8.1. Averaging model years for the gasoline-powered light-duty vehicles gives 1986.4 as the mean model year. This vehicle age distribution is similar to that seen in remote sensing studies in the Los Angeles area [1].

The concentrations of carbon dioxide, carbon monoxide, methane, non-methane hydrocarbons, sulfur hexafluoride, and ammonia measured inside and outside the tunnel [37] are reported in Table 8.1. These data are used to calculate emission rates based on fuel consumption, as well as the volumetric air flow rate through the tunnel.

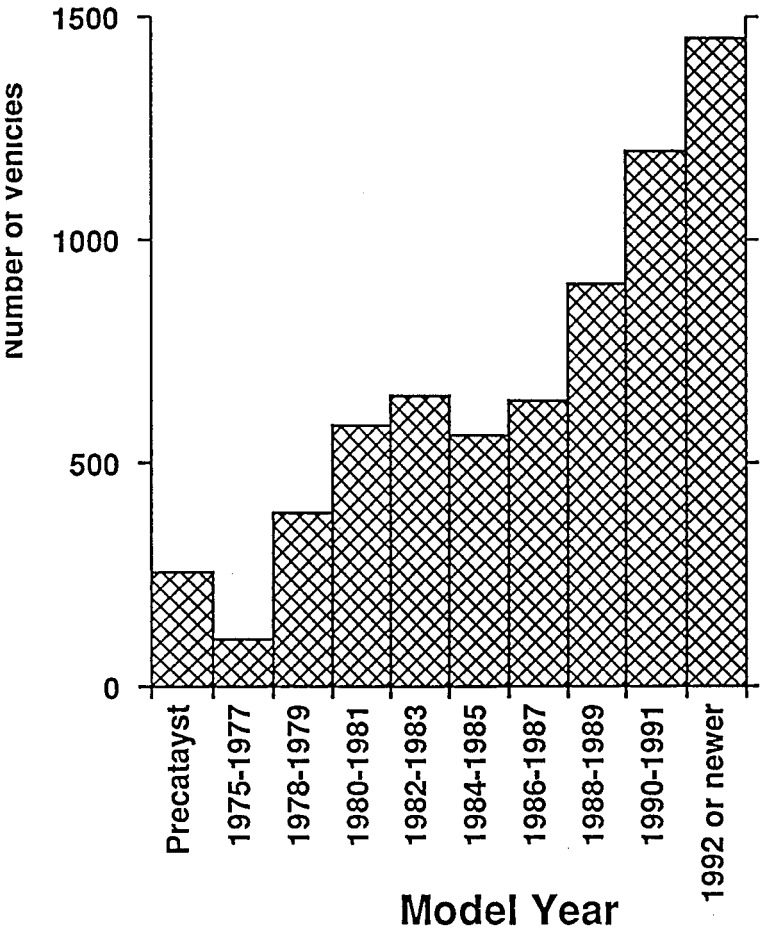

Figure 8.1:
Model year distribution of light-duty vehicles passing through the Van Nuys tunnel, 0600-1000 hours PDT, September 21, 1993.

Results of the SF_6 tracer experiment show volumetric flow rates inside the tunnel of 157 m^3 sec^{-1} during the instantaneous grab sampling period, and 133 m^3 sec^{-1} for the 29 min period of SF_6 release within the 4-h integrated sample, within reasonable agreement considering the expected fluctuations in tunnel ventilation rates. Using the longer period-average volumetric air flow rate calculated from the SF_6 release, the vehicle counts, the total carbon concentration increment measured in the tunnel that was due to vehicle exhaust emitted in the tunnel (difference between inside and outside samplers), and average fuel parameters (including fuel density and carbon weight fraction), the fleet-average fuel efficiency was calculated to be 6.3 km l^{-1} of gasoline-equivalent fuel (14.7 mi $gallon^{-1}$). By comparison, if a vehicle fleet with the same distribution of vehicle ages and types performed according to city driving fuel efficiency data published by the U.S. Environmental Protection Agency [38], the calculated fuel efficiency for the entire fleet (including heavy-duty trucks) would have been 8.6 km l^{-1} (20.3 mi $gallon^{-1}$). The fuel efficiency data published by the EPA are roughly 20% higher than observed fuel economy on the road [39], resulting in an expected fuel economy in acutal use of about 6.9 km l^{-1} (16.2 mi $gallon^{-1}$), a little higher than the 6.3 km l^{-1} measured for traffic in the tunnel. That the vehicle fleet in the Van Nuys tunnel on average was running rich is borne out not only by the low measured fuel economy but also by the high measured CO and volatile organic compounds (VOC) emissions rates which were 130 g l^{-1} (20.8 g km^{-1}) for CO and 9.1 g l^{-1} (1.5 g km^{-1}) for VOC when averaged over the entire vehicle fleet in the tunnel. These emissions rates are higher than reported from other tunnel studies conducted in other cities, but are within the range seen in Southern California. In 1994, emission rates of 78 g l^{-1} CO and 4.2 g l^{-1} VOC were measured in the Caldecott tunnel the San Francisco

Bay area [40]. In 1992, measurements made in the Ft. McHenry tunnel in Baltimore yielded emissions rates of 4.0 g km^{-1} CO and 0.4 g km^{-1} VOC [41]. But recent remote sensing studies of the southern California vehicle fleet, however, yielded emissions rates of 108±25 g l^{-1} CO [1], which are statistically indistinguishable from the CO emissions rates measured in the present study. By comparison, emissions rates measured in the Van Nuys tunnel during the 1987 SCAQS experiments were 13 g km^{-1} for CO and 1.7 g km^{-1} non-methane hydrocarbons (NMHC) [22, 42]. While the emissions rates presented here for CO and VOC are high, it is unlikely that this is due to artifacts of the experimental design. The emissions rates per unit of fuel burned are highly accurate, dependent only on the ratio of the concentration of the pollutant of interest in the tunnel to the total carbon concentration in the tunnel.

High concentrations of gas-phase ammonia were measured inside the tunnel (34 μg m^{-3}), compared to background concentrations outdoors above the tunnel entrance (1.9 μg m^{-3}), leading to a measured emission rate of ammonia per unit of fuel burned of 380 mg l^{-1} of gasoline-equivalent fuel. Given that the emissions of ammonia from dual-bed or three-way catalysts can be much higher than from either non-catalyst vehicles, oxidation catalyst-equipped vehicles or diesel engines [16-18] and knowing that the fleet distribution in the tunnel is made up mostly of vehicles with a dual-bed or three-way catalyst (dual-bed and three-way catalyst-equipped vehicles make up 81% of the vehicles in the tunnel), we will assume that dual-bed and three-way catalysts running rich are the main source of ammonia emissions. Using measured fuel economy data based on model year [38], the fraction of vehicles from each model year and each vehicle type that are equipped with three-way catalysts [43-44], and the observed age distribution of vehicles and

vehicle type, a rough estimate of the fraction of fuel burned the tunnel attributable to vehicles with dual-bed or three-way catalysts is possible. The resulting estimate is that 76% of the fuel burned inside the tunnel is burned by vehicles equipped with dual-bed or three-way catalysts. Using this result and attributing all ammonia in the tunnel to dual-bed and three-way catalyst vehicles, we estimate that the ammonia emission rate for these dual bed and three-way catalyst-equipped vehicles in on-road operation averages 72 mg km^{-1} (or about 480 mg l^{-1} after rough adjustment for the greater than average fuel economy of the three-way and dual bed catalyst vehicles). If the ammonia emissions were attributed equally across all vehicles in the tunnel, the emission rate is calculated to be 61 mg km^{-1}.

The most recent comprehensive ammonia emission inventory for light-duty gasoline-powered vehicles in southern California [45] was based on a literature review. Ammonia emission rates cited for vehicles in proper operation range from 0.4-10.9 mg km^{-1} for diesel vehicles, 2.5-5.0 mg km^{-1} for non-catalyst vehicles, 2.5-5.7 mg km^{-1} for oxidation catalyst-equipped cars, 2.6-20.1 mg km^{-1} for cars with dual-bed catalysts, and 3.6-60.8 mg km^{-1} for three-way catalyst-equipped vehicles. Average values adopted for use in the emission inventory for properly operating vehicles were 2.0, 3.3, 3.6, 9.4, and 16.1 mg km^{-1} for diesel, non-catalyst, oxidation catalysts, dual-bed and three-way catalyst equipped vehicles, respectively. Malfunctioning three-way catalyst-equipped light-duty vehicles are estimated in that emission inventory to emit ammonia at a rate of 67.0 to 166.6 mg km^{-1}, with an average emission rate of 115.9 mg km^{-1} and the fraction of malfunctioning vehicles was estimated to vary with vehicle age, ranging from 15% for 1981 and newer vehicles to 82% for 1979 and older model light-duty vehicles. Roadside survey data were used to estimate the fraction of "improperly" operating vehicles in

order to arrive at the weighted average emissions factor recommended, but no actual measurements of ammonia emissions were used to gauge how many vehicles fell into the properly operating versus improperly operating category. The weighted-average emissions rate of NH_3 for the light-duty vehicle fleet used in that emission inventory thus is fairly low, averaging 33.0 mg km^{-1} for all catalyst-equipped vehicles. In contrast, our measurements suggest a fleet-average emission rate that is roughly double the previous estimates that are in current use.

From the present experiment which looks at the vehicle fleet as a whole passing through the Van Nuys tunnel, it is not possible to tell whether the very high ammonia emissions are due to a large number of cars running rich or a smaller number of cars running very rich. That one or the other of these cases must be true is substantiated by the high CO and non-methane hydrocarbons emissions rates measured for the fleet in the tunnel. Fuel-rich operation can be caused by failures of oxygen sensors used to monitor and adjust the air/fuel ratio which is critical in the proper operation of three-way catalyst systems, by other types of vehicle malfunctions, or possibly by driving conditions not represented by the Federal Test Procedure urban driving cycle.

Control of ammonia emissions is important to control of fine particle ammonium nitrate levels in the South Coast Air Basin that surrounds Los Angeles. Peak 24-h average fine particle concentrations in the SoCAB measured during 1993 ranged from 75.3-139.2 $\mu g\ m^{-3}$ across the four air monitoring sites (Azusa, Central Los Angeles, Long Beach and Rubidoux) studied by Christoforou et al. [33], far higher than the newly adopted 24-h average fine particle National Ambient Air Quality Standard of 65 $\mu g\ m^{-3}$. Fine particle nitrate ion is the largest single contributor to those fine particle con-

centrations, accounting for 21-45% of the peak day concentrations, while fine particle ammonium ion contributed another 8-13% of the fine particle mass depending on the site considered. As a reasonable approximation, ammonium nitrate forms when the product of the gas-phase ammonia times nitric acid vapor concentrations in the atmosphere reaches the value of the equilibrium dissociation constant for NH_4NO_3 [19]. Beyond that point, further additions of NH_3 from vehicle exhaust will shift the atmospheric condition toward more NH_4NO_3 formation. Assume that the measured emission factor for ammonia from the Van Nuys tunnel can be scaled by fuel usage to obtain a range of estimates for daily ammonia emissions to the atmosphere of the SoCAB from the vehicle fleet as a whole. Daily fuel use in the basin by highway vehicles is approximately 14×10^6 gallons of gasoline and 3×10^6 gallons of diesel fuel per day [46]. Total fuel use when multiplied by the fuel-specific emissions factor from the tunnel study results in a total emission rate of ammonia in the SoCAB of 24 metric tons per day. Alternatively, estimated traffic in the air basin [46] amounts to 293×10^6 vehicle-miles travelled daily (471×10^6 km day^{-1}), which at 61 mg NH_3 km^{-1} yields an NH_3 emissions flux from the entire vehicle fleet of about 29 metric tons per day. The modest difference between 24 metric tons day^{-1} NH_3 computed from the fuel use data versus 29 metric tons day^{-1} computed from VMT is no larger than the uncertainty in the NH_3 emissions factor based on vehicle distance traveled which is known no more accurately than the range of the two measures of tunnel dilution obtained from the two SF_6 measurements. We believe that the fuel consumption-based emissions value is more accurate since that calculation relies on daily fuel useage and the carbon balance in the tunnel, both of which are more precisely known than the estimates of daily VMT and NH_3 emissions per-km-driven, respectively.

These estimates can be compared with the most important traditional source of ammonia emissions in the air basin, ammonia release from livestock waste decomposition at dairies, which has been estimated at roughly 27-30 metric tons NH_3 per day out of a total inventory of about 165-218 metric tons per day [25, 45]. Thus at this point, catalyst-equipped cars could be one of the most important NH_3 sources in the air basin. As further fleet turnover causes newer vehicles equipped with three-way catalysts to replace older pre-catalyst vehicles or oxidation-only catalyst vehicles, these ammonia emissions may increase somewhat. Ammonium nitrate concentrations can be reduced by controlling NO_x emissions, NH_3 emissions, or both [27], and conversely, increased emissions of NH_3 or NO_x will increase ammonium nitrate levels. If ammonium nitrate concentrations are to be reduced in the SoCAB, each of the major NH_3 sources should be examined to see if that source can be controlled. The major NH_3 sources now apparently include three-way and dual bed catalyst-equipped light duty vehicles operated under rich air/fuel ratio conditions.

Bibliography

[1] F. G. Viets. Cattle feedlot pollution. *Agricultural Sci. Rev.*, 9: 1-8, 1971.

[2] D. C. Adriano, P. F. Pratt and S. E. Bishop. Fate of inorganic forms of N and salt from land-disposed manures from dairies. In *Livestock Waste Management and Pollution Abatement*, American Society of Agricultural Engineers: St. Joseph, MI, 1971.

[3] D. C. Adriano, A. C. Chang and R. Sharpless. Nitrogen loss from manure as influenced by moisture and temperature. *J. Environ. Qual.*, 3: 258-261, 1974.

[4] J. Giddens and A. M. Rao. Effect of incubation and contact with soil on microbial and nitrogen changes in poultry manure. *J. Environ. Qual.*, 4: 275-278, 1975.

[5] R. E. Luebs, K. R. Davis and A. E. Laag. Ammonia and related compounds emanating from a large dairy area. *J. Environ. Qual.*, 2: 137-141, 1973.

[6] A. Wahhab, M. S. Randhawa and S. Q. Alam. Loss of ammonia from ammonium sulfate under different conditions when applied to soils. *Soil Sci.*, 84: 249-255, 1957.

[7] L. L. McDowell and G. E. Smith. The retention and reactions of anhydrous ammonia on different soil types. *Soil Sci. Soc. Am. Proc.*, 2:

38-42, 1958.

[8] J. H. Baker, M. Peech and R. B. Musgrove. Determination of application losses of anhydrous ammonia. *Agron. J.*, 51: 361-362, 1959.

[9] J. K. R. Gasser. Some factors affecting losses of ammonia from urea nad ammonium sulfate applied to soils. *J. Soil Sci.*, 15: 275-278, 1964.

[10] H. G. Walkup and J. L. Nevins. The cost of doing business in agricultural ammonia for direct application. *Agricultural Ammonia News*, 16: 96-100, 1966.

[11] L. F. Elliot, G. E. Schuman, F. G. Viets. Volatilization of nitrogen-containing compounds from beef cattle areas. *Soil Sci. Soc. Amer. Proc.*, 35: 752-755, 1971.

[12] L. K. Porter et al. Pollution Abatement from Cattle Feedlots in Northeastern Colorado and Nebraska. EPA-660/2-75-015. U.S. Environmental Protection Agency: Corvallis, OR, 1975.

[13] J. R. Miner. Production and Transport of Gaseous NH_3 and H_2S Associated with Livestock Production. EPA-600/2-76-239. U.S. Environmental Protection Agency: Ada, OK, 1976.

[14] O. T. Denmead, J. R. Freney and J.R. Simpson. A closed ammonia cycle within a plant canopy. *Soil Biol. Biochem.*, 8: 161-164, 1976.

[15] O. T. Denmead, R. Nulsen and G. W. Thurtell. Ammonia exchange over a corn crop. *Soil Sci. Soc. Amer. J.*, 42: 840-842, 1978.

[16] C. M. Urban and R. J. Garbe. Regulated and unregulated exhaust emissions from malfunctioning automobiles. *SAE Tech. Pap. Ser. No.*

790696, 1979.

[17] S. H. Cadle, G. J. Nebel and R. L. Williams. Measurements of unregulated emissions from General Motors' light-duty vehicles. *SAE Tech. Pap. Ser. No. 790694*, 1979.

[18] S. H. Cadle and P. A. Mulawa. Low molecular weight aliphatic amines in exhaust from catalyst-equipped cars. *Environ. Sci. Technol.*, 14: 718-723, 1980.

[19] A. G. Russell, G. J. McRae and G. R. Cass. Mathematical modeling of the formation and transport of ammonium nitrate aerosol. *Atmos. Environ.*, 17: 949-964, 1983.

[20] D. H. Stedman, G. Bishop, J. E. Peterson and P. L. Guenther. On-Road CO Remote Sensing in the Los Angeles Basin. report to the California Air Resources Board under Contract A932-189; University of Denver: Denver, CO 1991.

[21] D. R. Lawson, P. J. Groblicki, D. H. Stedman, G. A. Bishop and P. L. Guenther. Emissions from in-use motor vehicles in Los Angeles: a pilot study of remote sensing and the inspection and maintenance program. *J. Air & Waste Manage. Assoc.*, 40: 1096-1105, 1990.

[22] M. N. Ingalls, L. R. Smith and R. E. Kirksey. Measurement of on-road vehicle emission factors in the California South Coast Air Basin. Volume 1: regulated emissions. report to the Coordinating Research Council under Project SCAQS-1; Southwest Research Institute: San Antonio, TX 1989.

[23] R. A. Harley, A. G. Russell, G. J. McRae, G. R. Cass and J. H. Seinfeld. Photochemical modeling of the Southern California Air Quality Study. *Environ. Sci. Technol.*, 27: 378-388, 1993.

[24] F. W. Lurmann, A. S. Wexler, S. N. Pandis, S. Musarra, N. Kumar and J. H. Seinfeld. Modelling urban and regional aerosols. II. Application to California's South Coast Air Basin. *Atmos. Environ.*, 31: 2695-2715, 1997.

[25] A. G. Russell and G. R. Cass. Verification of a mathematical-model for aerosol nitrate and nitric-acid formation and its use for control measure evaluation. *Atmos. Environ.*, 20: 2011-2025, 1986.

[26] A. G. Russell, K. F. McCue and G. R. Cass. Mathematical modeling of the formation of nitrogen-containing air pollutants. 1. Evaluation of an Eularian photochemical model. *Environ. Sci. Technol.*, 22: 263-271, 1988.

[27] A. G. Russell, K. F. McCue and G. R. Cass. Mathematical modeling of the formation of nitrogen-containing pollutants. 2. Evaluation of the effect of emission controls. *Environ. Sci. Technol.*, 22: 1336-1347, 1988.

[28] S. M. Larson, G. R. Cass, K. J. Hussey and F. Luce. Verification of image processing based visibility models. *Environ. Sci. Technol.*, 22: 629-637, 1988.

[29] A. Eldering, S. M. Larson, J. R. Hall, K. J. Hussey and G. R. Cass. Development of an improved image processing based visibility model. *Environ. Sci. Technol.*, 27: 626-635, 1993.

[30] A. Eldering and G. R. Cass. Source-oriented model for air pollution effects on visibility. *J. Geophys. Res.*, 101: 19343-19369, 1996.

[31] H. A. Gray, G. R. Cass, J. J. Huntzicker, E. K. Heyerdahl and J. A. Rau. Characterization of atmospheric organic and elemental carbon particle concentrations in Los Angeles. *Environ. Sci. Technol.*, 20: 580-589, 1986.

[32] P. A. Solomon, T. Fall, L. G. Salmon, G. R. Cass, H. A. Gray and A. Davidson. Chemical characteristics of PM10 aerosols collected in the Los Angeles area. *J. Air Pollut. Control Assoc.*, 39: 154-163, 1989.

[33] C. Christoforou, L. G. Salmon, M. P. Hannigan, P. A. Solomon and G. R. Cass. Trends in fine particle concentration and chemical composition in Southern California. *submitted to J. Air Waste Manage. Assoc.*, 1997.

[34] M. P. Fraser, D. Grosjean, E. Grosjean, R. A. Rasmussen and G. R. Cass. Air quality model evaluation data for organics. 1. Bulk chemical composition and gas/particle distribution factors. *Environ. Sci. Technol.*, 30: 1731-1743, 1996.

[35] W. T. Bolleter, C. J. Bushman and P. W. Tidwell. Spectrophotometric determinations of ammonium as indophenol. *Anal. Chem.*, 33: 592-594, 1961.

[36] Method for the determination of non-methane organic compounds in ambient air using cryogenic preconcentration and direct flame ionization detection, EPA-600/4-89-018. U.S. Environmental Protection Agency: Research Triangle Park, NC, 1988.

[37] M. P. Fraser, G. R. Cass and B. R. T. Simoneit. Gas-phase and particle-phase organic compounds emitted from motor vehicle traffic in a Los Angeles highway tunnel. *submitted to Environ. Sci. Technol.*, 1997.

[38] J. D. Murrell, K. H. Hellman and R. M. Heavenrich. Light-duty automotive technology and fuel economy trends through 1993. EPA/AA/TDG-93/01. Office of Mobile Sources, U.S. Environmental Protection Agency: Ann Arbor, MI 1993.

[39] M. Mintz, A. D. Vyas and L. A. Conley. Differences between EPA-test and in-use fuel economy: are the correction factors correct? *Transportation Res. Record*, 1416: 124-130, 1993.

[40] T. W. Kirchstetter, B. C. Singer, R. A. Harley, G. R. Kendall and W. Chan. Impact of oxygenated gasoline use on California light-duty vehicle emissions. *Environ. Sci. Technol.*, 30: 661-670, 1996.

[41] W. R. Pierson, A. W. Gertler, N. F. Robinson, J. C. Sagebiel, B. Zielinska, G. A. Bishop, D. H. Stedman, R. B. Zweidinger and W. D. Ray. Real-world automotive emissions-summary of studies in the Fort McHenry and Tuscarora Mountain Tunnels. *Atmos. Environ.*, 30: 2233-2256, 1996.

[42] W. R. Pierson, A. W. Gertler and R. L. Bradow. Comparison of the SCAQS tunnel study with other on-road vehicle emission data. *J. Air & Waste Manage. Assoc.*, 40: 1495-1504, 1990.

[43] L. M. Lyons and R. J. Kenny. Trends in emissions control technologies for 1983-1987 model-year California certified light-duty vehicles. *SAE Tech. Pap. Ser. No. 872164*, 1987.

[44] Compilation of air pollution emission factors. Volume 2: Mobile Sources EPA/AP-42. Office of Mobile Sources, U.S. Environmental Protection Agency: Ann Arbor, MI 1985.

[45] R. J. Dickson. Development of the Ammonia Emission Inventory for the Southern California Air Quality Study. report to the Electric Power Research Institute under Grant 2333-4; Radian Corporation: Sacramento, CA, 1991.

[46] 1997 Air Quality Management Plan. South Coast Air Quality Management District: Diamond Bar, CA, 1996; Attachment C.

9 Particulate Organic Compounds in Vehicle Exhaust and the Ambient Atmosphere

9.1 Introduction

Epidemiological studies showing an association between fine particulate pollution levels and human health effects [1] followed by the adoption of a National Ambient Air Quality Standard for fine particulate matter in the United States have raised interest in the question of how the levels of fine particles in the ambient atmosphere might be controlled. Fine particulate matter is emitted from many sources including combustion, industrial processes and fugitive dust sources, and can be formed by gas-to-particle conversion processes as well. Thus reduction of ambient fine particle concentrations requires an accurate knowledge of the relative contribution of many different sources to the overall ambient air pollution problem [2].

Many air quality models that account for the ambient concentrations due to primary emissions of particles from motor vehicles use atmospheric transport calculations which rely on measurements made while the vehicles are operated on a chassis dynamometer. These dynamometer studies require precise control of the driving conditions which in turn allows the comparison between tests that is needed to evaluate the effect of different engine designs or fuel composition on pollutant emission rates. However, a number of studies over the past decade have found that the volatile organic compound

(VOC) and carbon monoxide (CO) emission rates from motor vehicles operated on the highway can be significantly different from the results obtained from dynamometer-based studies conducted in the laboratory [3, 4]. These discrepancies may arise from a difference in the way that vehicles are driven between standardized test conditions and real-world situations, or may result from differences between the maintenance condition of the fleet of vehicles tested in the laboratory versus the condition of the vehicle fleet as a whole. Indeed, studies suggest that the emissions from the vehicle fleet as a whole are dominated by a small fraction of the vehicles which emit pollutants at a very high rate [5, 6]. This raises concern about the use of dynamometer test results which measure emissions from only a very small fraction of the total vehicle fleet. Whether or not the vehicles voluntarily surrendered for dynamometer studies include a representative selection of these high-emitters is questionable.

An alternative approach is possible. The contribution of primary emissions from motor vehicles to airborne fine particle concentrations can be estimated based on emissions measurements made as the vehicle fleet is operated on the highway. Particulate matter emissions measured as many thousands of vehicles pass through a roadway tunnel can be related to ambient air quality via organic molecular tracer techniques.

Source contributions to airborne fine particle concentrations can be calculated using organic chemical tracer techniques [7]. In this method, compounds or compound classes that are characteristic of one emission source category but not others are used to track the presence of the emissions from the sources of interest in the ambient atmosphere. The tracer compounds used must be conserved during atmospheric transport (neither formed nor depleted by chemical reactions in the atmosphere) over the relatively short

urban time scale for transport from sources to receptor air monitoring sites. The compound classes capable of tracking the emissions of particles from motor vehicles consist of several homologous series of petroleum biomarkers. Petroleum biomarkers are molecular structures present in petroleum stemming from the microorganisms which created the deposits [8, 9]. These unique structures, including the hopanes and steranes, are present in lubricating oils and in particulate matter emitted from gasoline and diesel engines, and have been used successfully to track the emissions from motor vehicles in the ambient atmosphere [7, 10].

In the present paper, organic chemical tracer techniques will be used to relate data on the emissions of primary particles from motor vehicles in real-world operation that were collected in a Southern California roadway tunnel to the ambient levels of fine particulate matter collected at four urban sites in the Los Angeles area during a severe smog episode.

9.2 Experimental Design

Descriptions of the experiments needed to support the analysis conducted here have been given previously, and will only be briefly summarized [11, 12, 13]. Fine particle concentrations and chemical composition were characterized during two field projects. In one experiment, measurements were made of the direct particulate matter emissions from motor vehicle traffic in the Van Nuys tunnel in Los Angeles. The second study involved ambient fine particle sampling at Long Beach, Central Los Angeles, Azusa and Claremont, CA, over consecutive short term sampling periods during a two day summer smog episode. In both studies, measurements were made of fine particle mass, elemental and organic carbon content, ionic species, and trace metals accompanied by detailed speciation of the particulate organic

compounds present by gas chromatography-mass spectrometry (GC-MS).

9.2.1 Sampling Methods

Particle samples were collected using two different instruments: a low-volume particulate matter sampler used to construct a material balance on the bulk chemical composition of the airborne fine particulate matter [11], and a high-volume dichotomous sampler [14] used to collect enough particulate organic material to allow detailed organic chemical analysis. In both the tunnel experiment and the ambient field experiment, identical sampling equipment was used to allow results to be compared directly.

The low-volume particulate matter sampler used an AIHL cyclone separator [15] to remove coarse particulate matter ($d_p \geq 1.6$ μm), followed by collection of fine particulate matter on several 47 mm diameter filters operated in parallel. These filters included one quartz fiber filter (Tissuquartz 2500 QAO, Pallflex, Putnam, CT), two Teflon membrane filters (Teflo 0.5 μm pore size, Gelman, Ann Arbor, MI), and two nylon filters (Nylasorb, Gelman, Ann Arbor, MI). One of the two nylon filters was operated downstream of a magnesium oxide-coated diffusion denuder, and was used to determine particulate nitrate and chloride and vapor-phase nitric acid and hydrochloric acid by the denuder difference method [16, 17]. Additional ionic species concentrations were determined by ion chromatography (SO_4^{2-}) [18], atomic absorption spectroscopy (Na^+, Mg^{2+}) [19] and an indophenol colorimetric analysis (NH_4^+) [20] of the aqueous extract of one of the two Teflon membrane filters in each sample set. Before use, the quartz fiber filters were annealed at 550°C for at least 6-h to lower their carbon blanks, and nylon filters were washed in a dilute solution of sodium bicarbonate to lower their chloride blank levels. Overall ambient particulate mass concentrations were

determined by repeated weighing of the Teflon membrane filters. The fraction of the fine particulate matter attributable to elemental carbon and organic compounds was determined from samples collected on the quartz fiber filters by the method of Birch and Cary [21]. X-ray fluorescence analysis of the second Teflon membrane filter yielded data on 38 trace metals [22].

The fine-particle filters from the high-volume dichotomous sampler were used for detailed particulate organic compound speciation. Quartz fiber filters (Tissuquartz 2500 QAO, 102 mm diameter) were heat treated before use to remove organic compound contamination (550°C for at least 6-h). Following sampling, the filters were stored in pre-fired borosilicate glass jars with solvent-washed Teflon lid-liners and returned to the laboratory where they were frozen until analysis. Before extraction, filter samples were spiked with a known quantity of perdeuterated tetracosane ($\underline{n}$-$C_{24}D_{50}$) to monitor extraction efficiency and blow down losses. Samples were extracted by mild ultrasonic agitation, twice in n-hexane and three times in a 2:1 benzene:isopropanol mixture. All extracts were combined and reduced in volume to approximately 400 μl, and stored in the freezer until analyzed by GC-MS.

Analysis by GC-MS used a 30 m capillary column (DB-1701, 0.25 μm film thickness, J&W Scientific, Rancho Cordova, CA) and 1-phenyldodecane as a co-injection standard to monitor instrument response on a Finnigan GCQ ion trap system. Prior to GC-MS analysis, the organic extracts were divided into two aliquots, one of which was derivatized using diazomethane to convert organic acids for quantification as their methyl ester analogs. Filter extracts were concentrated to approximately 20 μl before GC-MS analysis, with the total sample volume determined immediately before injection of a 1 μl aliquot. The response of the instrument to petroleum biomarkers relative to the co-injection standard was determined using an authen-

tic standard of 20R,5α(H),14α(H),17α(H)-cholestane, and other compound classes were quantified using appropriate authentic standards. The other petroleum biomarkers were identified based on their relative GC retention time and known fragmentation patterns and the published elution order and mass spectra of authentic compounds [8, 23, 9]. Ambient concentrations of petroleum biomarkers were determined by correcting for extraction recovery and blow down losses based on quantification of the perdeuterated recovery standard, with overall recovery ranging between 21% and 110%, and averaging 61% over all samples. Blank filters extracted to assure the quality of the data collected, showed no signs of petroleum biomarkers. The overall precision of the quantification procedure based on propagation of uncertainties in volume determination, peak integration and repeatability of injections was estimated to be $\pm$20% (one standard deviation).

9.2.2 Tunnel Experiment

The Van Nuys tunnel is a major roadway tunnel in the Los Angeles area with three lanes of highway traffic traveling in each direction. During the morning traffic peak, 4-h integrated samples were collected simultaneously at two locations: at a traffic turnout in the east-bound bore of the tunnel (147 m from the tunnel entrance and 75 m from the tunnel exit) and at an outdoor background site immediately above the point where the vehicle traffic enters the tunnel [13].

Vehicle traffic counts and an estimate of vehicle speed were obtained from the analysis of video tapes recorded at the sampling location within the tunnel during the experiment. Those videotapes also were used to determine the distributions of vehicle age and type.

The air exchange rate through the tunnel was measured using sulfur hex-

afluoride (SF_6) as an artificial tracer. A known quantity of SF_6 was released continuously over a 29 minute period at the entrance of the tunnel, and the ambient concentration of the tracer at the tunnel sampling location was measured. The ratio of the ambient concentration of this artificial tracer at the sampling location and the known tracer emission rate was then used to convert the increase in the ambient concentrations of pollutants inside the tunnel above the outdoor background into vehicle emission rates. In this data set are the emission rates of petroleum biomarkers, including 15 individual compounds or isomer pairs. The GC-MS traces of the key ions used to quantify these petroleum biomarkers are shown in Figure 9.1, with mass to charge ratio 191 characteristic of the hopanes, and mass to charge ratios 217 and 218 characteristic of the steranes.

9.2.3 Ambient Sampling

During a severe photochemical smog episode in the Southern California area, samples of vapor-phase, semivolatile and fine particle-phase atmospheric pollutants were collected and analyzed [11, 12]. The resulting database includes fine particle total organic carbon concentrations determined by thermal evolution and combustion analysis as well as measurements of the concentrations of over 100 particle phase organic compounds, including the same 15 petroleum biomarkers that were quantified in fine particle emissions from motor vehicles in the Van Nuys tunnel [12].

Integrated samples of four-hour duration were collected every six-hours over a two-day period at four sites in urban Southern California. Additionally, samples were collected over longer time periods during this same two-day photochemical smog episode at San Nicolas Island, a regional background site upwind of the urban area. The short sampling times at the urban

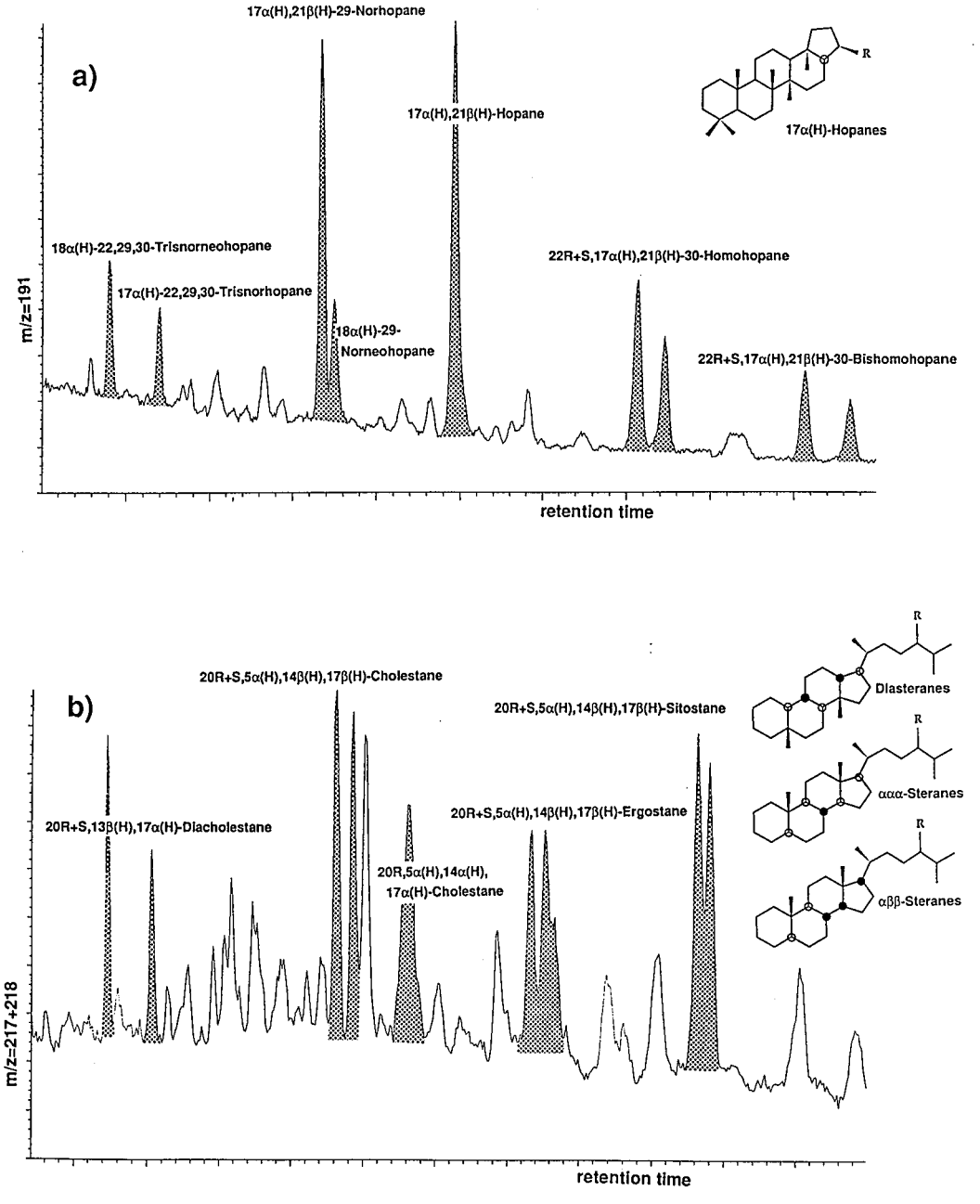

Figure 9.1:
GC-MS traces of the mass to charge ratio 191 (top) and 217+218 (bottom) fragmentograms which are used to quantify the hopanes and steranes, respectively, showing chemical structures and peak identification.

air monitoring sites permit quantification of the diurnal variations in pollutant concentrations, while longer periods (up to 11-h) at San Nicolas Island were employed to collect enough organic particulate matter for quantification of individual compounds at the lower particle concentrations present at the background site. However, even with these longer sampling periods, only unquantifiably small trace levels of petroleum biomarkers were seen at San Nicolas Island, indicating that the atmosphere over the ocean upwind of the city is for all practical purposes, nearly free of primary motor vehicle exhaust aerosol.

The four urban sites studied (Long Beach, Central Los Angeles, Azusa and Claremont) include regions of Southern California having air quality that is affected by different emission sources and with different pollutant characteristics. Central Los Angeles is at the center of the regional freeways, and air quality at this site is dominated by direct emissions from motor vehicles. Long Beach is near the region's port facilities, and its local air quality is affected by direct emissions from the local petroleum refineries, power plants and harbor activities. Azusa and Claremont are both located in interior valleys, where air quality during the summer months is dominated by high levels of secondary pollutants that are formed by atmospheric chemical reactions as air parcels are advected inland from the west to the east [24]. The air monitoring site in Azusa is located in a more industrial area (including an active gravel quarry and two local freeways) than the Claremont site, which is located in a relatively secluded suburban neighborhood next to the Claremont Colleges. These site locations allow the determination of the importance of primary vehicle emissions in different areas of the air basin that surrounds Los Angeles.

9.3 Results

The traffic flow through the tunnel during the experiment included 7060 vehicles, including 4546 catalyst-equipped automobiles, 1936 catalyst-equipped light trucks and vans, 256 pre-catalyst cars and trucks and 12 diesel-powered automobiles. The vehicle traffic also included 277 heavy-duty vehicles and 33 motorcycles. Of the heavy-duty vehicles, 186 were identified as diesel-powered with 91 identified as gasoline-powered.

Fine particulate matter samples collected inside the tunnel show an increase in particle concentrations that corresponds to an overall emission rate of 78 mg of fine particulate matter per vehicle km traveled, as seen in Figure 9.2a [13]. This includes significant contributions from ammonium nitrate, which is not known to be directly emitted from motor vehicles. A high emission rate of gas-phase ammonia was measured inside this tunnel [25] which apparently can lead to secondary NH_4NO_3 formation via reaction with gas-phase nitric acid. With secondary NH_4NO_3 removed from the mass balance, the overall primary fine particle mass emission rate becomes 65 mg km^{-1}, and the major identified primary species are carbonaceous fine particles, as shown in Figure 2b. Measurements of silicon and aluminum in fine particles show that contributions from fine crustal material emitted within the tunnel are small, indicating that direct tailpipe emissions from vehicles dominate over road dust generated by the vehicle traffic in this particular tunnel.

A material balance on the composition of the organic compounds present in motor vehicle emissions in this study was constructed as shown in Figure 9.3. The overall emission rate of organic compounds in fine particles is 22.5 mg km^{-1}. Of this organic material, 85% is extractable and will elute from the GC column using the described analytical procedures, resulting in

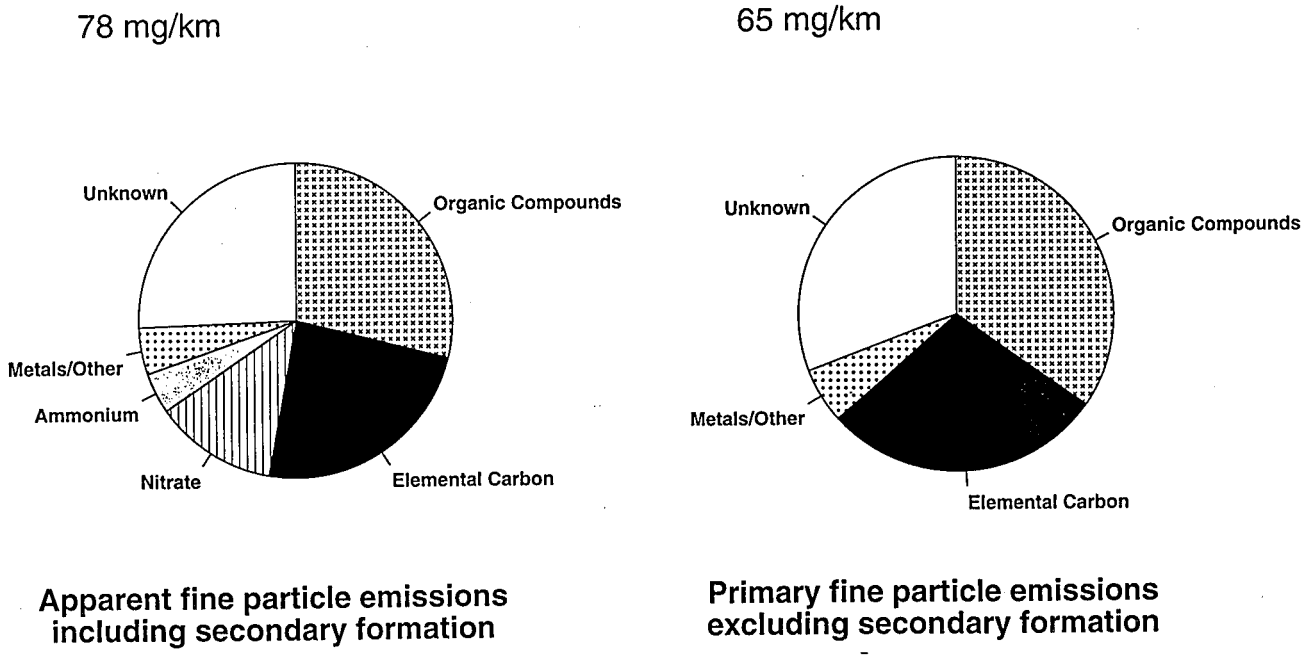

Figure 9.2:
Pie charts showing a material balance on the bulk chemical composition of the apparent emissions from motor vehicles (left), and the primary emissions excluding the secondary formation of ammonium nitrate (right). Van Nuys tunnel, September 1993.

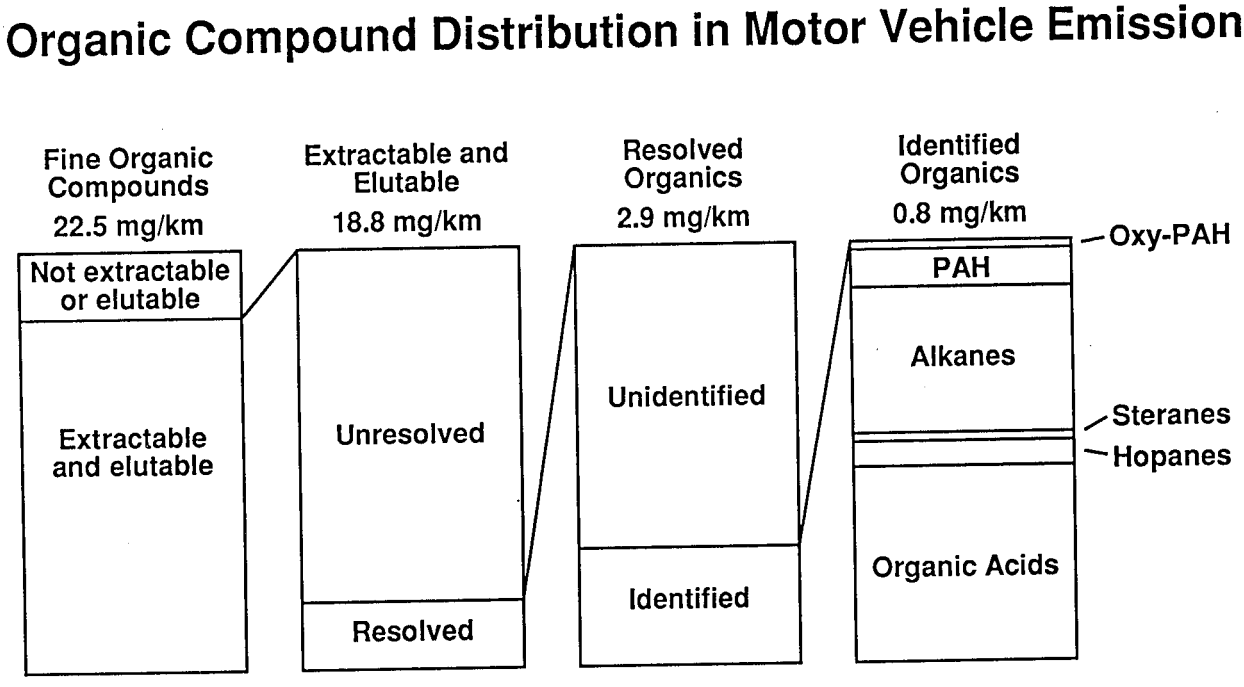

Figure 9.3:
Material balance on the composition of fine organic particulate matter emissions from motor vehicles in the Van Nuys tunnel, September 1993.

18.8 mg km^{-1} of emitted organic material that can be analyzed by GC-MS. A majority of this extractable and elutable material is present as an unresolved complex mixture (UCM) of petroleum resides consisting of highly branched and cyclic aliphatic material [8]. The resolved organic compounds that can be seen as individual peaks in the GC-MS analysis amount to 2.9 mg km^{-1}. Of these resolved peaks, the concentrations of the 97 identified compounds contribute a total of 0.8 mg km^{-1}, with contributions from organic acids, alkanes, polycyclic aromatic hydrocarbons (PAH), oxygenated PAH, and petroleum biomarkers (hopanes and steranes). While the identified material is only a fraction of the total organic material emitted from vehicles, it is important to note that the relationship between the emissions of petroleum biomarkers and the overall emission rate for fine organic particulate matter is understood.

Comparison of the tunnel traffic samples to the atmospheric samples begins with a comparison of the relative distribution of the petroleum biomarker concentrations in both sample sets. As seen in Figure 9.4, the relative compound distributions are nearly proportional to one another, lending support to previous findings [23, 7, 10] that these compounds can be used to track vehicle exhaust-derived particle concentrations in the Southern California atmosphere. Examination of the diurnal variation of the hopanes and steranes concentration in the outdoor air likewise supports the belief that these compounds are emitted from vehicle traffic. The concentrations of the petroleum biomarkers peak strongly during the early morning, when low mixing depths coincide with the morning traffic peak, as seen in Figure 9.5 for 17α(H),21β(H)-hopane. This peak in concentrations during the morning rush hour traffic period is most pronounced at Central Los Angeles, as expected.

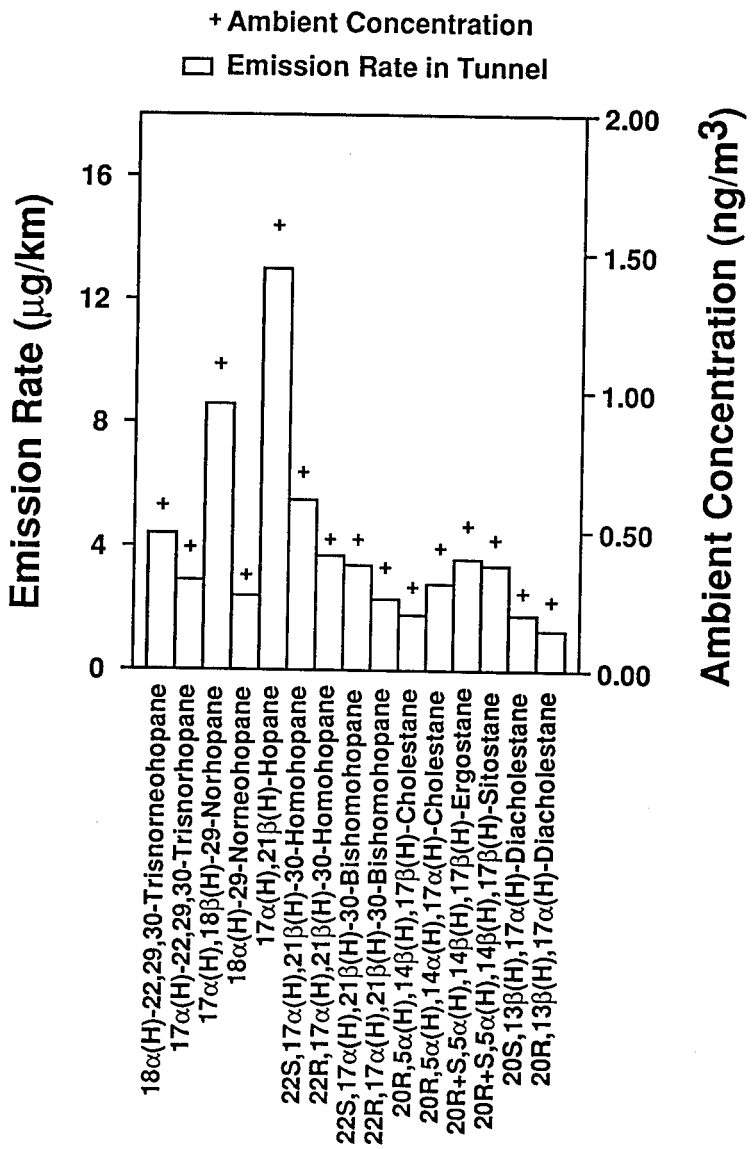

Figure 9.4:
Comparison of the ambient concentrations averaged over all Southern California monitoring sites and times on September 8-9, 1993 (from ref. 12), and emission rates quantified from the Van Nuys tunnel traffic (from ref. 13) for 15 petroleum biomarkers or isomer pairs.

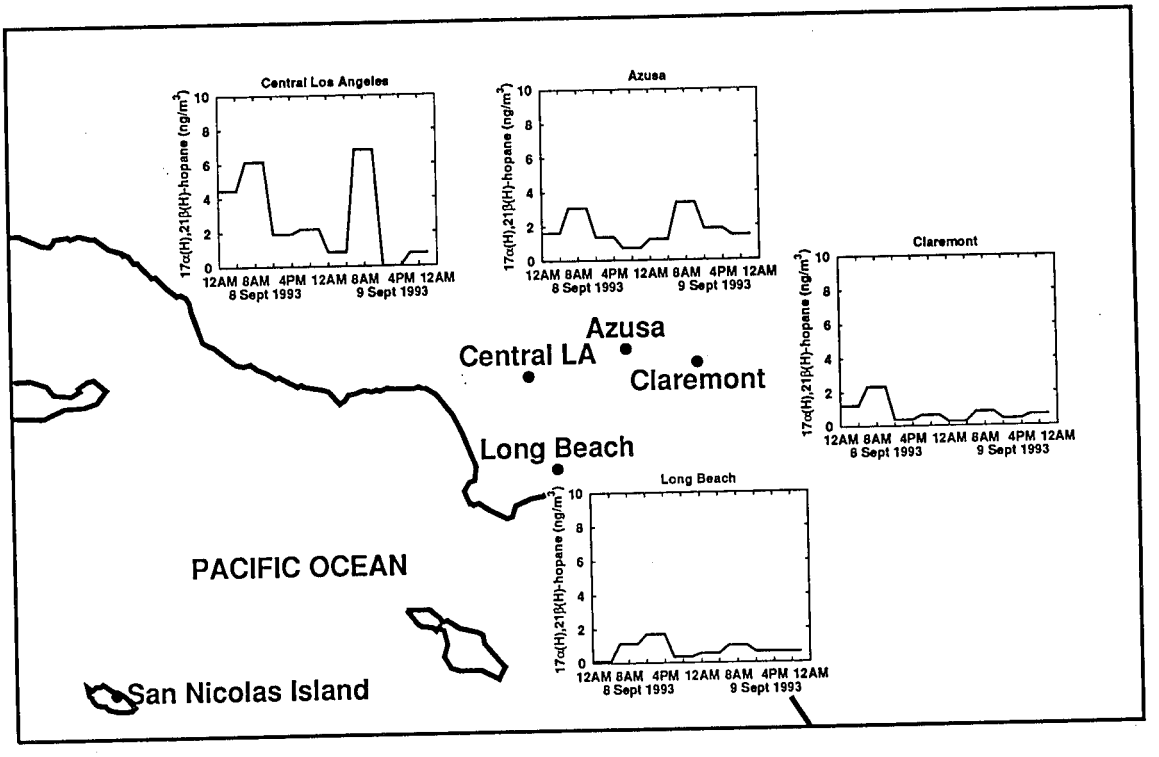

Figure 9.5:
Diurnal variation of 17α(H),21β(H)-hopane at each of the Southern California sites studied, September 8-9, 1993.

Table 9.1: Fine organic particulate matter concentrations attributable to motor vehicle traffic in comparison to the total fine organic particulate matter concentration in Los Angeles outdoor ambient air, September 8-9,1993.

	Fine Organic Matter Attributable to Motor Vehicle Traffic (μg m^{-3})	Ambient Fine Organic Particulate Matter (μg m^{-3})	Fraction of Fine Organics Attributable to Motor Vehicle Traffic
Averaged by site			
Long Beach	1.6	15.0	10.7%
Central Los Angeles	5.4	29.5	18.3%
Azusa	3.3	29.6	11.1%
Claremont	1.9	25.4	7.5%
Averaged by time of day			
0000-0400 PDT	2.5	17.5	14.3%
0600-1000 PDT	5.6	29.3	19.1%
1200-1600 PDT	2.1	33.6	6.3%
1800-2200 PDT	1.9	19.0	10.0%

Knowing the fraction of organic particulate matter which is made up of the sum of the individual petroleum biomarkers and also the ambient concentration of these same biomarkers, the contribution from primary motor vehicle emissions to the ambient concentrations of fine organic matter can be estimated. The results are shown in Figure 9.6, where they are averaged over each site at all times of the day and over all sites at each time of the day, thereby showing both the spatial and diurnal variations. Table 9.1 also summarizes the overall atmospheric fine organic particulate matter concentrations, the calculated contribution from motor vehicles, and the fraction of fine organic matter traced to motor vehicles. The data shown in Figure 9.6 and summarized in Table 9.1 show that the peak contributions from motor vehicle emissions occur at Central Los Angeles, consistent with the spatial distribution of traffic density in the air basin. At the Central Los Angeles site, 5.4 of the 29.5 μg m^{-3} of fine organic particulate matter is attributed to primary organic aerosol emissions from motor vehicle traffic. As air parcels pass from the most urbanized western region of the air basin

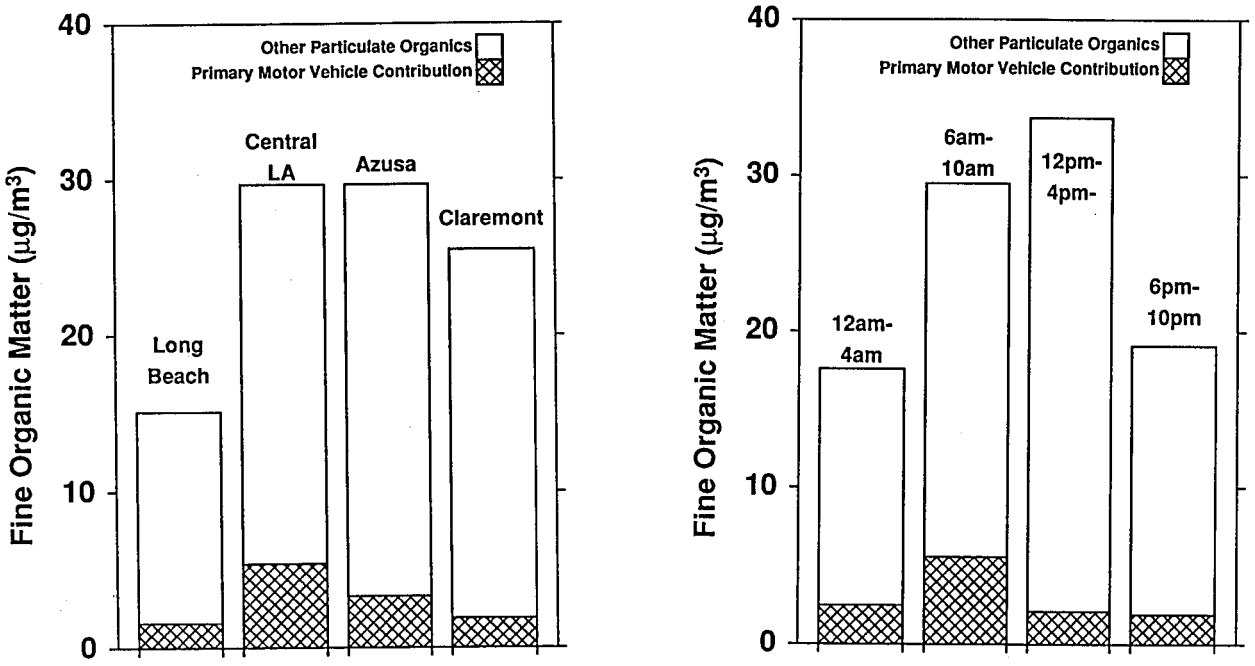

Figure 9.6:
Contribution of primary motor vehicle emissions to fine particulate organic matter averaged over all times at each site (left) and averaged over all sites as a function of time of day (right), Sept, 8-9, 1993.

towards the inland valleys, the proportion of fine organic matter contributed by direct particle emissions from motor vehicle traffic decreases to 11.1% in Azusa and 7.5% in Claremont. The explanation for this is that local motor vehicle traffic densities are lower there, increased vertical mixing in the atmosphere during the day causes dilution of those primary particle emissions that are transported from upwind, while secondary formation of airborne organic particulate matter due to the oxidation of primary volatile organic compounds adds organic matter to the air masses seen in the downwind areas like Azusa and Claremont which is not attributable to primary particle emissions from sources. The diurnal variations of the primary motor vehicle emissions generally show peak contributions from motor vehicle exhaust during the morning traffic peak between 0600-1000 Pacific Daylight Time (PDT). In the afternoon, a rapid decrease in the contribution from primary motor vehicle exhaust is seen; this is most likely caused by increased vertical mixing due to radiative heating combined with the reduction in primary motor vehicle traffic emissions following the morning traffic peak. In the evening, the fraction of fine particulate organic matter attributable to primary motor vehicle exhaust begins to build overnight, increasing to 10.0% of total fine particle organics from 1800-2200 PDT and to 14.3% from 0000-0400 PDT. These results are in agreement with previous studies of the annual average organic aerosol levels in Southern California, which apportion between 4.0%-17.9% of the fine organic particulate matter in the Southern California atmosphere to gasoline-powered vehicle exhaust [7].

Bibliography

[1] C. A. Pope, D. W. Dockery, and J. Schwartz. Review of epidemiological evidence of health effects of particulate air pollution. *Inhalation Toxicology*, 7:1–18, 1995.

[2] R. A. Harley, S. E. Hunts, and G. R. Cass. Strategies for the control of particulate air quality: least-cost solutions based on receptor-oriented models. *Environ. Sci. Technol.*, 23:1007–1014, 1989.

[3] M. N. Ingalls. On–road vehicle emission factors from measurements in a Los Angeles area tunnel. 1989. Paper No. 89-137.3, presented at the Air and Waste Management Association 82nd Annual Meeting.

[4] W. R. Pierson, A. W. Gertler, and R. L. Bradow. Comparison of the SCAQS tunnel study with other on–road vehicle emission data. *J. Air Waste Manage. Assoc.*, 40:1495–1504, 1990.

[5] D. R. Lawson, P. J. Groblicki, D. H. Stedman, G. A. Bishop, and P. L. Guenther. Emissions from in-use motor vehicles in Los Angeles: a pilot study of remote sensing and the inspection and maintenance program. *J. Air Waste Manage. Assoc.*, 40:1096–1105, 1990.

[6] D. H. Stedman, G. Bishop, J. E. Peterson, and P. L. Guenther. *On-road CO remote sensing in the Los Angeles basin.* Technical Report California Air Resources Board contract A939–189, University of Denver, Denver, CO, 1991.

[7] J. J. Schauer, W. F. Rogge, L. M. Hildemann, M. A. Mazurek, G. R. Cass, and B. R. T. Simoneit. Source apportionment of airborne particulate matter using organic compounds as tracers. *Atmos. Environ.*, 30:3837–3855, 1996.

[8] B. R. T. Simoneit. Application of molecular marker analysis to vehicular exhaust for source reconciliations. *Intern. J. Environ. Anal. Chem.*, 22:203–233, 1985.

[9] K. E. Peters and J. M. Moldowan. *The Biomarker Guide.* Prentice-Hall, Englewood Cliffs, NJ, 1993.

[10] W. F. Rogge, L. M. Hildemann, M. A. Mazurek, G. R. Cass, and B. R. T. Simoneit. Mathematical modeling of atmospheric fine particle-associated primary organic compound concentrations. *J. Geophys. Res.*, 101:19373–19394, 1996.

[11] M. P. Fraser, D. Grosjean, E. Grosjean, R. A. Rasmussen, and G. R. Cass. Air quality model evaluation data for organics. 1. Bulk chemical composition and gas/particle distribution factors. *Environ. Sci. Technol.*, 30:1731–1743, 1996.

[12] M. P. Fraser, G. R. Cass, B. R. T. Simoneit, and R. A. Rasmussen. Air quality model evaluation data for organics. 4. C2-C36 non-aromatic hydrocarbons. *Environ. Sci. Technol.*, 31:2356–2367, 1997c.

[13] M. P. Fraser, G. R. Cass, and B. R. T. Simoneit. Gas-phase and particle-phase organic compounds emitted from motor vehicle traffic in a Los Angeles highway tunnel. *submitted for publication in Environ. Sci. Technol.*, 1997a.

[14] P. A. Solomon, J. L. Moyers, and R. A. Fletcher. High-volume dichotomous virtual impactor for the fractionation and collection of particles according to aerodynamic size. *Aerosol Sci. Technol.*, 2:455–464, 1983.

[15] W. John and G. Reischl. A cyclone for size-selective sampling of ambient air. *J. Air Pollut. Control Assoc.*, 30:872–876, 1980.

[16] S. V. Hering et al. The nitric acid shootout: field comparison of measurement methods. *Atmos. Environ.*, 22:1519–1539, 1989.

[17] P. A. Solomon, S. M. Larson, T. Fall, and G. R. Cass. Basinwide nitric acid and related species concentrations observed during the Claremont nitrogen species comparison study. *Atmos. Environ.*, 22:1587–1594, 1989.

[18] J. Mulik, R. Puckett, D. Williams, and E. Sawicki. Ion chromatographic analysis of sulfate and nitrate in ambient aerosols. *Analyt. Lett.*, 9:653–656, 1976.

[19] Varian Corp. *Analytical Methods for Flame Spectroscopy.* Varian Techtron, Melbourne, Australia, 1972.

[20] W.T. Bolleter, C.T. Bushman, and P.W. Tidell. Spectrophotometric determination of ammonium as indophenol. *Anal. Chem.*, 33:592–594, 1961.

[21] M. E. Birch and R. A. Cary. Elemental carbon-based method for monitoring occupational exposure to particulate diesel exhaust. *Aerosol Sci. Technol.*, 25:221–241, 1996.

[22] T.G. Dzubay. *X-ray Fluorescence Analysis of Environmental Samples.* Ann Arbor Science, Ann Arbor, MI, 1977.

[23] W. F. Rogge, L. M. Hildemann, M. A. Mazurek, G. R. Cass, and B. R. T. Simoneit. Sources of fine organic aerosol 2. Noncatalyst and catalyst-equipped automobiles and heavy-duty diesel trucks. *Environ. Sci. Technol.*, 27:636–651, 1993.

[24] M. P. Fraser, G. R. Cass, B. R. T. Simoneit, and R.A. Rasmussen. Air quality model evaluation data for organics. 5. C6-C22 non-polar and semi-polar aromatic hydrocarbons. *submitted for publication in Environ. Sci. Technol.*, 1997b.

[25] M. P. Fraser and G. R. Cass. Detection of excess ammonia emissions from in-use vehicles and the implication for fine particle control. *submitted for publication in Environ. Sci. Technol.*, 1997.

10 Modeling the Ambient Concentrations of Organic Air Pollutants

10.1 Introduction

Mathematical models can be developed that simulate the atmospheric transport and chemical reactions which relate source emissions to ambient pollutant concentrations. These models, once verified by comparing model predictions of pollutant concentrations against ambient measurements, can then be used to simulate the effect of different emission control programs in advance of their adoption. Thus air quality models have evolved into important tools for determining the most effective proposed air quality improvement plans [1].

While atmospheric pollutants are comprised of inorganic and organic compounds, the atmospheric fate of single inorganic compounds (such as ammonia and the oxides of nitrogen) has been more thoroughly studied than the fate of single organic compounds. This situation is due in part to the fact that the number of individual inorganic compounds is small compared to the large number of organic compounds in the atmosphere.

Atmospheric models have been developed that track the inorganic pollutants such as the oxides of nitrogen from their emissions as gases, atmospheric conversion to form low vapor pressure reaction products, and condensation onto particles accompanied by atmospheric transport to inland smog receptor sites [2, 3], but no comparable models have been developed that simul-

taneously track both gas-phase and particle-phase organics at the level of predicting the concentrations of individual organic compounds. Air quality model development for organic compounds has progressed primarily along these fronts: aerosol processes modeling of bulk particulate organic compound mass [4, 5, 3, 6]; transport modeling of single organic compounds in the particle phase [7]; and separate photochemical modeling of vapor-phase organics with respect to ozone formation and toxic air pollutant concentrations [8, 9, 10, 11]. Research in aerosol modeling has led to development of procedures for calculating source/receptor relationships for primary particulate organic compounds (those directly emitted from sources) [7, 12]. Air quality modeling of volatile organic compounds (VOCs) has led to the capability to predict the atmospheric concentrations of more than 50 individual VOCs [13]. However, there has been little attempt to unify the treatment to track both individual gas-phase and particle-phase organic compounds simultaneously in a way that would support future calculations of gas/particle exchange for organics.

The motivation for pursuing this unified treatment is seen in the interconnection of two of the most prevalent urban air quality problems: increased ground level ozone and fine particulate matter concentrations. Atmospheric photochemical reactions involving vapor-phase organic compounds (VOCs) and nitrogen oxides (NO_x) lead to formation of both ozone and fine particulate matter. The oxidation of certain VOCs produces non-volatile organic compounds which can partition into the particle phase [4, 14]. Any complete understanding of atmospheric organics should include a simultaneous treatment of both the vapor and particle phase organic compounds.

Eularian air quality models have been developed which predict atmospheric total particulate carbon concentrations as well as VOC concentrations

[15, 6]. However, these models do not describe the molecular composition of the atmospheric carbon particles. Before models that do track individual particulate organic compound concentrations can be assembled and tested, it is necessary to have atmospheric measurements of the compounds of interest that are made over short consecutive time intervals throughout the airshed of interest. Measuring individual organic compounds present in the carbonaceous aerosol particles is a powerful tool for determining the origin of the total particulate carbon burden in the atmosphere [16, 12, 7]. Without detailed organic compound speciation, it is impossible to accurately tell the cause of any discrepancies between overall predicted atmospheric carbonaceous particle concentrations and measured total carbon values.

The major barrier to the development and testing of such a comprehensive model for atmospheric organic air pollutants is the absence of an equally comprehensive atmospheric data base against which such a model can be tested. As part of the present research effort, a data base that describes the detailed organic speciation of vapor-phase, particle-phase and semivolatile organic air pollutants has been assembled in Southern California [17, 18, 19, 20, 21]. Together with detailed measurements of the organic chemical speciation of the emissions from the major urban sources of organic air pollutants [22, 23, 24, 25], these data will be used to evaluate an air quality model designed to predict the ambient concentrations of primary gas-phase, semi-volatile and particle-phase organic species plus some secondary gas-phase species over a two-day photochemical smog episode. This model features the short time averaging needed to predict the diurnal variation of pollutant concentrations as well as their spatial variation across the South Coast Air Basin (SoCAB) that surrounds Los Angeles.

10.2 Model Formulation

The CIT airshed model is used here as the platform upon which the detailed model for organic air pollutants will be built [9, 2, 10]. This Eularian photochemical air quality model has been designed to simulate the emissions, atmospheric transport and chemical reactions of organic and inorganic pollutants in the atmosphere. The model numerically solves the atmospheric diffusion equation for individual species i that are linked by common chemical reactions:

$$\frac{\partial C_i}{\partial t} + \nabla \cdot (\vec{u} C_i) = \nabla \cdot (K \nabla C_i) + R_i \tag{10.1}$$

where C_i is the concentration of species i, $\vec{u}$ is the wind velocity, K is the eddy diffusivity tensor, and R_i is the rate of generation of species i by chemical reaction. The surface boundary condition relates the upward flux of the pollutant emissions of species i (E_i), the dry deposition velocity (v_g^i) and turbulent diffusion.

$$-K_{zz} \frac{\partial C_i}{\partial t} = E_i - v_g^i C_i \tag{10.2}$$

A no-flux boundary condition exists at the top of the modeling region, and initial conditions and boundary conditions at the horizontal edges of the modeling domain are set using measured pollutant concentrations.

10.2.1 Chemical Mechanism

Representation of the atmospheric chemistry of VOCs, NO_x, and radical species begins with the chemical mechanism complier described by Carter in 1990 [26]. The additions to this mechanism described by Harley and Cass [13] including 53 individual organic compounds and 11 lumped species groups are also adopted. These lumped species groups have been further subdivided to explicitly represent the reaction of 72 additional volatile and semi-volatile

organic compounds of interest to the present study. The final chemical mechanism includes 372 reactions and 206 chemical species or lumped species groupings. The additional organic species entered into the model beyond those employed by Harley and Cass [13] are listed in Table 10.1 along with their reaction rate with the hydroxyl radical. In addition to reaction with the hydroxyl radical, reactions between the olefins listed in Table 10.1 with the nitrate radical, atomic oxygen and ozone are included in the expanded chemical mechanism [26].

To track the emission of fuel components present in diesel fuels and diesel engine exhausts, aliphatic and aromatic hydrocarbons up to and including C_{24} compounds have been included in the chemical mechanism. The reaction kinetics of these compounds has been estimated using published kinetic data and estimates from structurally analogous compounds. For example, the reaction kinetics and products from reaction of the hydroxyl radical with the isoprenoid hydrocarbons norpristane, pristane and phytane were estimated to be equal to that of analogous reactions of the hydroxyl radical with C_{15}-branched hydrocarbons.

It is important to accurately describe radical production from photolysis of the aldehydes. In the present application, the lack of photolysis and reaction rate data for the higher molecular weight aldehydes has limited the analysis of aldehyde chemistry to formaldehyde, acetaldehyde, benzaldehyde, glyoxal, and methylglyoxal; all remaining higher molecular weight aldehydes are grouped within a lumped higher aldehyde category. All ketones are also grouped together in a general lumped ketones category. Photolysis and quantum yield data for formaldehyde are updated to recently suggested values [32].

Table 10.1: Additions to the chemical mechanism beyond those stated by Harley and Cass [13](a).

Compound	k_{OH}^{300C} (ppm^{-1} min^{-1})	Reference
n-decane	1.71×10^4	[26]
n-undecane	1.95×10^4	[26]
n-dodecane	2.09×10^4	[26]
n-tridecane	2.36×10^4	[26]
n-tetradecane	2.45×10^4	[26]
n-pentadecane	2.66×10^4	[26]
2,2-dimethylpropane	1.27×10^3	[26]
2-methylheptane	1.22×10^4	[26]
3-methylheptane	1.27×10^4	[26]
4-methylheptane	1.27×10^4	[26]
2,3-dimethylhexane	1.28×10^4	[26]
2,4-dimethylhexane	1.28×10^4	[26]
2,5-dimethylhexane	1.22×10^4	[26]
2,3,4-trimethylpentane	1.28×10^4	[26]
ethylcyclohexane	1.81×10^4	[26]
3-ethylhexane	1.56×10^4	b
norpristane	2.95×10^4	c
pristane	2.95×10^4	c
phytane	2.95×10^4	c
nonylcyclohexane	3.55×10^4	d
decylcyclohexane	3.55×10^4	d
undecylcyclohexane	3.55×10^4	d
dodecylcyclohexane	3.55×10^4	d
tridecylcyclohexane	3.55×10^4	d
tetradecylcyclohexane	3.55×10^4	d
pentadecylcyclohexane	3.55×10^4	d
hexadecylcyclohexane	3.55×10^4	d
heptadecylcyclohexane	3.55×10^4	d
octadecylcyclohexane	3.55×10^4	d
n-hexadecane	2.66×10^4	e
n-heptadecane	2.66×10^4	e
n-octadecane	2.66×10^4	e
n-nonadecane	2.66×10^4	e
n-eicosane	2.66×10^4	e
n-heneicosane	2.66×10^4	e
n-docosane	2.66×10^4	e
n-tricosane	2.66×10^4	e
n-tetracosane	2.66×10^4	e
m-ethyltoluene	3.46×10^4	f
o-ethyltoluene	2.01×10^4	g
p-ethyltoluene	2.10×10^4	h
naphthalene	3.17×10^4	[26]
1-methylnaphthalene	7.63×10^4	[26]
2-methylnaphthalene	7.63×10^4	[26]
dimethylnaphthalene	1.13×10^5	[26]
acenaphthene	1.5×10^4	[27]

Table 10.1: continued

Compound	k_{OH}^{300C} (ppm^{-1} min^{-1})	Reference
fluorene	2.4×10^4	[28]
dibenzofuran	5.8×10^3	[29]
phenanthrene	5.0×10^4	[30]
anthracene	1.6×10^5	[30]
fluoranthene	7.4×10^4	[31]
pyrene	7.4×10^4	[31]
2-methyl-1-butene	8.80×10^4	[26] m
2-methyl-2-butene	1.26×10^5	[26] m
1-pentene	4.56×10^4	[26] m
1-hexene	5.37×10^4	[26] m
cyclopentene	9.74×10^4	[26] m
d-limonene	2.51×10^5	[26] m
trans-2-pentene	9.62×10^4	[26] m
cis-2-pentene	9.62×10^4	[26] m
4-methyl-1-pentene	5.37×10^4	i, m
2-methyl-1-pentene	5.37×10^4	i, m
cis-4-methyl-2-pentene	9.62×10^4	j, m
trans-2-hexene	9.62×10^4	j, m
2-methyl-2-pentene	9.62×10^4	j, m
cis-2-hexene	9.62×10^4	j, m
2,4,4-trimethyl-1-pentene	5.37×10^4	k, m
2,4,4-trimethyl-2-pentene	5.37×10^4	l, m

(a) The individual organic compounds modeled by Harley and Cass [13] included methane, ethane, acetylene, propane, n-butane, n-pentane, n-hexane, n-heptane, n-octane, n-nonane, isobutane, isopentane, 2-methylpentane, 3-methylpentane, 2,2-dimethylbutane, 2,3-dimethylbutane, 2-methylhexane, 2,3-dimethylpentane, 2,4-dimethylpentane, 2,2,4-trimethylpentane(iso-octane), cyclopentane, cyclohexane, methylcyclopentane, methylcyclohexane, benzene, toluene, ethylbenzene, isopropylbenzene, n-propylbenzene, m-xylene, o-xylene, p-xylene, 1,3,5-trimethylbenzene, 1,2,3-trimethylbenzene, 1,2,4-trimethylbenzene, ethene, propene, 1-butene, trans-2-butene, cis-2-butene, isobutene, 1,3-butadiene, styrene, isoprene, α-pinene, β-pinene, 1,1,1-trichloroethane, perchloroethane, formaldehyde, acetaldehyde, benzaldehyde and acetone.
Rate constants for species that lack values explicitly in Carter [26] are estimated by analogy to similar compounds for which data are available in that reference as follows: (b) used 4-ethylheptane. (c) used 3,9-diethylundecane. (d) used 1,3,5-tripropylcyclohexane. (e) used n-pentadecane. (f) used m-xylene. (g) used o-xylene. (h) used p-xylene. (i) used 1-hexene. (j) used 2-hexene. (k) used C_8 terminal alkene. (l) used C_8 internal alkene. (m) reactions of olefins with ozone, the nitrate radical and molecular oxygen are also included in the model based on rate constants from reference [26].

10.2.2 Aerosol Processes Model

The mathematical model used to describe emissions of particulate matter, particle transport and deposition is developed from that described by Kleeman et al. [33]. The Lagrangian trajectory version of the particle model is expanded into an Eularian grid based model. Horizontal advection and diffusion are calculated based on particle number concentrations by a means analogous to that for the gas-phase species described above.

In this model framework, particles emitted from different source categories are represented in each active grid cell using particles of 15 sizes containing up to the 15 aerosol-phase inorganic chemical species employed by Kleeman et al. [33], plus a lumped organic compounds category and elemental carbon. The lumped organic compounds category is then disaggregated into as many individual primary organic compounds as desired in a particular model application, consistent with the availability of source emissions data and ambient concentration data. In the present work, the capabilities of the model will be evaluated by following the emission and fate of 31 individual primary particulate organic compounds that are chosen because they are characteristic of the emissions from specific source types. Because the focus of this work is to describe organic air pollutants, inorganic gas-to-particle conversion process calculations are not activated during the model calculations reported here.

10.3 Model Application

The model described above is applied to the study of air quality in the South Coast Air Basin (SoCAB) of Southern California over the two-day period, Sept. 8-9, 1993. The Southern California area, monitoring sites used in model evaluation, and the computational boundary within which model calculations

are made are shown in Figure 10.1. Input data, including meteorological fields, are developed over the entire 400×150 km region shown.

10.3.1 Meteorological Inputs

The accuracy of any model application is directly dependant on the accuracy of the input data used. For airshed modeling, complete and accurate meterological data are necessary. The meteorological data gathered to represent the SoCAB on September 8-9, 1993, include hourly observations of resultant wind speed and direction at 21 sites operated by the California Irrigation Management Information Service (CIMIS) and 32 sites operated by the South Coast Air Quality Management District (SCAQMD); temperature data from 21 sites operated by the CIMIS, 52 sites from the National Climatic Data Center (NCDC), and 13 sites operated by the South Coast Air Quality Management District; relative humidity (or dew point temperature) from 21 CIMIS sites, 52 NCDC sites, and 13 SCAQMD sites; hourly total solar radiation data from 21 CIMIS sites and 6 SCAQMD sites; and ultraviolet radiation data from one SCAQMD site. Hourly gridded meterological fields for temperature, relative humidity, solar radiation scaling (relative to predicted total solar radiation given clear-sky conditions), and ultraviolet radiation scaling were produced from the measured values according to the procedures of Harley et al [10] using the interpolation method of Goodin et al. [34].

Critical meterological inputs included data on the three-dimensional structure of the atmosphere, including specification of the height of the base of the temperature inversion that typically exists in the atmosphere above the Los Angeles area. Upper air soundings available during the smog episode of interest include one balloon sounding taken daily at Loyola Marymont Uni-

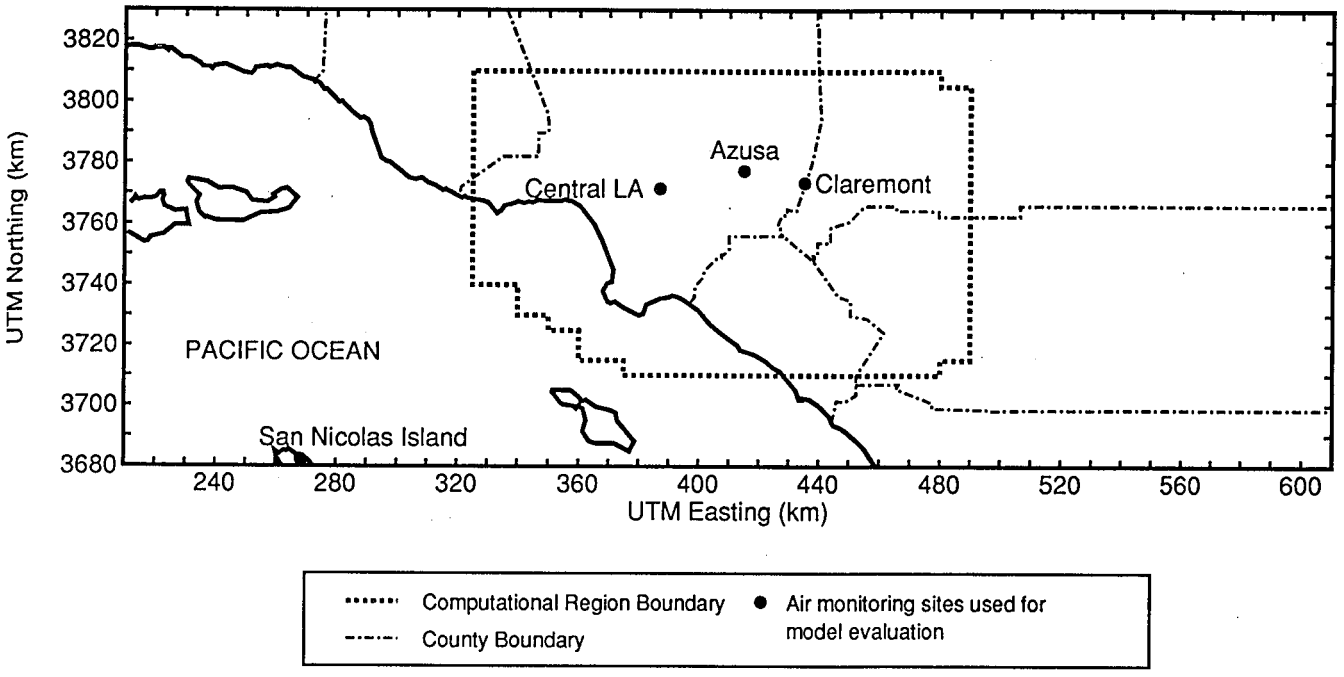

Figure 10.1:
Southern California region, showing computation region and sites used for model evaluation.

versity at 0500 hours PST, plus hourly radar profiler soundings collected at Claremont from which data have been reported between 0600 and 1400 hours PST [35]. From the available data, three-dimensional wind fields were generated using the diagnostic wind field model of Goodin et al. [36], and mixing depth fields were calculated hourly by combining the data on the temperature structure of the atmosphere and the hourly gridded surface temperature fields to compute hourly gridded mixing depths according to Holtzworth's method [37].

10.3.2 Vapor-Phase Emissions

Emissions of total (unspeciated) VOC mass, NO_x, and CO for the present application are based on emissions inventories supplied by the South Coast Air Quality Management District (SCAQMD) for the year 1993. These inventories include hourly emissions defined over a grid of 5×5 km cells that covers the SoCAB. Emissions from hundreds of different point source and area source categories are described. Mobile source emissions are calculated from modeled traffic patterns and emissions factors using the California Air Resource Boards emissions model EMFAC-7G. These estimates of mobile emissions have been shown to underpredict on-road emissions rates [38, 39, 40], and therefore in the present work the hot exhaust emissions of VOC and CO from highway vehicles are scaled upwards by a factor of 3 in order to match the results of measurements made in the Los Angeles Van Nuys traffic tunnel in 1993 a few days after the field experiments that will be used here for model evaluation [40]. The emissions rates of non-methane organic gases, CO and NO_x, are listed in Table 10.2.

Separation of total VOC emissions rates into emissions of individual organic compounds is based on the work of Harley et al. [41] combined with

Table 10.2: Emissions rates for non-methane organic gases (NMOG), carbon monoxide and nitrogen oxides in the South Coast Air Basin (in metric tons per day) from major source categories: September 8-9, 1993.

	Emissions (metric tons per day)		Rates
Category Type	NMOG	NO_x	CO
Fuel Combustion	12.4	105.7	46.9
Waste Burning	0.5	1.9	2.8
Solvent Use	335.2	0.3	0.2
Petroleum Process, Storage and Transfer	50.8	0.3	3.7
Industrial Processes	21.4	5.5	0.8
Miscellaneous Processes	65.9	1.0	9.3
On-Road Vehicles	1,117.6	701.5	9,236.9
Other Mobile	103.7	250.0	1,379.3
Other Sources	119.2	0.0	0.3
Totals for all categories	1,826.7	1,066.2	10,680.1

more recent source test data on VOCs reported by Schauer et al. [22, 23]. An expanded diesel engine exhaust composition profile that includes semi-volatile species up to C_{24} was used to model the emissions from diesel-powered vehicles. That profile was constructed by employing the heavy-duty diesel profile of Harley et al. [41] while unbundling the lumped n-C_{15} and higher hydrocarbons category into the emissions of 21 specific high molecular weight organic compounds in proportion to the speciation of semi-volatile organics emitted from medium-duty trucks as reported by Schauer et al. [23]. The source test data of Schauer et al. [22, 23] provide emissions rates for 33 vapor-phase semi-volatile organic compounds not traditionally included in air quality modeling source profiles that are now included within the present model.

10.3.3 Particle Emissions

Construction of the primary particle emissions inventory used in this work begins with the 1993 particle mass emissions inventory for the SoCAB provided by the South Coast Air Quality Management District. The SCAQMD emissions inventory next is modified to incorporate more recent mass emissions rate data for motor vehicles as described by Eldering and Cass [42]. Emitted particle size distributions are described by Eldering and Cass [42] based largely on the work of Hildemann et al. [43]. Emitted particles are modeled using 15 discrete particle sizes equally spaced on a logarithmic scale between 0.01 μm to 10.0 μm particle diameter. The resulting overall mass emissions rates from different source categories are listed in Table 10.3 for particles smaller than 10 μm, 2.5 μm, and 1.0 μm diameter (PM10, PM2.5 and PM1.0, respectively).

The bulk chemical composition of emitted particles is as described by Eldering and Cass [42] based largely on the work of Hildemann et al. [44], with new chemical composition data contributed by Schauer et al. [25, 22, 23, 45, 46], and Rogge et al. [47, 48]. Emitted particles are composed of up to 15 inorganic species as described by Kleeman et al. [33] in each of the 15 sizes. Primary particulate organic compounds are carried as a lumped category in the model from which individual organic compounds can be disaggregated at will. An inventory of lumped organic compound emissions showing the major source types is given in Table 10.4

The particulate species of most interest in this work include individual organic compounds that can be used to track emissions from specific source categories. These tracer compounds have been used in previous receptor modeling calculations to determine source contributions to ambient organic particulate matter concentrations [12] and also in atmospheric transport

Table 10.3: Emissions rates for particulate matter in the South Coast Air Basin (in metric tons per day) from major source categories: Sept. 8-9, 1993.

	Particulate Mass Emissions (metric tons per day)		
Category Type	PM10	PM2.5	PM1.0
Fuel Combustion	6.8	6.7	6.6
Waste Burning	0.3	0.3	0.3
Solvent Use	0.6	0.6	0.6
Petroleum Process, Storage and Transfer	0.9	0.6	0.4
Industrial Processes	11.9	9.7	8.3
Farming Operations	14.7	2.0	1.5
Construction and Demolition	30.5	6.7	3.1
Entrained Road Dust-Paved	141.0	26.3	12.1
Entrained Road Dust-Unpaved	46.0	10.1	4.7
Fugative Windblown Dust	66.7	14.6	6.7
Miscellaneous Processes	7.3	4.7	3.0
On-Road Vehicles	30.5	26.4	24.4
Other Mobile	24.1	22.8	21.8
Other Sources	0.0	0.0	0.0
Totals for all categories	381.3	131.4	93.4

Table 10.4: Emissions rates for particulate organic compounds (in metric tons per day) for the major source profiles for particulate organic compound emissions in the South Coast Air Basin: Sept. 8-9, 1993.

	Organic Compound Emissions (metric tons per day)		
Emission Profile	PM10	PM2.5	PM1.0
Unpaved road dust	6.7	1.5	0.7
Paved road dust	25.9	4.8	2.2
Diesel engines	8.8	8.4	8.0
Meat cooking operations	5.8	5.8	5.5
Non-catalyst gasoline engines	8.9	6.4	5.4
Catalyst-equipped gasoline engines	2.8	2.8	2.7
Other profiles	14.2	9.8	9.0
Totals for all profiles	73.1	39.5	33.5

models to explore the relationship between source emissions and ambient concentrations of these same tracer compounds [7]. The detailed chemical composition of the organic fraction of emitted aerosol particles from meat cooking operations, wood smoke, diesel engines, catalyst-equipped vehicles, non-catalyst vehicles, and paved road dust is entered into the model based on the work of Schauer et al. [25, 23, 45, 22, 46] and for tire dust and natural gas combustion based on the work of Rogge et al. [47, 48]. Thirty-three primary particulate organic compounds present in the emissions profiles of these sources and measured in the ambient air during the September 8-9, 1993, smog episode are chosen to illustrate the performance of this model. These compounds are listed in Table 10.5.

Emissions of plant and leaf waxes to the atmosphere are not included in the emissions inventories supported by the SCAQMD. As a result, the emissions inventory will be deficient in the emissions of the odd-carbon number high molecular weight n-alkanes in the range from about C_{29} to C_{33} [49].

10.3.4 Boundary and Initial Conditions

Initial and boundary conditions for vapor-phase organic compounds were set using measurements made on Sept. 8-9, 1993, at four urban sites and one offshore island background site as described by Fraser et al. [17, 20, 21] and Grosjean et al. [18, 19]. Previous modeling studies have shown that accurate knowledge of initial conditions and boundary conditions is very important to the predictions of the model [50]. Gridded maps of initial total non-methane hydrocarbons, formaldehyde, methylethylketone, and higher aldehydes were created for 0000 hours at the start of September 8 based on RHC measurements from six air monitoring stations operated by the SCAQMD plus five air monitoring sites operated as part of the present research program. The

Table 10.5: Particulate organic species tracked in the model.

Compound	Emission Sources
n-Tricosane	1,2,3,4,5,6,7,8
n-Tetracosane	1,2,3,4,5,6,7,8
n-Pentacosane	1,2,3,4,5,6,7,8
n-Hexacosane	1,2,3,4,5,6,7,8
n-Heptacosane	1,2,3,4,6,7,8
n-Octacosane	1,3,4,6,7,8
n-Nonacosane	1,3,4,6,7,8
n-Triacontane	6,7,8
n-Hetriacontane	6,7,8
n-Dotraicontane	6,7,8
n-Tritriacontane	6,7,8
n-Tetratriacontane	7
Hopanes (a)	2,3,4,7
Steranes (b)	3,4,7
Chrysene/Triphenylene	1,2,3,4,5,6,7
Benzo[k]fluoranthene	2,3,5,6
Benzo[e]acephenanthrylene	3,5,6
Benzo[e]pyrene	2,3,5,6,7
Benzo[a]pyrene	2,3,5,7
Perylene	2,5
Indeno[123-cd]fluoranthene	2,3,5
Indeno[123-cd]pyrene	2,3,5
Benzo[ghi]perylene	5
Antracene-9,10-dione	2,3,6
Benz[de]anthracen-7-one	5,6
Benz[a]anthracene-7,12-dione	6
Dehydroabietic acid	5,7,8
Hexanedioic acid	1
Octanedioic acid	1,2,3,4
n-Hexadecenoic acid	1,8
n-Hexadecanoic acid	1,5,6,7,8
n-Eicosanoic acid	1,2,3,5,7,8
n-Docosanoic acid	1,5,8

Category 1: Meat cooking operations. [25]
Category 2: Catalyst-equipped gasoline-powered vehicles. [22]
Category 3: Non-catalyst gasoline-powered vehicles. [22]
Category 4: Diesel engines. [23]
Category 5: Wood combustion. [45]
Category 6: Natural gas combustion. [48]
Category 7: Tire wear particles. [47]
Category 8: Paved-road dust. [46]
(a) This category represents the sum of 9 individual pentacyclic triterpanes.
(b) This category represents the sum of 8 individual steranes.

initial non-methane hydrocarbons concentrations field was then mapped into concentration fields for 79 individual organic compounds and 7 lumped compound groups, listed in Table 10.6, based the detailed organics speciation data collected during the first four-hour sampling period on Sept. 8-9, 1993 [17, 18, 19, 20, 21]. Meta and para-xylene, which are not resolved from each other by the techniques used to collect the ambient data, were each assigned half of the measured meta plus para-xylene concentrations.

Boundary conditions for organic compounds (including non-methane hydrocarbons, formaldehyde, acetaldehyde and acetone) over the ocean were set using values measured during this study at San Nicolas Island [18, 20, 21]. Additional boundary conditions for NO_x, O_3, CO, and methane over the ocean were set using values measured during the Southern California Air Quality Study [13]. Boundary values over the ocean assigned for NMHC, formaldehyde, acetaldehyde, acetone, CO, NO, NO_2, CH_4, and O_3 are given in Table 10.7. The speciation of NMHC along the boundaries was set equal to that of the initial conditions of the model persuant to the findings of this work that air quality over San Nicolas Island is similar in composition to aged, diluted air from the Southern California urban area [20, 21].

Boundary and initial conditions for aerosol species were set based on measured values at the urban and background sampling sites. A gridded map of initial particulate carbon was generated based on observations, and the particulate carbon at each grid square was speciated according to typically observed concentrations of the individual particulate organic compounds of interest in this study as shown in Table 10.8. The initial and background size distribution of the carbonaceous aerosol was based on size distributions collected during the SCAQS experiments [51].

Table 10.6: Relative composition of initial and background NMHC.

Compound	ppbC Species per ppmC NMHC
Toluene	80.7
2-Methylbutane	77.8
Ethane	60.5
Propane	58.2
Ethene	43.6
n-Pentane	36.7
2-Methyl-1-butene	36.7
n-Butane	35.5
Benzene	33.9
Acetylene	31.6
Naphthalene	28.7
2-Methylpentane	26.6
p-Xylene	24.0
m-Xylene	24.0
1,2,4-Trimethylbenzene	22.5
o-Xylene	19.5
2,2,4-Trimethylpentane(iso-octane)	18.4
Propene	17.9
3-Methylpentane	17.4
2-Methylpropane	17.2
n-Hexane	16.7
Methylcyclopentane	16.1
Ethylbenzene	14.2
3-Methylhexane	13.8
p-Ethyltoluene	13.8
2-Methylhexane	12.4
Methylcyclohexane	11.9
n-Heptane	11.0
2,3-Dimethylpentane	10.5
Isobutene	9.6
1,3,5-Trimethylbenzene	8.9
1,2,4-Trimethlybenzene	7.6
2,3-Dimethylbutane	7.6
Trichloroacetylene	7.6
m-Ethyltoluene	6.9
2,4-Dimethylpentane	6.7
n-Decane	6.6
2-Methyl-2-butene	5.7
n-Octane	5.3
2-Methylheptane	5.1
o-Ethyltoluene	5.1
trans-2-Pentene	5.0
1-Butene	4.6

Table 10.6: continued.

Compound	ppbC Species per ppmC NMHC
1,3-Butadiene	4.4
Cyclohexane	4.4
Cyclopentane	4.3
n-Nonane	4.1
n-Propylbenzene	4.1
trans-2-Butene	3.2
1-Pentene	3.0
2,2-Dimethylbutane	3.0
Isoprene	2.8
2,4-Dimethylhexane	2.8
cis-2-Pentene	2.8
2,3-Dimethylhexane	2.7
cis-2-Butene	2.7
2-Methylnaphthalene	2.3
1-Methylnaphthalene	2.3
d-Limonene	2.1
a-Pinene	2.1
Perchloroethene	1.9
trans-2-Hexene	1.8
3-Methyl-1-butene	1.4
1-Hexene	1.4
2,2,4-Trimethyl-1-pentene	1.4
Cyclopentene	1.2
2-Methyl-1-pentene	1.2
Dimethylnaphthalene	1.2
Cresols	1.0
i-Propylbenzene	0.9
cis-2-Hexene	0.7
4-Methyl-1-pentene	0.7
Phytane	0.4
n-Octadecane	0.3
Pristane	0.3
n-Nonadecane	0.2
n-Docosane	0.2
Fluorene	0.2
n-Heneicosane	0.1

Table 10.7: Boundary conditions over the ocean.

Species	Boundary Condition (ppbV)	Reference
NMHC	60	[20, 21]
formaldehyde	1	[18]
acetaldehyde	1	[18]
acetone	1	[18]
CO	200	[13]
NO	1	[13]
NO_2	1	[13]
CH_4	1700	[13]
O_3	40	[13]

10.3.5 Model Evaluation Data

The measured four-hour average concentrations of VOCs, aldehydes, semi-volatile and particle-phase organic compounds and bulk elemental and organic carbon collected at Central Los Angeles, Azusa and Claremont, CA by Fraser et al. [17, 20, 21] and Grosjean et al. [18, 19] provide the principal model evaluation data set used in this study. In addition, hourly observed pollutant concentration data available from the SCAQMD for use in model evaluation studies include data from 23 sites for NO, NO_2 and NO_x; 6 sites for NMHC; 36 sites for ozone; 22 sites for carbon monoxide; and 11 sites for sulfur dioxide.

10.4 Results

Model performance over the range of volatile, semi-volatile and particulate organic compounds is illustrated in Figures 10.2 and 10.3. These figures report the range of observed ambient four-hour average concentrations measured at Central Los Angeles, Azusa and Claremont on September 9, 1993, (taken as the mean over all times and stations$\pm$one standard deviation) compared to the mean of the model predicted concentrations for the same sampling locations and times for normal alkanes (Figure 10.2) and aromatic hy-

Table 10.8: Speciation of initial and boundary particulate organic carbon.

Compound	Speciation of Organic Carbon ng compound per μg OC
n-Tricosane	0.35
n-Tetracosane	0.56
n-Pentacosane	0.69
n-Hexacosane	0.56
n-Heptacosane	0.60
n-Octacosane	0.40
n-Nonacosane	0.41
n-Triacontane	0.23
n-Hetriacontane	0.29
n-Dotraicontane	0.12
n-Tritriacontane	0.25
n-Tetratriacontane	0.00
Hopanes	1.10
Steranes	0.44
Chrysene/Triphenylene	0.05
Benzo[k]fluoranthene	0.04
Benzo[e]acephenanthrylene	0.04
Benzo[e]pyrene	0.04
Benzo[a]pyrene	0.04
Perylene	0.01
Indeno[123-cd]fluoranthene	0.02
Indeno[123-cd]pyrene	0.06
Benzo[ghi]perylene	0.16
Antracene-9,10-dione	0.07
Benz[de]anthracen-7-one	0.03
Benz[a]anthracene-7,12-dione	0.01
Dehydroabietic acid	0.03
Hexanedioic acid	0.93
Octanedioic acid	0.06
n-Hexadecenoic acid	0.31
n-Hexadecanoic acid	4.45
n-Eicosanoic acid	0.00
n-Docosanoic acid	0.27

drocarbons (Figure 10.3). Model predictions and ambient observations at Long Beach are not included in this (or later analyses) because of difficulty in confirming the accuracy of the emissions inventory for local industrial sources in the port region. When reporting the modeled and measured concentrations of semi-volatile compounds that exist both in the particle phase and the vapor-phase, concentrations are summed. Figures 10.2 and 10.3 show that the model is capable of predicting the ambient concentrations of these compounds directly from emissions and meteorological data over a wide range of species volatilities, ranging from the most volatile VOCs including ethane, propane, and benzene, through the semi-volatile compounds to the heaviest particle phase hydrocarbons.

A more rigorous and complete description of model performance for 104 vapor-phase, semivolatile and particle-phase organic species carried by the model is reported in Table 10.9. That table states the mean of the observed four-hour average concentrations at Central Los Angeles, Azusa and Claremont on September 9, 1993, the standard deviation of these concentration measurements, the absolute model bias and absolute gross error statistics reported in ambient concentration units along with normalized bias and normalized gross error statistics. While there are several individual organic compounds that are not well modeled in the present application, the model accurately predicts the ambient concentrations of more than half of the organic compounds studied with a normalized bias of less than $\pm 50\%$. A more thorough discussion of the model performance for specific compounds of interest follows.

In Figure 10.4, model predictions (circles) are compared to the observed carbon monoxide concentrations at two locations (Central Los Angeles and Azusa) where ambient data are available from the SCAQMD. Carbon monox-

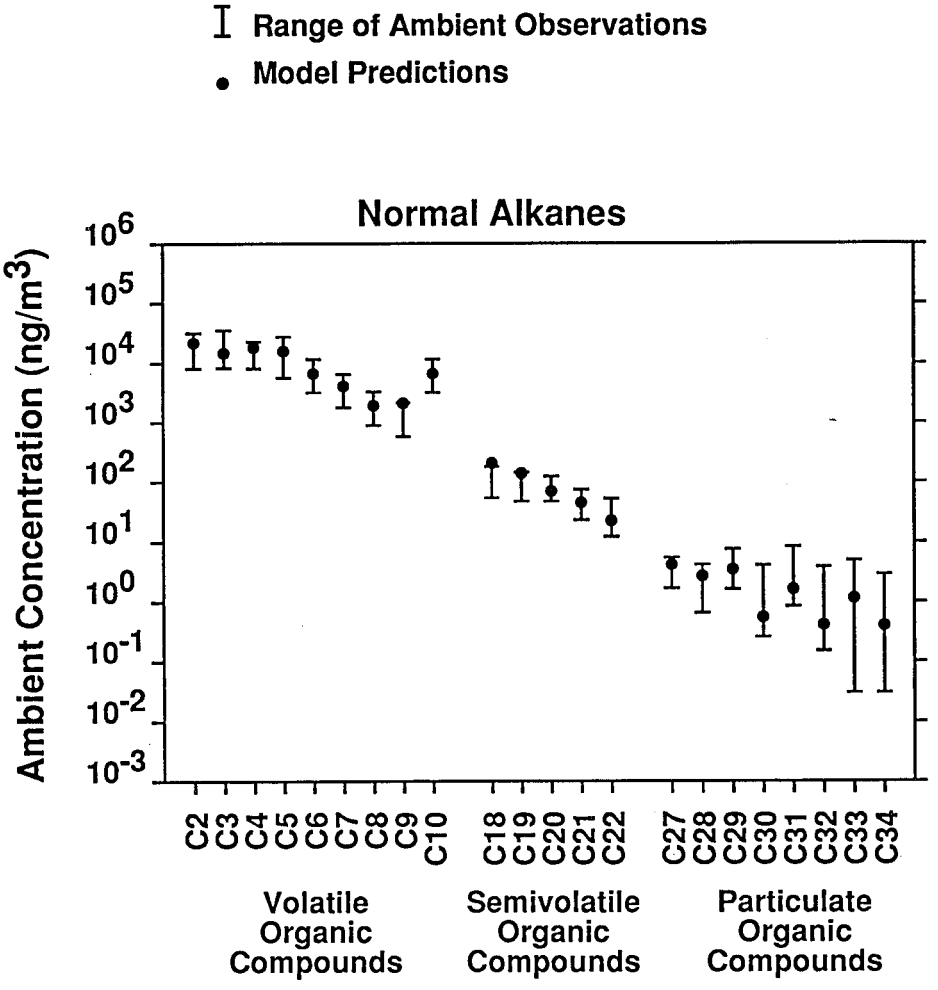

Figure 10.2:
Mean of hourly predicted n-alkane concentrations at Central Los Angeles, Azusa, and Claremont, CA, on September 9, 1993, (circles) compared to range of four-hour average ambient observations at those sites (taken as the mean±one standard deviation).

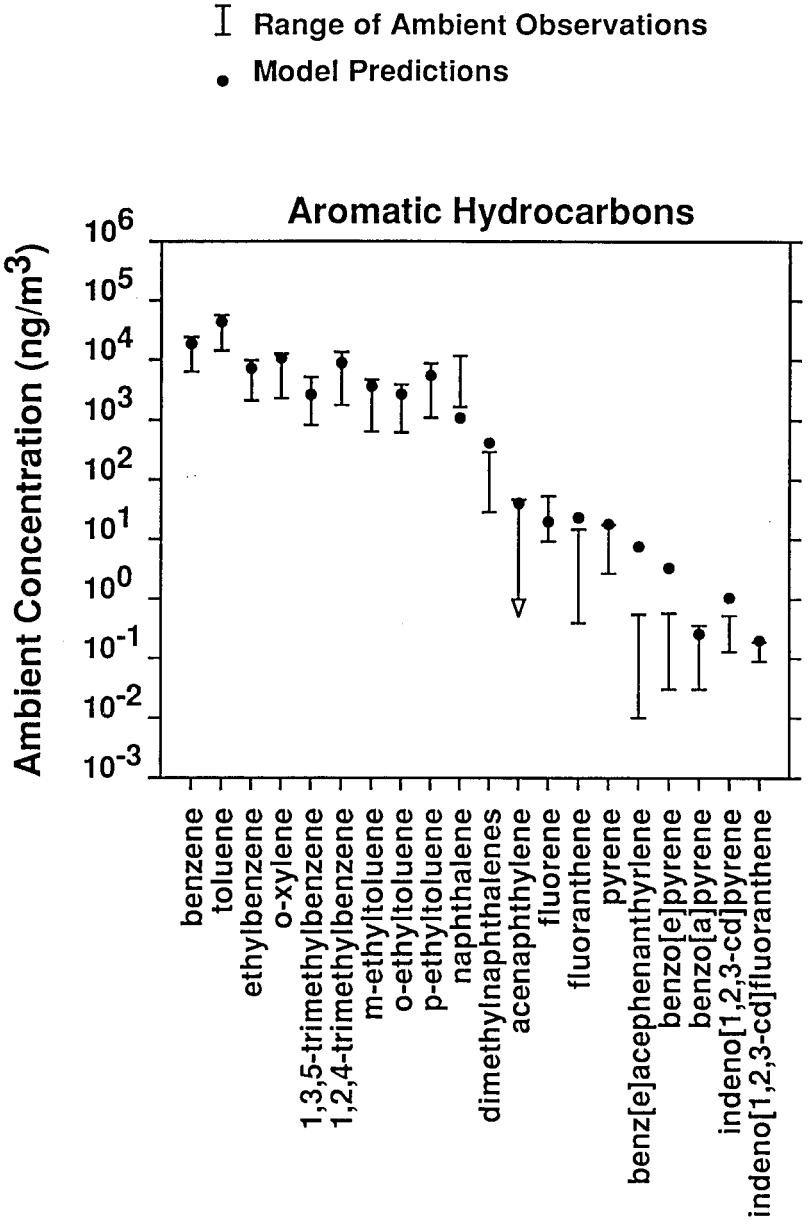

Figure 10.3:
Mean of hourly predicted aromatic hydrocarbon concentrations at Central Los Angeles, Azusa, and Claremont, CA, on September 9, 1993, (circles) compared to range of four-hour average ambient observations at those sites (taken as the mean±one standard deviation).

Table 10.9: Model performance for individual organic compounds

Compound	units	Observed Ambient Conc.[a] (mean±σ)	Absolute Bias[b]	Normalized Bias[b]	Absolute Gross Error[c]	Normalized Gross Error[c]
ethane	$\mu g\ m^{-3}$	19.9 ± 11.7	2.2	0.40	8.4	0.61
propane	$\mu g\ m^{-3}$	21.6 ± 13.4	-6.9	-0.17	8.3	0.31
n-butane	$\mu g\ m^{-3}$	15.3 ± 7.3	2.7	0.19	5.4	0.33
n-pentane	$\mu g\ m^{-3}$	16.8 ± 11.1	-0.8	0.08	7.0	0.38
n-hexane	$\mu g\ m^{-3}$	7.3 ± 4.1	-0.7	-0.04	2.4	0.33
n-heptane	$\mu g\ m^{-3}$	4.1 ± 2.3	-0.1	0.04	1.6	0.39
n-octane	$\mu g\ m^{-3}$	2.0 ± 1.2	-0.1	-0.03	0.8	0.40
n-nonane	$\mu g\ m^{-3}$	1.4 ± 0.8	0.8	0.59	1.0	0.71
n-decane	$\mu g\ m^{-3}$	2.0 ± 1.3	1.0	0.66	1.3	0.78
2-methylpropane	$\mu g\ m^{-3}$	7.2 ± 3.9	-0.2	0.06	2.3	0.31
2-methylbutane	$\mu g\ m^{-3}$	35.4 ± 19.6	12.7	0.42	16.7	0.51
2-methylpentane	$\mu g\ m^{-3}$	11.6 ± 6.7	1.4	0.18	4.2	0.40
3-methylpentane	$\mu g\ m^{-3}$	7.5 ± 4.4	0.4	0.11	2.6	0.37
2,2-dimethylbutane	$\mu g\ m^{-3}$	1.1 ± 0.6	1.4	1.41	1.4	1.41
2,3-dimethylbutane	$\mu g\ m^{-3}$	3.2 ± 1.9	2.1	0.72	2.2	0.75
2-methylhexane	$\mu g\ m^{-3}$	5.2 ± 2.8	0.4	0.10	2.0	0.40
3-methylhexane	$\mu g\ m^{-3}$	5.9 ± 2.9	-0.2	-0.02	2.3	0.38
2,3-dimethylpentane	$\mu g\ m^{-3}$	4.4 ± 2.6	4.5	1.05	4.6	1.08
2,4-dimethylpentane	$\mu g\ m^{-3}$	2.8 ± 1.6	2.0	0.79	2.2	0.85
cyclopentane	$\mu g\ m^{-3}$	1.7 ± 0.9	0.1	0.11	0.6	0.32
methylcyclopentane	$\mu g\ m^{-3}$	6.6 ± 4.1	-6.1	-0.90	6.1	0.90
cyclohexane	$\mu g\ m^{-3}$	1.4 ± 0.8	2.1	1.46	2.1	1.47
methylcyclohexane	$\mu g\ m^{-3}$	5.4 ± 4.6	-1.7	-0.10	2.9	0.42
acetylene	$\mu g\ m^{-3}$	15.9 ± 9.7	18.7	1.40	18.7	1.40
ethene	$\mu g\ m^{-3}$	17.3 ± 12.1	9.6	0.61	11.2	0.71
propene	$\mu g\ m^{-3}$	6.3 ± 5.2	3.9	0.63	5.2	0.89
trans-2-butene	$\mu g\ m^{-3}$	1.2 ± 0.9	0.6	0.23	1.0	0.76
cis-2-butene	$\mu g\ m^{-3}$	0.8 ± 0.6	0.3	0.23	0.7	0.78
isobutene	$\mu g\ m^{-3}$	2.6 ± 2.3	4.0	1.12	4.2	1.25
1-butene	$\mu g\ m^{-3}$	1.4 ± 1.0	-1.1	-0.79	1.1	0.79
2-methyl-1-butene	$\mu g\ m^{-3}$	16.8 ± 11.1	-14.4	-0.86	14.4	0.86
3-methyl-1-butene	$\mu g\ m^{-3}$	0.5 ± 0.3	0.1	0.19	0.3	0.59
cyclopentene	$\mu g\ m^{-3}$	0.5 ± 0.3	-0.1	-0.51	0.4	0.79
1-hexene	$\mu g\ m^{-3}$	0.8 ± 0.4	-0.2	-0.19	0.4	0.55
1-pentene	$\mu g\ m^{-3}$	1.1 ± 0.8	-0.2	-0.23	0.7	0.55
4-methyl-1-pentene	$\mu g\ m^{-3}$	0.6 ± 0.4	-0.2	-0.38	0.3	0.45
2-methyl-1-pentene	$\mu g\ m^{-3}$	0.6 ± 0.3	-0.1	-0.07	0.4	0.78
trans-2-pentene	$\mu g\ m^{-3}$	1.5 ± 1.2	-0.3	-0.38	1.1	0.73
cis-2-pentene	$\mu g\ m^{-3}$	0.9 ± 0.6	-0.3	-0.42	0.7	0.76
trans-2-hexene	$\mu g\ m^{-3}$	0.8 ± 0.4	-0.3	-0.46	0.4	0.57
cis-2-hexene	$\mu g\ m^{-3}$	0.5 ± 0.0	-0.3	-0.52	0.4	0.68
1,3-butadiene	$\mu g\ m^{-3}$	1.1 ± 0.7	-0.7	-0.58	0.7	0.58
isoprene	$\mu g\ m^{-3}$	1.1 ± 1.3	-0.8	-0.59	0.9	0.81
α-pinene	$\mu g\ m^{-3}$	1.6 ± 1.2	-1.4	-0.89	1.4	0.89

Table 10.9: continued

Compound	units	Observed Ambient Conc.[a] (mean±σ)	Absolute Bias[b]	Normalized Bias[b]	Absolute Gross Error[c]	Normalized Gross Error[c]
benzene	$\mu g\ m^{-3}$	15.1 ± 8.8	3.6	0.36	5.2	0.44
toluene	$\mu g\ m^{-3}$	35.5 ± 21.4	8.6	0.31	14.4	0.43
ethylbenzene	$\mu g\ m^{-3}$	5.9 ± 3.8	1.3	0.28	2.4	0.42
n-propylbenzene	$\mu g\ m^{-3}$	1.6 ± 1.0	0.4	0.42	0.8	0.56
m+p-xylene	$\mu g\ m^{-3}$	19.6 ± 14.5	-17.5	-0.89	17.5	0.89
o-xylene	$\mu g\ m^{-3}$	7.3 ± 5.1	3.3	0.48	4.2	0.60
1,3,5-trimethylbenzene	$\mu g\ m^{-3}$	3.0 ± 2.1	-0.3	-0.17	1.5	0.51
1,2,4-trimethylbenzene	$\mu g\ m^{-3}$	7.6 ± 5.8	1.3	0.14	3.6	0.45
m-ethyltoluene	$\mu g\ m^{-3}$	2.6 ± 2.0	1.0	0.38	1.8	0.65
o-ethyltoluene	$\mu g\ m^{-3}$	2.3 ± 1.6	0.4	0.24	1.1	0.48
p-ethyltoluene	$\mu g\ m^{-3}$	4.9 ± 3.8	0.5	0.20	2.0	0.45
i-propylbenzene	$\mu g\ m^{-3}$	0.9 ± 0.7	-0.6	-0.63	0.6	0.63
formaldehyde	$\mu g\ m^{-3}$	7.5 ± 3.0	17.2	2.60	17.2	2.60
acetaldehyde	$\mu g\ m^{-3}$	7.4 ± 4.1	13.0	2.33	13.0	2.33
glyoxal	$\mu g\ m^{-3}$	2.4 ± 2.7	-1.4	0.18	1.7	0.90
methylglyoxal	$\mu g\ m^{-3}$	3.7 ± 1.8	-1.88	-0.30	2.0	0.49
trichloroethane	$\mu g\ m^{-3}$	15.5 ± 9.1	1.5	0.35	6.4	0.52
2,2,4-trimethylpentane	$\mu g\ m^{-3}$	8.0 ± 4.6	7.4	1.05	7.5	1.06
2,3-trimethylhexane	$\mu g\ m^{-3}$	1.1 ± 0.7	0.6	0.63	0.8	0.75
2,4-trimethylhexane	$\mu g\ m^{-3}$	1.4 ± 1.0	1.3	1.17	1.5	1.27
naphthalene	$\mu g\ m^{-3}$	7.8 ± 5.8	-6.7	-0.80	6.7	0.80
pristane	$ng\ m^{-3}$	92.7 ± 60.5	64.8	0.68	83.5	0.87
phytane	$ng\ m^{-3}$	120.4 ± 83.0	32.5	0.26	56.7	0.46
n-nonylcyclohexane	$ng\ m^{-3}$	9.6 ± 5.1	-0.7	-0.09	5.1	0.43
n-decylcyclohexane	$ng\ m^{-3}$	12.6 ± 9.0	0.8	0.03	6.2	0.45
n-undecylcyclohexane	$ng\ m^{-3}$	18.7 ± 14.4	-10.1	-0.56	10.4	0.59
n-dodecylcyclohexane	$ng\ m^{-3}$	18.0 ± 9.8	-11.7	-0.68	11.7	0.68
n-tridecylcyclohexane	$ng\ m^{-3}$	19.6 ± 8.2	-13.5	-0.71	13.5	0.71
n-tetradecylcyclohexane	$ng\ m^{-3}$	20.5 ± 9.5	-14.8	-0.72	14.8	0.72
n-pentadecylcyclohexane	$ng\ m^{-3}$	20.7 ± 8.1	-15.5	-0.75	15.5	0.75
n-octadecane	$ng\ m^{-3}$	116.8 ± 62.9	87.4	0.65	98.8	0.80
n-nonadecane	$ng\ m^{-3}$	96.3 ± 49.4	42.9	0.43	71.8	0.73
n-eicosane	$ng\ m^{-3}$	84.4 ± 37.8	-15.3	-0.15	49.8	0.52
n-heneicosane	$ng\ m^{-3}$	49.1 ± 26.0	-4.1	0.05	32.8	0.61
n-docosane	$ng\ m^{-3}$	32.0 ± 20.0	-9.5	-0.09	19.8	0.58
hopanes	$ng\ m^{-3}$	20.79 ± 47.04	-8.25	2.75	18.6	3.05
steranes	$ng\ m^{-3}$	12.04 ± 31.74	-6.75	1.37	11.5	1.62
docosanoic acid	$ng\ m^{-3}$	3.40 ± 2.91	-2.03	-0.29	2.5	0.76
eicosanoic acid	$ng\ m^{-3}$	4.73 ± 3.01	-3.05	-0.46	3.4	0.69
hexadecanoic acid	$ng\ m^{-3}$	88.37 ± 54.33	-31.81	-0.05	57.8	0.72
hexadecenoic acid	$ng\ m^{-3}$	3.76 ± 1.64	3.26	1.27	4.6	1.58
benzo[a]pyrene	$ng\ m^{-3}$	.19 ± .16	.07	0.33	0.2	1.38

Table 10.9: continued

Compound	units	Observed Ambient Conc.[a] (mean±σ)	Absolute Bias[b]	Normalized Bias[b]	Absolute Gross Error[c]	Normalized Gross Error[c]
acenaphthylene	ng m^{-3}	20.7±26.4	20.3	3.94	27.4	4.14
fluorene	ng m^{-3}	32.0±22.6	-11.9	0.76	15.4	1.64
anthracene	ng m^{-3}	6.6±7.4	-0.3	0.96	5.4	1.30
pyrene	ng m^{-3}	7.6±7.2	15.8	2.77	16.3	2.86
fluoranthene	ng m^{-3}	10.2±7.5	7.9	1.51	11.4	1.85
dehydroabietic acid	ng m^{-3}	.71 ± .97	2.33	11.73	2.3	11.73
n-heptacosane	ng m^{-3}	3.60 ± 1.91	.61	0.70	2.5	1.11
n-octacosane	ng m^{-3}	2.44 ± 1.79	.23	0.78	2.3	1.33
n-nonacosane	ng m^{-3}	4.67 ± 3.03	-1.19	0.37	4.3	1.24
n-triacontane	ng m^{-3}	2.19 ± 1.93	-1.64	-0.48	1.7	0.65
n-hentriacontane	ng m^{-3}	4.52 ± 3.69	-2.88	-0.34	3.6	0.82
n-dotraicontane	ng m^{-3}	1.96 ± 1.81	-1.55	-0.55	1.7	0.71
n-tritriacontane	ng m^{-3}	2.43 ± 2.40	-1.29	-0.02	2.1	0.95
n-tetratriacontane	ng m^{-3}	1.44 ± 1.41	-1.04	-0.26	1.3	0.85
indeno[1,2,3-cd]pyrene	ng m^{-3}	.33 ± .20	.71	2.79	0.7	2.79
indeno[1,2,3-cd]fluoranthene	ng m^{-3}	.14 ± .05	.06	0.31	0.2	1.19
anthracene-9,10-dione	ng m^{-3}	.27 ± .16	.20	1.12	0.4	1.47
hexanedioic acid	ng m^{-3}	7.63 ± 5.24	-6.7	-0.85	6.7	0.85

(a) Statistics computed using measured ambient concentrations at Central Los Angeles, Azusa and Claremont on September 9, 1993.
(b) Absolute ias is calculated as the mean residual concentration (predicted - observed) based on comparison of all individual four-hour average observations to model predictions. Normalized bias values are calculated by normalizing each residual to the corresponding observed concentration before averaging.
(c) Absolute gross error is defined as the mean absolute value of the residuals, with normalized gross error calculated in a manner analogous to the normalized bias.

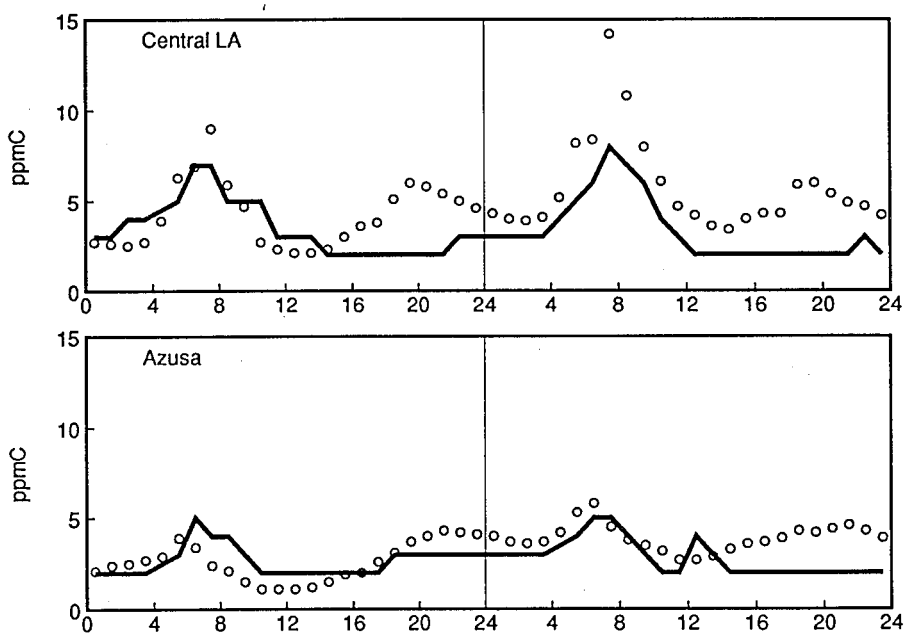

Figure 10.4:
Model predictions (circles) compared to ambient observations (solid line) for carbon monoxide. Ambient observations are from the South Coast Air Quality Management District, and are reported to only one significant digit.

ide provides a useful test of the ability of the airshed model to track the primary emissions and transport of motor-vehicle exhaust-derived pollutants. CO does not react to an appreciable extent over the transport times modeled here. The model predicts that peak concentrations of carbon monoxide occur during the morning traffic peak, as expected.

Figure 10.5 shows the ambient predictions versus measured values of p-ethyltoluene at three sites across the air basin. The data shown were collected during the field experiment described earlier and are plotted as four-hour average values. This example shows the ability of the model to accurately predict the ambient concentrations of compounds that are emitted from emissions sources that have been well characterized. Since the historical focus of hydrocarbon speciation research has been aimed at modeling ozone formation, the emissions sources of volatile organic compounds such as p-ethyltoluene are better understood than is the case for semi-volatile or particle phase organic compounds.

The reaction of aromatic hydrocarbons to form secondary products can be investigated by comparing predicted and measured values of the primary emitted compounds and their known reaction products. One such example is presented in Figure 10.6. Gas-phase photooxidation of toluene and other aromatic hydrocarbons leads to glyoxal and methylglyoxal formation [52, 26]. With the exception of the midafternoon glyoxal concentrations prediction on the first day of the simulation (which may be influenced by initial conditions which are uncertain), primary species and reaction product concentration predictions are reasonably close to observed values. The model, however, does not predict the observed increasing concentrations of the dicarbonyls with advection inland. When peak concentrations are observed at Claremont [18], the model does not accurately capture the observed values.

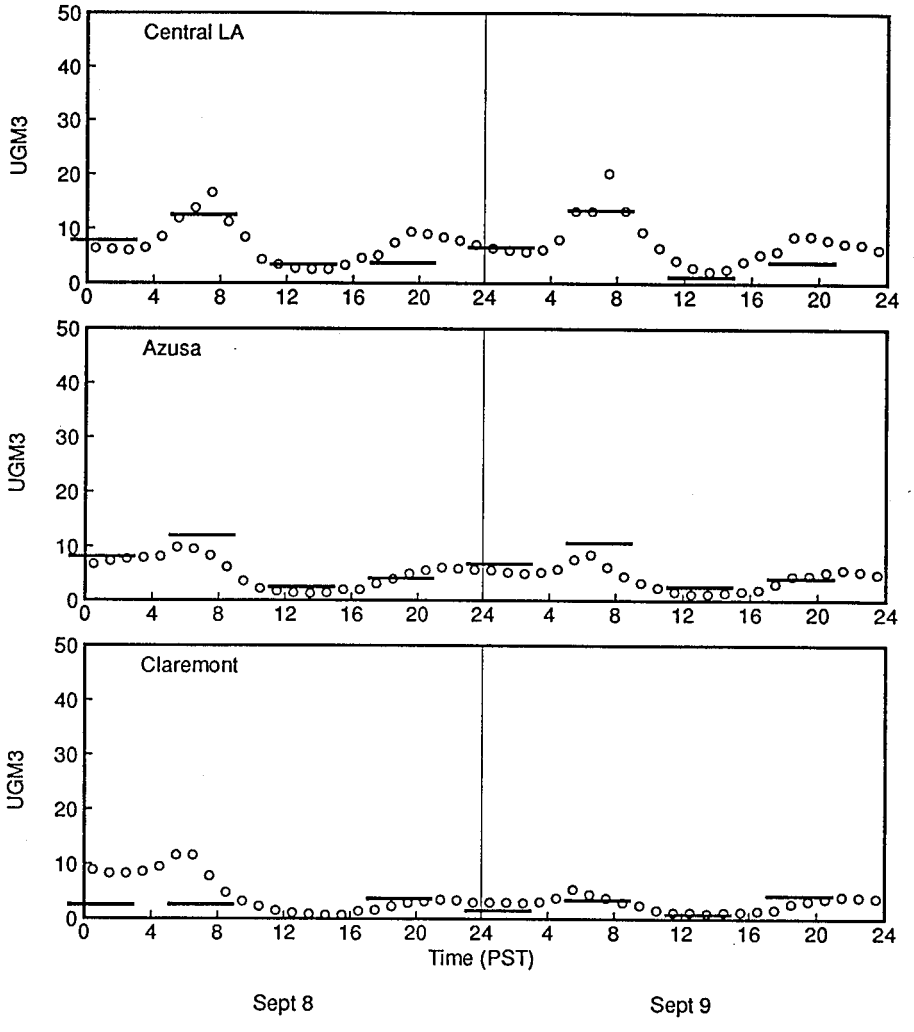

Figure 10.5:
Model predictions (circles) compared to ambient observations (solid lines representing four-hour average samples) for p-ethyltoluene.

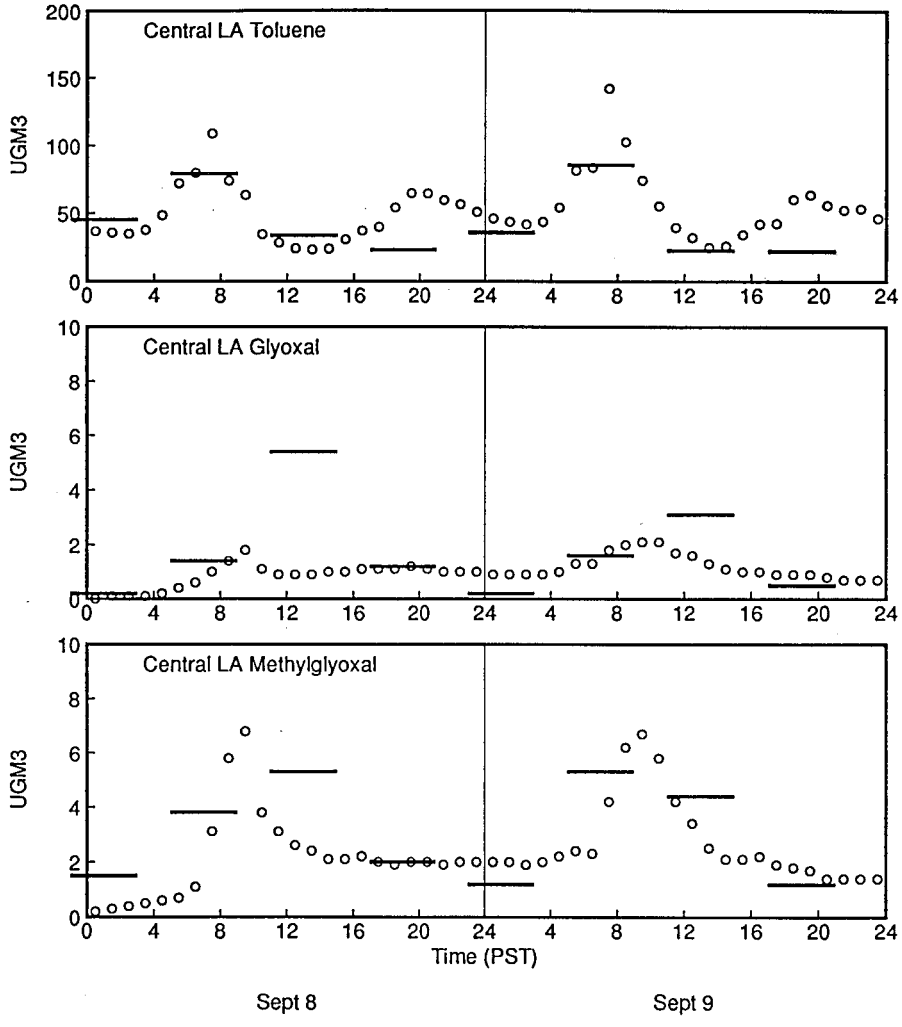

Figure 10.6:
Model predictions (circles) compared to ambient observations (solid lines representing four-hour average samples) for toluene, glyoxal and methylglyoxal at Central Los Angeles.

Figure 10.7 shows model predictions and observations for an olefinic hydrocarbon, 1-hexene. The peak hydrocarbon concentrations that occur during the morning traffic peak are accurately modeled, along with the rapid chemical reactions that lead to ambient concentrations below detection limits during the afternoon photochemically active period.

Figure 10.8 describes model performance for the semi-volatile organic compound phytane. Phytane (or 2,6,10,14-tetramethylhexadecane) is an isoprenoid hydrocarbon present in diesel fuels, and present in emissions from both diesel and, and at a trace level, gasoline-powered vehicles [23, 22]. The emissions of unburned diesel fuel components have not received much attention in the study of urban air pollution. However, measurement of ambient concentrations of isoprenoid hydrocarbons, alkylcyclohexanes and n-alkanes in the distillation range of diesel fuel during the field experiments conducted as part of the present research [20, 21] permits the inclusion of these compounds in this current modeling effort.

The measured and predicted lumped sterane concentrations are shown in Figure 10.9. This category is formed from the sum of 8 individual organic compounds in the homologous series of sterane hydrocarbons. Motor vehicle exhaust emissions have been shown to dominate steranes concentrations in the urban atmosphere [53, 7, 12]. Present in lubricating oils, these compounds are emitted from both diesel and gasoline engines. The model predictions and ambient data for these particle-bound species show peak concentrations at Central Los Angeles during the morning traffic rush hours, accompanied by much lower concentrations in the outlying suburban areas.

The ambient concentrations and model predictions for four organic acids at Central Los Angeles are shown in Figure 10.10. For hexadecanoic acid, numerous primary emissions sources have been identified [54, 46, 49, 48, 45].

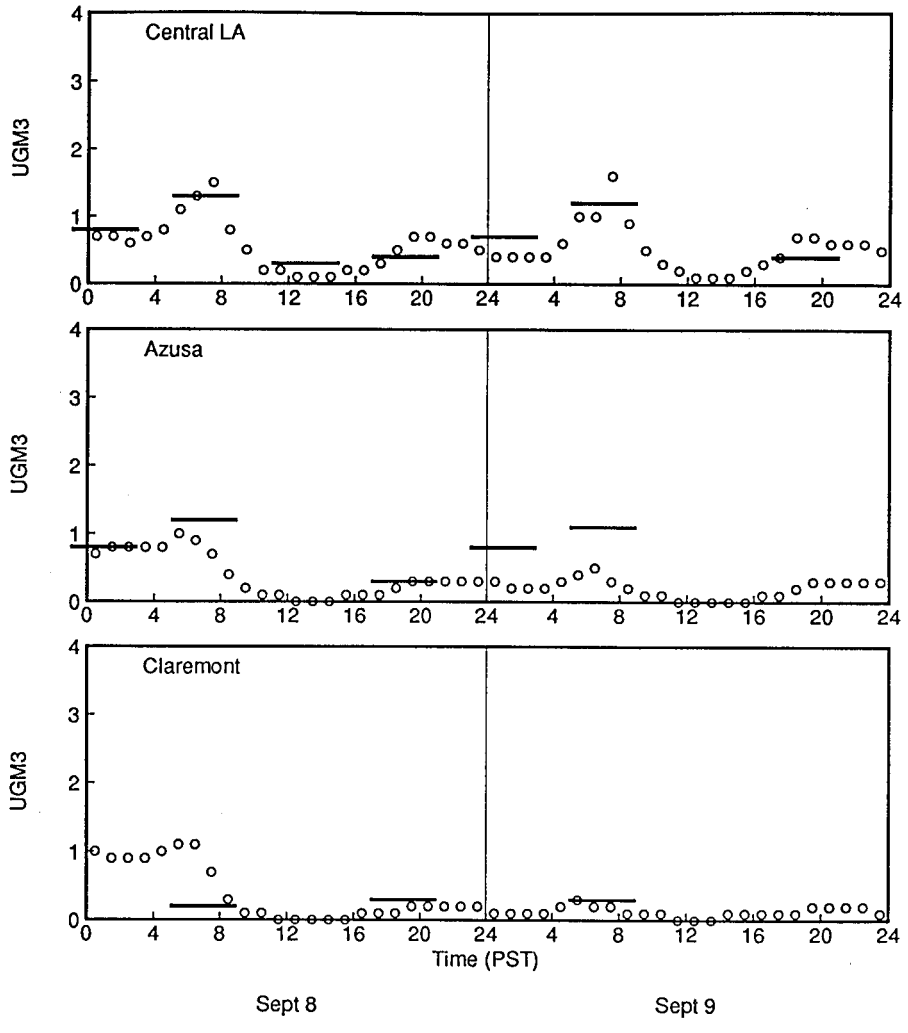

Figure 10.7:
Model predictions (circles) compared to ambient observations (solid lines representing four-hour average samples) for 1-hexene.

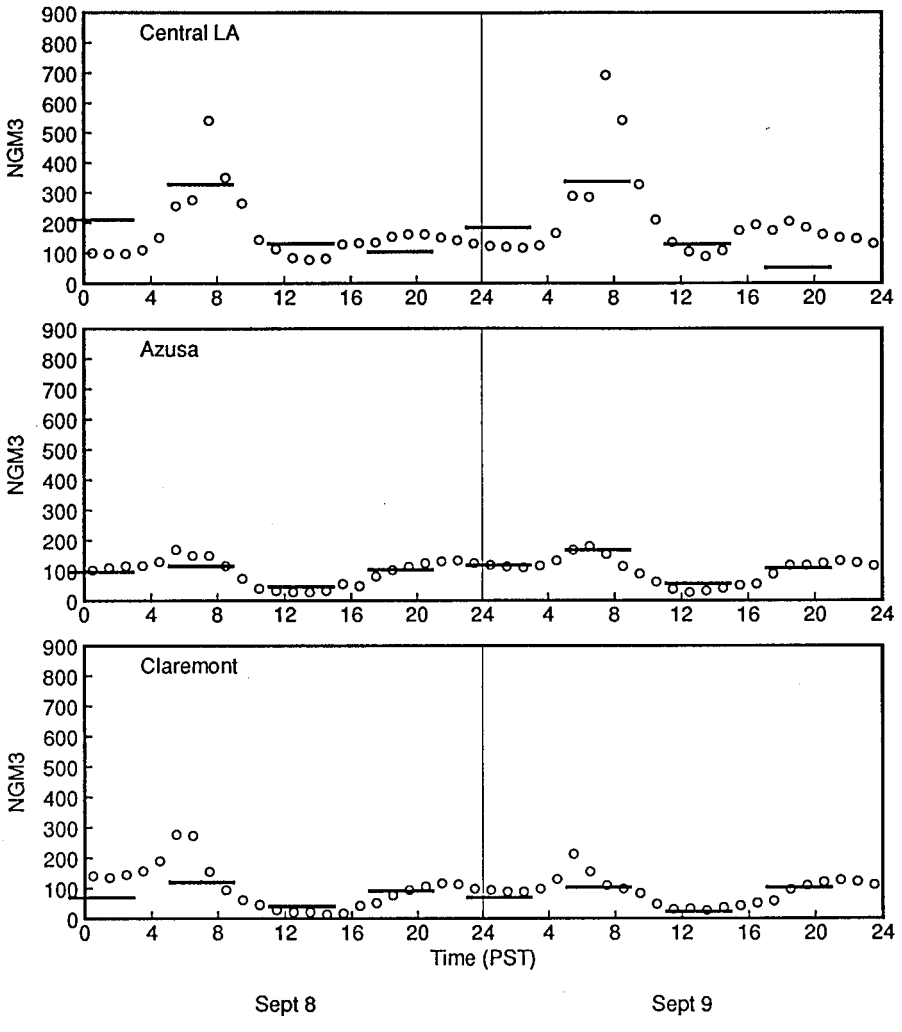

Figure 10.8:
Model predictions (circles) compared to ambient observations (solid lines representing four-hour average samples) for phytane.

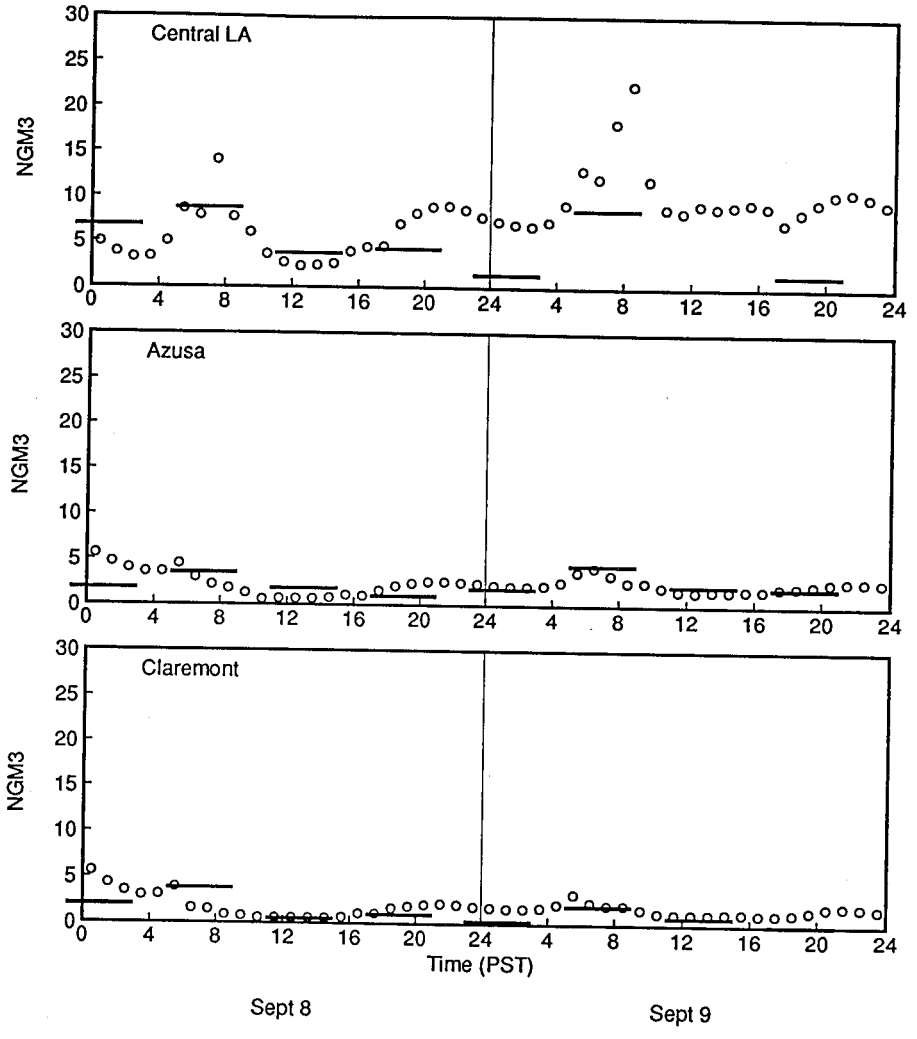

Figure 10.9:
Model predictions (circles) compared to ambient observations (solid lines representing four-hour average samples) for steranes.

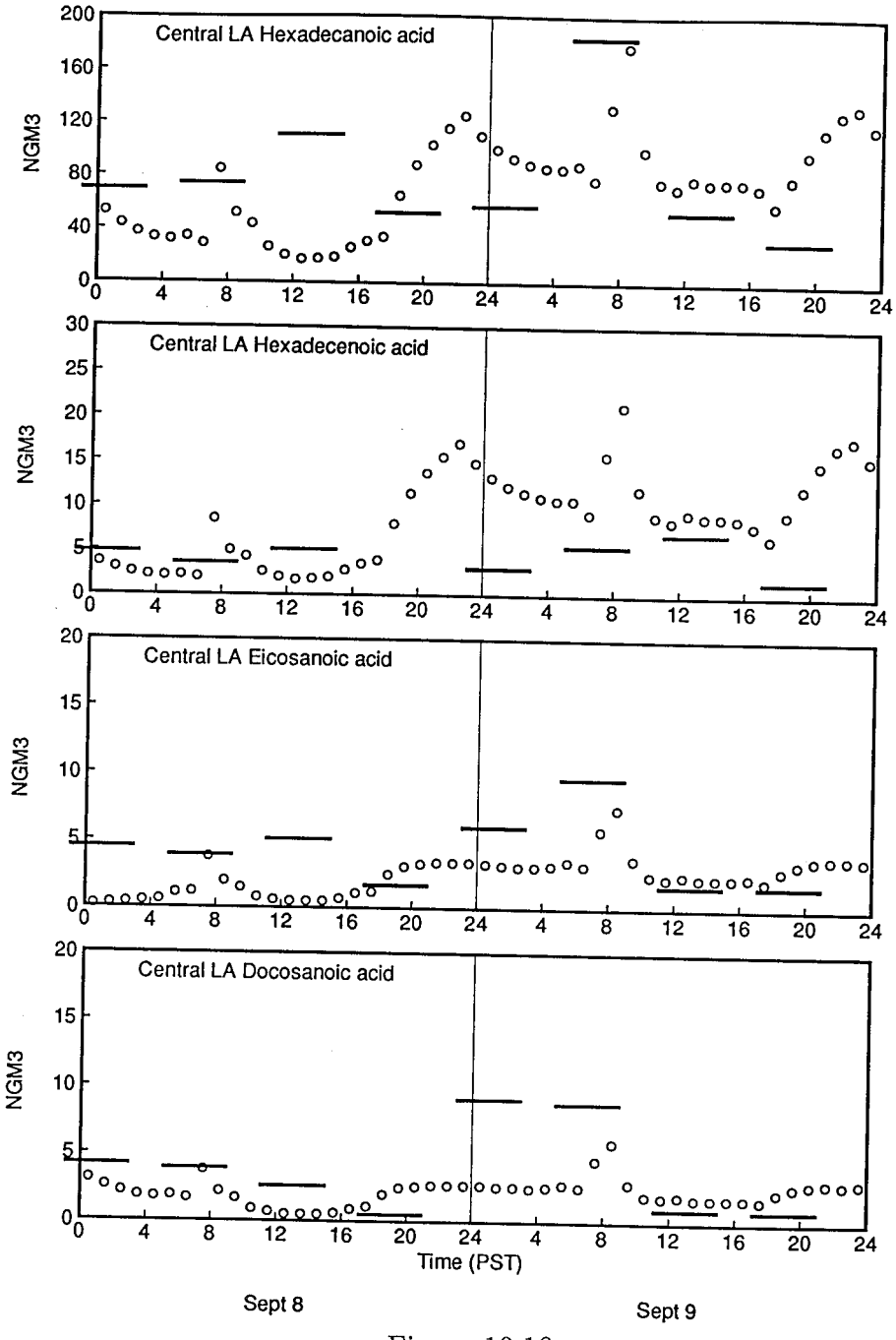

Figure 10.10:
Model predictions (circles) compared to ambient observations (solid lines representing four-hour average samples) for four organic acids at Central Los Angeles.

Overall, the model predicts roughly the correct ambient concentrations, but does not capture the mid-day peak observed on the first day of model application. The unsaturated fatty acid hexadecenoic acid is present in particles emitted from meat-cooking operations [54, 25] and is present at trace levels in paved road dust [46]. This compound has been used as a tracer for the contribution of meat cooking operations to the atmosphere [7, 12]. Hexadecenoic acid concentration predictions are higher than observations late at night, which suggests that the diurnal variation of meat smoke emissions within the SCAQMD emissions inventory should be examined more closely. Model predictions and observations for eicosanoic acid and docosanoic acid also are shown in Figure 10.10. Both eicosanoic and docosanoic acids are present in paved road dust particles [46] and in meat smoke aerosols [54, 25]. Additional emissions of eicosanoic acid are contributed by motor vehicle exhaust [22], wood smoke [45], and tire dusts [47]. In general, the model predicts approximately the correct ambient concentrations of the four primary organic acids depicted in Figure 10.10; additional surveys of area source activity levels for meat smoke, road dust and other fugative sources should be conducted to help refine the diurnal variation of the emissions from the most important sources of primary organic acids.

Bibliography

[1] National Research Council. *Rethinking the ozone problem in urban and regional air pollution.* National Academy Press, Washington, D.C., 1991.

[2] A. G. Russell, K. F. McCue, and G. R. Cass. Mathematical modeling of the formation of nitrogen-containing pollutants — 1. Evaluation of an Eulerian photochemical model. *Environ. Sci. Technol.*, 22:263–271, 1988.

[3] Z. Meng, D. Dabdub, and J. H. Seinfeld. Chemical coupling between atmospheric ozone and particulate matter. *Science*, 277:116–119, 1997.

[4] S. N. Pandis, R. A. Harley, G. R. Cass, and J. H. Seinfeld. Secondary organic aerosol formation and transport. *Atmos. Environ.*, 26A:2269–2282, 1992.

[5] S. N. Pandis, A. S. Wexler, and J. H. Seinfeld. Secondary organic aerosol formation and transport. II. Predicting the ambient secondary organic aerosol size distribution. *Atmos. Environ.*, 27A:2403–2416, 1993.

[6] F. W. Lurmann, A. S. Wexler, S. N. Pandis, S. Musarra, N. Kumar, and J. H. Seinfeld. Modelling urban and regional aerosols. II. Application to California's South Coast Air Basin. *Atmos. Environ.*, 31:2695–2715, 1997.

[7] W. F. Rogge, L. M. Hildemann, M. A. Mazurek, G. R. Cass, and B. R. T. Simoneit. Mathematical modeling of atmospheric fine particle-

associated primary organic compound concentrations. *J. Geophys. Res.*, 101:19373–19394, 1996.

[8] G. J. McRae, W. R. Goodin, and J. H. Seinfeld. Development of a second-generation mathematical model for urban air pollution — I. Model formulation. *Atmos. Environ.*, 16:679–696, 1982.

[9] G. J. McRae, W. R. Goodin, and J. H. Seinfeld. Development of a second-generation mathematical model for urban air pollution — II. Model evaluation. *Atmos. Environ.*, 17:501–522, 1983.

[10] R. A. Harley, A. G. Russell, G. J. McRae, G. R. Cass, and J. H. Seinfeld. Photochemical modeling of the Southern California Air Quality Study. *Environ. Sci. Technol.*, 27:378–388, 1993.

[11] R. A. Harley and G. R. Cass. Modeling the concentrations of gas-phase toxic organic air pollutants: direct emissions and atmospheric formation. *Environ. Sci. Technol.*, 28:88–98, 1993.

[12] J. J. Schauer, W. F. Rogge, L. M. Hildemann, M. A. Mazurek, G. R. Cass, and B. R. T. Simoneit. Source apportionment of airborne particulate matter using organic compounds as tracers. *Atmos. Environ.*, 30:3837–3855, 1996.

[13] R. A. Harley and G. R. Cass. Modeling the atmospheric concentrations of individual volatile organic compounds. *Atmos. Environ.*, 29:905–922, 1995.

[14] J. R. Odum, T. P. Jungkamp, R. J. Griffin, H. J. L. Forstner, R. C. Flagan, and J. H. Seinfeld. Aromatics, reformulated gasoline and atmo-

spheric organic aerosol formation. *Environ. Sci. Technol.*, 31:1890–1897, 1997.

[15] C. Pilinis and J. H. Seinfeld. Development and evaluation of an eularian photochemical gas-aerosol model. *Atmos. Environ.*, 22:1985–2001, 1988.

[16] B. R. T. Simoneit. Application of molecular marker analysis to vehicular exhaust for source reconciliations. *Intern. J. Environ. Anal. Chem.*, 22:203–233, 1985.

[17] M. P. Fraser, D. Grosjean, E. Grosjean, R. A. Rasmussen, and G. R. Cass. Air quality model evaluation data for organics. 1. Bulk chemical composition and gas/particle distribution factors. *Environ. Sci. Technol.*, 30:1731–1743, 1996.

[18] E. Grosjean, D. Grosjean, M. P. Fraser, and G. R. Cass. Air quality model evaluation data for organics. 2. C_1 – C_{14} carbonyls in Los Angeles air. *Environ. Sci. Technol.*, 30:2687–2703, 1996.

[19] E. Grosjean, D. Grosjean, M. P. Fraser, and G. R. Cass. Air quality model evaluation data for organics. 3. Peroxyacetyl nitrate and peroxypropionyl nitrate in Los Angels air. *Environ. Sci. Technol.*, 30:2704–2714, 1996.

[20] M. P. Fraser, G. R. Cass, B. R. T. Simoneit, and R. A. Rasmussen. Air quality model evaluation data for organics. 4. C2-C36 non-aromatic hydrocarbons. *Environ. Sci. Technol.*, 31:2356–2367, 1997c.

[21] M. P. Fraser, G. R. Cass, B. R. T. Simoneit, and R.A. Rasmussen. Air quality model evaluation data for organics. 5. C6-C22 non-polar and

semi-polar aromatic hydrocarbons. *submitted for publication in Environ. Sci. Technol.*, 1997b.

[22] J. J. Schauer, M. J. Kleeman, G. R. Cass, and B. R. T. Simoneit. Measurement of emissions from air pollution sources. 4.C1 through C29 organic compounds from gasoline powered motor vehicles. *to be submitted to Environ. Sci. Technol.*, 1997.

[23] J. J. Schauer, M. J. Kleeman, G. R. Cass, and B. R. T. Simoneit. Measurement of emissions from air pollution sources. 3.C1 through C29 organic compounds from medium duty diesel trucks. *to be submitted to Environ. Sci. Technol.*, 1997.

[24] J. J. Schauer, M. J. Kleeman, G. R. Cass, and B. R. T. Simoneit. Measurement of emissions from air pollution sources. 7.C1 through C14 organic compounds from spray coating operations. *to be submitted to Environ. Sci. Technol.*, 1997.

[25] J. J. Schauer, M. J. Kleeman, G. R. Cass, and B. R. T. Simoneit. Measurement of emissions from air pollution sources. 1.C1 through C29 organic compounds from meat charbroiling. *to be submitted to Environ. Sci. Technol.*, 1997.

[26] W. P. L. Carter. A detailed mechanism for the gas–phase atmospheric reactions of organic compounds. *Atmos. Environ.*, 24A:481–518, 1990.

[27] R. Atkinson and S. M. Aschmann. Kinetics of the reactions of acenaphthene and acenaphthylene and structurally-related aromatic compounds with OH and NO_3 radicals, N_2O_5, and O_3 at 296±2K. *Inter. J. Chem. Kin.*, 20:513–539, 1988.

[28] E. S. C. Kwok, R. Atkinson, and J. Arey. Kinetics of the gas-phase reactions of fluorene and 9,10-dihydroxyanthracene with OH radicals, NO_3 radicals and O_3. *Inter. J. Chem. Kin.*, 27:299–309, 1997.

[29] E. S. C. Kwok, J. Arey, and R. Atkinson. Gas-phase atmospheric chemistry of dibenzo-p-dioxin and dibenzofuran. *Environ. Sci. Technol.*, 28:528–533, 1994.

[30] H. W. Biermann, H. MacLeod, R. Atkinson, A. W. Winer, and J. N. Pitts. Kinetics of the gas-phase reactions of the hydroxyl radical with naphthalene, phenanthrene and antracene. *Environ. Sci. Technol.*, 19:244–248, 1985.

[31] R. Atkinson, J. Arey, B. Zielinska, and S. M. Aschmann. Kinetics and nitro-products of the gas-phase OH and NO_3 radical initiated reactions of naphthalene-d8, fluoranthene-d8 and pyrene. *Inter. J. Chem. Kin.*, 22:999–1014, 1990.

[32] W. P. L. Carter. Computer modeling of environmental chamber studies of maximum incremental reactivities of volatile organic compounds. *Atmos. Environ.*, 29:2513–2527, 1995.

[33] M. J. Kleeman, A. Eldering, and G. R. Cass. Modeling the airborne particle complex as a source-orientated external mixture. *J. Geophys. Res.*, 102(D17):21355–21372, 1997.

[34] W. R. Goodin, G. J. McRae, and J. H. Seinfeld. A comparison of interpolation methods for sparse data: application to wind and concentration fields. *J. Applied Met.*, 18:761–771, 1979.

[35] D. Wolfe, B. Weber, D. Wuertz, D. Welsh, D. Merritt, S. King, R. Fritz, K. Moran, M. Simon, A. Simon, J. Cogan, D. Littell, and E. Measure. An overview of the Mobile Profiler System: preliminary results from field tests during the Los Angeles Free Radical Study. *Bull. Amer. Meteor. Soc.*, 76:523–534, 1995.

[36] W. R. Goodin, G. J. McRae, and J. H. Seinfeld. An objective analysis technique for constructing three-dimensional urban-scale wind fields. *J. Applied Met.*, 19:98–108, 1980.

[37] G. C. Holtzworth. Mixing depths, wind speeds and air pollution potential for selected locations in the United States. *J. Applied Met.*, 6:1039–1044, 1967.

[38] M. N. Ingalls. On–road vehicle emission factors from measurements in a Los Angeles area tunnel. 1989. Paper No. 89-137.3, presented at the Air and Waste Management Association 82nd Annual Meeting.

[39] W. R. Pierson, A. W. Gertler, and R. L. Bradow. Comparison of the SCAQS tunnel study with other on–road vehicle emission data. *J. Air Waste Manage. Assoc.*, 40:1495–1504, 1990.

[40] M. P. Fraser, G. R. Cass, and B. R. T. Simoneit. Gas-phase and particle-phase organic compounds emitted from motor vehicle traffic in a Los Angeles highway tunnel. *submitted for publication in Environ. Sci. Technol.*, 1997a.

[41] R. A. Harley, M. P. Hannigan, and G. R. Cass. Respeciation of organic gas emissions and the detection of excess unburned gasoline in the atmosphere. *Environ. Sci. Technol.*, 26:2395–2408, 1992.

[42] A. Eldering and G. R. Cass. Source-orientated model for air pollutant effects on visibility. *J. Geophys. Res.*, 102(D14):19343–19369, 1997.

[43] L. M. Hildemann, G. R. Markowski, M. C. Jones, and G. R. Cass. Submicrometer aerosol mass distributions of emissions from boilers, fireplaces, automobiles, diesel trucks, and meat–cooking operations. *Aerosol Sci. Technol.*, 14:138–152, 1991b.

[44] L. M. Hildemann, G. R. Markowski, and G. R. Cass. Chemical composition of emissions from urban sources of fine organic aerosol. *Environ. Sci. Technol.*, 25:744–759, 1991a.

[45] J. J. Schauer, M. J. Kleeman, G. R. Cass, and B. R. T. Simoneit. Measurement of emissions from air pollution sources. 5.C1 through C14 organic compounds from fireplace combustion of wood. *to be submitted to Environ. Sci. Technol.*, 1997.

[46] J. J. Schauer. California Institute of Technology, Pasadena, CA, 1997.

[47] W. F. Rogge, L. M. Hildemann, M. A. Mazurek, G. R. Cass, and B. R. T. Simoneit. Sources of fine organic aerosol 3. Road dust, tire debris and organometallic brake lining dust: roads as sources and sinks. *Environ. Sci. Technol.*, 27:1892–1904, 1993.

[48] W. F. Rogge, L. M. Hildemann, M. A. Mazurek, G. R. Cass, and B. R. T. Simoneit. Sources of fine organic aerosol 5. Natural gas home appliances. *Environ. Sci. Technol.*, 27:2736–2744, 1993.

[49] W. F. Rogge, L. M. Hildemann, M. A. Mazurek, G. R. Cass, and B. R. T. Simoneit. Sources of fine organic aerosol 4. Particulate abrasion products

from leaf surfaces of urban plants. *Environ. Sci. Technol.*, 27:2700–2711, 1993.

[50] D. A. Winner, G. R. Cass, and R. A. Harley. Effect of alternative boundary conditions on predicted ozone control strategy performance: A case study in the Los Angeles area. *Atmos. Environ.*, 29:3451–3464, 1995.

[51] W. John, S. M. Wall, J. L. Ondo, and W. Winklmayr. Acidic aerosol size distributions during SCAQS. 1990. Report to the California Air Resources Board under contract A6-112-39.

[52] R. Atkinson, W. P. L. Carter, K. R. Darnall, A. M. Winer, and J. N. Pitts. A smog chamber and modeling study of the gas phase NOx-air photooxidation of toluene and cresols. *Inter. J. Chem. Kin.*, 12:779–836, 1989.

[53] B. R. T. Simoneit. Characterization of organic-constitutents in aerosols in relation to their origin and transport- a review. *Intern. J. Environ. Anal. Chem.*, 23:207–237, 1986.

[54] W. F. Rogge, L. M. Hildemann, M. A. Mazurek, G. R. Cass, and B. R. T. Simoneit. Sources of fine organic aerosol 1. Charbroilers and meat cooking operations. *Environ. Sci. Technol.*, 27:1112–1125, 1991.

11 Conclusion

11.1 Summary

Field experiments and atmospheric models have been used to explore the relationship between air pollutant source emissions and ambient air quality for individual organic compounds. The approach taken is to view the distribution of organic compounds in the atmosphere not as containing separate groups of gas and particle phase species, but rather to view organic air pollutants as a continuum, ranging in carbon number from C_1 through polymeric material that changes progressively from solely gas phase substances through semi-volatile organics that exist simultaneously in both the gas and particle phases to purely particulate organics at higher molecular weights. In the present work C_1 - C_{36} organics are examined in great detail. Methods developed are demonstrated by characterizing the emissions/air quality relationships for organic air pollutants during a severe photochemical smog episode in Los Angeles during September, 1993.

11.1.1 Experimental Program

During the period of September 8-9, 1993, the South Coast Air Basin that surrounds Los Angeles experienced the worst photochemical smog episode in recent years; ozone concentrations exceeded 0.29 ppm one-hour average and NO_2 concentrations peaked at 0.21 ppm one-hour average. Field measurements were conducted at a five-station air monitoring network to obtain comprehensive data on the identity and concentration of the individual or-

ganic compounds present in both the gas and particle phases during that episode. The data were taken according to an experimental design that serves to support tests of air quality models designed to study organic air pollutant transport and reaction. Air samples taken in stainless steel canisters were analyzed for 141 volatile organic compounds by GC/ECD, GC/FID and GC/MS; PAN and PPN were measured by GC/ECD; particulate organics collected by filtration were analyzed for total organic and elemental carbon by thermal evolution and combustion and for individual organic compounds by GC/MS; semi-volatile organics were analyzed by GC/MS after collection on polyurethane foam cartridges.

At the farthest downwind site studied, Claremont, extensive modification of primary pollutants by atmospheric chemical reactions was evident during the peak photochemical smog period: vapor-phase olefins and aromatics were depleted, the majority of the nitrogen-containing pollutants were present as organic plus inorganic nitrates, the fraction of organics in the particle phase rose to 12.5% (versus 2.6%-5.4% at the coast), one fourth of the pollutant-derived nitrogen was in the particle phase, and nearly all of the Cl^- had been removed from the particle phase. Of the total nitrate measured at Claremont, on average only 33.6% was present as organic nitrates, which is a much lower ratio of organic nitrate to total nitrate than has been seen in previous years.

11.1.2 PAN, PPN and Carbonyls

Ambient levels of peroxyacetyl nitrate (PAN, $CH_3C(O)OONO_2$) and peroxypropionyl nitrate (PPN, $CH_3CH_2C(O)OONO_2$) were measured during the 2-week period August 28 - September 13, 1993, at four locations in the urban Southern California area. Highest concentrations recorded were 9.9 ppb for PAN and 1.5 ppb for PPN. Diurnal and spatial variations were consis-

tent with photochemical production with eastward (inland) transport. The amount of PAN lost due to thermal decomposition near the time of the daily ozone peak was calculated and was found to be comparable in magnitude to the PAN concentration remaining in the atmosphere. PAN decomposition thus is a major source of NO_2 and radical species that have the capability to increase ozone concentrations near the time of the daily ozone peak.

Twenty-three carbonyls were identified and their concentrations measured: 14 aliphatic aldehydes (from formaldehyde to tetradecanal), two aromatic aldehydes (benzaldehyde and m-tolualdehyde), three ketones (acetone, 2-butanone, and cyclohexanone), one unsaturated carbonyl (crotonaldehyde) and three dicarbonyls (glyoxal, methylglyoxal, and biacetyl). Another ten carbonyls were tentatively identified. Formaldehyde (urban average concentration 5.3 ppb), acetaldehyde, and acetone accounted for 24%, 18% and 7%, respectively, of the total carbonyls on a ppbV basis. The nine high molecular weight carbonyls (C_8 - C_{14}) accounted for 11-14% of the total carbonyls. Ranking of the measured carbonyls with respect to removal of the hydroxyl radical showed acetaldehyde to be the most important followed by formaldehyde and nonanal. It was discovered that the high molecular weight aldehydes (those heavier than acetaldehyde) that are seldom measured in either the atmosphere or source emissions are collectively as important to atmospheric chemical reactivity as is the case for formaldehyde or acetaldehyde individually.

11.1.3 C_2 to C_{36} Non-Aromatic Hydrocarbons

The concentrations of 143 non-aromatic hydrocarbons were quantified during the Los Angeles area photochemical smog episode studied. Gas phase, semivolatile and particle phase organic compounds were viewed simultane-

ously across the carbon number range from C_2 to C_{36}. Compound classes studied included the *n*-alkanes, branched alkanes, *n*-alkenes, branched alkenes, diolefins, alkynes, saturated cyclic hydrocarbons, unsaturated cyclic hydrocarbons, biogenic hydrocarbons, petroleum biomarkers, and the unresolved complex mixture contained within the semivolatile and particle-phase organics samples. The abundance of the *n*-alkanes declines almost exponentially with increasing *n*-alkane carbon number, and the distribution of the *n*-alkanes between the gas and particle phase followed vapor/particle partitioning theory. The concentrations of individual low molecular weight alkenes declined during transport across the urban area in about the order expected given their initial rates of reaction with the hydroxyl radical. The most pronounced change found in non-aromatic hydrocarbons concentrations between historical data and the current study was a reduction in the concentration of the lightest blending components of gasoline (e.g., butanes), which reflected new regulations that limit the Reid vapor pressure of gasoline.

11.1.4 C_6 to C_{22} Non-polar and Semi-polar Aromatic Compounds

The concentrations of 86 vapor-phase, semivolatile, and particle-phase aromatic compounds were measured in the Southern California atmosphere. Compound classes formed by grouping all aromatic hydrocarbons having the same number of aromatic rings showed progressively declining concentrations as the number of aromatic rings increased. Examination of the partitioning of the polycyclic aromatic hydrocarbons (PAH) between the gas and particle phases showed the transition from purely gaseous PAH at low molecular weight to purely particle-phase PAH at high molecular weight, with compounds such as the mutagen cyclopenta[cd]pyrene present about equally in both gas and particle phases. Primary aromatics, both the vapor-

phase mono-aromatics and the PAH, showed evidence of depletion by atmospheric chemical reaction over downwind transport with apparent depletion rates generally increasing as the degree of substitution of the aromatic rings increased. In contrast, many nitro-PAH and some oxy-PAH accumulated during downwind transport, consistent with their likely formation as products of atmospheric chemical reactions. Historical data generally showed that aromatics concentrations declined substantially from the 1950's to the 1980's, but that concentrations measured during the present 1993 experiment are similar to those measured during the mid-1980's including the August episode of the 1987 Southern California Air Quality Study (SCAQS) experiment. The present experiment provided baseline data prior to the introduction of California Phase II reformulated gasoline that can be used in future years to examine the effect of the reduced aromatic content of that Phase II gasoline.

11.1.5 Organic Acids

The atmospheric concentrations of 46 semi-volatile vapor phase and particle phase organic acids were quantified during a severe Los Angeles area photochemical smog episode. Compound classes studied include C_8 and higher n-alkanoic acids, alkenoic acids, alkanedioic acids, benzene monocarboxylic acids, benzene polycarboxylic acids, one polycarboxylic aromatic dicarboxylic acid, and resin acids. Analysis of these data suggest that the concentrations of different acids are governed by different atmospheric processes. Benzoic acid, phthalic acid and octanedioic acid display temporal and spatial patterns that suggest that secondary formation by chemical reaction during atmospheric transport across the Los Angeles basin dominates local concentrations. Benzene dicarboxylic acids other than phthalic acid

(e.g., 1,3- and 1,4-benzene dicarboxylic acids) track the concentrations of petroleum biomarkers in the urban atmosphere suggesting that direct emissions from motor vehicle exhaust dominate their ambient concentrations. Low molecular weight aliphatic dicarboxylic acids (e.g., propanedioic acid, butanedioic acid and hexanedioic acids) are found in background air at San Nicolas Island upwind of Los Angeles at 44%-76% of the concentrations measured in the urban atmosphere, suggesting that these diacids are contributed in part either by long range transport of polluted air, or by marine sources, or by atmospheric oxidation of natural background hydrocarbons.

11.1.6 Organic Compounds Emitted from Motor Vehicle Traffic

The emission rates for 221 vapor-phase, semivolatile, and particle-phase organic compounds from motor vehicles, plus fine particulate matter mass and some inorganic particle-phase species, were calculated based on measurements made inside and outside a Los Angeles roadway tunnel. These emission rates were calculated based on fuel consumption to remove any uncertainties based on tunnel dilution rates or air circulation. The results showed carbon monoxide emissions rates of 130 g per liter of gasoline-equivalent fuel burned and volatile organic compound (VOC) emissions of 9.1 g l^{-1}. These values were higher than predicted by the baseline version of California's EMFAC 7G emissions inventory program but were within the range of 108 ± 25 g l^{-1} CO reported by roadside remote sensing studies in Los Angeles [1]. When the VOC emissions composition in the tunnel is compared to that of tailpipe emissions source test data and to the composition of additional unburned whole gasoline, the tunnel atmosphere is found to be consistent with a linear combination of these major contributors over a fairly broad range of about 74% to 97% vehicle exhaust depending on the tailpipe profiles used. Fine

particulate emissions within the tunnel consisted largely of carbonaceous material accompanied by a significant amount of ammonium nitrate apparently formed by gas-to-particle conversion processes within the tunnel atmosphere. Certain gas-phase and particulate organic compounds traditionally thought to be the secondary products of atmospheric chemical reactions were enriched inside the tunnel, and from this enrichment, the primary emission rates of aromatic alcohols, aliphatic dicarboxylic acids, and aromatic polycarboxylic acids were calculated. Petroleum biomarkers (e.g., hopanes and steranes) emissions rates were measured in the tunnel so that they could be used as tracers to estimate primary vehicle exhaust fine particulate matter concentrations in the urban atmosphere.

11.1.7 Detection of Excess Ammonia Emissions from In-Use Vehicles

The emission rate for ammonia from in-use vehicles was calculated based on measurements made inside the Los Angeles roadway tunnel. Using fleet distributions by vehicle age and type, known catalyst distributions and fuel economy by model year and vehicle type, and attributing all ammonia to vehicles equipped with three-way catalysts or three-way catalysts plus oxidizing catalysts (dual-bed catalysts), an average ammonia emission rate of 72 mg km^{-1} was estimated for these vehicles, or 61 mg km^{-1} driven by the vehicle fleet as a whole. These emissions can emanate from vehicles running under rich air-fuel conditions, with three-way catalytic converters designed to reduce NO_x to N_2 and O_2 in addition forming NH_3, which will lead to increased emissions of ammonia from vehicle traffic as fleet turnover causes newer vehicles equipped with three-way catalysts to replace older pre-catalyst vehicles or oxidation-only catalyst vehicles. Resulting calculations estimated

ammonia emissions of 24-29 metric tons NH_3 per day from the vehicle fleet for the South Coast Air Basin (SoCAB) that surrounds Los Angeles. This represented an increase in the daily emissions of ammonia attributable to motor vehicles in the SoCAB from 2% of basin-wide emissions before the introduction of catalyst-equipped automobiles to 15% based on the current experiment. The air basin-wide emission rate of ammonia from motor vehicles was compared to ammonia emissions from livestock waste decomposition at local dairies, and the implications for control of fine particle ammonium nitrate concentrations were discussed.

11.1.8 Motor Vehicle Exhaust in the Urban Atmosphere

The emission rate of particle-phase petroleum biomarkers in vehicular exhaust was compared to the concentrations of these biomarkers in ambient air. From this comparison, the particulate organic compound concentration due to primary particle emissions from motor vehicles in the Southern California atmosphere was determined. A material balance on the organic particulate matter emitted from motor vehicle traffic in a Los Angeles highway tunnel first was constructed to show the proportion which was solvent-extractable and which will elute from a GC column, the ratio of resolved to unresolved compound mass, the portion of the resolved material that can be identified as single organic compounds, and the contribution of different classes of organic compounds to the overall identified fraction. It was shown that the outdoor ambient concentrations of the petroleum biomarkers track primary emissions measured in the highway tunnel, confirming that direct emissions of these compounds from vehicles govern the observed ambient petroleum biomarker concentrations. Using organic chemical tracer techniques, the portion of fine organic particulate matter in the Los Angeles atmosphere which

is attributable to direct particle emissions from vehicle exhaust is calculated to vary from 7.5% to 18.3% at different sites throughout the air basin during a summertime severe photochemical smog episode. A similar level of variation in the contribution of primary motor vehicle exhaust to fine particulate organic matter concentrations during different times of day was seen. While peak atmospheric concentrations of fine particulate organic carbon were observed during the 1200-1600 PDT afternoon sampling period, only 6.3% of that material was apportioned to the directly emitted particles from vehicle exhaust. During the morning traffic peak between 0600-1000 PDT, 19.1% of the fine particulate organic material was traced to primary emissions from motor vehicles.

11.1.9 Modeling the Atmospheric Concentrations of Individual Organic Compounds

An Eularian photochemical airshed model was adapted to track the concentrations of individual vapor-phase, semi-volatile and particle-phase compounds over the carbon number range from C_1 to C_{34}. The model incorporates primary emissions of organic gases and particles from sources based on recent source tests conducted specifically to support this model development effort. These emissions are processed through a photochemical airshed model whose chemical mechanism has been expanded to explicitly follow the reaction or formation of 125 individual vapor-phase organic compounds plus 11 lumped compound groups. Primary organic compounds in the particle phase can be disaggregated at will from a lumped primary organic compound category; in the present model application, 31 individual primary particulate organic compounds are tracked as they are transported from sources to receptor air monitoring sites. The model is applied to study air quality relationships

for organics in California's South Coast Air Basin that surrounds Los Angeles during the severe photochemical smog episode that occurred on September 8-9, 1993. The ambient concentrations of all normal alkanes and most aromatic hydrocarbons are predicted within the correct order of magnitude over 6 orders of magnitude concentration change from most abundant gas-phase to least abundant particulate species studied. A formal evaluation of model performance shows that, with the exception of a few outliers, the concentrations of over 100 organic compounds studied were reproduced with an average bias of $\pm 58\%$ and with roughly equal numbers of compounds underpredicted (42) versus overpredicted (62). The time series of observed aromatic hydrocarbons concentrations are reproduced closely, production of methylglyoxal from aromatic precursors is tracked, olefinic hydrocarbons such as 1-hexene decline dramatically in concentration due to chemical reaction and dilution during downwind transport as is observed in the ambient monitoring data base. This ability to simultaneously account for the concentrations of individual gas-phase and particulate organic compounds lays a foundation for future calculations of secondary organic aerosol formation and gas/particle repartitioning in the atmosphere.

11.2 Suggestions for Future Research

The semi-volatile organic compound concentrations reported here in many cases provide the first description of the atmospheric behavior of compounds of this type. These data now exist in one city for a two day period during an extreme photochemical smog episode. Much further work is needed to characterize the conditions that occur in other urban, rural and remote locations, and during other seasons of the year. In the course of that future work, opportunities exist to improve the atmospheric measurement technol-

ogy used during the experiments reported here. The apparent distribution of semi-volatile organics between the gas and particle phases can be distorted by sampling artifacts if gas phase organics adsorb to the surface of quartz fiber filters used in this work before they can be collected on the sorbent beds (PUF cartridges) that follow the filters in the present experiments. To reduce this potential problem, diffusion denuder technology should be developed to the level where it is practical for use in experiments that must operate over short (e.g., four-hour) consecutive sampling intervals at a network of air monitoring sites. In such denuders, semi-volatile organic vapors would be removed by diffusion to sorbent-coated surfaces upstream of the particle filter, while a sorbent trap downstream of the particle filter would capture any semi-volatile particulate organics that evaporate from the filter. Such systems presently exist [2, 3]. The challenge is to design and produce them inexpensively. At present cost is a serious barrier to deploying hundreds of expendable denuder cartridges within a typical field campaign because such denuder/filter/sorbent bed systems can cost thousands of dollars each.

Beyond improvements to sample collection methods, advances can be made in the chemical analysis methods used in the present study. Hundreds of organic compounds have been quantified in the gas and particle phases in this work. The low molecular weight gaseous species analyses conducted here do account for an overwhelming majority of the gas phase organic material in the atmosphere. But in the particle phase, while total carbon can be measured completely, the individual organic compounds identified at the molecular level account for a small fraction of the organic compound mass that is present. Methods for further characterization of the remaining particulate organic compounds are needed, especially for the highly polar or polymeric organics that do not dissolve in the solvent systems used in the

present work or that will not pass through the chromatographic columns used here.

The air quality model developed as part of this research represents the first use of an Eulerian photochemical airshed model to simultaneously transport both gas phase, semi-volatile and particle phase organic compounds that are described at the single organic compound level. This is the level of detail ultimately needed to support accurate calculations of reactant/reaction product relationships and gas/particle repartitioning of the reaction products. Separate methods recently have been developed by others for modeling the gas-phase photochemical production of low vapor pressure reaction products and their partitioning into the particle phase [4, 5], but with less detailed description of the primary semi-volatile and particulate organic matter emissions and their ability to repartition in the atmosphere than is contained in the airshed model developed in the present research. This separate knowledge of primary plus secondary organic compound behavior can be combined in the future into a more complete treatment of the overall problem.

Air quality models are powerful tools in the investigation of the likely effect of proposed air quality improvement plans. With the level of detail described in the airshed model presented here, it is possible to evaluate the effect of different proposed emissions control programs on the concentrations of many toxic organic compounds in the ambient atmosphere (e.g., benzene, PAH, aldehydes, nitroaromatics). Further, recent work with Lagrangian trajectory models has shown that atmospheric particles emitted from different sources can be tracked separately through aerosol processes model calculations, thereby directly showing how different emissions sources contribute to ambient particle concentrations [6]. The expansion of the airshed model described here to track the emissions from different sources separately would

allow the same information to be obtained from a model that can depict the spatial distribution of air quality in three dimensions.

Bibliography

[1] B. C. Singer and R. A. Harley. A fuel-based motor vehicle emission inventory. *J. Air Waste Manage. Assoc.*, 46:581–593, 1996.

[2] J. J. Schauer, M. J. Kleeman, G. R. Cass, and B. R. T. Simoneit. Measurement of emissions from air pollution sources. 1.C1 through C29 organic compounds from meat charbroiling. *to be submitted to Environ. Sci. Technol.*, 1997.

[3] W. X. Cui, J. Machir, L. Lewis, D. J. Eatough, and N. L. Eatough. Fine particulate organic material at Meadview during the Project MOJAVE summer intensive study. *J. Air Waste Manage. Assoc.*, 47:357–369, 1997.

[4] J. F. Pankow. An absorption model of gas/particle partitioning of organic compounds in the atmosphere. *Atmos. Environ.*, 28:185–188, 1994.

[5] J. R. Odum, T. P. Jungkamp, R. J. Griffin, H. J. L. Forstner, R. C. Flagan, and J. H. Seinfeld. Aromatics, reformulated gasoline and atmospheric organic aerosol formation. *Environ. Sci. Technol.*, 31:1890–1897, 1997.

[6] M. J. Kleeman and G. R. Cass. Source contributions to the size and composition distribution of urban particulate air pollution. *submitted for publication in Atmos. Environ.*, 1997.